Development of a surfactant-based in situ extraction from authentic feedstocks

Vom Promotionsausschuss der
Technischen Universität Hamburg

zur Erlangung des akademischen Grades

Doktor-Ingenieurin (Dr.-Ing.)

genehmigte Dissertation

von

Ralena Racheva

aus

Sofia, Bulgarien

2020

1. Gutachterin: Prof. Dr.-Ing. Irina Smirnova
2. Gutachter: Prof. Dr.-Ing. Andreas Jupke

Tag der mündlichen Prüfung: 22. November 2019

ACKNOWLEDGMENT

This thesis was completed during my time as a research assistant in the Institute of Thermal Separation Processes at the Hamburg University of Technology. I would like to thank the following people without whom I would not have made it through my PhD degree!

First, I would like to express my sincere gratitude to Prof. Dr. Irina Smirnova. I appreciate her dedicated support and her never-misleading guidance, from the start of my PhD journey towards becoming a young professional. The scientific skills and the personal learnings, which I obtained as her PhD student, are always going to be essential for my life track.

In addition, I would also like to thank Prof. Dr. Andreas Jupke for taking over the co-examination. Furthermore, to Prof. Dr. Kerstin Kuchta for organizing a smooth examination procedure and for the great atmosphere during my defense.

My next acknowledgments go to Prof. Dr. Gerrit Luinstra, Prof. Dr. Sascha Rohn, Dr. Martin Kerner, Dr. Stefan Hindersin, and all the co-workers in their teams, with whom we managed to achieve competitive results and derive new learning regarding the valorization of valuable compounds from the microalgae.

I would like to say a special thank you to all my former colleagues from the institute. I enjoyed the time with you so much and I always look back with a smile to the days of "V8". Wish you all the best for the days to come, you all deserve it! I also would like to thank all my students for their collaborative effort during data collection. Without you, this thesis was not going to happen.

Finally, I would like to thank my family for believing in my success and for the support and love, no matter the far-away distance.

Last but not least, I would like to express the deepest gratitude to my boyfriend René. Thank you for the care, patience, love, and for motivating me to finish this work!

ABSTRACT

Nonionic surfactants are a diverse class of amphiphilic compounds, which can form two-phase systems in an aqueous solution. At an elevated temperature above the cloud point temperature, these mixtures split into a surfactant-rich phase and aqueous phase. This work aimed to develop an in situ extraction of sensitive biomaterials from authentic feed solutions using surfactant-based cloud point systems in a technically relevant scale. Therefore, investigations on the separation in a cloud point system were performed in the laboratory, technical and pilot scale. Foremost, amphiphiles with low cloud point temperature were identified. That after, suitable process conditions were determined, based on the liquid-liquid equilibria of the three surfactants Triton X-114, Silwet L-7230 and ROKAnol NL-5 and their corresponding physical properties. Consequently, a successful recovery of the model solute cinnamic acid in the surfactant-rich phase was observed in batch and continues mode.

Further, a strategy to increase the solute loading of the extract without using additional heat or solvents was achieved by recycling the solvent during the continuous process in technical scale. In addition, a cloud point extraction with a surfactant, which was permitted in the final market formulation (leave-in surfactant), such as Silwet L-7230 and ROKAnol NL-5, was proposed. Hence, there was no need for a cost-intensive separation (or just a rough separation) of the target molecule from the surfactant.

Based on the process realization with the model solute, the cloud point extraction was conducted with natural feedstocks. A successful accumulation of phenolic compounds and pigments from authentic pineapple juice was demonstrated using the "leave-in surfactant" ROKAnol NL-5. Moreover, a long-term in situ extraction from genuine microalgae culture with recycling of the solvent was carried out in a continuous mode. A good biocompatibility, stable performance, and product accumulation were achieved in technical scale. Finally, a pilot plant for the continuous cloud point extraction from microalgae cultures was designed and operated.

Ultimately, the successful demonstration of a cloud point extraction from authentic feedstocks represented the technique as an attractive separation tool with high technical relevance.

TABLE OF CONTENTS

1 INTRODUCTION

Surfactants, also named surface-active agents, are mainly used to improve the properties of aqueous formulations. In 2014, a global revenue of 32.2 billion US dollar was achieved in the surfactant market. Their main applications were detergents and cleaners, where the surfactant enhances the rinsing performance of water mixtures. That segment represented 56 % of the world surfactant demand in 2014. Personal care, agricultural chemicals, textiles industry, paints, lacquers and processed food products were denoted as further application areas for the surfactants [1,2].

The diversity in the applications leads to a variety of commercial surfactants. Depending on the charge of their molecule, surfactants can be anionic, cationic and nonionic. However, all these chemical have a common property. Once added to a solution, their monomers arrange into micelles. For instance, in an aqueous bulk, the micelles possess a hydrophobic core surrounded by an outer layer of the hydrophilic moieties. Thus, oil-soluble species can be solubilized in the core and thus can be evenly distributed in the aqueous solution [3].

Some nonionic surfactants are known for a further phenomenon. Their micellar solutions separate into two phases in case of a temperature elevation. That after, a surfactant-rich phase coexists with a surfactant-lean phase. However, the main component in both fractions remains water. Such biphasic systems are regarded to as aqueous two-phase systems [4].

Often, aqueous two-phase systems are not hazardous and comprehend low toxicity to microorganisms. Therefore, these systems are used for the extraction of sensitive organic compounds, such as proteins. Moreover, due to their excellent biocompatibility, the systems are applied for the direct product removal in the whole-cell biotechnology [5].

The extraction based on nonionic surfactant aqueous two-phase systems is described as a mild technique for direct isolation of sensitive biomaterials from genuine feed solutions. However, there is a limit number of investigations, which focus on such separations in a multistage apparatus. Moreover, there are even fewer studies on the implementation of surfactant-based extraction for direct

product removal from a biological suspension. Despite the mild conditions in a surfactant-based aqueous two-phase system, their application for the recovery of biomaterials in industrial or pilot scale is rarely studied [6–9].

Therefore, the general aim of this work is the development of a separation process for mild recovery of biomaterials using nonionic surfactants. In order to reach this goal, well-studied but also commercial surfactants have to be tested for their suitability for mild and direct (in situ) product removal. In addition, concepts for process intensification and surfactant regeneration have to be proposed. Subsequently, the combination of the selected amphiphiles with the process set-up has to be tested on its biocompatibility with authentic natural feedstocks. Based on these conditions, an extraction process cab be designed in batch and continuous mode, which can make the technique attractive for larger-scale applications. As a final proof of the concept for in situ product removal using micellar systems, the extraction from a natural feedstock using a nonionic surfactant has to be realized in technical and pilot scale.

2 THEORETICAL BACKGROUND

This chapter provides a general overview of the knowledge required to develop a separation process using nonionic surfactants. At first, a brief description of the thermodynamic equilibria in the two-phase system is presented. That after, the basics in the design and scale-up of liquid-liquid extraction are summarized. Attention is given to the in situ product removal as well. Consequently, the phase behavior of nonionic surfactants considering its potential as in situ separation media is described. Finally, the properties of the two authentic feedstocks, applied in this work, are summarized.

2.1 PHASE EQUILIBRIA IN LIQUID SYSTEMS

When a thermal separation process is applied, heat and mass are transferred between the phases of the open thermodynamic system. Mass transfer ends when phase equilibrium is reached [10]. The system exists at equilibrium state when the total internal energy U is at its minimum, as well the total entropy S, volume V and molar amount of each component n_i are constant [11]:

$$U = U^{\alpha} + U^{\beta} + \cdots + U^{\pi} = min$$

$$S = S^{\alpha} + S^{\beta} + \cdots + S^{\pi} = const$$

$$V = V^{\alpha} + V^{\beta} + \cdots + V^{\pi} = const$$

$$n_i = n_i^{\alpha} + n_i^{\beta} + \cdots + n_i^{\pi} = const, i = 1, \ldots, n$$

Equation 2-1: Conditions for the thermodynamic equilibrium

U^{φ}: internal energy; S^{φ}: entropy; V^{φ}: volume; $n_i{}^{\varphi}$: molar amount of component i of the phase φ

The Gibbs equation for each phase φ is then as follows:

$$dU^{\varphi} = T^{\varphi} dS^{\varphi} - P^{\varphi} dV^{\varphi} + \sum_{i=1}^{n} \mu_i^{\varphi} d\, n_i^{\varphi}$$

Equation 2-2: Gibbs equation for each coexisting phase

U^{φ}: internal energy; T^{φ}: temperature; S^{φ}: entropy P^{φ}: pressure; V^{φ}: volume; μ_i^{φ}: chemical potential of component i; n_i^{φ}: molar amount of component i of the phase φ

By applying the method of Lagrange multipliers to locate the minimum of dU^{φ}, the Gibbs equilibrium conditions are defined as:

$$T^{\alpha} = T^{\beta} = \cdots = T^{\varphi}$$

$$P^{\alpha} = P^{\beta} = \cdots = P^{\varphi}$$

$$\mu_i^{\alpha} = \mu_i^{\beta} = \cdots = \mu_i^{\varphi}, i = 1, \ldots, n$$

Equation 2-3: Gibbs conditions for thermal, mechanical and chemical equilibrium

T^{φ}: temperature; P^{φ}: pressure; μ_i^{φ}: chemical potential of component i of the single phase φ

2.2 PARTITION COEFFICIENTS

The chemical equilibrium of a multicomponent two-phase system is defined through the identical chemical potential for each component in the coexisting phases. The chemical potential is also referred as partial molar Gibbs free energy [12]:

$$\left(\frac{\partial G}{\partial n_i}\right)_{p,T,n_j} = \mu_i$$

Equation 2-4: Partial molar Gibbs free energy

G: Gibbs free energy; n_i: mole amount of the component i≠j; μ_i: chemical potential of component i

The chemical potential of one component in a mixed phase can be estimated using the following sum:

$$\mu_i = \mu_i^o + \Delta\mu_i$$

Equation 2-5: Chemical potential in a mixed phase, μ_i

μ_i: chemical potential; μ_i^o: chemical potential in standard state; $\Delta\mu_i$: partial molar free energy of mixing of component i

Whereas, the partial molar free energy of mixing is calculated as follows:

$$\Delta\mu_i = RTln(\gamma_i x_i)$$

Equation 2-6: Partial molar free energy of mixing $\Delta\mu_i$

R: molar gas constant; T: temperature; γ_i: activity coeffitient; x_i: molar fraction of component i

The distribution of a solute between two phases can be expressed by applying **Equation 2-3**, **Equation 2-5**, and **Equation 2-6**. As the standard state for two liquid phases is the same, the partition of one component between these phases can then be described according to Nernst's distribution law:

$$K_i^{\alpha\beta} = \frac{x_i^\alpha}{x_i^\beta}$$

Equation 2-7: Partition coefficient $K_i^{\alpha\beta}$

x_i: molar fraction of component i in the phases α or β

For two ideally diluted phases, the partition can also be expressed regarding concentrations instead of molar fractions. The resulting partition coefficient ($P_i^{\alpha\beta}$) is calculated as denoted in eq. Equation **2-8**. For the comparison of separation processes, commonly the logarithmic value of this partition coefficient ($logP$) is applied [13].

$$P_i^{\alpha\beta} = \frac{c_i^\alpha}{c_i^\beta}$$

Equation 2-8: Partition coefficient $P_i^{\alpha\beta}$

c_i: concentration of component i in phase α or β

An uneven distribution of a solute leads to a $logP$ value lower or greater than zero. In this thesis, the partition coefficient P was measured towards the evaluation of different two-phase systems as suitable for liquid-liquid extraction. Hence, the major points for the design of extraction processes are presented in chapters 2.3 and 2.4.

2.3 LIQUID-LIQUID EXTRACTION

The principle of a liquid-liquid extraction is the mass transfer of a target substance (solute) from one liquid phase (feed) to another (solvent). Therefore, the solute must have a higher solubility in the solvent than in the feed phase and both liquid phases must be either entirely or at least partially immiscible. The resulting solute-rich solvent is referred to as an extract and the second phase, lean in solute, is referred to as a raffinate. Liquid-liquid extraction finds typical applications in the treatment of wastewater since the volatility of the impurities does not differ much to the one of water. The Udex process is also an example of an industrial separation of aromatics from aliphatics by liquid-liquid extraction. Further, the separation of heat-sensitive substances may be more cost-effective in two-phase extraction systems than in adsorption units [10,14].

A crucial issue for the design of an extraction process is the right solvent choice. The requirement for a suitable solvent are listed below [14]:

- pronounced selectivity for the target substance,
- high solubility of the substance of interest;
- high capacity for solute accumulation;
- low or no solubility in the raffinate;
- cost-efficient recovery from the extract;
- high density difference compared to the feed;
- low interfacial tension;
- low toxicity.

The simple approach of applying the suitable solvent for the separation of the target substance is the single theoretical stage extraction. This is a typical laboratory technique of stripping the extract from raffinate after reaching the

thermodynamic equilibrium [14]. Hence, the accumulation of the solute is limited by the partition coefficient (**Equation 2-7** or **Equation 2-8**).

Multistage extraction processes are introduced to reach better recovery of the target substance. These consist of multiple extraction stages, with concurrent, crosscurrent, or countercurrent flow direction as depicted in Figure 2.1.

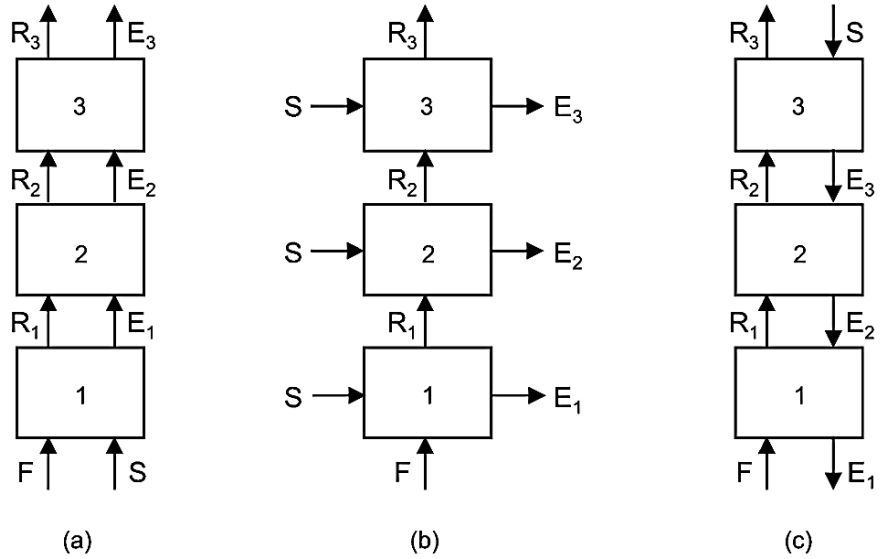

Figure 2.1: Schematic illustration of (a)con-, (b) cross- and (c) countercurrent extraction [15].

One extraction stage consists of feed (F), solvent (S), extract (E), and a raffinate (R). The crosscurrent technique is advantageous for laboratory applications since the sampling of extract and raffinate is possible after each stage. However, crosscurrent extraction demands high solvent amount. Hence, this scheme is less economically attractive. On the other hand, depending on the solvent and feed properties, the countercurrent process can be more beneficial, since it is known to reach up to 12 equivalents of the equilibrium stage in industrial scale. The apparatus, utilized for the countercurrent liquid-liquid extraction are classified to stage-wise (mixer-settler) and differential (continuous) contactors [14].

Widely used differential contactors with introduced stirring are the rotating disc contactor (RDC), the Kühni, the Scheibel and the Oldshue-Rushton (ORC) column types. These apparatus have in common that they consist of several compartments. In each compartment mixing energy is introduced by a rotated, centrally located agitator [10]. Two Lightnin Mixer (Oldshue-Rushton) extraction columns of different scale were subject to investigation in this work and therefore are presented more detailed.

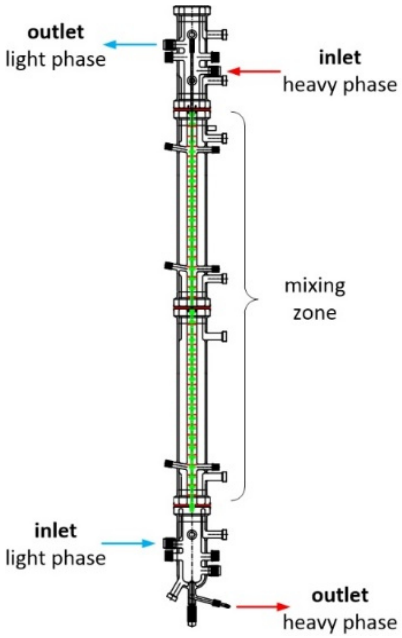

Figure 2.2: Scheme of an Oldshue-Rushton column (ODC) with a heating jacket.

An extraction column of the type applied in this thesis is presented in figure **Figure 2.2**. The continuous contactor is equipped with a central agitator (in green) and stators (in red). Agitators and stators are alternating along the height of the mixing zone. On both ends, the mixing zone is connected to the top and bottom parts, where the settling of the phases takes place. The light and the dense phase enter the column at the bottom and the top, respectively. Then, the raffinate and extract exit the column vice-versa. In this way, the column is operated in a countercurrent mode. Depending on its density, the solvent can be introduced at the top or at the bottom of the contactor. Further, the solvent is the disperse phase in most columns. Hence, the agitation in the mixing zone leads to the dispersion of the solvent in the feed [13]. It is important to note, that in case of poor solute concentration in the disperse phase the extract flow can be recycled as solvent until the desired concentration is reached [10]. In this way, the stage efficiency is expected to increase [14].

The countercurrent extraction in contactors with stirring is well studied in organic but also in aqueous media. For instance, a multistage countercurrent contactor is applicable for the purification of enzymes in the aqueous two-phase system of polyethylene glycol [16]. Furthermore, the biotransformation of penicillin G is possible in a modified Kühni extractor, which contains the carrier Amberlite LA 2 loaded with enzyme [5]. A further contribution to the application of aqueous

biphasic mixtures is presented in this work, focusing on aqueous surfactant-based systems for the continuous extraction.

Stirred columns allow density differences between feed and solvent greater 0.05 $g \cdot cm^{-3}$ and viscosity of the continuous phase similar to water [17]. Hence, the column type was suitable for the investigations in this thesis.

The optimal operation in a stirred column can be reached by varying the mechanical energy input, as well as the feed and solvent flows. The agitation speed directly influences the extraction efficiency in an ODC. The stirrer provides the needed mass transfer area between the two phases by dispersing the solvent in droplets among the feed [18]. Hence, the droplet size distribution, as well as the breakage or coalescence, are influencing the enrichment of solute. Moreover, through the axial forces of the stirrer blade, small droplets are held up in the mixing zone. This phenomenon is referred to as backmixing [10]. A simplified representation of the influence of the agitation speed on the extraction efficiency is presented in Figure 2.3.

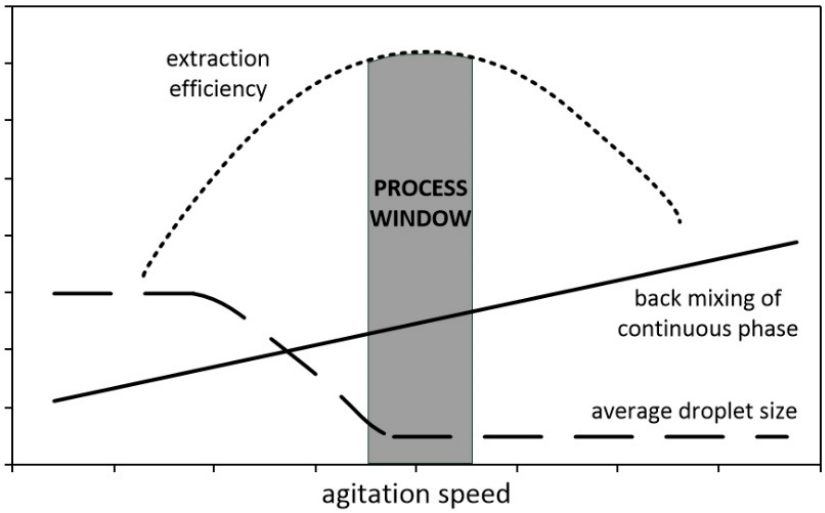

Figure 2.3: Influence of the agitation speed on the droplet size, backmixing of the continuous phase and the extraction efficiency (own simplified representation according to [18,19]).

The droplet size does not decrease with intensive stirring until a critical value of the agitation speed is reached. Then, the droplets are getting smaller, and thus the mass transfer is elevated. However, the adverse axial mixing effect is also more pronounced at higher stirring speeds. Therefore, it is essential to define a

process window providing highest mass transfer surface at less significant amount backmixing [18].

The feed and solvent flow are further parameters, which provide the amount of free phase accepting the target substance from the feedstock. The feed-to-solvent ratio and the capacity are the two primary values used to characterize extraction processes.

The feed-to-solvent ratio in stirred columns usually ranges from 1 to 10 [17]. The ratio is referred to as ν and is defined as:

$$\nu = \frac{\dot{F}}{\dot{S}}$$

Equation 2-9: Calculation of the feed-to-solvent ratio ν

$\dot{F}$: feed stream; $\dot{S}$: solvent stream

In liquid-liquid extraction, the physical constraints on solvent usage can be estimated to calculate the minimum and maximum feed-to-solvent ratio. In theory, the minimum amount of solvent needed to transfer a high fraction of solute is the amount corresponding to maximal yield, while in practice this value is about 30% higher [20]. Hence, the minimum solvent-to-feed ratio is:

$$\nu_{min} = \frac{1.3}{K_i^{\alpha\beta}}$$

Equation 2-10: Calculation of the minimum feed-to-solvent ratio ν_{min}

$K_i^{\alpha\beta}$: partition coefficient of component i

Consequential the maximum feed-to-solvent ratio (ν_{max}) is defined as the amount of solvent necessary to dissolve the feed phase, whereby the entering feed does not contain extraction solvent, and thus obtaining [20]:

$$v_{max} = \frac{1}{1 - c_S^{sat}}$$

Equation 2-11: Calculation of the maximum feed-to-solvent ratio v_{max}

c_S^{sat}: concentration of extraction solvent in the extract phase at equilibrium

Besides the feed-to-solvent ratio, the capacity of the column is also essential for the process design. The column capacity is calculated as follows:

$$b = \dot{F} + \dot{S}$$

Equation 2-12: Calculation of the column capacity b

$\dot{F}$: feed stream; $\dot{S}$: solvent stream

The capacity is an important parameter when designing extraction equipment since it is applied when upscaling the diameter. Furthermore, it is known, that stirred columns possess an upper limit of the throughput (capacity/cross-section). The maximal capacity is reached when flooding is observed. An apparent or measurable disturbance of the countercurrent fashion through the column at a specific capacity is defined as flooding [21]. On the one hand, flooding occurs in case of low stirring and high capacity. The reason for this is the large droplet size resulting in a phase inversion. On the other hand, by high agitation speed and lower capacity, flooding is also possible, as a result of the small dispersed droplets that are carried out with the continuous phase [18].

Even below the flooding point, the disperse phase can be partially hindered to move in a countercurrent manner. This part of the disperse phase is regarded to as dynamic liquid hold-up. Additionally, a static liquid hold-up can remain in corners, in dead spots, and on the baffles [10]. The total hold-up in this work is defined as the fraction of the total liquid flowing in the column, occupied by the disperse phase [22]. The hold-up is depending on the stirring intensity since the agitation is responsible for the different droplet sizes in the mixing zone. Hence, by adjusting the power input by stirring, the hold-up can be maintained in such a way so that minimal amount of the disperse phase is carried out with the raffinate flow [14].

The plot of the flooding point as a function of the capacity and agitation speed is known as a flooding curve. The flooding curve of a multistage mixer column of the Oldshue-Rushton type is depicted in Figure 2.4.

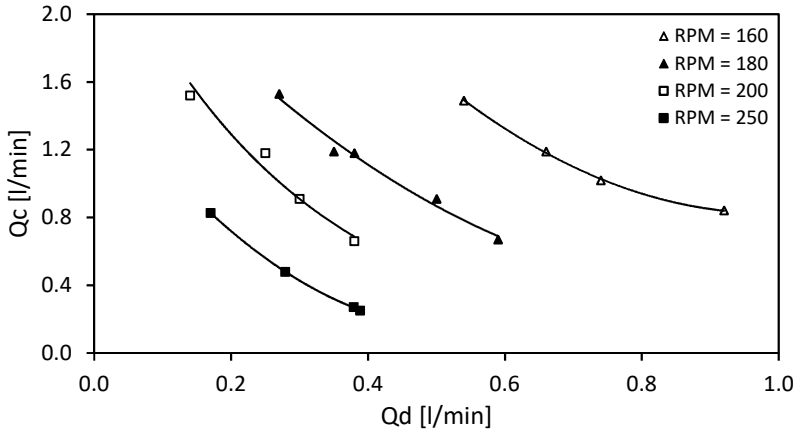

Figure 2.4: Continuous (Q_c) and dispersed phase (Q_d) flow rates at flooding with agitation speed (rpm) as a parameter (own representation according to [23]).

The diagram indicates that with increasing agitator speed the flooding curves are shifted to a lower region in the flooding diagram. Thus, the phase flow rates have to be smaller. Furthermore, the flooding point is depending on the overall capacity of the column, which is the sum of the continuous and dispersed phase flow rate.

However, even when operating below the flooding point, the process can be accompanied by significant losses of the dispersed phase. While some studies use specific values and model equations to calculate operating conditions below the flooding point, for instance, 50% of the superficial flooding velocity [18,23], the acceptable dispersed phase loss is highly dependent on the specific process. Therefore, in this work, an alternative term, stress limit, was used to describe operating conditions that do not fulfill all aspects of a flooding point. When the stress limit was reached the loss of dispersed phase is above a self-determined acceptable amount of 10 wt%, as described in detail in the experimental part.

Finally, values regarding the accumulation of target substance in the extract phase as well as dynamic productivity and efficiency are calculated to evaluate the performance of the extraction process.

Firstly, the enrichment factor represents the ratio between the solute concentration in the extract and raffinate, respectively [13]:

$$T_i = \frac{c_i^E}{c_i^R}$$

Equation 2-13: Calculation of the enrichment factor T_i

c_i^E: concentration of component (i) in the extract; c_i^R: concentration of component (i) in the raffinate

Secondly, the efficiency is evaluated according to the yield of the continuous extraction:

$$Y_{cont.} = \frac{\dot{m}_i^E}{\dot{m}_i^F}$$

Equation 2-14: Calculation of the extraction yield $Y_{cont.}$

$\dot{m}_i^E$: mass flow of component (i) in the extract; $\dot{m}_i^F$: mass flow of component (i) in the feed

Thirdly, the productivity of the continuous extraction is calculated as:

$$F_i = c_i^E \cdot \dot{E}$$

Equation 2-15: Calculation of the extraction productivity F_i.

c_i^E: component (i) concentration in the extract; $\dot{E}$: total extract mass flow

Lastly, the number of theoretical stages (or mass-transfer units) is calculated to estimate the mass transfer at different operating conditions, as follows [10,14]:

$$N_{theo} = \frac{\ln\left[(\varepsilon - 1)\left(\frac{w_i^F}{w_i^R} + \frac{w_i^S}{w_i^R}\right) + 1\right]}{\ln(\varepsilon)} - 1$$

Equation 2-16: Calculation of the number of theoretical stages $N_{theo.}$

ε: extraction factor; w_i: weight fraction of component (i) in feed (F), solvent (S) and raffinate (R)

With the extraction factor:

$$\varepsilon = P_i \frac{\dot{E}}{\dot{R}}$$

Equation 2-17: Calculation of the extraction factor ε

P_i: partition coefficient; $\dot{E}$: extract flow; $\dot{R}$: raffinate flow

Please note, that **Equation 2-16** and **Equation 2-17** are applied with the assumption, that the partition coefficient is constant at the studied concentration ranges, as well as the ratio between feed and solvent flow is equal to the ratio between the raffinate and extract flow [10,14].

When designing an extraction process, attention is given to the process characteristics described in this chapter. Thus, it is possible to evaluate the economic and operational side of the extraction. An important issue of the process design, which is essential for this work, is the scalability of the extraction [24]. Hence, the theoretical background concerning the scale-up of stirred extraction units is summarized in the following chapter (see chapter 2.4).

2.4 SCALE-UP OF THE LIQUID-LIQUID EXTRACTION

The scale-up of extraction equipment requires the consideration of three types of similarities. Firstly, two vessels are geometrically similar if the ratio between all corresponding dimensions is equal. Secondly, the two geometrically similar vessels have a kinematic similarity only if the ratio between corresponding velocities in the equivalent positions is the same. Thirdly, the vessels are dynamically similar in case of a kinematic similarity and if all force ratios are equal in corresponding positions [14]. Based on these requirements, the scale-up of an extraction column is conducted in three steps, starting from experimental data regarding laboratory columns with inner diameter from 32 to 80 mm [17].

Initially, a flooding curve (see **Figure 2.4**) at chosen stirring speed and feed-to-solvent ratio are obtained based on experimental data. Then an operation point is set in such a manner so that the highest extraction efficiency and a maximal number of theoretical stages are maintained. The capacity is usually at 80% of the

flooding value ensuring maximal productivity [17]. Further, the specific throughput is then calculated from the capacity [21]:

$$(v_f + v_s) = \frac{\dot{F} + \dot{S}}{\pi \cdot d^2/4}$$

Equation 2-18: Calculation of the throughput $(v_f + v_s)$

$\dot{F}$: feed stream; $\dot{S}$: solvent stream; d: column inner diameter

The throughput allows obtaining the diameter of the column at a known capacity. Thus, the geometry of the new column can be derived from the ratio to the diameter. By applying the throughput, the geometrical and the kinematic similarities are ensured. It is important to notice that with the higher diameter the height of the new column has to be increased as well. However, a limitation in the allowed building height is often reported. Hence, a deviation from the geometrical similarity may take place [17]. Nevertheless, to scale-up the height of a stirred column is possible according to the following correlation [18]:

$$\frac{h_{c1}}{h_{c2}} = \left(\frac{d_{c1}}{d_{c2}}\right)^{\alpha}, \alpha = 0.38 \div 0.5$$

Equation 2-19: Geometrical similarity of height and diameter [18]

h: height; d: column inner diameter; c: column 1 or 2

As an alternative approach to the throughput calculation, the velocities of the streams can be calculated from the residence time. The laboratory scale column's active volume is divided by the column's capacity to calculate the residence time (**Equation 2-20**). The pilot scale column capacity yielding an equal residence time is then obtained through division of the residence time by the pilot scale column's actual volume [14]. In case of a constant ratio between mixing zone volume and free cross-section, both calculations should lead to equal results.

$$\tau = \frac{V_a}{W}$$

Equation 2-20: Calculation of the residence time τ

V_a : Active column volume; W: Column capacity

The residence time is essential in case of systems that separate slowly or for extractive catalysis. When the velocity of the streams is too high, there might be not enough time to react in the mixing zone or to separate in the settler part of the column. Therefore, it is of importance to assess the retention time when designing an extraction process [14].

Further, the energy input of the mixer has to be calculated so that the dynamic similarity is maintained. Moreover, the agitation input has to be kept unchanged as the flooding curve is kept [17].

To this purpose, first, the Reynolds Number (N_{Re}) is calculated according to **Equation 2-21** for the given laboratory scale geometry and chosen agitation speed.

$$N_{Re} = \frac{N_a * D_a^2 * \rho}{\eta}$$

Equation 2-21: Calculation of the dimensionless Reynolds Number N_{Re} (modified for agitation).

η: Viscosity; D_a: Impeller diameter; ρ: Density; N_a: Agitation speed

Subsequently, using a correlation curve diagram (**Figure 2.5**), the Power Number N_P (also known as Newton Number) can be obtained as a correlation to the Reynolds Number. Each type of agitator has its characteristic correlation curve [14].

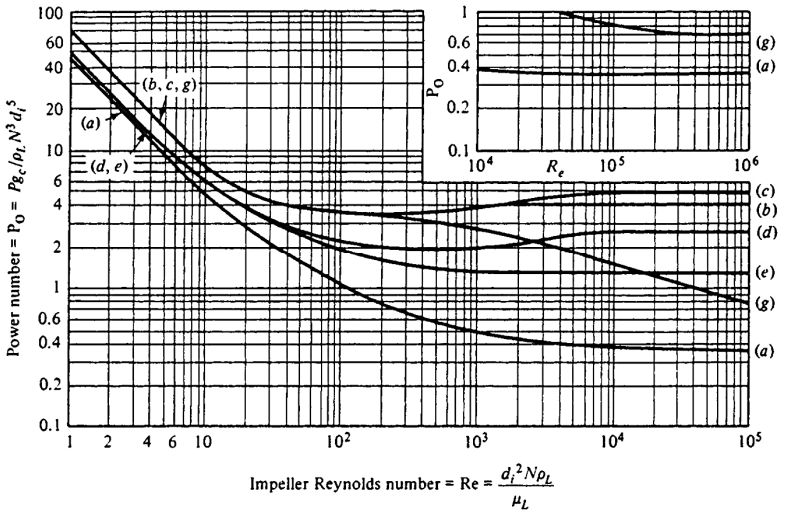

Figure 2.5: Correlation of Power Number (Ne) and Reynolds Number (Re) for different types of agitators [14]

The agitator's total power input can then be calculated from the obtained Power Number for a given laboratory scale geometry, agitation speed, and a number of impellers by **Equation 2-22** [25].

$$N_P = \frac{P}{D_a^5 * \rho * N_a^3}$$

Equation 2-22: Calculation of the dimensionless Power Number N_P.

P: Power input; D_a: Impeller diameter; ρ: Density; N_a: Agitation speed

Thus, the total power input represents the energy transferred into the fluid by the impellers. Finally, by dividing the total power input by the column's mixing zone volume, the parameter power per unit volume is obtained.

Vice versa, the power per unit volume can be calculated for a given pilot scale geometry. As the values for laboratory and pilot scale should match, the agitation speeds at both scales have to be adjusted iteratively.

A successful scale-up from laboratory to pilot equipment is thus possible by following the described calculation scheme. The calculation is universal, and the type of system does not influence it. Hence, the method is applicable for organic and aqueous two-phase systems. The surfactant-based biphasic systems are an example of a suitable extraction media for the continuous extraction in a column [13]. These systems were studied in this thesis as well. Therefore, the primary points regarding surfactant-water mixtures as an extractive media are presented in the next chapter.

2.5 SURFACTANT-BASED AQUEOUS BIPHASIC SYSTEMS FOR EXTRACTION PROCESSES

Surfactants are amphiphilic molecules, composed of a hydrophilic head and one or more hydrophobic tails. They are classified regarding their head-group's charge as anionic (negatively charged head-group), cationic (positively charged head-group), zwitterionic (a head-group carrying a positive and negative charge), or nonionic (uncharged but polar head-group) [26]. The investigations in this thesis focused on the nonionic surfactants due to their application in extraction processes.

The chemical structure of three nonionic surfactants of importance for this work is presented in Figure 2.6.

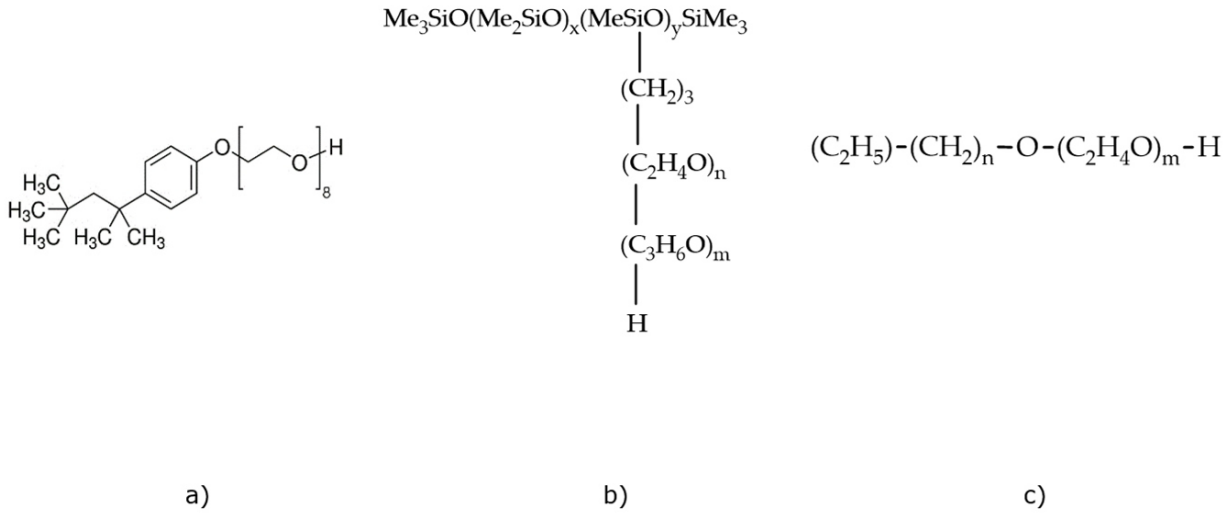

Figure 2.6: Chemical structure of Triton X-114 (fig. a): average number of EO in head group 8 [27]; Silwet L7230 (fig. b): poly(ethylene oxide) (m)/poly(propylene oxide) (n) = 40/60 wt% and polydimethylsiloxane (x)/ polymethylsiloxane (y) = 21/79 wt% (own representation according [28]; and ROKAnol NL-5 (fig. c): number of C-atoms in tail (n) = 7-11 and number of EO in head group (m) = 3-5 (own representation according chemical data sheet). Me: methyl group.

A typical nonionic surfactant consists of a hydrophobic alkyl chain group and hydrophilic ethylene oxide groups. The molecules of Triton X-114 (fig Figure 2.6a) and ROKAnol NL-5 (fig. Figure 2.6c) represent such chemical structure. Triton X-114 is an alkylphenol ethoxylate with a hydrophobic branched tail containing an aromatic ring. The molecule of ROKAnol NL-5 is represented by a fatty alcohol (C = 7-11) which is ethoxylated with 3-6 ethylene oxide moieties [3]. Silwet L7230 (fig. Figure 2.6b) represents another class of nonionic surfactants. This amphiphile is a block copolymer of silicone, ethylene oxide, and propylene oxide. The hydrophobic part of the molecule is built of a siloxane backbone which is grafted to the ethylene oxide-propylene oxide head group [28].

Due to the diversity of their chemical structures, nonionic surfactants exhibit variations in their chemical and physical properties. For instance, the hydrophilic-lipophilic balance (HLB) can change by adjusting the weight ratio between the head group and the tail moiety. The HLB is specific for each surfactant and is expressed on a scale of 3.5 to 18 divided in water-in-oil (w/o) emulsifiers (HLB=3.5÷6), wetting agents (HLB=7÷9), oil-in-water (o/w) emulsifiers (HLB=8÷18), detergents (HLB=13÷15), and solubilizers (HLB=15÷18) [29,30]. In case of Silwet

L7230, the HLB-value is 6.3 which makes the amphiphile less soluble in water than ROKAnol NL-5 (HLB = 11.6).

Nonionic surfactants can form complex structures, such as bilayers, liquid crystals, and spherical or cylindrical vesicular structures (micelles). A typical phase diagram for an aqueous nonionic surfactant binary mixture (C_5E_{12}/water) is shown in **Figure 2.7**

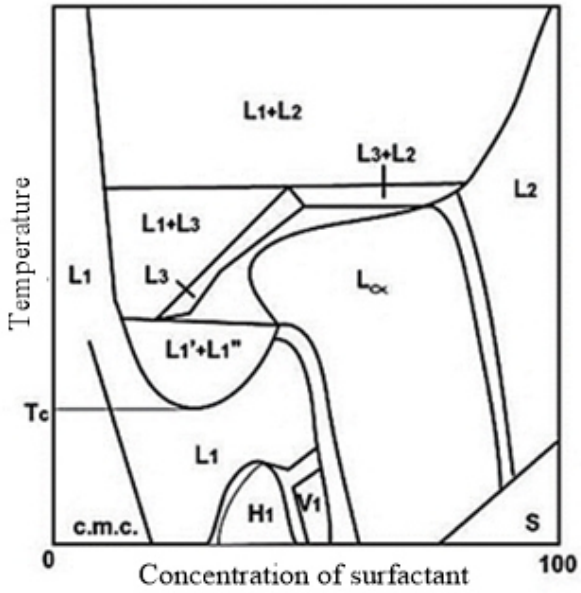

Figure 2.7: Phase diagram for C_5E_{12}/water [31].

In aqueous surfactant solutions, a change in the surfactant concentration or the system temperature leads to different phase transitions, as illustrated in **Figure 2.7**. At low concentrations and temperatures, the surfactant dissolves entirely into a single isotropic liquid phase.

However, above the critical micelle concentration (cmc) regular micellar solutions (L_1) and reverse micellar solutions (L_2) are formed. The normal micelle is a dynamic aggregate composed of a hydrophobic core, formed by the lipophilic tails of the monomers, and a hydrophilic outer layer of the water-soluble monomer moieties. The reversed micelle structure is the opposite. The hydrophobic core of the micelles can solubilize lipophilic substances (solutes). Hence, by solubilizing an oil-soluble substance in the micelle, one can homogeneously disperse it in an aqueous bulk. This property is the reason for the broad application of surfactants in cleansing agents, food and cosmetic products [32].

At higher temperatures, above the cloud point temperature (T_c), the micellar solution separates into one surfactant-lean phase (L_1') and one surfactant-rich phase (L_1'').

Additionally, a sponge-like phase (L_3) can also exist in surfactant/water mixtures. At low temperatures but higher concentration, the formation of lyotropic phases can be observed, viz. hexagonal (H_1), cubic (V_1) and lamellar (L_α) liquid crystalline phases, with the latter characteristically extending into the two-phase area [33,34]. The liquid crystalline lamellar, hexagonal, cubic phases, as well as the sponge-like phase, are highly structured. As a result, high viscosity may be exhibited in these phase regions [34–36].

The coexistence of the phases L_1' and $L_1''$is of higher importance for separation processes and is further discussed in this chapter. An aqueous solution containing a nonionic surfactant above the cmc can undergo a temperature-induced clouding. The temperature, at which the solution turns turbid, is referred to as cloud point temperature (CPT) [37,38]. The thermodynamic mechanisms behind the clouding are complex. It is assumed, that elevated temperatures lead to dehydration of the micelles' hydrated outer layers. Consequently, repulsive forces are decreased and attractive micellar interactions are more pronounced. Hence, the size of the aggregates increases and the solution becomes turbid [3,32].

For commercial water-soluble surfactants, the CPT is commonly defined at a surfactant concentration of 1 wt % in deionized water. Further, at a surfactant concentration, the minimum clouding temperature, also known as minimal lower critical solution temperature (LCST), is exhibited [39]. However, there are diverse methods to determine a CPT and the LCST at different solvents. Thus, one has to consider the manufacturer's data concerning the CPT and LCST carefully.

The molecular structure or the solution composition can affect the CPT of nonionic surfactants. These factors can cause steric hindrance, charge repulsion, or influence the solvent's solubility [26,33]. The LCST values of an aqueous nonionic surfactant solution decrease with a lower number of ethylene oxide groups and increasing length of the alkyl chain [4]. However, electrolytes have the most significant influence on aqueous nonionic surfactant solutions. It is distinguished between electrolytes lowering the CPT, and such increasing the CPT. The first effect

is caused by a dehydration of the surfactant's ethylene oxide chain and its consequently decreased solubility in water (salting-out effect). Vice versa, the second effect is caused by an increased solubility of the surfactant (salting-in effect) [38,40].

Moreover, if the aqueous surfactant solution (S) is further heated to a point above the coexistence curve (in the two-phase region, above the CPT), a macroscopic phase separation may occur (**Figure 2.8**).

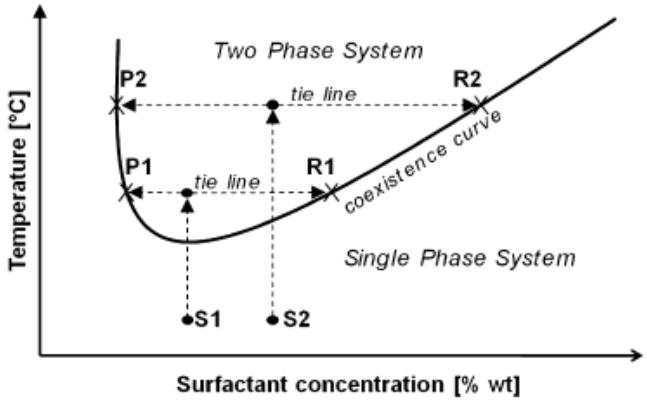

Figure 2.8: Liquid-liquid equilibrium of water-surfactant solution. Phase separation mechanism [41].

Then the mixture splits into a surfactant-rich phase (R) and a surfactant-lean aqueous phase (P), as shown in **Figure 2.8** [41]. The concentration of surfactant in the micellar phase (R) is a function of the temperature. The aqueous phase is poor in micelles whereas the concentration of surfactant is close to the cmc [42].

This type of phase behavior and the ability of the micelles to solubilize solutes, make surfactant-based aqueous two-phase systems (ATPS) attractive for separation processes. Hence, a technique for recovery of target substances from an aqueous bulk, referred to as cloud point extraction (CPE), is presented in **Figure 2.9** [4]:

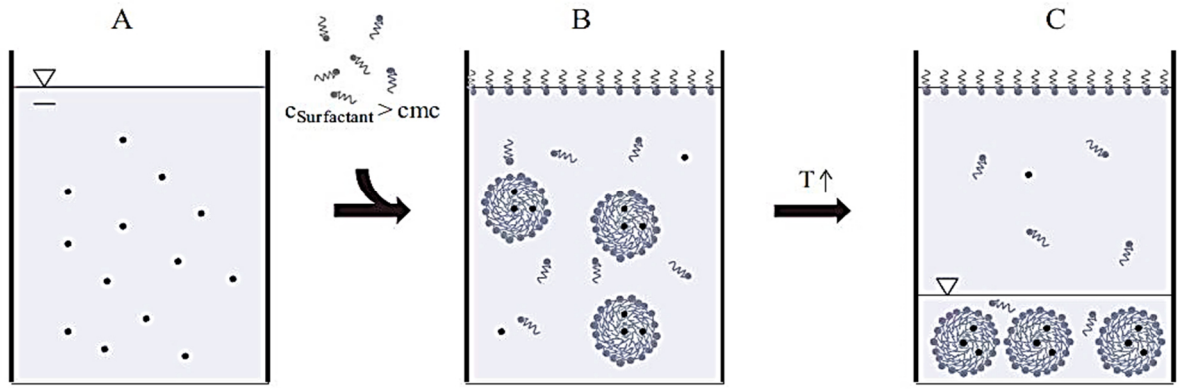

Figure 2.9: Scheme of the cloud point extraction with nonionic surfactants [43].

The feedstock for the CPE may be any solution that contains predominantly water, as well as dissolved organic compounds (**Figure 2.9** A). Further, by addition of nonionic surfactant at a concentration above the cmc, micelles occur in the aqueous media. Thus, the dissolved hydrophobic solutes are solubilized in the micelle cores (**Figure 2.9** B). By elevating the temperature of the solution, the macroscopic phase separation takes place as described previously (**Figure 2.9** C). Consequently, the micellar phase is rich in surfactant and hydrophobic solutes, leaving only low concentrations of both components in the aqueous phase [4]. The uneven distribution of the solute makes possible the separation of organic components from diluted bulks by CPE.

The general principles of the CPE are thereby analogous to a conventional liquid-liquid extraction, except that the solvent is completely miscible with the feed solution below CPT [39]. Additionally, the density difference between the micellar and the aqueous phase should be high enough to allow a proper phase separation [13].

Some nonionic surfactant solutions possess CPT similar to the ambient temperature [4]. In additions, some amphiphiles are known for their low toxicity [44]. Therefore, the cloud point system represents a suitable media for biotransformation. Moreover, it can be used to remove sensitive compounds due to the mild temperature. The basic knowledge regarding such in situ product removal techniques is presented in the next chapter.

2.6 IN SITU EXTRACTION

The in situ product removal (ISPR) is a technique, which allows the immediate separation of a product from the producing cell. Hence, the goal of the approach is to obtain the target substance as it formed directly from the cultivation media. The separation of the product is conducted by introducing an immiscible second phase or by an indirect removal via evaporation or permeation [45].

The ISPR is beneficial in two ways. Firstly, the short accumulation time of the target product in the cultivation broth leads to lower product loses due to cross-interactions with the cells and their environment. Secondly, the number of steps for the preparation of the biomaterial for the product separation as well as less the downstream steps are reduced [45–47]. The in situ approach can also lead to the minimization of the energy costs. For instance, the in situ removal of acetone, butanol, and ethanol via solvent extraction from the cultivation medium can result in lower energy input in comparison with adsorption or stripping with N_2 [48].

ISPR operations such as extraction with organic solvents, supercritical CO_2 or aqueous two-phase systems, adsorption, pervaporation or filtration can be applied in a batch or continuous mode [45]. An essential criterion for a suitable separation is the type of contact between the cell culture and the product separation phase. The contact can be direct by introducing a second immiscible liquid phase or an adsorbent. However, if the solvent or solid adsorbent has an inhibitory effect on the cells, indirect contact is applied [5,45,49]. Despite the toxicity aspect, the direct contact mode does not require any additional costs for membrane operations or energy input for evaporation [50].

The direct in situ extraction of solutes from biological feedstock was of particular interest for this work. Therefore, the indirect ISPR methods are not discussed further.

Two types of configurations are applicable for the in situ extraction from whole cells feedstocks. The direct contact can take place within the reactor (**Figure 2.10** a) or in an external loop (**Figure 2.10** b) [5].

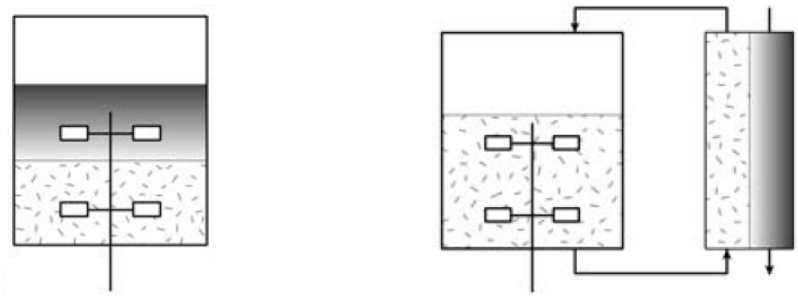

(a) (b)

Figure 2.10: ISPR configurations with direct contact: (a) internal removal, (b) external removal (adapted from [5]).

The internal contact is beneficial due to the simple tank design. However, the latter can lead to high solids accumulation or long-term exposition toxicity. The medium is circulated externally for specific product separation to minimize the adverse effect of the long-term exposition. Hence, the cultivation and the separation can be operated continuously [45]. The development and realization of the direct in situ extraction in both settings were studied in this thesis.

The design of an in situ extraction in one of the shown configurations is similar to the conventional extraction (see chapter 2.3) since the apparatus can be tanks or continuous contactors. The requirements concerning the solvent in the conventional extraction are valid for the in situ process as well. Hence, a favorable partitioning of the target product and the present substrate, a stable phase separation and an easy recovery of the solvent are crucial for a successful implementation.

However, the effect of the cells in the feedstock has to be taken into account. The presence of cells can lead to the stabilization of the emulsion and thus hinder the phase separation [51]. Furthermore, in case of growing cells, the solvent has to be biocompatible with the culture. Therefore, the chemical and phase toxicity has to be given attention. Additionally, growing cells support less harsh environments and cannot tolerate severe stirring. Moreover, when bypassing a living culture (**Figure 2.10** b), the cell demand for nutrition or oxygen has to be accounted [5,46,52].

By the diverse applications of the ISPR with whole cells, the target compound may be intracellular (in the cell) or extracellular (distributed in the broth). The two

utilized mechanisms for transport of the solute from the cell to the extract are the excretion of the product (exudates) and the partial cell wall permeabilization (**Figure 2.11**). However, the extreme permeabilization of the membrane leads to cell rupture. Thus, cell fragments become accessible for the solvent as well [53].

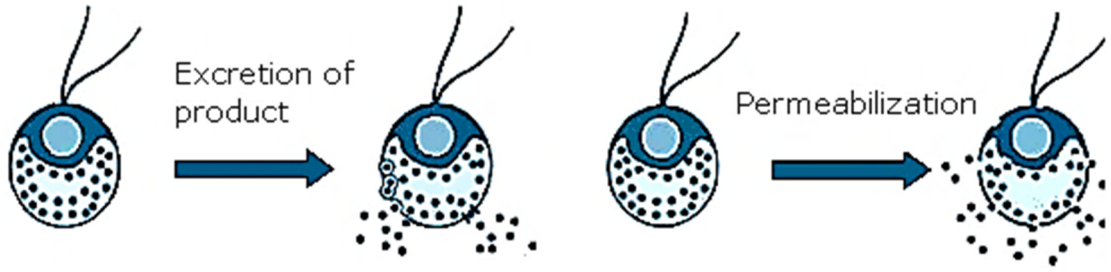

Figure 2.11: Schematic illustration of product excretion and cell wall permeabilization (adapted from [53]).

Due to the diversity on solvents, liquid-liquid extraction operations are applied for the ISPR of low- and high-molecular-weight solutes. In particular, organic solvents are suitable for separation of hydrophilic as well as hydrophobic species, with low and high volatility. Additionally, the aqueous biphasic systems can be applied with sensitive solutes with complex molecular structure, such as enzymes. The in situ extraction is compatible with yeast and bacteria but also with plant cells [5,45].

The utilization of the aqueous two-phase systems based on non-ionic surfactants offers an in situ extraction media for accumulating sensitive biomaterials [13]. Significant attention to this technique was given in this work. In order to present the suitability of the ISPR using nonionic surfactant systems, studies on the in situ extraction from plant whole cell culture (green microalgae) as well as from fruit juice (pineapple) were part of this work. Therefore, the corresponding composition and properties of the studied feedstocks are summarized in chapters 2.7 and 2.8.

2.7 VALUABLE COMPOUNDS IN GREEN MICROALGAE

Algae are a very diverse group of organisms that contain valuable compounds, such as polar and non-polar lipids; pigments and sterols; starch, alginates and other complex polysaccharides; amino acids and secondary metabolites [54]. Microalgae are a group of microscopic phototrophic algae, which are a promising source of plant products. For instance, the microalgal neutral lipids with a lower degree of unsaturation are applicable in the biodiesel production. Furthermore, some species accumulate omega-3 fatty acids as well as plant proteins and thus can provide a high-value food supplement [55,56]. The growing interest for natural colorants also draws the attention to carotenoids such as astaxanthin, lutein, β-carotene, chlorophyll a and b, and phycocyanin, commonly found in the microalgae cells [57,58]. Carotenoids, as well as phenolic and cinnamic acid derivatives, are natural antioxidants present in the green microalgae [59,60]. This diversity of valuable compounds leads to applications of the algal biomass as fertilizer or in the human and animal nutrition. Besides, isolated products of microalgal origin are ingredients in cosmetics, natural dyes, and antioxidants in food, or active compounds in pharmaceuticals supporting human eye-health [58,61].

To generate these valuable compounds, microalgae can be cultivated in aqueous media using sunlight, carbon dioxide, and salts. Standard culture systems use open-air pounds. The type of systems, according to the mixing, can be circular stirring reactors or paddle wheel raceway pounds. However, these cultivation solutions possess limited gas transfer, complicated scalability and no temperature and species control due to the direct contact with the environment [62]. As an alternative, closed photobioreactors are introduced to make the cultivation less influenced by local climate. At the controlled environment of a tubular or flat-panel reactor (stable temperature, mixing with a controlled gas flow), the photosynthetic efficiency is increased, and thus a higher cell mass is reachable [55,63]. The green microalgae applied in this work were cultivated in a bubble column or in an outdoor flat-panel photobioreactor system (see chapter 4.4).

The strain *Acutodesmus obliquus* (*A. obl.*) was cultivated for the experiments in this work. These green microalgae are regarded to as "equivalent to laboratory rats for limnology" since they serve as a standard for comparison to different

species [64,65]. The microalgae's physiological appearance is depicted in Figure 2.12.

Figure 2.12: *Acutodesmus obliquus* microalgae cells [micrograph: algaebase]

The cells of *A. obl.* are elliptical or spindle-shaped and have an average size of 10 µm. Usually, four, six or sixteen cells are combined to form a cell colony [66]. The applied microalgae are known to possess highly resistant cell walls, which makes the species stable at shear stress and in the presence of organic solvents [65,67]. The robustness of the algae can be derived from the trilaminar cell wall containing sporopollenin-like polymers and ketocarotenoids. These compounds are insoluble and resistant to organic solvents and thus relate to the pronounced stability of the cell wall [68,69]. Furthermore, *A. obl.* cells can grow in freshwater at temperatures from 15 to 45 °C, which makes them suitable for cultivation in the region of North Germany [63,70].

The green microalgae *A. obl.* can accumulate hydrophobic molecules in their cells. For instance, up to 45 % total lipids per gram biomass can be reached at nitrogen limitation. The fatty acid composition, in this case, differs according to the nutrition media. The palmitic acid (16:0) remains the most abundant in the *A.obl*. fatty acid pattern (38 % from total yield). The second most often-occurring fatty acid is the stearic acid (18:0). Sometimes instead of 18:0, vaccenic (18:1) and the linoleic (18:2) acids are accumulated [64,71]. Pigments such as neoxanthin, loroxanthin, violaxanthin, lutein, and chlorophyll b are found in cultures of the studied microalgae strain. The pigment composition is also highly influenced by the cultivation conditions and culture age [65].

The isolation of these hydrophobic compounds from algae biomass has always been a challenge due to the high energy costs of the algae harvest and the robustness of the cells [54]. Kleinegris et al. presented an alternative to the

methods, utilizing the cell-harvest, in the means of in situ extraction with a biocompatible solvent (dodecane) [53]. In their studies, a simultaneous cultivation in the solvent-free phase and an accumulation of hydrophobic products in the dodecane phase was possible. However, the authors experienced a drawback of the system due to the observed phase toxicity and the formation of a stable emulsion. An alternative approach for the in situ extraction of hydrophobic microalgae products could be the application of surfactant-based aqueous two-phase systems [9]. Hence, the application of nonionic surfactants with green microalgae was studied in this thesis.

Fruit and vegetable materials also contain unsaturated oils, natural pigments, antioxidants, and vitamins. The majority of those compounds are hydrophobic and highly sensitive to heat and organic solvents. That makes the mild conditions in the cloud pint system attractive for the isolation of plant biomaterials. A more in-depth look at the composition of the relevant fruits for this work is given in the next chapter.

2.8 VALUABLE COMPOUNDS IN FRUITS

Fruits and fruit juices are an essential part of human nutrition. The peel of various citrus fruits contains fine essential oils, which are applied in food or cosmetic. The essential oil is a concentrate of lipophilic terpenes that can be volatile and give the oil the specific aroma. Plants also produce fatty oils containing hydrophobic triglycerides. There are also flavoring materials whose attractiveness is regarded to the alkaloids, polyphenols or antioxidants. Furthermore, fruits and vegetables are rich in natural pigments. These natural colorants can be used in food, drugs, and cosmetics as an alternative to often undesirable synthetic dyes [72]. Annually, the industry, as well as the private households, produce a vast amount of fruit waste that is disposed at landfills. Furthermore, the food-processing industry generates high volumes of aqueous wastes, including fruit residues and discarded items, stillage and other residues from wineries, distilleries, and breweries. Most of these liquids are diluted suspensions with a low amount of dissolved materials. All these fruit waste are attractive as a feedstock for reusable materials and valuable chemicals as pigments, polyphenols, antioxidants, and flavoring compounds [73].

Pineapple, for instance, is one of the most popular non-citrus fruits grown in the tropical and subtropical regions. The production of canned pineapple generates waists including fruit, juice and shell fiber, which still contain valuable compounds. Pineapple is a vital source of the enzyme bromelain which is applied in food, medicine and cosmetics [74]. Pigments such as β-carotene and β-cryptoxanthin are responsible for the light yellow color of pineapple [75]. Besides that, the fruit is also rich in phenolic compounds (flavonoids, phenolic acids, and other polyphenolic compounds). The most present non-flavonoid phenolic substances in pineapple juice are p-hydroxybenzoic acid, p-coumaroylquinic acid, caffeic acid, ferulic acid, p-coumaric acid, sinapic acid and syringic aldehyde [76,77]. Different types of plant material preparation (drying, size reduction) and separation steps (steam destination, solvent extraction, cold pressing) can be applied to isolate valuable substances in fruit oils or concentrates. However, these conditions can affect the stability of the concentrate: extreme pH, exposure to light, the presence of enzymes or high temperature [72,78]. For instance, elevated temperature affects the fruit matrix by leaching of soluble compounds from the surface layer,

partial inactivation of enzymes due to denaturation of protein, and oxidation affecting flavor, color, and aroma. The antioxidant activity is also decreasing at a higher temperature since polyphenols and pigments are prone to degradation [61].

Green production processes are developed to keep the valuables in the fruit feedstock. The latter contribute to the reuse of the waste and minimize the impact on the environment [73]. Accordingly, the enzyme bromelain can be obtained from pineapple peels by salt-induced phase separation in an aqueous system of polyethylene glycol. This application is an example of a green process since it does not utilize any organic solvents [79]. Furthermore, bromelain can be recovered from the pineapple stem residue using aqueous micellar two-phase systems with ionic liquid as co-surfactants. In this case, the hydrophilic enzyme accumulates in the surfactant-poor phase of the Triton X-114 micellar system. The remaining hydrophobic compounds were separated in the surfactant-rich phase [80].Hence, the extraction with nonionic surfactants is also attractive for the direct separation of hydrophobic compounds (e.g., pigments, polyphenols, oils, antioxidants) out of pineapple feedstocks. Therefore, the in situ separation of antioxidants and pigments from pineapple juice using nonionic surfactants was investigated in this work (see 6.4.1).

Finally, as described in chapters 2.7 and 2.8., the sensitive compounds in diluted plant cultures or in fruit juices, can be mildly separated using ISPR based on nonionic surfactants. In order to develop this process from the laboratory to the pilot scale, the state of the art concerning similar applications is essential. Hence, a review of different surfactant-based two-phase systems and their phase behavior, application and scalability are presented in the following chapter.

3 STATE OF THE ART

This chapter presents an overview of different extraction processes utilizing nonionic surfactants. The focus is given to essential aspects for the development of separations with amphiphiles. Hence, the phase behavior of surfactants in water is summarized. Attention is given to the phenomena in these aqueous mixtures that are significant for the separation process. Further, the different applications of surfactant-based aqueous two-phase systems for extraction or as mild biotransformation media are described. Those include examples for laboratory studies but also for large-scale operations are highlighted. Further, the regeneration of surfactant from organic compounds is revised due to its relevance for the process design. Based on this literature overview, the significant knowledge gaps are emphasized. Ultimately, the objectives of this thesis are derived in accordance with the knowledge gaps.

3.1 NONIONIC SURFACTANTS AND THEIR BEHAVIOR IN AQUEOUS SOLUTION

Amphiphilic molecules are termed surfactants (or surface-active agents) corresponding to their ability to arrange on interfaces. Schwarz and Reid described their property and the resulting reduction of the interfacial tension as the main reason for their industrial application. Moreover, the addition of surface-active material would lead to increased solubility of oil in aqueous media and wetting of hydrophobic surfaces. According to the authors, the correct implementation of the amphiphilic compound depends on its chemical composition and solubility [81].

Nonionic surfactants are a diverse class of surfactants with polar but uncharged head group. They are commercially available from different manufacturers that often provide similar products under different trade names. Hence, it is essential to introduce a universal classification so that the nonionic surfactant is applied correctly. Griffin was the first to introduce the hydrophilic-lipophilic balance as a parameter for surfactant classification. The author proposed an empirical calculation of the HLB as a function of the hydrophobic and the hydrophilic part of the molecule. The resulting values were between 3.5 and 18, whereby amphiphiles were divided in w/o emulsifiers, wetting agents, o/w emulsifiers, detergents, and solubilizers. More importantly, the HLB of homologs was a linear function of the

molar weight [29]. Later on, Davis correlated the HLB-value with the coalescence kinetics. Thus, the surfactants were distinguished as o/w emulsifiers if an oil droplet settled faster from the aqueous to the oil phase than vice versa. Those experiments were correlated to the Bancroft rule. The latter stated that the phase in which the stabilizing agent is more soluble was the continuous phase of the emulsion. Hence, based on experiments and solubility, it was possible to calculate HLB values in a universal way [82]. After that, Schott correlated the HLB-value of different nonionic surfactants with the corresponding octanol/water partition coefficient (K_{ow}). That made the selection of a suitable surfactant possible using standard solubility data such as K_{ow} [83]. According to those studies, several surfactants were selected based on their HLB-values for the investigations in this work.

The phase behavior of mixtures containing such nonionic surfactants and water are distinguished with the formation of dynamic aggregates, temperature-induced separation, and transitions to liquid-crystalline phases. Molecules of nonionic surfactants arrange into micelles when added to an aqueous solution above their critical micelle concentration (cmc). Hait and Moulik reported a linear correlation between the logarithmic cmc and the lnHLB of surfactants within the homolog Tween (polysorbates), Brij (PEG-monoether) and Triton (octylphenol ethoxylates) series. That was due to the proportionality of the HLB to the fraction of hydrophobic groups in the monomer. Hence, the cmc decreased with increasing length of the hydrophobic moiety for a fixed hydrophilic group. The cmc of nonionic surfactants decreased with lower hydrophilic content in the molecule [84]. That observation was in good agreement with Wolszczak and Miller, who also stated a linear correlation between the cmc values and the number of ethylene oxide units in Triton X surfactants [27].

Such aqueous surfactant solutions can undergo a temperature-induced clouding followed by a phase separation into a coexisting surfactant-rich (micellar) phase and a surfactant-lean aqueous phase. The temperature, at which the phases separate, is referred to as cloud point temperature (CPT). Nandin et al. found that CPT, as well as the cmc, are functions of the chemical composition of the monomer. According to their results, the higher the cmc, the higher was the clouding temperature [85].

The composition of the coexisting phases above the clouding temperature depends on the surfactant concentration and the temperature. Lang and Morgan extensively described the phase behavior of the primary alcohol ethoxylate $C_{10}E_4$ in water among the temperature range between 0 - 90 °C and ambient pressure. An aqueous solution of the surfactant above its cmc coexisted with the hexagonal liquid crystalline phase up to 20 °C. At higher temperatures up to 65 °C, the cloud point separation was represented by a miscibility gap between surfactant-lean aqueous phase and a surfactant-rich phase. Further heating above 65 °C lead to a two-phase region of the diluted phase (approx. cmc) and the inversed micelle phase with surfactant concentration greater 78 wt%. A small gap between 45 and 64 °C was characteristic for a mixture of a normal micellar phase and a lamellar liquid crystal phase [86]. Lavergne et al. reported similar kind of phase behavior for another class of amphiphiles, namely isosorbide-based nonionic surfactants. In their study, a succession of three liquid crystalline phases – hexagonal, bicontinuous cubic and lamellar occurred when increasing the surfactant concentration at 10 °C. The hexagonal phase was the most viscous one. At 23.5°C, the authors stated the lowest LCST. However, the two-phase region where the cloud point separation took place was too narrow for precise characterization [34]. A phase behavior including separation above a cloud point temperature was reported for polyoxyethylene trisiloxane surfactants by He et al. Typical colloidal phases such as diluted micellar phase; surfactant-rich inversed micelle phase, as well as lamellar and hexagonal liquid crystalline phases, were observed for the silicone-based amphiphiles. The authors also described the influence of the polyoxyethylene head group. The larger the hydrophilic moiety, the broader was the region of the normal micellar solution [87].

The phase behavior of siloxane-based surfactant solutions is strongly influenced by nonelectrolyte additives as well. Soni et al. reported that nonelectrolyte co-solvents such as alcohols and glycols influence the cmc and the CPT value of silicone surfactants in water. The tested short-chain alkyl alcohols (<C=3) increased the solubility of the surfactant in water and thus lead to higher cmc values. Due to that effect, the CPT of 1 wt% surfactant solutions were elevated by the addition of those alcohols. On the other hand, higher less water-soluble alcohols favored the micelle-formation and the clouding [88]. Accordingly, additives also shift the transition temperature and concentration for the liquid

crystalline phases. Iwanaga and Kunieda reported a pronounced effect of polyols on the hexagonal liquid crystalline structure of silicone-surfactants. It was shown, that ethylene glycol, polyethylene glycol and 1,3-butane diol increase the formation temperature of the hexagonal phase. The authors explained that phenomenon according to the salting-in effect of the studied additives [89].

Salts influence the properties of surfactant solutions as well. Ritter et al. studied the influence of inorganic salts on the phase equilibrium of Triton X-114 aqueous two-phase systems. The authors reported a salting-out effect among the cations following the series $\mathrm{Na^+} > K^+ > \mathrm{NH_4^+} > \mathrm{Li^+}$. A more pronounced effect was observed among the anions, whereby the salting-out effect decreased in the order $\mathrm{HPO_4^{2-}} \approx \mathrm{SO_4^{2-}} > \mathrm{Cl^-} > \mathrm{Br^-} > \mathrm{I^-}$. Moreover, all salts distributed predominantly in the aqueous phase and thus a higher surfactant concentration was induced in the micellar phase [90]. The sugar sucrose also decreased the cloud point temperature of Triton X-114 according to Koshy et al. [38]. Apparently, it was possible to adjust a known phase behavior of a surfactant aqueous solution by adding suitable co-solvents or inorganic substances. The effect of the additives should to be considered when developing a formulation with multiple components including surfactants. A study on the phase behavior of a surfactant/water mixture is essential since liquid crystalline phases can be formed or a phase separation is possible even at low temperatures and concentrations. These phenomena can affect the process set-up or the product formulation.

The behavior of surfactants in aqueous solutions as well as the ability of the micelles to solubilize hydrophobic compounds is the reason for the diverse applications of the amphiphiles. For instance, according to Somasundaran et al., nonionic surfactants are applied for creating a wide variety of dispersed systems, such as suspensions and emulsions in personal care products [91]. Moreover, Kralova and Sjörblom stated the ability of surfactants to control the stability and rheology of emulsions in food products [92]. Mulligan et al. gave attention to the enhanced remediation of contaminated soil by addition of biosurfactants to water. In that case, it was possible to increase the solubility of the impurities by solubilizing them into the micelles [93]. Moreover, a nonionic surfactant was applied to distribute hydrophobic sulfur compounds from bunker-C oil in a suspension for biodesulfurization of the target compounds [94]. Such

biotransformations were improved by solubilization of the hydrophobic precursors into the micelles. Hence, the probability for the hydrophobic compounds to penetrate the cell membrane was increased [95].

Furthermore, the coexistence of two macroscopic phases above the clouding temperature gives rise to the application of biphasic surfactant solutions as extraction media. Hinze and Pramauro presented an extensive overview of commercial nonionic surfactants regarding their cmc and CPT. Their summary provided useful data of cloud point temperatures exhibited in more than 50 different micellar solutions. Moreover, the authors summarized specific applications of surfactant-based biphasic systems for separation and purification of metal chelates, biomaterials, and organic compounds [4]. That review, together with the later work of Quina and Hinze [96], demonstrated the potential of the cloud point extraction as an environmentally benign alternative separation approach. Surfactant-mediated extraction processes were given significant attention in this work as well. Therefore, the next chapter presents an overview of different applications of the cloud point extraction.

3.2 CLOUD POINT EXTRACTION

3.2.1 BATCH APPLICATIONS

The simplest way to implement an extraction is the batch process. The most studies on the cloud point extraction from diluted aqueous solutions describe a single-stage operation. For instance, Frankewich and Hinze estimated the extraction efficiency of a phenol and 4-chlorophenol separation using homologs among the primary alcohol ethoxylates. The cloud point temperature of different 1 wt% surfactant solutions was determined, and the cloud point extraction of both solutes was conducted at temperature 15 °C higher as the CPT. An enhanced extraction efficiency (max. 85 %) was reached with more hydrophobic surfactants. However, the enrichment of solute decreased with the surfactant hydrophobicity. That was due to the higher volume of the micellar phase and the corresponding lower solute concentration. Additionally, the authors demonstrated that a sufficient equilibration time is needed to reach the maximal efficiency [97]. Kimchuwanit et al. also reported an increase of the surfactant concentration in the micellar phase

with elevated extraction temperature of the system Igepal CA-620 (octylphenol ethoxylate)/water. The temperature and the initial surfactant concentration also influenced the distribution of trichloroethylene. A more favorable partition coefficient was reached at increased temperature and higher initial surfactant concentration [42]. In a later study, Haga et al. implemented the micellar two-phase system based on the primary alcohol ethoxylate $C_{10}E_4$ for the extraction of clavulanic acid as a model solute. Contrary to their expectations, the authors observed a decrease of the partition coefficient at elevated temperature. That was regarded to the lower solubility of the hydrophilic solute in the more hydrophobic surfactant-rich phase. Hence, an addition of a cationic surfactant lead to charged mixed micelles and thus enhanced the separation performance [98]. The cloud point extraction with nonionic surfactants is influenced by different process conditions as described above. Therefore, Silva et al. proposed an experimental design using response surface methodology as a suitable tool for determination of the optimal temperature and Triton X-114 initial concentration for the extraction of phenol. That approach minimized the number of experiments, and the optimal conditions were reported at 38 °C and surfactant fraction of 13 wt% Triton X-114 [99].

The applicability of nonionic surfactants for the accumulation of trace solutes in aqueous media makes the technique attractive for analytical purposes. Bezzera et al. described cloud point extraction as a tool for separation of trace metals from different matrices. By building a complex between the cation and a hydrophobic ligand, it was possible to concentrate the metal in the surfactant-rich phase. The extraction was coupled with a spectrophotometric determination, an atomic absorption analysis, ICP optical emission spectrometry, or ICP - mass spectrometry. The technique was beneficial due to the low cost, high enrichment factors and environmental safety [100]. Cloud point extraction prior chromatography or electrophoresis was applied for analysis of organic compounds as well. According to Carabias-Martinez and Ballesteros-Gomez, the technique was suitable for the isolation of proteins, phenolic derivatives, dyes, or vitamins since it ensured mild separation and high yield. Additionally, in both contributions, a sufficient compatibility of the surfactants with the spectrophotometric detection was reported because most surfactants were not active in UV-Vis [101,102]. Analytical protocols combining cloud point extraction with HPLC analysis were also

applied for solid sample materials from plants. Tan et al. used the technique to determine pesticides [103]. Ameur et al. reported a method for separation of the alkaloid tetrahydrocannabinol from cannabis resin [104]. The CPE is a suitable pre-treatment in food constituent analysis, such as the pesticide, antibiotic and mycotoxin residue determination. In addition, the separation technique can also be applied as a mild media for the extraction of bioactives from food processing byproducts or from medicinal plants or for protein isolation [106].

Hydrophobic membrane proteins were separated from hydrophilic ones by inducing phase separation in a mixture of sucrose, NaCl, Tris-HCl buffer and 0.5 – 1 wt% Triton X-114 [105]. Fricke also described a method to concentrate the membrane protein from different solubilizates containing a surfactant. The separation of the system was triggered by temperatures between 0- 20 °C and in case of high CPT - the addition of NaCl or $(NH)_4SO_4$ [107]. Arnold and Linke revised the utilization of different surfactants including Triton, Tween and Brij families, for the isolation of membrane proteins. According to the authors, the approach for a cloud point extraction of membrane protein was as follows: addition of a surfactant, salt, and buffer; temperature increase; phase separation by centrifugation; collecting of the micellar phase. Aspects concerning the stability of the proteins in high surfactant or salt concentration, the possible high viscosity of the extract as well as the stripping of protein from the micellar phase were essential for the choice of surfactant system and the conditions [108].

Schneider et al. reported the isolation of other hydrophobic compounds, namely triterpenes oleanolic acid and ursolic acid, from sage leaves using cloud point extraction. The performance of the aqueous solutions of the nonionic surfactants Genapol X-080, Brij 56 and Tween 65 and that of alcohols, heptane, hexane, and toluene as solvents were compared. The concentration factor of the hydrophobic acids in the micellar phase was of the same magnitude as in the alcohol with the longest chain. The authors recommended the use of nonionic surfactants as solvents due to their lower toxicity, biodegradability and higher purity [109]. Leite et al successfully presented the accumulation of chlorophylls from spinach leaves using nonionic surfactants. The authors reached the highest separation efficiency when utilizing amphiphiles with HLB from 10 to 13 (such as Triton X-114). In addition, a morphological change in the leaf structure was observed when the pigments were extracted with a surfactant solution [112]. Chen et al. also

suggested micelle-mediated extraction as an alternative to organic solvents for the separation of lipids and proteins from wet microalgal biomass. Prior the extraction, an algae slurry (96 % moisture) underwent a lysis using heating and enzymes to release the hydrophobic intracellular products. A subsequent cloud point separation yielded 88 % of the lipids and 62 % of the proteins, which was more efficient in comparison to traditional hexane extraction [110].

Further, cloud point separations were implemented for extraction of phenolic compounds or pigments. Gortzi et al. reported a recovery of such natural antioxidants from olive mill wastewater using Genapol-X-080 and NaCl as CPT reducing agent. In order to determine the selectivity of different compounds, experiments with individual polyphenols were conducted. The results revealed up to 100 % yield of tocopherols and recoveries between 20 and 98 % of the phenolic gallic acid, protocatechuic acid, oleuropein, coumaric acid, rutin, epicatechin, luteolin, syringic acid, and tyrosol. The efficiency of the separation was enhanced by increasing the surfactant concertation. However, the hydrophilicity of some solutes was more pronounced and resulted in the barrier of the yield. The trend from the model separation was analogous to the CPE from genuine olive mill wastewater, which reached a total phenolic recovery of 89 % [111]. A later study by that group revealed the suitability of Tween 20 and Tween 80 biphasic systems for the separation of phenolic compounds and carotenoids from the red-flesh orange juice. A total carotenoid recovery of 79% was obtained after a two-step cross flow extraction with Tween 80 [7]. That after, the same research group reported the successful application of Genapol X-080 for the removal of polyphenols from wine sludge. By applying four v/v% surfactant at 55 °C and pH of 3.5 for 30 minutes, 75.8 % of the target compounds were accumulated in the micellar extract [113]. The latter three applications also maintained the high antioxidant activity of the extract according to the DPPH method (see chapter 5.11.4). El Abbassi et al. confirmed the applicability of the cloud point extraction of phenolic compounds from olive mill wastewater with Triton X-100 cloud point system, registering a 67 % recovery of the total phenolic compounds in a single-stage extraction [114]. Sharma et al. tested the suitability of different nonionic surfactant systems for the cloud point extraction of phenolic compounds from apple, sweet lemon, and mango juice. According to their results, the Brij-58 biphasic media yielded a higher amount of gallic acid equivalents in comparison to

ethanol or acetone. Additionally, the antioxidant activity of that extract was the highest among all test systems [115].

A successful cloud point separation with commercially available nonionic surfactants was reported for the isolation of anthraquinones from the roots of chees fruit tree [116], of isoflavones from soybean flour [117], of mangostins from eggplants [118], of flavonoids and alkaloids from rattlepods [119], and of phorbol esters from pressed seeds of physic nut [120]. All those contributions illustrated the suitability of a surfactant solution to isolate and concentrate hydrophobic species from biomaterials. Ultimately, the cloud point extraction was indicated as a universal technique to recover high-value components from plants or food production wastes.

Nonionic surfactants are also applied in biotechnological suspensions. Singh et al. revised the role of amphiphiles considering the production of extracellular and intracellular compounds. The addition of a surfactant to the cultivation media above the cmc increased the enzyme secretion and the recovery of hydrophobic proteins due to permeabilization or lysis of the cell envelope [121]. Furthermore, Ulloa et al. took advantage of the dual influence of Tween and Triton surfactants for lysis of the cell wall and subsequent extraction of antioxidants from microalgae cells [122]. However, the mild process conditions that can be maintained in a cloud point system can also provide a media for biocompatible in situ product removal.

The works of Zhilong Wang focused mainly on biotransformation in cloud point media. Initially, Wang et al. introduced novel transformation of cholesterol to androst-1,4-diene-3,17-dione and androst-4-ene-3,17-dione in the cloud point two-phase system of Triton X-100 and Triton X-114. The surfactants were chosen based on their biocompatibility with the applied microorganisms. A conversion yield of 93% was achieved [123]. Later on, the group presented a similar resting cell biotransformation of phytosterol to androsta-diene-dione in a cloud point system of Triton surfactants. The authors emphasized the benefits of biotransformation of hydrophobic compounds in the tested environment in the spare of sterile conditions, prolonged biocatalyst activity of the cells and increased product yield [124]. In the following work, the same research group reported a successful in situ extraction of a polar product during a microbial transformation of benzaldehyde with baker’s yeast. The process took place in a biphasic system

of Triton X-100 in the presence of PEG 2000 at a moderate temperature, which ensured a mild media for the cells [125].

An extractive catalysis of penicillin G to into phenylacetic acid and 6-amino penicillanic acid, initially reported in the biphasic system of the surfactant $C_{10}E_4$ [126], was studied extensively by Wang et al. Immobilized penicillin acylase distributed in the aqueous phase of a biphasic Tergitol TMN-3 surfactant system together with the educt. Subsequently, the hydrophobic phenylacetic acid partitioned in the micellar phase, and thus the inhibition by the latter on the enzyme was omitted [127]. That advantage of the cloud point system allowed the authors to implement a fed-batch hydrolysis of penicillin G [6]. Aiming further intensification, Wang et al. presented a discrete countercurrent experiment with the same reaction. Hence, the product yield was increased from 50 to 65% in comparison with the batch process [128].

Wang et al. developed a submerged cultivation of *Monascus* fungus in the micellar system. They aimed to enhance the production of intracellular pigments by an in situ separation of the target hydrophobic dye in the micelles. To that purpose, the cells were grown in a cultivation media containing the biocompatible Triton X-100. Subsequently, the cell debris was collected from the broth. Finally, a phase separation above the CPT led to the accumulation of the hydrophobic pigment in the micellar phase. [129]. The authors also demonstrated a fed-batch operation mode, at which the concentration of the pigments was further elevated [44]. In the following study, the same group reported the effect of different nonionic surfactants on the export rate of intracellular pigments. Despite that the organism grew well in the presence of all tested amphiphiles, extracellular pigments were found only in the in the Triton X-100, Triton X-114, and Tween 80 solutions. That was due to the substantial solubilization capacity of the micelles, which eliminated the pigments degradation by preventing direct contact with bacteria [130]. That approach illustrated a successful indirect in situ product removal in a micellar system.

A similar in situ product separation in Triton X-114 cloud point systems was applied for purification of green fluorescent proteins from endotoxins [131]. Moreover, Pan et al. implemented a surfactant-based aqueous two-phase system for the extractive biodecolorization of triphenylmethane dyes with *Aeromonas hydrophila*

[8]. However, the described contributions presented a two-stage process of biotransformation in a homogeneous surfactant solution, followed by cell harvest, and a final cloud point separation in the cell-free supernatant. Such approach is beneficial due to the enhanced product yield. However, the cell harvest before the extraction is cost-and energy-intensive.

In order to develop a simultaneous cultivation and separation of hydrophobic compounds from green microalgae cultures, Glembin et al. suggested the cloud point system as a suitable two-phase medium. Therefore, the authors studied the biocompatibility of different algae strains with the surfactants Triton X-114, Tergitol 15-S-7 and Tergitol TMN 6. Their results illustrated the importance of the biocompatibility for the design of in situ separations with direct contact since only the *Scenedesmus obliquus* microalgae tolerated surfactant addition at the required concentration (1 wt%). Based on their findings, a batch CPE of fatty acids from the culture with the surfactant Triton X-114 was conducted in laboratory and pilot scale. After the phase separation, the cells accumulated in the aqueous phase and could be further cultivated. The products (myristic and palmitic acid) were accumulated in the micellar phase [132]. Chávez-Castilla and Aguilar also reported an integrated process for the direct in situ recovery of prodigiosin (red pigment) from a culture of *Serratia marcescens* bacteria. Triton X-114 (2 v/v%) was mixed in the cultivation media and did not inhibit the cell growth. The pigment production was maintained higher than in the surfactant-free control. Moreover, the authors presented a continuous application in a chemostat. Two heated separators were connected to the outlet, where the micellar phase collected. Finally, the extract was treated with a mixture of 80% cyclohexane and 20% dichloromethane to recover prodigiosin from the surfactant. The pigment was finally purified via preparative HPLC. That direct extractive fermentation in the biocompatible media resulted in 81% recovery of prodigiosin in batch mode and 88% in the chemostat [133].

The essential part in the design of direct in situ product separation is the compatibility of the solvent with the cells. Hence, when developing a cloud point system for that purpose, the toxicity of the surfactant has to be evaluated. The influence of commercial amphiphilic materials on green algae is studied to determine the environmental impact on marine systems. Those data can be adapted for the screening of surfactants as solvents. For instance, Ernst et al.

reported that nonionic alcohol ethoxylates decreased the growth of the microorganisms with increasing hydrophilicity [134]. However, Lewis reviewed numerous studies on the chronic toxicity of detergents towards microalgae and concluded that the species sensitivity varied as much as the effect of different surfactants on the same microorganism. Nevertheless, cationic detergents had a more pronounced toxicity compared to nonionic and anionic ones [135]. Lüring reported such culture-specific phenomenon. The author described a colony-inducing effect of an anionic surfactant on the microalgae *Scenedesmus obliquus*, which could be related to the robustness of the cells in stress conditions [136]. Masakorala et al. measured the impact of Triton X-100 on marine microalgae by monitoring the photosynthetic activity. Relative toxicities were attributed to the affinity of the surfactant for the algal surface and the tendency to disrupt cell membrane (lysis) [137]. Dias et al. reported morphological and physiological changes in eukaryotic protists *Tetrahymena pyriformis* in the presence of Triton X-100. The amphiphiles did not aggressively denature cell proteins. However, cytoskeletal alterations and changes of the cell membrane were observed in micrographs [138]. Those effects can be correlated to the affinity of surfactants to adsorb on cell walls and membranes. According to Shafer and Bukovac, Triton X-100 sorption of tomato fruit cuticles changed with the surfactant concentration whereby the equilibrium state was reached faster at levels below the cmc [139]. The adsorption behavior of Triton X-100 and Tween 80 on a *Pseudomonas aeruginosa* strain was characterized by short equilibration time and fitted the Freundlich equation well. Higher temperature weakened the adsorption on the cell surface [140].

The surface effect of the amphiphiles has to be taken into account when conducting a CPE from cells or plant materials. Such examples were extensively described in the literature overview presented in this work. However, the regarded contributions were predominantly batch mode applications. Thus, the product recoveries were limited by the single stage efficiency. Nevertheless, cloud point extraction is possible in a continuous set-up as well. That can make cloud point extraction an attractive method for industrial applications. Hence, examples of the continuous utilization of the CPE are summarized in the next chapter.

3.2.2 CONTINUOUS APPLICATIONS

Yao and Yang suggested the ultrasonic-assisted cloud point extraction of polycyclic aromatic hydrocarbons using Tergitol TMN-6. Ultrasonication accelerated the phase separation. Hence, a mixing vessel coupled to a sonicated heated unit provided the needed conditions for the continuous cloud point extraction [141]. Further, Benkhedja et al. reported an efficient cross-flow cloud point extraction of phenol, benzyl alcohol and 1-phenylethanol in a mixer-settler device. The nonionic surfactants Tergitol 15-S-7 and Simulsol NW342 were utilized for the removal o the pollutants using a six-stage apparatus [142]. In a series of publications, Trakultamupatam et al. investigated the removal of aromatic compounds such as benzene, toluene, and ethylbenzene from wastewater using a nonionic surfactant from the Triton family. In their first study, the authors investigated the extraction method under batch conditions. A partition ratio of up to 160 for ethylbenzene was reached at 50°C. Furthermore, a yield of almost 95% was achieved under the same conditions [39]. Later on, the cloud point extraction of the same components was studied under continuous experimental conditions in a rotating disc contactor. The influence of disc rotation speed, feed-to-solvent ratio, temperature, and added NaCl were investigated in particular. The group found that the concentration of solute in the extract increased with elevated agitator speed and feed-to-solvent ratio, due to the enhanced mass transfer. Additionally, the concentration of solute in the extract increased with higher temperatures and NaCl concentrations due to the improved phase separation. While the partition ratio for ethylbenze was increased to 193, the surfactant partition ratio decreased drastically from 1300 in the batch experiments to 156 in the continuous set-up as result of entrainment of the surfactant with the aqueous raffinate phase [143,144].

The group of Smirnova et al. studied the continuous countercurrent CPE of syringic acid, vanillin, phenol, and salicylic acid from aqueous solutions with Triton X-114 in a stirred column. The authors found that increasing the extraction temperature helped to reduce the loss of surfactant through the raffinate phase and increased the enrichment factor. Additionally, up to eight theoretical stages per meter column were reached by the extraction of vanillin [43]. In a subsequent work, mixed surfactant systems containing Triton X-114 and ionic surfactants (CTAB and SDS) were applied for a continuous extraction of ionized solutes in the same contactor unit. Hence, the recovery of dissociated vanillin reached up to 64% at

60°C [145]. The same research group presented a continuous extraction method in a stirred column, which utilized a Tergitol 15-S-7 cloud point system. The addition of sugar promoted a more stable separation in the otherwise unstable biphasic system. The authors implemented a stationary countercurrent process resulting in an enrichment factor of 19.94 for the model solute vanillin [146].

Fischer et al. presented a novel continuous approach for protein purification of using functionalized magnetic nanoparticles in aqueous micellar two-phase systems. Proteins bound to a magnetic sorbent in a bulk surfactant solution below the transition temperature of Emulgin ES. Subsequently, the solution was heated above the CPT and was separated in a specially designed magnetic vessel [147]. However, that contribution is preferably specific for protein separation. There were no further studies on continuous in situ product removal from cell cultures in a surfactant solution. Therefore, one of the particular aims of the present thesis is to contribute to this knowledge gap.

3.3 CLOUD POINT EXTRACTION IN LARGER SCALE

The state of the art of cloud point extraction in large-scale is revised in this chapter. As for the continuous operations, the utilization of surfactants for industrial or pilot separations is mainly specific.

Minuth et al. reported a successful separation of surfactant-based aqueous two-phase systems for the direct extraction of the membrane-bound enzyme CHO from a cultivation medium containing *Nocardia rhodochrous.* The extraction was examined on a pilot scale (up to 21 kg). The authors applied the nonionic $C_{12\text{-}18}E_5$. Despite the low density differences between the two liquid phases (0.003–0.005 $g \cdot cm^3$), the low interfacial tensions (5–10 $\mu N \cdot m^{-1}$) and the complex rheological behavior of the micellar phase, the authors conducted continuous operations in disc stack centrifuge or a nozzle-discharged disc stack centrifuge. Since both machines were not equipped with a thermostat, the feed was preheated. The solids were collected with the dilute phase, and the extract was a clear top phase. The biomass led to a fluctuation in the surfactant concentration in the extract. The authors reported a yield >87% combined with a 4-fold product accumulation, which was comparable to the batch scale experiments, yielding more than 90% of the enzyme [148].

Kepka et al. utilized a cloud point phase separation in pilot scale for the purification of enzymes from a polymer aqueous solution. That operation was conducted with a $C_{12-18}E_5$ surfactant in a disk-stack centrifugal separator as well. A 71 % recovery of the enzyme in the surfactant-lean phase was achieved. Additionally, the influence of the original bacterial culture, which produced the enzyme, was omitted by a biomass harvest step [149].

Furthermore, the batch surfactant-mediated extraction of proteins from a culture broth was implemented in a total volume of 0.010 l and in 1200 l. The authors reported yields up to 61 % in the Agrimul NRE 1205 coacervate phase. The separation was conducted in a biomass-free supernatant [150]. In contrast, Glembin et al. performed a batch micelle-mediated extraction of fatty acid from a microalgal culture without previously separating the biomass. Using the surfactant Triton X-114, the authors implemented the process in laboratory and outdoor plant. In both cases, an accumulation of palmitic acid was registered in the micellar phase [9].
The variety of separation processes utilizing cloud point systems in laboratory and small technical scale is contradictory to the vast amount of larger scale applications. That can be due to the laborious methods to regenerate the surfactant from the solutes in the extract phase. Nevertheless, several studies are describing the stripping of the amphiphilic material from the target compounds. Some examples are summarized in the next chapter.

3.4 SEPARATION OF ORGANIC COMPOUNDS FROM SURFACTANT SOLUTIONS

Despite the diverse applications of the cloud point extraction as an alternative to the extraction with organic solvents, the technique faces a significant drawback in the form of the problematic and often cost-intensive surfactant recovery and solute purification. According to the review by Cheng and Sabatini, the principals for the separation of organic compounds from the surfactant solution were the solute's interphase mass transfer, surfactant micelle removal, and manipulation of the phase behavior. Volatile solutes were recovered from the micellar media by air or vacuum stripping and by pervaporation. In case of hydrophobic substances with high boiling point, an organic liquid was applied instead of an airflow. Another possibility was to deplete the micelles, and thus the solute could separate in a

second phase. That was possible by cooling below the Kraft temperature or by extreme dilution below the cmc. Lastly, the authors emphasized the shifting of the emulsion type as possible stripping techniques [151].

Further, Dhamole et al. conducted a cloud point extraction of butanol with a block-copolymer with a high boiling point. Hence, it was possible to separate the surfactant from the solute using distillation [152]. Lebeuf et al. recovered piperine by evaporating the volatile surfactant, which was used for the CPE [153]. Topf et al. utilized pervaporation as a unit operation for the removal of the more volatile toluene from the micellar phase of the Triton X-114 cloud point systems [154]. In order to recover the extracted saponins from the micellar phase, containing Triton X-100 and phenolics, Ribeiro et al. used the Amberlite FPX-66 selective resin. Hence, it was possible to adsorb the undesired compounds due to the high selectivity of the resins [155].

Furthermore, there are reported techniques for the separation of solutes with a high boiling point or thermal sensitivity as well. Liang et al. introduced a novel system based on polyethylene glycol and a hydrophilic surfactant to allow stripping of organic compounds from the aqueous surfactant solution with Winsor I microemulsion extraction. The authors successfully regenerated compounds such as phenol, p-nitrophenol and, 1-naphthol phenol [156]. An extraction with Winsor I emulsion was used to separate tannic acid from the micellar phase rich in Triton X-114. The authors selected diethyl ether as excess oil phase and thus separated tannic acid and the surfactant from each other. Subsequently, the solute-free coacervate was successfully applied for a second extraction [157].

It can be concluded, that the recovery of the surfactant and the products from the micellar phase is mainly depending on the structure and properties of the compounds. Hence, that step has to be given attention and has to be designed when developing a separation process using surfactant-based two-phase systems. Therefore, the search for alternative separation techniques or for strategies to omit the surfactant recovery is still challenging.

3.5 DERIVATION OF THE OBJECTIVES BASED ON THE STATE OF THE ART

This work aims to fulfill the described knowledge gaps by developing a cloud point extraction for the in situ product recovery of biomaterials in technical and pilot scale.

According to the state of the art, the mild clouding temperature, the high water content and the good biocompatibility, define surfactant-based biphasic systems as suitable for the direct in situ product removal from authentic plant-based feedstocks and cell cultures. Hence, the primary goal of this work is the design of an in situ cloud point extraction, which:

- is stable in a batch and in a continuous mode;
- requires no expensive and laborious extract processing;
- is compatible with sensitive biomaterials and living cells;
- is applicable in technical and pilot scale.

Firstly, the application of a well-established cloud point system as a potential media for an ISPR has to be studied. The two-phase system based on the surfactant Triton X-114, widely applied for CPE, has a potential for a mild extraction media for sensitive materials. To realize the extraction using Triton X-114, a combination of process settings (including the capacity, feed-to-solvent ratio, and agitation speed) should be derived in such a way that it can fulfill the requirements for a stable and fast direct in situ product removal from sensitive biomaterials.

Furthermore, the range of surfactants, suitable for the continuous cloud point extraction needs to be extended. Therefore, a screening among the nonionic surfactants, commonly applied in food and cosmetics is required. Their phase behavior and physical properties should be beneficial for a fast and stable separation. If all needed requirements are fulfilled, a batch and continuous ISPR from biological mixtures can be performed in the selected aqueous two-phase systems.

The continuous separation of dissolved biomaterials in cloud point systems should be further straightened by less laborious process concepts. On the one hand, possibilities to increase the solute concentration in the surfactant-rich phase have

to be developed. In this work, attention is given to the recirculation of the surfactant-rich phase during the multistage process and to the nanofiltration for the retention of the loaded micelles from the bulk water in the extract. On the other hand, a more beneficial extraction scheme utilizing permitted surfactants (such as food-grade and cosmetic-grade amphiphiles) could decrease the cost and effort for the solvent stripping. Therefore, the CPE using permitted amphiphiles has to be evaluated regarding the need of surfactant regeneration.

The compatibility of the cloud point extraction using the chosen amphiphiles with genuine suspensions should be demonstrated as well. Therefore, the efficiency of the CPE from different media (such as fruit juices and aqueous cell cultures) has to be performed in batch and in continuous mode. This can illustrate the potential of the CPE for the batch and continuous ISPR, which represent the fast and effective extraction of natural products in combination with low negative effect on the feedstock.

The stable, fast CPE in a surfactant-based cloud point system, which can be performed directly from the genuine feedstock and does not involve laborious extract processing, should give the base for a process design in a pilot application. A transfer of the set-up and the conditions should be performed so that the continuous cloud point extraction from an authentic feedstock can finally be run in a pilot-sized installation.

Ultimately, this work should illustrate the milestones on the way to a pilot scale application of the nonionic surfactants for the isolation of natural products directly from their original source. Thus, the potential behind the CPE as a technique for the laboratory, technical and pilot scale can be demonstrated.

4 MATERIALS AND EQUIPMENT

The following chapter summarizes the materials and the equipment used for the experiments presented in this thesis.

4.1 SURFACTANTS

All commercial nonionic surfactants applied in this thesis are summarized in **Table 4.1**. Information concerning the chemical class, CAS-number, molar weight and HLB-value for all studied surfactants is available as well.

The nonionic surfactant Triton X-114 was applied for the micellar extraction process as a model surfactant with well-known behavior and properties. The amphiphile is characterized with a cmc of 0.22 mM [27] and a CPT at 1 wt% in aqueous solution at 23 °C [90].

All other surfactants were tested for their suitability for the cloud point extraction. Subsequently, Triton X-114, Silwet L7230, and ROKAnol NL5 were applied at the batch and the continuous experiments. All surfactants were used as received.

Table 4.1: Studied surfactants with corresponding supplier, chemical class, CAS-number, molar weight (Mn) and HLB-value

surfactant	supplier	chemical class	CAS-No.	M_n [g/mol]	HLB
Triton X-114	AppliChem	t-Octylphenoxy polyoxyethylene ethers	9036-19-5	537	12.4
Polysorbate 20	Aquanova	Polysorbates	9005-64-5	523	16.7
Polysorbate 80	Aquanova	Polysorbates	9005-65-6	1228	15.0
Silwet L7002	Momentive	Silicone-Polyether Block copolymer, pendant graft structure	67762-87-2	8000	7.6
Silwet L7230	Momentive	Silicone-Polyether Block copolymer, pendant graft structure	68937-55-3	29,000	6.3
Synperonic 91/5	Croda	Ethoxylated alcohols	68439-46-3	380	12.5
Synperonic PE L/31	Croda	EO/PO block copolymers	9003-11-6	1100	4.5
Synperonic PE L/62	Croda	EO/PO block copolymers	9003-11-6	2900	6.3
Brij C2	Croda	Ethoxylated alcohols	9004-95-9	330	5.3
Brij C10	Croda	Ethoxylated alcohols	9004-95-9	683	12.9
Brij O2	Croda	Ethoxylated alcohols	9004-98-2	357	5.0
ROKAnol DB7W	PCC Exol	Ethoxylated alcohols	68131-39-5	530	12.0
ROKAnol L5P5	PCC Exol	Ethoxylated , propoxylated alcohols	68439-51-0	730	6.0
ROKAnol NL5	PCC Exol	Ethoxylated alcohols	160901-09-7	380	11.6
ROKAnol NL8P4	PCC Exol	Ethoxylated , propoxylated alcohols	154518-36-2	740	9.5
Sympatens-ALM/040	KOLB	Ethoxylated alcohols	68439-50-9	360	9.5
Imbetin-AG/124S/060	KOLB	Ethoxylated alcohols	68439-50-9	460	11.5

4.2 ADDITIONAL CHEMICALS

All additional chemicals used for the different experimental set-ups are listed in Table 4.2. Information concerning their supplier and use in this thesis are presented as well.

Table 4.2: Table of additional chemicals

compound	supplier	use
(2E)-3-phenylprop-2-enoic acid	Sigma-Aldrich	model solute
Manna LIN M	Manna	microalgae nutrition
Foamdoctor F2768	Pennwhite	antifoam agent
Sodium hydroxide	Carl Roth	pH regulation of algae culture
Acetonitrile	Sigma-Aldrich	HPLC analysis
Gallic acid hydrate	Riedel-de Haën	phenolic compounds analysis
2,2-diphenyl-1-picrylhydrazyl	Sigma-Aldrich	antioxidant capacity analysis
Methanol	Sigma-Aldrich	antioxidant capacity analysis
3,5-dinitrosalicylic acid	Sigma-Aldrich	sugar analysis
D-Glucose, monohydrate	Merck	sugar analysis

All chemicals used for the external analysis are not listed.

Trans-cinnamic acid ((2E)-3-phenylprop-2-enoic acid, Sigma Aldrich) was chosen as a model substance for all extraction experiments. This solute has a water solubility of 0.29 $g \cdot l^{-1}$ at 30 °C and a logarithmic partition coefficient between octanol and water equal to 2.19 [158]. Therefore, cinnamic acid (CA) represents a suitable hydrophobic model solute for the process design of the cloud point extraction of biomaterials with nonionic surfactants.

The molecular structure of CA is illustrated in Figure 4.1:

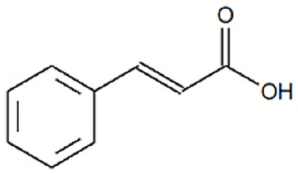

Figure 4.1: Structure of trans-cinnamic acid [159]

4.3 MICROALGAE

The green microalgae strain *Acutodesmus obliquus* (no. 10169) was obtained from the "Microalgae and Zygnematophyceae Collection Hamburg" (MZCH-SVCK). Please note that the investigated microalgae were previously denoted as *Scenedesmus obliquus.* The culture was cultivated according to Hindersin et al. [63].

Nutrition for the cultivation medium was provided with Manna Lin M fertilizer (Manna, Ammerbruch, Germany). The exact composition of the fertilizer is given in appendix A1. Additionally, excessive foaming due to pressurized air agitation was prevented with Foamdoctor F2768 antifoam agent (Pennwhite, United Kingdom).

The cultivation of the microalgae culture in technical scale was carried out in a cylindrical tank with a volume of 0.02 m^3. Illumination was provided by five strips of red LED-lamps, which were evenly distributed over the outer surface of the tank. The obtained inoculum was added to the bubble column containing 20 liters culture media consisting of tap water, 0.5 g·l-1 fertilizer "Manna LIN M," and 100 ppm defoamer. A constant carbon dioxide flow was provided as a carbon source for growth. A flow of pressurized air (ca. 4 vol %) aerated and stirred the microalgae.

The pH value was controlled by a pH regulator from Aqua Medic GmbH (Bissendorf, Germany), which was connected to a peristaltic pump of the type ISMATEC SA (IDEX Health & Science GmbH (Wertheim, Germany).The pH was set constant at 7.25 by carbon dioxide addition and was further controlled by addition of sodium hydroxide solution (2 M). The temperature of the cultivation tank varied depending on the environment temperature with an average value of 28.2 ± 0.5 °C.

The amount of algae cells in the culture was determined by measuring the optical density (OD) at 750 nm with a photometer Evolution 300 UV-Vis from "ThermoScientific." The cell density (CD) was calculated according to **Equation 4-1**.

$$CD\ [g \cdot l^{-1}] = 0.187 \cdot OD_{750}$$

Equation 4-1: Calculation of the cell density CD

CD: cell density; OD_{750}: optical density at 750 nm

Microalgae culture from the bubble column was applied for the continuous cloud point extraction with Triton X-114 at technical scale (see chapter 5.8). The photosynthetic activity of that feedstock was monitored during the biocompatibility test with ROKAnol NL5 and Triton X-114 as well (see chapter 5.11.8).

4.4 BIQ ALGAE HOUSE

Studies in corporation with the Strategic Science Consult Ltd. (SSC) were performed at the BIQ Algae House. The BIQ Algae House is a building with family apartments on four floors that has a house facade equipped with outdoor flat-panel photobioreactors. Green microalgae are cultivated in each of the photobioreactors. Due to the dark green color of the microalgae, heat is accumulated by the liquid and is applied as a heat source for the household needs. The BIQ Algae House in Wilhelmsburg, Hamburg is illustrated in **Figure 4.2**.

Figure 4.2: BIQ Algae House [160]

Two sides from the facade are covered with 129 modules with a total light contact area equal to 200 m^2. The total culture volume equals 3800 liters. The reactors are coupled as a cascade in four separated lines for each floor. The culture is circulated through the cascade by a pumping. A schematic representation of the lines coupling is depicted in appendix A2.

A central system is applied for the monitoring and control of the circulation intensity, heat exchange, and pH. When a sufficient cell density is reached, the biomass is harvested directly from the cascade or via a flotation machine. Thus, a suspension (further referred to as "flotate") with higher microalgal concentration can be obtained. The culture from the BIQ Algae House was applied for the cloud point extraction in pilot scale. Furthermore, the suspension was utilized for batch separations with nonionic surfactants.

4.5 PINEAPPLE JUICE

In order to obtain natural juice, without additives or conservatives, fresh pineapples were purchased from the local market. For the preparation of pineapple juice, small pieces of the fruit, excluding its shell, were cut and introduced to the juice extractor Greenis Slow Juicer F-9007. Afterwards, the juice was frozen at -20°C. A day before every experimental trial, the juice was placed to defrost at 5°C. Before the extraction process, the juice was vacuum filter with the filter from Rotilabo®-Rundfilterns, type 13A (Cellulose, φ 70 mm). The filtrated juice was applied as a feed for the cloud point extraction with ROKAnol NL5.

4.6 TECHNICAL SCALE EXTRACTION EQUIPMENT

The following **Figure 4.3** shows the double jacket borosilicate glass column, which was used for the continuous extraction of technical scale.

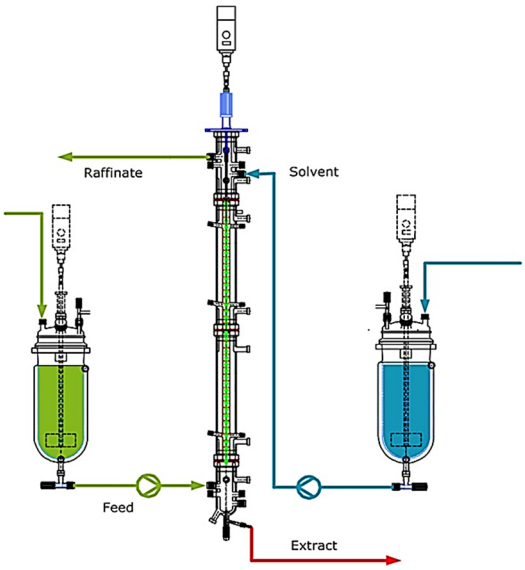

Figure 4.3: Schematic representation of the technical scale extraction set-up (exemplary representation for a lighter continuous phase and heavier disperse phase)

Both the feed and the solvent vessels were double jacket borosilicate glass tanks, each capable of holding a volume of 0.01 m³. The feed tank was connected to a gear pump of the type ISMATEC ISM901, which was coupled to the inlet of the column. The solvent tank was connected to a peristaltic pump of the type ISMATEC MCP, which was coupled to the inlet of the column. Both pumps were provided by IDEX Health & Science GmbH.

Each tank was stirred by an agitator of the type RZR 2021, which was provided by Heidolph Instruments GmbH. An agitator of the type RZR 2101, which was provided by Heidolph Instruments GmbH, was installed in the column. It had a framework with 32 stirred cells, each consisting of a *Rushton turbine* type impeller with six stirring blades. The impeller had a diameter of 18 mm and a width of 3.6 mm. Symmetrically arranged stator discs between each stirring cell restricted axial backmixing. This type of continuous differential contactor is also known as *Oldshue-Rushton column* (see chapter 2.3).

The extraction column, the feed tank, and the solvent tank were tempered by a water bath of the type Eco RE 630, which was provided by LAUDA Dr. R. Wobser

GmbH. The temperature in the column was indicated by three temperature sensors, with one at the head, one at the bottom, and one in the middle of the mixing zone. The sensors were connected to a measurement device of the type Almemo 2590, which was provided by Ahlborn Mess- und Regelungstechnik GmbH.

The column's geometric parameter are listed in Table 4.3.

Table 4.3: Geometric parameters of the laboratory scale extraction column

dimension	size	unit
total volumetric capacity	0.002	m^3
inner diameter (mixing zone)	0.030	m
inner diameter (head and bottom)	0.052	m
active volume	0.00183	m^3
active height	1.64	m
volume mixing zone	0.00086	m^3
settler volume/total volume	53	%
free cross-section	0.0003	m^2
free cross-section/total cross-section	41	%

4.7 PILOT SCALE EXTRACTION PLANT

A pilot-scale plant for the continuous cloud point extraction of microalgae was realized at the BIQ Algae House (see chapter 4.4). A P&I scheme of the plant is presented in Figure 6.29. The corresponding control diagram is given in appendix A 3. All valve positions for the different modes of operation are summarized in appendix A 4

In the center of the set-up, a differential contactor unit was designed similarly to the technical scale equipment. The double jacket borosilicate glass column from NORMAG Labor- und Prozesstechnik GmbH is illustrated in appendix A 5.

As in technical scale, column and agitator were set up as *Oldshue -Rushton column*, with 20 stirred cells, each containing a *Rushton turbine* type impeller with six stirring blades, an impeller diameter of 72 mm, and an impeller width of 14.4 mm. An agitator of the type NRW 80/35/M/ATEX was applied for the stirring and was provided by NORMAG Labor- und Prozesstechnik GmbH. The geometric

parameters describing the extraction column in pilot scale are presented in **Table 4.4**

Table 4.4: Geometric parameters of the pilot scale extraction column

dimension	size	unit
total volumetric capacity	0.0351	m^3
inner diameter (mixing zone)	0.150	m
active volume	0.0325	m^3
active height	1.93	m
volume mixing zone	0.0261	m^3
settler volume/total volume	19.5	%
Free cross section	0.0071	m^2
free cross-section/total cross-section	40	%

The temperature in the mixing zone was maintained with a thermostat D20 KP from LAUDA. Additional heating with a heating band from NORMAG Labor- und Prozesstechnik GmbH was installed at the settler, where the two phases separated from each other. The temperature in the column was measured with a sensor PT100, type GA2510 from LABOM Ltd. The temperature in the top part of the column was monitored with a Ni-Cr-Ni-thermoelement.

The solvent was introduced at the column's inlet via a gear pump of the type ISMATEC ISM901. The weigh of the solvent tank was measured with a scale SF 890 from Nohlex GmbH.

The feed flow could be set manually with a needle valve. The flow was measured via a magnetic inductive flow meter VMZ 081 from Sika GmbH.

Additionally, a system to set the feed automatically using a control valve 565 coupled with a positioner 1434 µPos from GEMÜ GmbH was developed in collaboration with "Electrical Engineering Research Workshop" at the Technical University of Hamburg. The feed indication and control system was calibrated using a calibrator MetraHIT 18C from Gossen Metrawatt GmbH.

The flow meter, the positioner, and the temperature sensor were coupled through a Programmable Logic Controller (PLC), Simatic S7 from Siemens. The interconnections, as well as the specification of the PLC, are presented in appendix A6. The parameters used by the PLC were motored and controlled via an HMI-

Module from Siemens. Its interface is presented in appendix A 7. The PLC was connected to a desktop computer using a communication interface with the software Snap7. All data logs were automatically saved on the hard drive of the computer. Moreover, by connecting the LabView 2013 software (NI National Instruments), it was possible to calibrate and control the control valve. A representation of the LabView screen is presented in appendix A 8.

5 METHODS

The practices for the presented experiments are summarized in this chapter. Additionally, the applied analytical procedures and tests are presented below.

5.1 SURFACTANT SCREENING

In order to identify suitable surfactants for the cloud point extraction from dissolved biomaterials, an initial screening was conducted among the surfactants in Table 4.1 (excluding Triton X-114, which has a well-established application for cloud point extraction). To that purpose, the CPT and the phase separation of the amphiphiles were investigated as described by Ingram et al. [43]. Aqueous solutions with surfactant concentrations of 1 wt% were prepared. The samples were cooled down to 5 °C and subsequently heated by 0.5 °C·min^{-1} in a water bath (Lauda D20 KP). The cloud point temperature was defined as the temperature at which the sample turned turbid. All experiments were performed in triplicates.

Additionally, in order to evaluate the phase separation, the phase behavior was recorded visually one hour after the observed clouding. Depending on whether two clear phases were present, the surfactants were classified as follows: fast separation and clear interfacial border; slow separation and unstable interfacial border, and bad separation and no clear interfacial border. Only the surfactants with a fast and stable phase separation and defined cloud point temperature were further investigated for their application in the cloud point extraction.

5.2 LIQUID-LIQUID EQUILIBRIUM DETERMINATION

The liquid-liquid equilibria (LLE) of the surfactant/water systems were measured to determine the conditions for the cloud point extraction with the suitable surfactants. In accordance, the temperature and the initial surfactant concentration in the feed were set for all extraction experiments. Please note, that the equilibrium data for the Triton X-114/water system was obtained from Ingram et al. [43]. However, for the aqueous systems of Silwet L7230, Synperonic 91/5, and ROKAnol NL5, there were no data available.

Hence, their LLE was obtained by measuring several points of the coexistence curve. To this purpose, the clouding temperatures of aqueous solutions with different surfactant concentrations were visually determined. This method was further referred to as "cloud point method."

Additionally, several points of each coexistence curve were validated gravimetrically. Hence, samples, contacting a specific surfactant fraction, were mixed thoroughly by shaking and were tempered in a water bath at the separation temperature for 48 hours. Subsequently, the samples were centrifuged at 2500 rpm for 45 minutes at the chosen temperature. Afterwards, the micellar and the aqueous phase were separated, and 10 mL of each surfactant-rich phase were given in pre-dried and weighed sample tubes. Finally, the samples were kept in an oven at 80 °C until their weight remained constant. By assuming that only the water amount was transpired, the surfactant concentration was determined by weight difference according to **Equation 5-1**:

$$w_{M,S} = \left(\frac{m_{S,M}}{m_{total,M}}\right) * 100\% = \left(\frac{m_2 - m_{empty}}{m_1 - m_{empty}}\right) * 100\%$$

Equation 5-1: Gravimetric method: Calculation of the surfactant concentration within the micellar phase $w_{M,S}$

$m_{S,M}$: Mass of surfactant in the micellar phase; $m_{total,M}$: Total mass of the micellar phase ; m_{empty}: Mass of the empty sample tube; m_1: Mass of the sample before drying; m_2: Mass of the sample after drying

This method is further denoted as "gravimetric method."

All points of the coexistence curves were determined in triplicates.

5.3 CLOUD POINT EXTRACTION OF THE MODEL SOLUTE CINNAMIC ACID

Batch experiments

The preliminary assessment, whether the selected surfactant-based aqueous two-phase systems are suitable for the separation of hydrophobic biomaterials, was conducted based on the partitioning of cinnamic acid. CA was chosen as a tracer, since it was of plant origin and its molecule distributed predominantly in oil phases (see chapter 4.2). Therefore, the partitioning of the model solute between the micellar and the aqueous phase was studied in single-stage CPE.

Samples containing 200 mg·l^{-1} CA and surfactant in initial concentrations of 1, 2, 3, 4 or 5 wt%, were prepared in triplicates. The homogenized samples were placed in a water bath for 24 h at the chosen temperature according to the LLE. Thus, samples containing Triton X-114 were tempered at 40 °C. The systems based on Silwet L-7230 were kept at 39°C. The mixtures of ROKAnol NL5 – at 45 °C. Subsequently, to ensure the settling of the phase equilibria, all vials were centrifuged at 2500 rpm over 40 minutes in a preheated centrifuge at the corresponding temperature. Finally, the CA concentration in each of the coexisting phases was analyzed using HPLC (see chapter 5.11.1). Hence, the partition coefficient (see chapter 2.2) of the model solute could be calculated as a ratio between the concentrations in the micellar and aqueous phase (**Equation 5-2**).

$$P_{CA} = \frac{c_{CA}^{M}}{c_{CA}^{A}}$$

Equation 5-2: Calculation of the partition coefficient of cinnamic acid (P_{CA}) in batch experiments

c_{CA}: concentration of the cinnamic acid in the micellar (M) or aqueous (A) phase

Furthermore, the yield of the batch extraction was calculated as the ratio between the CA mass in the micellar phase and the CA mass in the initial sample (**Equation 5-3**):

$$Y_{Batch} = \frac{c_{CA}^{M} \cdot V_M}{c_{CA}^{0} \cdot V_0}$$

Equation 5-3: Calculation of the yield of cinnamic acid (Y_{Batch}) in batch experiments

c_{CA}: concentration of the cinnamic acid in the micellar (M) phase or the feed(0); V: volume of the micellar phase (M) or the initial sample (0)

By calculating the partition coefficient and the single-stage extraction efficiency, it was possible to characterize the performance of the different nonionic amphiphiles. Moreover, in the case of the Triton X-114 two-phase system, it was possible to determine the loading of the micelles according to **Equation 5-4**:

$$Y_{Micelle} = \frac{n_{SysCA} \cdot n_{Agg}}{n_{SysSurf} - n_{cmc}}$$

Equation 5-4: Calculation of the micelle loading ($Y_{Micelle}$) in batch experiments

n_{sysCA}: amount of CA molecules in the system; n_{sysCA}: amount of surfactant molecules in the system; n_{Agg}: aggregation number = 220; n_{Agg}: aggregation number

Whereby, the aggregation number was assumed to be equal to 220 [161]. Additionally, n_{cmc}. was calculated by applying the cmc value for Triton –X 114. $n_{SysSurf}$ and n_{SysCA} were calculated using the concentrations of the surfactant and the tracer, and the volume of the micellar and aqueous phases. Since micelle formation starts only above the cmc, all surfactant molecules needed to maintain the cmc were excluded from the estimation [162].

Continuous experiments

Three surfactants, namely Triton X-114, Silwet L-7230 and ROKAnol NL5, were applied for the continuous cloud point extraction of cinnamic acid in technical scale. To that purpose, the set-up described in chapter 4.6 was applied. For all continuous experiments, CA solution in distilled water (approx. 200 mg·l^{-1}) was set as feed. The continuous extraction was carried out in countercurrent mode. The temperature at the column and the tanks was the same as the one during the batch experiments (Triton X-114 - 40 °C, Silwet L-7230 - 39°C, ROKAnol NL5 - 45 °C).

Firstly, Triton X-114 was utilized for the extraction of cinnamic acid in the stirred column. Each extraction experiment lasted 8 hours to ensure that the steady state was reached (around four hours) [43]. The solvent was introduced at the top of the column (heavy phase) via the peristaltic pump. An aqueous solution containing 20 wt% Triton X-114 was used as extracting agent. The concentration of the surfactant in the solvent flow was chosen in accordance with the tie-line at 40 °C (see LLE Triton X-114/water in appendix A 9, the mass fraction of Triton X-114 in the micellar phase= 0.20). The feed flow was introduced at the bottom of the column (light phase) by a gear pump. The calibration curves for both pumps are depicted in appendix A 10. The following parameters were varied according to the experimental design (see chapter 5.4): speed (n), feed-to-solvent ratio (v) and column capacity (b).

Subsequently, continuous cloud point extraction of cinnamic acid was conducted using Silwet L-7230 and ROKAnol NL5. The solvent was a surfactant solution, containing 20 wt% Silwet L-7230 or 15 wt% ROKAnol NL5. Those values corresponded to the surfactant mass fraction in the micellar phase at the chosen temperature. Further, in case of Silwet L-7230, the solvent represented the dense phase and was therefore pumped in at the top of the column, whereas the feed as a lighter phase entered the column at its bottom. In case of ROKAnol NL5, the procedure was vice versa. The duration of each continuous experiment was 5 or 7 hours for Silwet L-7230 and ROKAnol NL5, respectively. The extraction parameters temperature, agitation speed, feed flow, and solvent flow for the latter two systems are presented in **Table 5.1**.

Table 5.1: Parameters for the continuous cloud point extraction with Silwet L-7230 and ROKAnol NL-5

surfactant	temperature [°C]	feed flow [$l \cdot h^{-1}$]	solvent flow [$l \cdot h^{-1}$]	agitation speed [rpm]
Silwet L-7230	39	0.67	0.13	25
ROKAnol NL5	45	0.57	0.12	15

In addition, a recirculation of the collected extract was investigated for Triton X-114, Silwet L-7230 and ROKAnol NL5 at 40°C, 39°C, and 45 °C, respectively. Hence, several experiments with the surfactants were conducted, whereby after 150 minutes the solvent stream was switched from fresh solvent solution to the collected extract. The conditions for the continuous extraction were set as shown for Silwet L-7230 and ROKAnol NL5 in **Table 5.1**. The parameter combination for Silwet L-7230 was applied with Triton X-114. The solvent composition was set at 20 wt% surfactant amount in water, for the Silwet L-7230 and Triton X-114 experiments. The solvent for the ROKAnol NL-5 extraction contained 15 wt% surfactant in water.

During all experiments, samples were collected from the feed, raffinate and extract phases. Hence, profiles of the CA concentration in the raffinate and extract were used to evaluate the performance. Moreover, to compare the time profiles of the CA amount in the raffinate phase during different sets of experiments, the relative raffinate concentration (C_{rel}) was defined as shown in **Equation 5-5**:

$$c_{rel.} = \frac{c_{CA}^{R}}{c_{CA}^{F}}$$

Equation 5-5: Calculation of the relative raffinate concentration C_{rel}

c_{CA}^{R}: concentration of cinnamic acid in the raffinate; c_{CA}^{F}: Concentration of cinnamic acid in the feed

The experiments with Triton X-114 were evaluated using the cinnamic acid yield ($Y_{cont.}$) and productivity (F_{CA}) according to **Equation 2-14** and **Equation 2-15,** respectively.

The performance of the continuous extraction with Silwet L-7230 and with ROKAnol NL5 was assessed by the enrichment factor (T_{CA}) and the cinnamic acid yield ($Y_{cont.}$). Those were calculated according **Equation 2-13** and **Equation 2-14,** respectively. The number of theoretical stages (N_{theo}) was also calculated according **Equation 2-16** with **Equation 2-17.**

5.4 DESIGN OF EXPERIMENT: PARAMETER OPTIMIZATION PROCEDURE

The software "Stat-Ease Design-Expert Version 8" was used for the experimental design of the optimization for the continuous CPE of the tracer CA with the model surfactant Triton X-114. A response surface method was applied to reflect the chosen responses depending on the factor combinations. The responses were yield and productivity of cinnamic acid (**Equation 2-14** and **Equation 2-15**). The studied factor combinations consisted of column capacity, feed-to-solvent ratio and agitator speed.

Moreover, the continuous cloud point extraction of cinnamic acid was restricted by the surfactant concentration in the raffinate. A surfactant fraction higher than 0.2 wt% in the raffinate led to the accumulation of Triton X-114 in the raffinate. That resulted in a high loss of surfactant or accumulation of the amphiphile in the surfactant-lean stream. Thus, an additional separation of the surfactant from the raffinate could be needed. A maximal concentration limit of 0.2 wt% Triton X-114 in the raffinate was restricted to minimize the surfactant loss. The reaching of a surfactant concentration in the raffinate equal to 0.2 wt% was defined as "stress limit."

The influence of the agitation speed from 20 to 80 rpm on the Triton X-114 concentration in the raffinate was tested at capacities in the range of 1 – 2 $l \cdot h^{-1}$ at

a solvent-to-feed ratio equal to 6 and 10, respectively. The surfactant concentration in the raffinate was measured over 3.5 hours. The stress limit was reached in case 0.2 wt% were exceeded. All stress limit points were presented as a function of the capacity and the agitation speed. This plot represented the limiting operating conditions for the design of experiments.

The experimental design applied in this thesis is referred to as "Optimal Design." This design is developed for parameter intervals with irregular process space. After defining the factors and the parameter ranges for the system, the multilinear constraint of the stress limit points was introduced in the edges of the parameter area [163].

Multifactor constraints were given in Design-Expert in the form of **Equation 5-6**.

$$\beta_L \leq \beta_1 A + \beta_1 B \ldots \leq \beta_U$$

Equation 5-6: Multifactor constrain

β: lower (L) and upper (U) limit of the multilinear constraint; A, B: empiric constants

The provided constraint tool of the Design-Expert software was used to develop the multilinear constraint.

None of the experiments was permitted to lay outside of the valid operating conditions area. Hence, a precise investigation of the optimal operating conditions required the implemented final multilinear constraints to be lower than the possible stress limit point.

In general, the stability and accuracy of the experimental design were increased by choosing a design type with a high optimality. In this study, "Optimality IV" was chosen as a well-conditioned design type for modeling the cloud point extraction. Therefore, Design-Expert software required data of 20 distributed factor combinations and their corresponding responses. Ten data points were needed as model points to develop a stable model, five data points were needed for the lack of fit test, and the remaining five data points were replicates.

Initially, a fit summary was conducted in which the software fits a linear, two-factor interaction, quadratic, and cubic polynomials to the responses. To find the most suitable model, each fit was analyzed by a "Sequential Model Sum of Squares" regarding how increasing complexity contribute to the total model. Hence, a "Lack of Fit" test, "Predicted Residual Sum of Squares" (PRESS) and R-squared values were calculated to conclude which model had a stable and precise

estimation for an underlying system. Thus, a suitable model was chosen and further analyzed by analysis of variance (ANOVA) to confirm adequacy. Thereby each term of the model was evaluated. Finally, the form of the model was presented as an equation.

5.5 SHEAR RATE CALCULATION

The Metzner-Otto method was used to calculate the shear rate ($\dot{\gamma}$) in an agitated tank. The Metzner-Otto constant for a *Rushton turbine* type impeller is 12 [164]. By multiplying the Metzner-Otto constant with the agitation speed, the shear rate was obtained, as shown in **Equation 5-7**:

$$\dot{\gamma} = N * K_S$$

Equation 5-7: Calculation of the shear rate in an agitated tank $\dot{\gamma}$

N: Agitation speed; K_S: Metzner-Otto constant

5.6 SEPARATION OF TRITON X-114 FROM AQUEOUS MEDIA USING NANOFILTRATION

The separation of Triton X-114 from an aqueous solution using nanofiltration was performed in collaboration with the "Department of Chemical Engineering," University of Chemical Technology and Metallurgy, Sofia. The experiments were carried out in a Dead-end METcell using the membrane Microdyn-Nadir NP 030. The temperature was set at 20.1 °C. The feed was a 16.995 wt% Triton X-114 solution. The concentration of the surfactant in the permeate and the retentate was measured via UV- absorbance at 277 nm using the calibration curve in appendix A 11. The membrane performance was evaluated as described by Peshev et al. [165]. First, the permeate flux was obtained by measuring the volume permeating per unit filtration area and per unit time. After the instantaneous sampling from the retentate and the permeate, the Triton X-114 rejection was calculated according to **Equation 5-8**.

$$R_T = 1 - \frac{C_{Per.}}{C_{Ret.}}$$

Equation 5-8: Calculation of the rejection of Triton X-114 R_T

C: Triton X-114 concentration in permeate (Per.) and in retentate (Ret.)

5.7 CLOUD POINT EXTRACTION FROM PINEAPPLE JUICE

Pretreated pineapple juice, as described in chapter 2.8, was utilized as feed for the cloud point extraction of phenolic compounds using the surfactant ROKAnol NL5. The separation of those valuable compounds was performed as a single-stage process, similar to the batch extraction of the model solute cinnamic acid.
The extraction of pineapple juice was performed in 50 mL Falcon tubes that were filled with 50 g of a solution containing three wt% ROKAnol NL5 dissolved in the juice. After proper shaking, the tubes were let into the water bath (D20 KP) at 45 °C to promote the phase separation. When the two phases were completely separated, samples were collected from the micellar and aqueous phase.
The concentration of phenolic compounds (gallic acid equivalents) was determined via UV spectrometry (see 5.11.3). Additionally, the antioxidant capacity and the sugar amount were measured as described in the next chapter. The extraction efficiency was evaluated by calculating the yield of the phenolic compounds according to **Equation 5-3**.

5.8 CONTINUOUS CLOUD POINT EXTRACTION FROM MICROALGAE CULTURES IN TECHNICAL SCALE

Green microalgae was applied for the continuous cloud point extraction using the surfactant Triton X-114. The process set-up is presented in **Figure 5.1**.

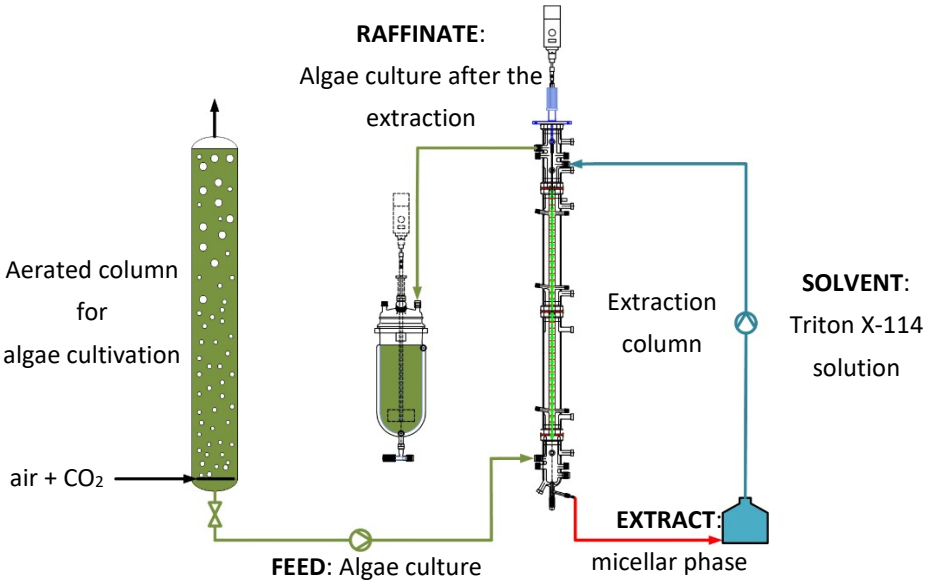

Figure 5.1: Set-up for the continuous extraction from green microalgae in technical scale.

Green microalgae culture of the strain *A. obl.* (see chapter 4.3) was utilized as feed. The extraction column and the additional instruments are described in chapter 4.6. The feed was introduced at the bottom and was subsequently collected as raffinate at the top of the column (green arrow). The solvent was a Triton X-114 solution, which was pumped in into the column head (blue arrow). The extract stream was the micellar phase that separated at the bottom of the contactor. The recirculation of the solvent was maintained by transferring the extract to the solvent vessel (red arrow).

The process parameters were set as summarized in **Table 5.2.**

Table 5.2: Parameters for the continuous cloud point extraction from microalgae culture using Triton X-114

Process parameter	value	unit
temperature	40.0	°C
agitation speed	40	rpm
column capacity	0.8	$L \cdot h^{-1}$
feed-solvent-ratio	5	-
feed flow rate	0.667	$L \cdot h^{-1}$
solvent flow rate	0.136	$L \cdot h^{-1}$
surfactant concentration in the solvent	20	wt%

The extraction duration was 24 hours, with the beginning of the recirculation after three hours. Samples were collected from the raffinate and extract streams and were analyzed for their Triton X-114 concentration via HPLC (see chapter 5.11.1). The cell debris was removed from the samples by a 0.2 µm syringe filter.

A qualitative investigation of the total mass of algae substances in the extract was made to characterize the continuous extraction of microalgae cultures. For this purpose, samples of the extract were collected at the end of the experiment. Subsequently, the surfactant concentration was measured by HPLC, and the total amount of solutes and surfactant was determined gravimetrically after by transpiring the water at 55 °C and atmospheric pressure. Thus, the total yield of algae products per unit feed was calculated as shown in **Equation 5-9**.

$$Y_{Algae} = \frac{(m_{Pr} \cdot \dot{S})}{(m_{Ex} \cdot \dot{F})}$$

Equation 5-9: Calculation of the yield of algae products Y_{Algae}

m: total amount of collected extract (Ex) and of extracted product (Pr); S: solvent flow; F: feed flow

The total yield of microalgal products was compared to the extraction of the model solute CA at the optimal process conditions.

Additionally, the photosynthetic activity (PA) of the algae cells in the raffinate was monitored as described in chapter 5.11.8.

The morphology of microalgae cells in the presence of Triton X-114 was investigated using scanning electron microscopy to identify the effect of the surfactant on the microalgae structure. To obtain samples, *A. obl.* was incubated with the surfactant for three hours (compared to 3.5 hours residence time in the column) at 40 °C. Algae cells were collected from the surfactant-lean phase and an untreated reference culture. Subsequently, samples were prepared according to Patzelt et al. [66], and scanning electron micrographs were taken with a Leo 525 SEM (Zeiss, Germany).
Finally, photosynthetic activity of the microalgae was evaluated in the presence of 1 wt% of the surfactants Silwet L-7230 and ROKAnol NL-5. The photosynthetic yield was measured according to the method in chapter 5.11.8.

5.9 REALIZATION OF THE CONTINUOUS CLOUD POINT EXTRACTION IN PILOT SCALE

5.9.1 DESIGN, CONSTRUCTION, AND COMMISSIONING

A plant for the continuous cloud point extraction from microalgae cultures was build at the site of the BIQ Algae House (see chapter 4.4). The column, the heating unit, piping, valves, sensors, and control units were installed according to the P&I scheme (see Figure 6.29). Hence, the extraction set-up, described in chapter 4.7 was completed.

The commissioning was conducted in four parts. Firstly, a stable and constant temperature profile along the height of the column was maintained. Secondly, the pressure of the feed streams (algae culture or tap water) was set at a constant value. Thirdly, the installed pump for the solvent was calibrated for the needed flow range. The corresponding calibration curve is presented in appendix A 12. Lastly, the indicators for the inlet flow and the temperature, as well as the control units for the feed were calibrated and tested for their stable performance. The calibration of the positioner and the control valve are presented in appendix A 13.

5.9.2 CALCULATION OF THE PROCESS PARAMETER

The continuous CPE in pilot scale was performed correspondingly to the experiments with microalgae in technical scale. In addition, a recirculation of the solvents was applied by the pilot scale flow scheme. After the successful commissioning, the process parameters were transferred from the technical to the pilot scale. Table 5.2 summarizes the initial conditions for the continuous cloud point extraction with Triton X-114 in technical scale, which were subjected to the scale-up (see chapter 5.3).

The process parameters for the pilot scale extraction with Triton X-114 were calculated according to the approach in chapter 2.4. Hence, the agitation speed was transferred using the specific energy input of the mixer. The laboratory and pilot scale agitation speeds yielding the same power per unit volume were determined iteratively. The Reynolds Number was calculated for the given geometries according to Equation 2-21. The Power Number correlated to the calculated Reynolds Number was obtained from curve c (Rushton turbine type impeller) in Figure 2.5. As a result, a fitting curve was derived, which gave a direct

correlation between the energy input and the agitation level setting at the pilot scale stirrer of the column.

Additionally, the residence time and the stream velocities in the technical column were applied for the calculation of flow rates in the pilot scale. On the one hand, the residence time was maintained constant by adjusting the column capacity for the volume of the mixing zone following **Equation 2-20**.

On the other hand, the feed and solvent flow were calculated using the following equations, when considering a feed-to-solvent ratio equal to 5:

$$\dot{F} = v_F \cdot A_f \cdot \frac{5}{6}$$
$$\dot{S} = v_S \cdot A_f \cdot \frac{1}{6}$$

Equation 5-10: Calculation of the flow rates $\dot{F}$ and $\dot{S}$

v: velocity of the feed (F) and the solvent (S); A_f: free cross-section

The temperature and the surfactant concentration in the solvent were kept equal to the optimal conditions for the continuous extraction with Triton X-114 in technical scale. A feed-to-solvent ratio of 5 was set for all experiments.

Based on those calculations, experiments with a test system containing Triton X-114 and tap water were conducted. Therefore, it was possible to evaluate the performance of the set-up. Moreover, a comparison with the technical scale was conducted as well.

5.9.3 VALIDATION EXPERIMENTS WITH THE BINARY SYSTEM TRITON X-114/WATER

The experiments with water were performed at the denoted "Normal mode." Hence, V-2 was held open, while V-8 and V-9 were closed. The feed flow was set using V-1. The solvent was pumped in the column using the pump E-1. The extract flow was set using V-7 (blue line in **Figure 6.29**).

The solvent was mixed additionally and contained 20 wt% Triton X-114. The temperature in the heating jacket was set to 40 °C. The heating in the extract settler was maintained at 52 °C. The agitation level of 0.5 was applied for all experiments.

The feed stream was monitored using the flow meter. The data were then obtained from the Lab-View software. As an alternative, that flow was determined manually, by measuring the volume over a specific time interval.

The extract flow was set manually in the same manner as the feed flow. Additionally, an installed scale indicated the weight of the solvent tank during the experiment. Hence, it was possible to derive the solvent stream, as well as the extract flow after the beginning of its recirculation (solvent=extract).

Samples were collected from the raffinate, extract, as well as from the initial solvent. At the end of each experiment, the agitator was turned off so that the micellar phase can settle from the aqueous phase. Hence, the hold-up was determined. Additionally, samples were obtained from the micellar and the aqueous part of the hold-up. The Triton X-114 amount was subsequently analyzed via HPLC as described in chapter 5.11.1.

Based on the measurements, time profiles of the flow rate and the Triton X-114 were used to evaluate the performance of the set-up.

The mass balance regarding the surfactant Triton X-114 was applied as an indicator of the accuracy of the measured values. The used amount of the surfactant in the solvent was compared to the sum of the Triton X-114 mass in the raffinate, extract and the hold-up in the column:

$$m_{S,0} - m_{S,1} = m_R + m_E + m_{M,H} + m_{A,H} + m_P, \text{ where } m_i = c_i \cdot V_i$$

Equation 5-11: Calculation of the Triton X-114 mass balance

m_i: Triton X-114 mass in initial solvent (S,0); final solvent (S,1); raffinate (R); extract (E); micellar phase hold-up (M,H); aqueous phase hold-up (A,H); loss due to sampling (P); c_i: Triton X-114 concentration; V_i: volume.

5.10 CLOUD POINT EXTRACTION FROM MICROALGAE CULTURES IN PILOT SCALE

Initially, a continuous in situ extraction from *Acutodesmus obliquus* culture using the surfactant Triton X-114 were performed. As a reference, a 24-hour experiment at technical scale was conducted.

The experiments with the fresh of *Acutodesmus obliquus* culture from the BIQ Alage House were conducted in "Normal mode," whereby the valve V-8 was kept closed because the culture was not cultivated further (green line in **Figure 6.29**). The feed was taken from the line 4 (4th floor of the Algae house, see appendix A 2). The biomass concentration was obtained from the central monitoring system of the BIQ.

The experiment was carried out in the same manner as the validation extraction with Triton X-114 (see 5.9.3). The duration was extended to 22 hours. An extra filtration step of all samples using 0.2 µm syringe filters was performed prior the HPLC analysis. Samples from the extract were analyzed at the University of Hamburg using SEC (see 5.11.2).

Moreover, an additional settling of the raffinate was conducted using a beaker and a funnel, as shown in **Figure 5.2**.

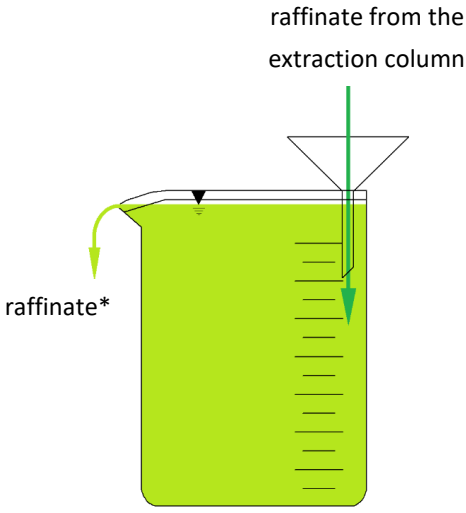

Figure 5.2: Additional settler for the raffinate.

The algae culture after the extraction was lead through a funnel into a beaker. The temperature in the vessel was approx. 33 °C (above the CPT of the raffinate). The micellar phase settled at the bottom of the beaker, and the algae culture was separated at the top.

Further in situ extraction experiments from the same microalgal culture were performed with the surfactant ROKAnol NL-5. A batch extraction with ROKAnol NL5 was carried out in the 35 L stirred column as a separation vessel (figure in appendix A 5). Firstly, the microalgal culture was applied as feed. The cell density was obtained from the BIQ control system. The culture was mixed with the surfactant

to a ROKAnol NL5 concentration of 5 wt%. A subsequent mixing at 43.75 rpm (agitation level 1.5) and temperature of 42.5 °C of the heating jacket and 52 °C of the heating stripe was operated over 24 hours. That after, the stirring was interrupted and the mixture was let to settle over 24 hours. Finally, the micellar phase was collected at the top of the vessel and the surfactant-lean phase was separated from the bottom valve of the column.

A second batch experiment was conducted with flotate as feed. The flotate was a slurry with higher biomass concentration obtained from the flotation unit of the BIQ Algae House (see chapter 4.4). The experiment was carried out identically to the batch extraction from fresh culture.

A final continuous cloud point extraction from *Acutodesmus obliquus* using the surfactant ROKAnol NL5 was conducted utilizing the pilot plant. The setting was the "Normal mode" according to the green line in Figure 6.29. Since the solvent phase containing ROKAnol NL5 is lighter than the microalgal culture, the column was operated vice versa to the Triton X-114 experiment. Hence, the extract was collected at the top of the column. However, other process parameters were applied. The temperature was set at 45 °C. The feed flow rate was at 7 $L \cdot h^{-1}$. The solvent stream amounted 2.3 $L \cdot h^{-1}$. That resulted in a feed-to-solvent ratio of 3. The agitation rate was 15 rpm. The solvent consisted of 15 wt% ROKAnol NL5 in tap water. The duration was 6 hours, and the recirculation of the solvent began after 2 hours.

Samples from the extract phases obtained from the three ROKAnol NL5 experiments were analyzed for their pigment concentration. Firstly, UV-VIS spectra in the wavelength range 200-750 nm were measured in quartz SUPRASIL cuvettes in using the spectrophotometer Art Evolution 300 UV-VIS from Thermo Scientific. Additionally, an analysis using inversed phase high-performance chromatography system was performed at the "Cell biology and phycology" department of the University of Hamburg. The aim was to determine the pigment concentration. The mobile phase consisted of tetrahydrofuran, acetonitrile, and methanol. The solvent was pumped in an isocratic mode. The pigments neoxanthin, violaxanthin, lutein, alpha-carotene, chlorophyll a, and chlorophyll b were were detected using a diode array detector. Calibration curves were preliminary obtained for each pigment standard.

5.11 ANALYTICS

5.11.1 HIGH-PERFORMANCE LIQUID CHROMATOGRAPHY

The determination of Triton X-114 and cinnamic acid concentrations were performed with an Agilent 1200 series HPLC system (Agilent Technology Inc., Santa Clara, USA). The injection volume was 2 µL, the flow rate 1 ml min^{-1}. The mobile phase consisted of acetonitrile and water. The gradient of the two solvents was set over time as follows: 0-2 min: 60%/40%; 2 – 4.5 min: linear increase from 60%/40% to 100%/0%; 4.5 – 6 min: 100%/0%; 6 – 6.5 min: linear decrease from 100%/0% to 60%/40%; 6.5 – 10 min: 60%/40%. All measurements were performed at 55°C column temperature. The components were both detected at a wavelength of 275.8 nm, with retention times of about 2 min for cinnamic acid and about 6 min for Triton X-114. The respective calibration curves are given in appendices A14 and A15.

5.11.2 SIZE-EXCLUSION CHROMATOGRAPHY

Samples, containing a surfactant, water, and algae products were analyzed by size-exclusion chromatography (SEC) in collaboration with the "Institute for Technical and Macromolecular Chemistry," University of Hamburg. The aim was to separate the products from the surfactant and thus qualify the extract composition. The samples were prepared for the analysis as follows. 30 g sample was transferred into a 100 mL round-bottom flask. The sample was lyophilized. The residue was extracted three times for 5 min with chloroform, and the extract was filtered through a 0.2 µm syringe filter into a 50 mL pear-shaped flask. The solvent was completely evaporated in a rotary evaporator.
Then, the final residue was diluted in 5 g tetrahydrofuran, and one mL was measured by SEC (calibration using polystyrene).

5.11.3 DETERMINATION OF THE GALLIC ACID EQUIVALENTS

The yield of phenolic compounds after the cloud point extraction from pineapple juice was determined using the gallic acid equivalents (GAE) as a standard quantification method of total phenols content [166]. The GAE determination was conducted using the spectrophotometer Art Evolution 300 UV-VIS from Thermo

Scientific. To avoid external absorbance disturbances, two quartz SUPRASIL cuvettes from Hellma were used. Before every determination, they were filled with distilled water and used as reference cell and after, one of them was replaced with the sample.

In order to obtain the specific wavelength of the phenolic compounds among all the components in the surfactant-rich sample, the absorption spectra in a range from 190 to 400 nm was obtained separately for each compound.

The absorbance spectra were measured for the following samples: ROKAnol NL5 (0.01 wt%), gallic acid (1 mg/L), and pineapple juice (0.002 wt%). The results are presented in Figure 5.3.

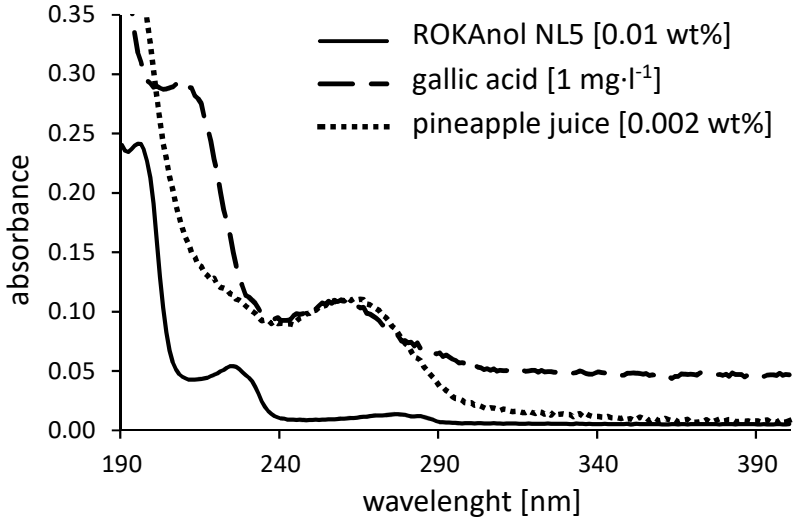

Figure 5.3: Absorbance spectra of the single compounds

The spectra of the gallic acid had two maximums at 210 and 265 nm. In accordance, pineapple juice had a similar behavior to gallic acid, having a maximum absorbance peak at 265 nm. This behavior was expected due to its composition rich in phenolic compounds [76,77]. On the other hand, the surfactant ROKAnol NL5 showed only a maximum absorbance at 225 nm, and because of the low absorbance at other wavelengths, it was assumed that the surfactant did not influence in the determination of phenolic compounds.

The total phenol content of pineapple juice in the present work was measured by reading the absorbance at a wavelength of 275 nm. A calibration curve of absorbance against gallic acid concentration is shown in appendix A 16.

5.11.4 DETERMINATION OF THE ANTIOXIDANT CAPACITY

The antioxidant capacity was used for the evaluation of the CPE from pineapple juice. The analysis was performed according to Peshev et al. [165]. The antioxidant radical 2,2-diphenyl-1-picrylhydrazyl (DPPH) that has a maximal spectrophotometric absorbance at 517 nm was applied. The antioxidants in the sample reacted with DPPH to DPPH-H and thus decreased its the absorbance. For the analytical procedure, a standard methanolic solution containing 0.1 mmol·L^{-1} DPPH was prepared. Its absorbance was measured using an UV-photometer at 517 nm after 30 minutes and was used as a reference value. Additionally, 0.25 mL of each sample were mixed with 0.75 mL standard solution and their absorbance signal was monitored every 10, 20 and 30 min as well. A baseline was obtained using pure methanol. Hence, antioxidant capacity was calculated as "quenched DPPH" in mmol DPPH/g sample according to **Equation 5-12**.

$$quenched\ DPPH = (A_R - A_S)/A_R$$

Equation 5-12: Calculation of quenched DPPH

A: Absorbance of the reference (R) and the sample (S)

5.11.5 DETERMINATION OF THE REDUCING SUGARS

The sugar distribution during the cloud point extraction from pineapple juice was determined via photometric analysis of total reducing sugar using DNS-reagent. The 3,5-dinitrosalicylic acid (DNS) is reduced to 3-amino-5-nitrosalicylic acid, which strongly absorbs light at 540 nm [167]. The sample was diluted to match the valid absorbance range of the applied UV-photometer. Afterwards, 0.167 ml of the sample mixed with 0.333 ml 0.05 M citrate buffer and 1 ml DNS-reagent into 2 ml centrifuge tubes. The mixture is boiled in a water bath for 5 minutes and cooled in iced water immediately to stop the reaction. 0.1 ml of the boiled sample was diluted with 1.25 ml of demineralized water in a polystyrene cuvette. Subsequently, the UV-absorbance was measured at 540 nm. A calibration for glucose was conducted before the sample analyses (appendix A 17).

5.11.6 DENSITY MEASUREMENTS

The density of surfactant solutions at a specific temperature was determined with a density meter of the type DMA 4500 M from Anton Paar GmbH. Samples of 1 mL were fed into the pre-heated measuring tube, and density values obtained when temperature equilibrium was reached.

5.11.7 VISCOSITY MEASUREMENTS

The viscosity of the samples was determined using a rheometer of the type Kinexus pro from Malvern Instruments. The geometry used for the determination was a PL65-CP-20. The sample and the measuring surface of the bottom geometry were tempered by a cryo-compact circulator of the type CF41, supplied by JULABO GmbH.

5.11.8 DETERMINATION OF THE RELATIVE PHOTOSYNTHETIC ACTIVITY

The photosynthetic activity (PA) of the green microalgae *Acutodesmus obliquus* was determined according to Glembin et al. [132]. The PA of the microalgae photosystem II was measured by Pulse Amplitude Measurement (PAM) with a MAXI – Imaging-PAM chlorophyll fluorimeter (Heinz Walz GmbH). Before the fluorescence took place, the samples were dark adapted to have a maximal number of active chlorophyll centers. The integrated camera captured the maximal fluorescence. The PA value was transferred to the Imaging-WIN Software. Thus, the relative photosynthetic activity (RPA) of each sample was calculated as a ratio between the sample's PA value and the one of the reference surfactant-free microalgae culture.

5.12 ASSUMPTIONS

The following assumptions were applied when reasonable:

- Unless otherwise stated, the density of water and water-rich mixtures of water and surfactant was assumed to be 1 kg dm^{-3}.
- Unless otherwise stated, the viscosity of water and water-rich mixtures of water and surfactant was assumed to be 1 mPa s.
- Although cinnamic acid is a dissociable solute, the influence of the pH was neglected in this thesis. Therefore, neither was the pH measured during the experiments nor was distinguished between the dissociated and non-dissociated form of cinnamic acid for calculations of the partition coefficient.

5.13 ERROR ANALYSIS

Unless specially denoted, experimental values are given in the form $\bar{x} \pm s_x$. The mean value ($\bar{x}$) and the population's standard deviation (s_x) are defined as denoted in **Equation 5-13** and **Equation 5-14**:

$$\bar{x} = \frac{1}{N}\sum_{i=1}^{N} x_i$$

Equation 5-13: Calculation of mean values $\bar{x}$

N: Number of samples; x: Value of sample (i)

$$s_x = \left[\frac{1}{N-1}\sum_{i=1}^{N}(x_i - \bar{x})^2\right]^{1/2}$$

Equation 5-14: Calculation of the population's standard deviation s_x

N: Number of samples; x_i : Value of sample (i)

6 RESULTS AND DISCUSSION

The results illustrating the development of the cloud point extraction from authentic feed solutions in batch and continuous mode are presented in this chapter. Firstly, the design of stable cloud point systems based on experiments with a model solute is discussed. That after, strategies for the more favorable extract processing are proposed. Based on these observations, a cloud point extraction is carried out with an authentic fruit juice. Moreover, the feasibility of a continuous surfactant-based in situ extraction from green microalgae culture is presented in technical scale. Finally, the design and operation of a plant for the CPE in pilot scale is presented and evaluated. Based on the results, a general strategy for the design of a mild separation using nonionic surfactants is proposed.

6.1 CLOUD POINT EXTRACTION OF CINNAMIC ACID USING TRITON X-114*

* *The results in this chapter were published in the contribution: "In situ continuous countercurrent cloud point extraction of microalgae cultures"* [168]. *The experiments were partly completed by Nick Tietgens for his Master thesis* [159].

The knowledge gap concerning the surfactant-based two-phase mixtures as media for a continuous ISPR was the reason to study a well-established system for that application. Therefore, the nonionic surfactant Triton X-114 was used, because of its successful application for a direct in situ product removal from microorganism cultures in batch mode [9,132,133]. Moreover, the Triton X-114 cloud point system was suitable for the continuous extraction of model phenolic compounds [43,145,146]. According to those studies, an extraction temperature of 40 °C was selected, since a good biocompatibility and stable operation in continuous mode could be maintained at that temperature level.

Additionally, a model feedstock, which had a constant composition during all experiments was needed. Hence, it was possible to study the influence of the operating conditions. Due to the fluctuating composition of the biological materials, a natural suspension was not directly applicable. Therefore, cinnamic acid was chosen as tracer since it represents substances with high abundance in plant cells and has lipophilic properties. The objective was to determine optimal process

parameters for a continuous countercurrent surfactant-based in situ extraction of dissolved biomaterials using Triton X-114.

It was essential to develop an approach to identify the suitable parameters. Primarily, the cinnamic acid partitioning was studied in a single-stage extraction so that the tracer's suitability was evaluated. Subsequently, the crucial process parameters: feed-to-solvent ratio, total column capacity, and stirring speed were varied in a defined operating window, and their influence on the tracer yield and productivity was investigated. The optimal operating conditions were determined based on the experimental design procedure described in chapter 5.4.

6.1.1 PARTITIONING BEHAVIOR OF CINNAMIC ACID IN TRITON X-114/WATER SYSTEMS

Cinnamic acid was chosen as a tracer for the optimization of the extraction. Therefore, it was essential to study the CA distribution between the micellar and the aqueous phase of Triton X-114/water systems regarding overall partition coefficient, yield, and micelle loading in case of different initial surfactant fractions. Based on these values, the minimal amount of surfactant, which was needed to reach the highest yield, was determined and later transferred to the continuous process via the feed-to-solvent ratio as a maximal value for the parameter range.

The value of $10logP_{CA}$ = 1.2±0.2 was estimated, confirming that the tracer was predominantly distributed in the micellar phase, and is thus suitable for the modeling of the continuous extraction.

The achieved extraction yield of the batch experiments was calculated according to **Equation 5-3**. Hence a later comparison with the continuous experiments was possible. The cinnamic acid yield as a function of the initial surfactant concentration is presented in **Figure 6.1**.

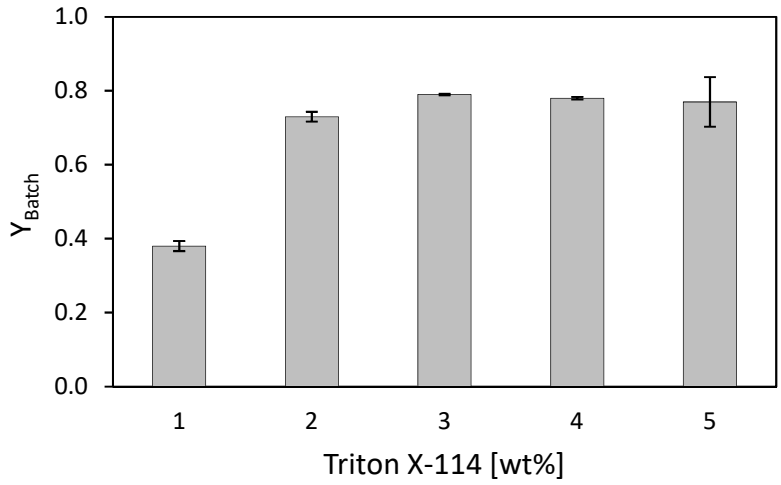

Figure 6.1: Yield of cinnamic acid in the micellar phase at different initial surfactant concentrations, at 40 °C, in batch experiments. Initial CA concentratioN=200 mg·l^{-1}. Error bars indicate the standard deviation, N=3.

An initial surfactant concentration of 1 wt% resulted in a yield of 38 ± 1 % indicating that the solubilization capacity of the surfactant was not sufficient. When the Triton X-114 fraction was increased up to 3 wt%, the obtained yield was also higher. The yield at 3 wt% Triton X-114 concentration was 79.1± 0.2 %, and the value did not increase further with higher surfactant concentrations. Tan et al. reported a similar tendency of achieving a saturation of the micellar phase when extracting mangostins from eggplant [118]. This result confirms the expectations since in case of 1 wt% initial surfactant concentration, Triton X-114 could only extract as much solute as the maximum loading of the micelles allowed. The remaining tracer was distributed in the aqueous phase. When the surfactant fraction was higher, more cinnamic acid could be extracted from the aqueous phase, and thus the yield increased (the initial CA concentration in all samples was kept constant at 200 mg·l^{-1}). Hence, in case of 4 and 5 wt% initial Triton X-114 concentration, the micelles in the surfactant-rich phase had lower cinnamic acid loading than at the lower Triton X-114 concentration. The reason for the latter was that the fraction of CA absolute quantity per mass unit Triton X-114 was lower.

For better understanding, the micelle loading was calculated according to **Equation 5-4**. The amount of CA per single micelle at different initial surfactant concentrations is presented in **Figure 6.2**.

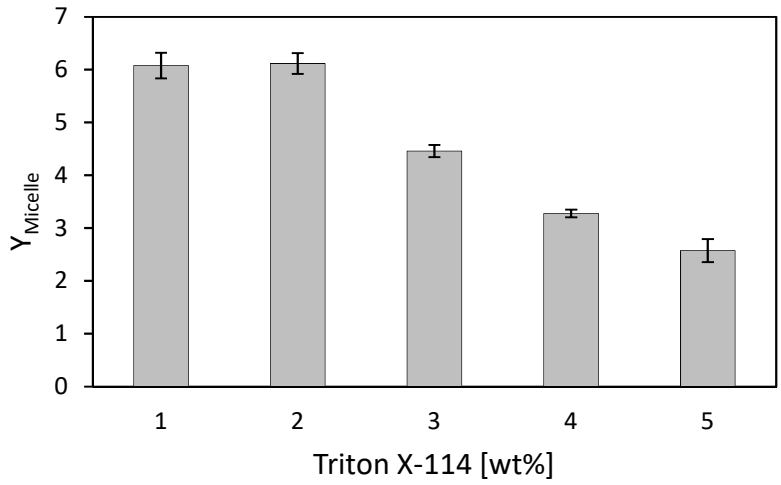

Figure 6.2: Micelle loading at different initial surfactant concentrations at 40 °C, in batch experiments. Initial CA concentratioN=200 mg·l^{-1}. Error bars indicate the standard deviation, N=3.

As expected, the micelle loading started to decrease at a specific concentration when the solubilization capacity of the micelles exceed the total solute amount in the solution. Each micelle could approximately be loaded with six CA molecules (calculated from the molar weight of CA) at initial Triton X-114 concentrations of 1 and 2 wt%. The observed tendency concerning the loading was in agreement with the yield decrease.

The range of the feed-to-solvent ratio was defined by the observed yield dependency on the initial surfactant concentration. Hence, the fraction of the surfactant in the column during all experiment was set below 3 wt%. Further, a Triton X-114 concentration range in the mixing zone was chosen between 1.8 and 3.5 wt%. The solvent flow composition was constant at 20 wt% surfactant in deionized water. Thus, the feed flow was varied in such a manner, that the concentration of Triton X-114 was within the defined interval. In this way, the range for the feed-to-solvent ratio was defined as the lowest value of 6 (3.5 wt%) and the highest ratio of 10 (1.8 wt%), respectively.

6.1.2 PROCESS WINDOW AND PARAMETER VARIATION

The process window for the CPE in the extraction set-up, presented in chapter 4.6, was designed as follows.

Since plant tissues and living microorganisms can be highly sensitive to a temperature above 45 °C (see chapters 2.7 and 2.8), 40 °C was set as a constant operating temperature for the extraction column although higher temperatures were shown to improve the extraction efficiency [13]. The cinnamic acid concentration in the feed flow was kept constant at 200 $mg \cdot l^{-1}$.

The surfactant concentration in the solvent amounted to 20 wt% in accordance with the surfactant-rich phase at 40 °C (see LLE Triton/water in appendix A 9). The fraction of Triton X-114 in the extraction column was set by the feed-to-solvent ratio. Overall, the surfactant concentration in the active volume varied from 1.8 wt% (F/S = 10) to 3.5 wt% (F/S=6).

Additionally, the feed range was restricted considering the residence time of the stream in the column. The exposition to heat and high surfactant concentration was set from 1 to 2 hours corresponding to the reported studies utilizing sensitive biomaterials [9,111,122]. Hence, the feed flow rate varied from 0.85 to 1.81 $l \cdot h^{-1}$. Therefore, the column capacity range was adjusted between 1 and 2 $l \cdot h^{-1}$ according to the surfactant concentration in the mixing zone and the feed flow range.

The stirring speed was varied based on the stress limit determination. A concentration of Triton X-114 = 0.2 wt% in the raffinate flow at a certain parameter combination of agitation speed, capacity, and feed-to-solvent ratio was defined as stress limit. The stress limit was introduced to maintain minimal surfactant loss with the raffinate. Hence, a potential extraction from cell cultures could allow a subsequent cultivation of the cells after the ISPR. The difference between an experiment at and above the stress limit is exemplary shown in **Figure 6.3** for a total capacity = 2 $l \cdot h^{-1}$, feed-to-solvent ratio = 10 and stirring speed = 40 and 50 rpm, respectively.

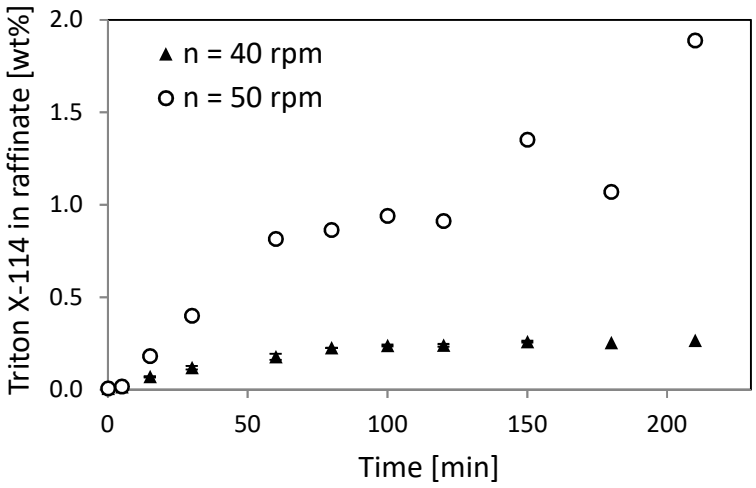

Figure 6.3: Surfactant concentration profile in the raffinate over the time at two different agitation speeds (n=40, n=50 rpm); v = 10, b = 2 $l \cdot h^{-1}$; T = 40 °C.

The impact of different agitation intensities was observed in the concentration profile of the surfactant in the raffinate over time. While a constant surfactant fraction was reached at 40 rpm, the amount of Triton X-114 in the raffinate was increasing at 50 rpm. Hence, at 40 rpm the steady state was reached with the Triton X-114 concentration equal to 0.2 wt%. On the other hand, flooding was observed at 50 rpm. Hence, the stress limit was registered at n = 40 rpm, v = 10, b = 2 $l \cdot h^{-1}$. Moreover, the plots in **Figure 6.3** illustrate the benefits of the stress limit restriction at the experimental design. Namely, not only the surfactant loss with the raffinate could be minimized but also any possible flooding could be omitted.

The needed agitation speed to reach the stress limit was registered for the entire capacity interval while applying the minimum and maximum of the feed-to-solvent ratio. All registered restriction points are presented in **Figure 6.4**. Please note, that the agitator speed was varied in steps of 10 rpm and thus the actual restriction points could be slightly higher than presented.

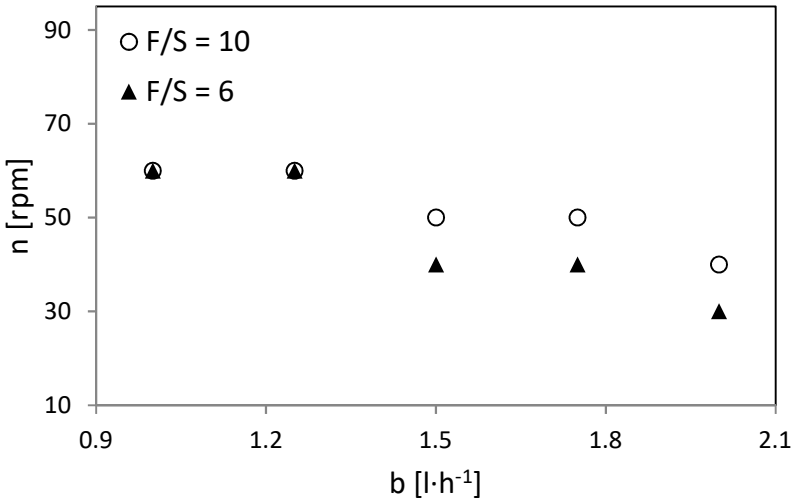

Figure 6.4: Stress limit point as a function of agitation speed (n) and column capacity (b) at feed-to-solvent ratio v = 6 and v = 10. T = 40 °C.

For all investigated column capacities, the stress limit point could be located. As shown in **Figure 6.4**, the lowest column capacity of 1 $l \cdot h^{-1}$ could be applied with an agitation speed of 60 rpm. Corresponding to the expectations, an increase in the stirring speed limited the column capacity. At the highest column capacity of 2 $l \cdot h^{-1}$ only stirring at 40 rpm was possible. The reason for the stress limit being depended on the stirring speed and column capacity is the higher velocity of the feed flow in conjunction with the turbulences, axial backmixing, and smaller droplet size distributions due to the agitation (see **Figure 2.3**). These effects influence the descent of the dense phase to the bottom of the column [169]. Summarized, with chosen feed-to-solvent ratio and column capacity, the maximal agitator speed, was determined.

Based on this dependence, by applying the tools of the "Stat-Ease Design-Expert Version 8" software, linear constraints were formed. Subsequently, those were merged to a plane. Accordingly, all measuring points were distributed below this plane. The plane was defined by **Equation 6-1** as a multilinear constraint.

$$20 \cdot b + n - 5 \cdot \nu \leq 30$$

Equation 6-1: Plane of the multilinear constrain

b: capacity; n: agitation speed; v:feed-to-solvent ratio

Ultimately, by combining the ranges concerning the parameters feed-to-solvent ratio, agitator speed and column capacity, the process window for the investigated system at which all measuring points were distributed was defined (**Figure 6.5**).

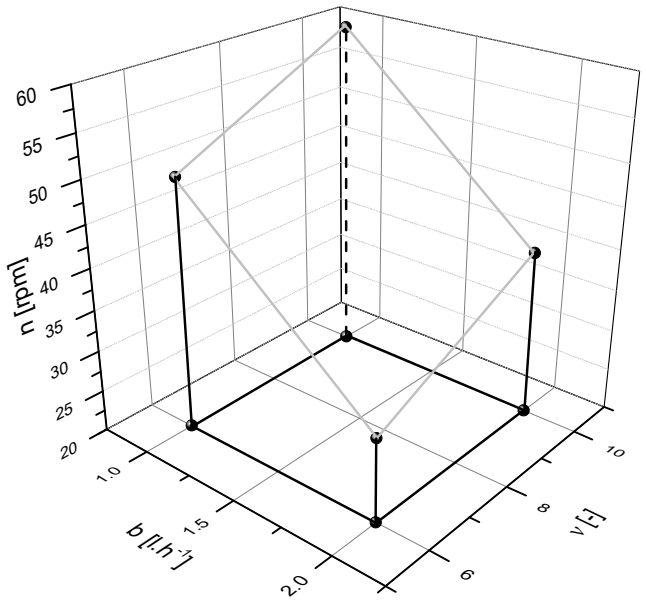

Figure 6.5: Process window of the parameters influencing the continuous cloud point extraction.

The three-dimensional field represented the limitations for the developed yield and productivity models. It was assumed, that outside of this system both models would not work correctly and would give incorrect responses. The performed statistical analysis observed each response factor separately. An overview of the exact location of all measuring points and their corresponding responses is provided in appendix A 18.

6.1.3 YIELD OPTIMIZATION

The CA yield could be obtained for all 20 experiments by applying **Equation 2-14**. The yield values within the system ranged between 0.195 and 0.425 (appendix A 18). The table in appendix A 19 shows the model summary statistics for different data fits. Initially, four different models were applied to fit the measured points: Linear, two-level factorial, quadratic and a cubic model. The models were compared in their quality. More specifically, their standard deviation, different r-squared values, and their PRESS determined the quality. The r-squared measures how much variability in the observed response values could be explained by the experimental factors and their interaction. Commonly, values above 0.90 can be considered as a good result [170]. According to the experimental results, a quadratic equation is

recommend to model the yield. With a high r-squared of 0.954 and a low standard deviation and PRESS, the quadratic model had the best quality. The linear and two-level factorial r-squared value lied in comparison only under 0.85. Although the cubic model had a lower standard deviation and higher r-squared value than the quadratic model, it was aliased. The latter derives from the chosen design, which provides too few unique points to determine all terms in a cubic model.

Additionally, "Sequential Model Sum of Squares" and "Lack of fit"-tests confirmed the quality of the quadratic model for the yield (see appendix A 19).

Hence, the yield could be estimated by using the operating condition values (**Equation 6-2**):

$$Y_{cont.} = \quad -0.002 \cdot b \; + 0.006 \cdot n - 0.242 \cdot \nu - 0.001 \cdot n \cdot \nu + 0.013 \cdot \nu^2 + \; 1.328$$

Equation 6-2: Model equation for the yield of cinnamic acid ($Y_{cont.}$)

b: capacity; n: agitation speed; v:feed-to-solvent ratio

When comparing the model terms, it was apparent that the feed-to-solvent ratio had the most definite impact on the yield. A low feed-to-solvent ratio was equivalent to a high surfactant concentration, and thus the yield increased with a decrease in the feed-to-solvent ratio. Both, the agitator speed and the column capacity had a less significant influence on the yield.

The model was assessed based on the normal probability of a residual vs. run plots. The corresponding plots regarding the yield model are presented in appendix A 19. The normal probability plot was a function of the internally standardized residuals. That assessment was the most important for the model diagnostics. A precise and stable model had all data points close to the linear function. The developed model for the yield give satisfying results, and no outliers were observed. Additionally, a residual vs. run plots indicated which measuring points differed more from its predicted value. While there were some values, which were further of the predicted value, all measuring points were within the coded confidence level of 3. Thus, the total fluctuation of the residuals was no cause for concern, since it illustrates that they vary only due to common-cause variations [171]. Overall, the residual diagnosis confirms the quality of the model which provided reasonable results.

In Figure 6.6, the surface contour plots for the agitator speed and capacity (a) and the feed-to-solvent ratio and capacity (b) are illustrated.

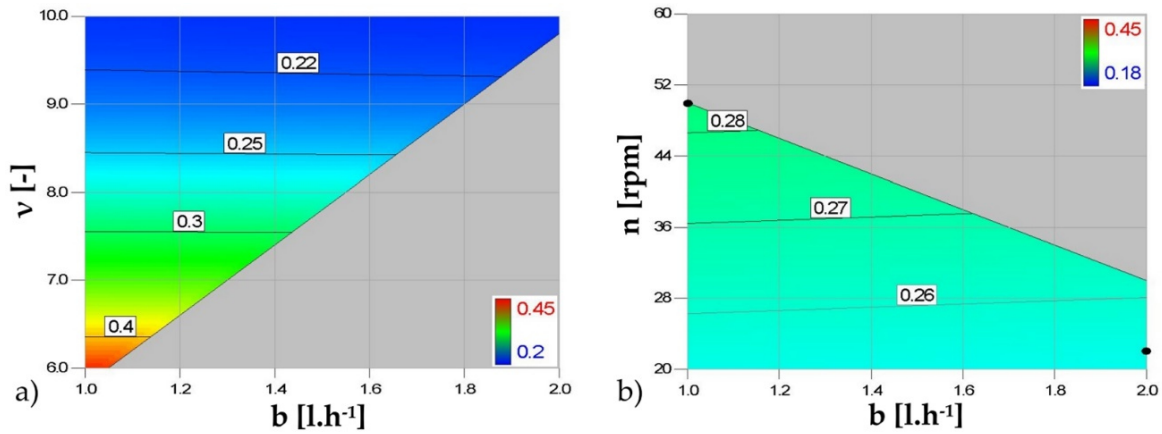

Figure 6.6: Contour plots of the yield as a function of the feed-to-solvent ratio (v) and capacity (b) at agitation speed (n) = 40 rpm (plot a), and as a function of n and b at v = 8 (plot b). Colored for the yield; at T = 40°C.

The influence of the feed-to-solvent ratio on the yield (Figure 6.6 a) was pronounced at 40 rpm and feed-solvent-ratio = 8. Overall, when the feed-to-solvent ratio was the highest (10), a yield of approx. 22 % was reached at average agitator speed. By decreasing the feed-to-solvent ratio to the minimum (6), the obtained yield was nearly doubled.

Contrary to the expectations, the agitator speed did not dominate the yield change through the control of the surfactant dispersion in the column (Figure 6.6 b). A possible reason for this could be the fact that the phase ratio between the aqueous and micellar phase at the narrow surfactant concentration range in the mixing zone did not change significantly. Thus, an increase in the stirring speed would lead to a better dispersion of the similar amount of surfactant-rich phase. Hence, no significant improvement in the mass transfer rate could be reached [170].

Furthermore, a high column capacity had an adverse effect on the yield. The agitator speed – capacity contour plot at a constant average feed-to-solvent ratio (Figure 6.6 b) confirmed the limited significance of the column capacity. Additionally, a considerable area of the plot was restricted due to the stress limit. The reason for that is the multilinear constraint, which allows the highest surfactant concentration in the raffinate only at low column capacities.

Overall, according to the model, the best yield value was located in one of the corner points of the surface plot, at a moderate agitator speed and the lowest feed-to-solvent ratio. The highest yield was calculated at a column capacity of 1 $l \cdot h^{-1}$, agitator speed of 40 rpm and a feed-to-solvent ratio of 6. At these conditions, a maximum yield of 43.9 % and enrichment factor of 3.2 (calculated according to **Equation 2-13**) were reached. An experiment under the described operation conditions was able to obtain a yield of 42.5 %, which confirms the calculated result of the model.

However, during the batch CPE, a yield of 79 % was reached. Contrary to the expectation, the yield of a continuous process at 3 wt% Triton X-114 in the mixing zone reached the half of the corresponding single-stage value. The reason for this could be the limited residence time in the column. When conducting the batch experiments, the solubilization of CA occurred 24 hours before the subsequent phase separation. On the other hand, at the continuous process, the solubilization and phase separation took place simultaneously, with a residence time of the feed of approx. one hour. In comparison, Ingram et al. were able to extract vanillin in the continuous cloud point extraction system with a yield of 76.7 wt% at 40 °C [43]. However, the feed flow was lower and the residence time in the column higher due to the lower applied column capacity. Further, the authors were able to use an increased agitation of 100 rpm, which was not possible in this work due to the stress limit. The different operating conditions could be the reason for the significantly reduced mass transfer, and thus for the reduced yield. The productivity, on the other hand, was enhanced in comparison to the batch experiment and previous works [43]. Nevertheless, it was possible to develop a quadratic model, which provided valid results for the estimation of the yield of the continuous cloud point extraction.

6.1.4 PRODUCTIVITY OPTIMIZATION

In this chapter, the results for the achieved productivity of the continuous CPE of CA are discussed. The productivity was calculated according to **Equation 2-15** for all conducted experiments. Hence, the response within the system varied between 34.8 and 113.6 (see table in appendix A 18). The fit of four different models was investigated for the productivity. As for the yield, the different model statistics are presented in appendix A 20. In order to model the productivity, a linear model was

recommended by Design-Expert. The r-squared value of the quadratic model was with 0.920 slightly higher than the r-squared value of the linear model with 0.903. However, the linear model excelled in a lower standard deviation, PRESS and especially in a much better predicted R-squared value. Overall, the linear model had the better quality and was chosen as the model for the productivity. Although the cubic model had the highest R-squared, it was aliased and cannot be applied.

The "Sequential Model Sum of Squares" and "Lack of fit"-tests confirm the quality of the linear model for the productivity and are listed in appendix A 20 as well.

Hence, s linear equation was developed to model the productivity (**Equation 6-3**).

$$F_{CA} = \quad 37.3 \cdot b - 0.1 \cdot n - 9.0 \cdot \nu + 90.7$$

Equation 6-3: Model equation for the productivity of cinnamic acid F_{CA}

b: capacity; n: agitation speed; v:feed-to-solvent ratio

According to the model equation, the productivity increases significantly with the column capacity. That was due to the elevated feed and solvent flows, and to the resulting increase in the raffinate and extract flows. Regarding the feed-to-solvent ratio, a high solvent flow positively affected the productivity. The reason for this was the yield since a higher surfactant concentration significantly increased the amount of extracted CA. Likewise the yield, a high surfactant concentration was beneficial for the productivity.

For assessment of the quality of the model, the normal probability plot and the residual vs. run plot were observed (appendix A 20). Both plots were similar to yield diagnostics. The normal probability plot indicated satisfactory results regarding linearity. However, a light S-shaped curve was be observed. That was due to the result of the max-to-min ratio of the productivity. Only a max-to-min of greater than 10 was an indicator for required transformation. However, only max-to-min values of 3 or lower had no significant influence on the model. That indicated that the max-to-min ratio of the productivity model with 3.26 had a small but negligible effect. There was one outlier in the measured data, which can be observed in both diagrams. However, according to the residual vs. run plot, this outlier was within the confidence level. Thus, all residuals show, as for the yield, only common-cause variation.

As already described, the column capacity and feed-to-solvent ratio had a significant influence on the productivity. This relation is illustrated on **Figure 6.7**.

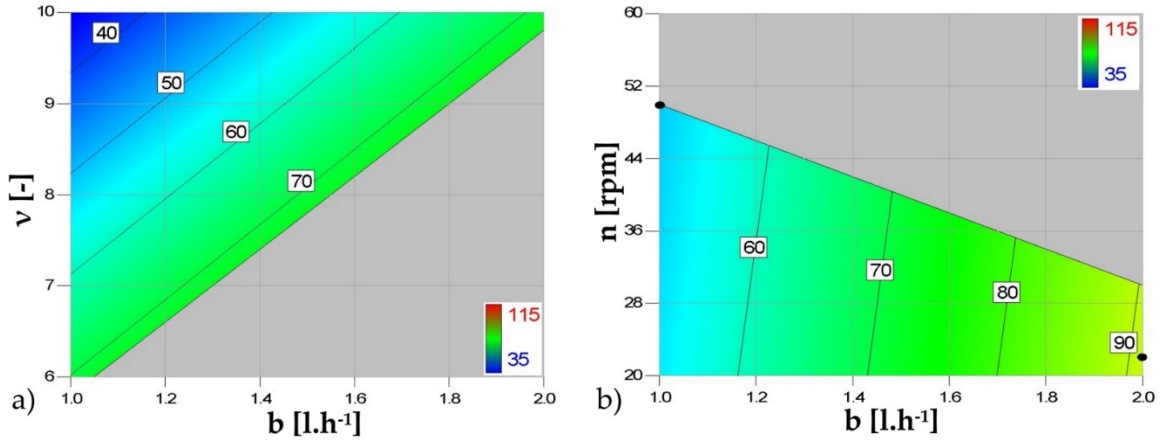

Figure 6.7: Contour plots of the productivity ($g \cdot h^{-1}$) as a function of the feed-to-solvent ratio (v) and capacity (b) at agitation speed (n) = 40 rpm (plot a) and as a function of n and b at v = 8 (plot b). Colored for the productivity; at T = 40°C.

As in the model equation, the pronounced influence of the capacity on the productivity can be observed in **Figure 6.7** a. However, an increased agitator speed influences the productivity (**Figure 6.7** b) negatively. A high surfactant concentration and high column capacity could be maintained in case of low agitation. The agitator speed did not directly influence the productivity, but the impact on the stress limit was indirectly responsible for a decrease in the productivity.

Overall, the highest productivity was found along the border of the system approaching the stress limit. In contrast to the yield, which has a maximum that can not be exceeded, the productivity was ultimately depending on physical limitations when designing the column. At the highest surfactant concentration in the mixing zone, the multilinear constraints restricted a considerable area of the investigated system. Thus only a narrow window for the location of the optimal operating conditions remained. As a result, the highest productivity value was calculated at the lowest stirring speed and highest capacity. Hence, an optimum for the productivity could also be registered within the used parameter field.

The highest productivity was achieved at a column capacity of 2 $l \cdot h^{-1}$, an agitator speed of 20 rpm and a feed-to-solvent ratio of 6. Whereby, a productivity of 109.3 $g \cdot h^{-1}$ CA was obtained. An experiment, which was performed under the described operation conditions, was able to validate the model optimum by obtaining a

productivity of 113.6 $g \cdot h^{-1}$. Thus, it was possible to develop an accurate linear model for estimation of the productivity in the chosen process window.

Finally, the statistical experimental design could be applied to optimize not a single response factor but also for locating operating conditions, which simultaneously assure a high productivity and yield. In case of an equal weighting for both responses, the optimized operating conditions were equivalent to the optimal productivity parameter combination. In this case, the yield was equal to 39.3 % and the productivity to 109.3 g/h, respectively. This parameter combination was defined as optimum for the tested process window of the continuous cloud point extraction of cinnamic acid.

Based on the results in this chapter, a stable operation of the continuous extraction could be maintained with an established cloud point system. Moreover, the optimal combination of the process parameters ensured mild temperature, low exposure to heat and stirring of the feed and minimized Triton X-114 loss with the raffinate. Thus, these conditions were applicable for the continuous in situ extraction of dissolved biomaterials with Triton X-114.

However, Triton X-114 biphasic systems had a general drawback as a solvent for biomaterials. The surfactant has no permission for food, cosmetic or drugs. Additionally, the aromatic ring in its molecule raised the environmental awareness regarding the amphiphile. Therefore, a potential cloud point extraction of a natural product with Triton X-114 would be disadvantageous. These issues lead to the need of alternative surfactants, which are permitted in market goods and commercially available. Therefore, the utilization of commercial-grade surfactant systems, suitable for the cloud point extraction, is presented in the next chapter.

6.2 CONTINUOUS CLOUD POINT EXTRACTION WITH COMMERCIAL SURFACTANTS*

** The results in this chapter were published in the contribution: "Aqueous food-grade and cosmetic-grade surfactant systems for the continuous countercurrent cloud point extraction" [172]. The experimental work was part of the Master thesis by Dennis Wenzel [173] and the Project work by Clemens Müller [174].*

Based on the stable process behavior of the CPE, it was beneficial to identify suitable commercial aqueous surfactant system for the cloud point extraction of hydrophobic biological compounds. Therefore, a screening of sixteen food-grade and cosmetic-grade surfactants based on their cloud point temperature and phase separation kinetics was conducted. The amphiphiles with fast separation kinetics and a mild clouding temperature were further investigated concerning their phase behavior in water and their ability to extract a model solute. Hence, the liquid-liquid equilibria of the aqueous surfactant systems, as well as the partitioning of the model substance cinnamic acid between the coexisting phases, were determined. A further assessment of the suitability of these systems for extraction processes was conducted based on density and viscosity measurements. Finally, extraction experiments in batch and continuous mode were conducted to demonstrate the applicability of the chosen surfactants in the CPE of products with a natural origin.

6.2.1 SURFACTANT SCREENING

Sixteen surfactants were chosen as potentially suitable for the cloud point extraction due to their food- or cosmetic-grade approval, solubility in water, as well as the cloud point temperature. The screening was conducted according to the approach in chapter 5.1.

The obtained values regarding their clouding temperature in an aqueous solution, together with the visual observations concerning the separation kinetics, are presented Table 6.1. The surfactants, which are permitted as food additives in Europe and Switzerland are denoted with the corresponding E-number (E-No.). Additionally, all surfactants with a cosmetic application are listed with their corresponding names according to the International Nomenclature of Cosmetic Ingredients (INCI).

Table 6.1: Chosen surfactants for the preliminary screening with the corresponding supplier, food additive number (E-No.) or international nomenclature of cosmetic ingredients name (INCI), and cloud point temperature (°C, CPT) in 1 wt% dest. water solution

surfactant	supplier	E-No.	INCI	CPT[a]	CPT[b]	phase separation[c]
Polysorbate 20	Aquanova	E432/PS 20	Polysorbate 20	76	77.2±0.9	o
Polysorbate 80	Aquanova	E433/PS 80	Polysorbate 80	65	64±1	o
Silwet L7002	Momentive	E 900	PEG/PPG-50/50 Copolymer	39	39.5±0.5	o
Silwet L7230	Momentive	E 900	PEG/PPG-50/50 Copolymer	40	37.4±0.1	+
Synperonic 91/5	Croda	-	C9-C11 Pareth-5	36	37.9±0.3	+
Synperonic PE L/31	Croda	-	Poloxamer 237	29	32.0±0.7	-
Synperonic PE L/62	Croda	-	Poloxamer 182	32	27.4±0.4	-
Brij C2	Croda	-	Ceteth-2	unknown	dispersible	-
Brij C10	Croda	-	Ceteth-10	unknown	dispersible	-
Brij O2	Croda	-	Oleth-2	unknown	dispersible	-
ROKAnol DB7W	PCC Exol	-	C12-C15 Pareth-7	51	54.3±0.3	-
ROKAnol L5P5	PCC Exol	-	PEG-5-Laureth-5	28	30.5±0.2	o
ROKAnol NL5	PCC Exol	-	C9-C11 Pareth-5	34	36.5±0.2	+
ROKAnol NL8P4	PCC Exol	-	Oleth-3	46	44.2±0.4	-
Sympatens-ALM/040	KOLB	-	Laureth-4	unknown	dispersible	-
Imbetin-AG/124S/060	KOLB	-	C12-14 Pareth-7	41-46	39.5±0.6	-

[a] chemical data sheet; [b] experimentally determined within this work, error indicate the standard deviation, n = 3; [c] "+" fast separation (relative fast separation and clear interfacial border); "o" slow separation, (relatively slow separation and wide interfacial border); "–" bad separation (very slow or no separation and no clear interfacial border.

The cosmetic-grade surfactants Brij C2, Brij C10, Brij O2, and Sympatens ALM/040 did not dissolve in water completely, being present partially as a dispersion. Hence, no cloud point could be determined by the experimental set-up. For this reason, these cosmetic-grade surfactants were not examined further.

All obtained CPT values were slightly different from the suppliers' data. This can be due to the fact, that commercial surfactants often contain a mixture of polymers, which can differ slightly in different production batches. This observation corresponds to the previous studies of Smirnova et al. [9,43]. Further, Polysorbate 20, Polysorbate 80 and ROKAnol DB7W only underwent a clouding at temperatures above 50 °C. If the extraction is carried out at such temperatures, it could affect the stability of phenolic and other aromatic substances (see chapter 2.8). Therefore, these surfactants were neglected for further studies as well. All other nine tested surfactants turned turbid at temperatures below 50 °C. However, most of them did not undergo a phase split (marked with "-" in Table 6.1). The solutions of Silwet L7002 and ROKAnol N5P5 slowly formed an interfacial boundary, which was wide and unstable (marked with "o" in Table 6.1). Hence, Silwet L7002 and ROKAnol N5P5 were not studied further. On the other hand, the aqueous Silwet L7230, Synperonic 91/5 and ROKAnol NL5 systems separated rapidly at a temperature below 50 °C (marked with "+" in Table 6.1). Both, Synperonic 91/5 and ROKAnol NL5 were denoted as C9-C11 Pareth-5 from the supplier. This means that both surfactants consist of a comparable mixture of ethoxylated alcohols with similar properties. Hence, Synperonic 91/5 was subjected to only particularly further investigation.

Ultimately, based on the screening, the two commercial surfactants Silwet L7230 (E 900) and ROKAnol NL5 (C9-C11 Pareth-5) were chosen for further investigations and applied for the cloud point extraction. Their structures are illustrated in Figure 2.6.

6.2.2 BINARY LIQUID-LIQUID EQUILIBRIUM OF AQUEOUS SURFACTANT SYSTEMS

The liquid-liquid phase equilibrium of the system was essential to choose the right extraction temperature and surfactant amount in the feed. The LLE of the Silwet L-7230/water and the ROKAnol NL5/water mixtures were determined in terms of a binodal by the cloud point method [97]. The region of the surfactant-rich phase

was validated additionally with the gravimetric method since the concentration of surfactant in this region corresponded to the solvent at the extraction process (see chapter 5.2). The LLE of the binary Silwet L-7230 and ROKAnol NL5 aqueous systems are presented in **Figure 6.8**. The equilibrium data of the binary aqueous system Synperonic 91/5 is presented in appendix A 21. The measured values were equivalent to the binary aqueous system of ROKAnol NL5 illustrated below.

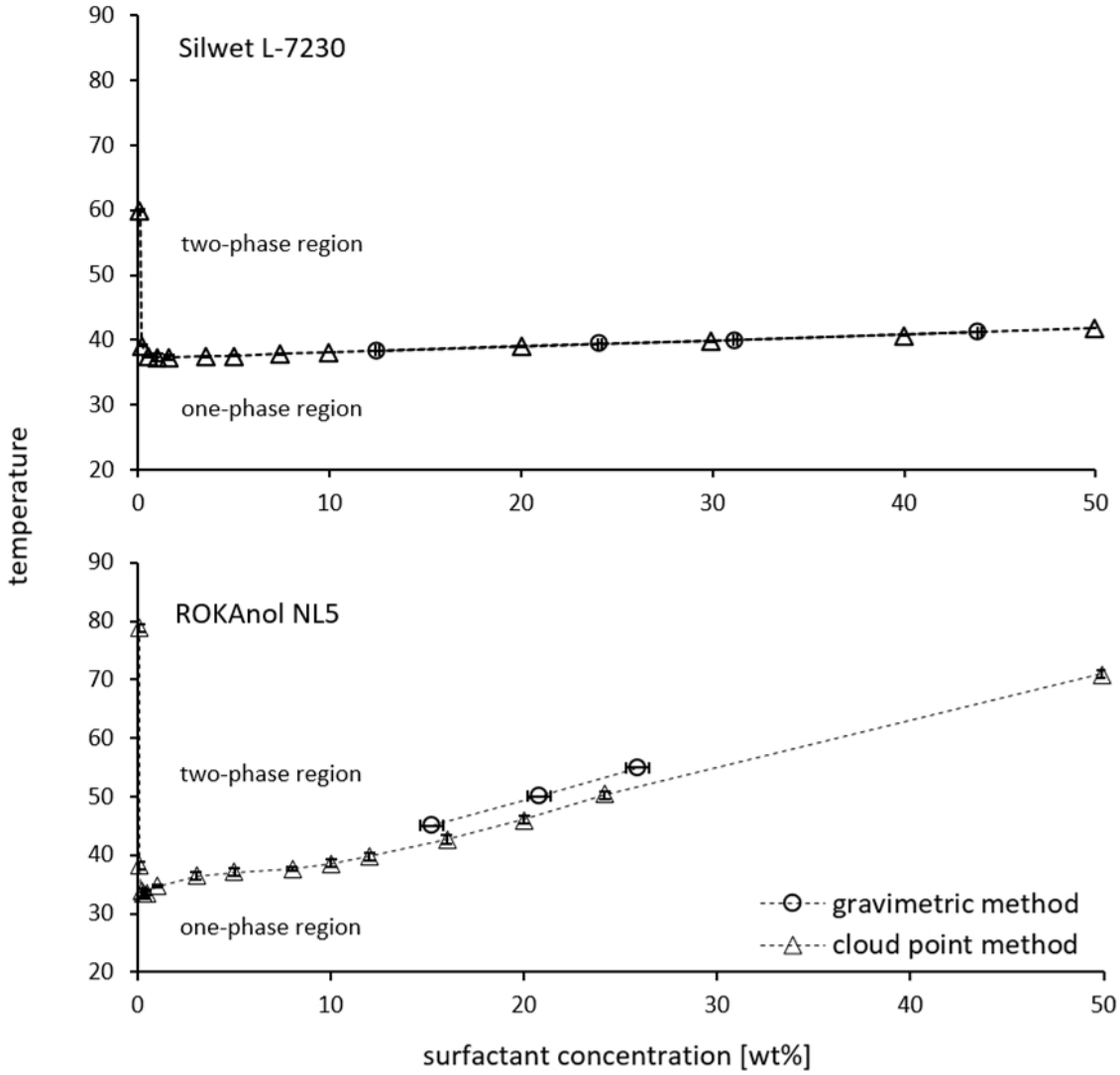

Figure 6.8: Liquid-liquid equilibrium of the binary systems Silwet L-7230/water and ROKAnol NL5/water. Error bars indicate the standard deviation, n=3. Lines are added to guide the eyes.

Clouding temperatures up to 60 °C were measured for Silwet L-7230 aqueous solutions, whereas the minimal lower critical solution temperature (LCST) at 1 wt% was determined to be 37.3°C. That finding was contrary to results by Nemeth et al. [28], who stated a CPT of 40°C for a Silwet L-7230 concentration of 1 wt%. The deviation could be due to production variations since different lots of Silwet L-7230 can contain polymers of different chain length and degree of ethoxylation

and propoxylation. Furthermore, the residual monomer content of octamethylcyclotetrasiloxane from silicone polymer production can vary up to 1 wt%. In case of the ROKAnol NL5/water mixture, CPTs were determined in the range from 33.5 °C to 78.8 °C, with the lowest LCST = 33.5 °C at 0.3 wt%. Since ROKAnol NL5 is a mixture of polymers (see **Figure 2.6**), a comparison with a single ethoxylated alcohol is not reasonable. However, Hinze and Pramauro summarized LCST values for the pure polymers (CxEy), included in the surfactant mixture, from 8 °C up to 60 °C at a concentration range of 0.1 wt% to 5 wt% [4]. The obtained value was in good agreement with the given range and corresponded to a product mainly containing C_8E_4 and $C_{10}E_4$.

Several points of the coexistence curve (at the left part of the binodal) were validated with the gravimetric method. No remarkable deviation from the values obtained by the cloud point method occurred for the Silwet L-7230/water system. However, the values for the ROKAnol NL5/water system differed more pronouncedly. That could be due to the elevated temperature used to transpire the water in the gravimetric method, whereas some molecules with a lower boiling point in the surfactant mixture could have evaporated as well.

Based on the points of the coexistence curve, a defined miscibility gap was measured for both surfactant systems under study. Further, the miscibility gap for the Silwet L-7230 system was broader than the one of the ROKAnol NL5 mixtures. On the one hand, this led to more concentrated surfactant-rich phases at equal temperatures in case of Silwet L-7230. Since the micellar phase is the extract in CPE process, that phase behavior could be utilized for the continuous production of an extract even richer in surfactant. On the other hand, the system Silwet L-7230/water exhibited an extremely temperature sensitive phase separation. Hence, micellar phases with 20 wt% surfactant were formed at 39°C, while at 40°C micellar phases with 30 wt% of surfactant were observed. That posed a significant challenge for process control since small deviations in temperature could already have a strong influence on the resulting phase composition. On the contrary, the ROKAnol NL5/water system showed significantly lower temperature sensitivity and was expected to be more stable during an extraction process.

Consequently, the process temperature for the extraction was set to 39 °C and 45 °C for Silwet L-7230 and ROKAnol NL5, respectively. Under these conditions, a

surfactant fraction of 20 wt% and 15 wt% in the micellar phase was expected for Silwet L-7230 and ROKAnol NL5, respectively. These values corresponded to the solvent flow composition applied in the continuous experiments.

The phase ratio (micellar-to-aqueous, calculated according to the lever rule) was 0.16 for the Silwet L-7230 system and 0.24 for the ROKAnol NL5 system when the initial surfactant concentration in the homogenous feed was set to, e.g., 3 wt%. By setting the temperature, as well as the surfactant concentration in the solvent, sufficient quantity of the extract, as well as mild extraction conditions were ensured. The choice of the extraction conditions based on the binary LLE illustrates the significance of the phase behavior for the process design.

6.2.3 PARTITIONING BEHAVIOR OF CINNAMIC ACID IN THE SURFACTANT/WATER SYSTEMS

An essential criterion for the design of a surfactant-based extraction was the favorable partitioning of target substances in the surfactant-rich phase. The distribution of CA between the coexisting phases was studied, representing the extraction of a hydrophobic compound with a plant origin. Hence, the partition coefficient of CA was determined at different initial surfactant concentrations and temperature = 39 °C and 45 °C for Silwet L-7230 and ROKAnol NL5, respectively (Figure 6.9).

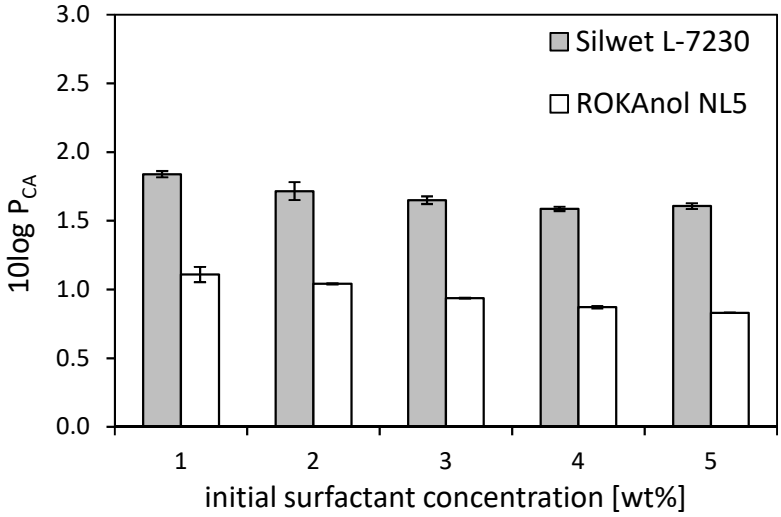

Figure 6.9: Logarithmic partition coefficient of cinnamic acid ($10logP_{CA}$) as a function of the initial surfactant concentration. Error bars indicate the standard deviation; N = 3.

As shown in Figure 6.9, the logarithmic partition coefficient was considerably higher for Silwet L-7230 (average $10logP_{CA} = 1.6 \pm 0.1$) than the values obtained for

ROKAnol NL5 (average $10logP_{CA} = 0.9 \pm 0.1$) at all concentrations. This result was expected, as Silwet L-7230/water formed a micellar phase of 20 wt% surfactant at 39°C, while the micellar phase of the ROKAnol NL5 system contained 15 wt% surfactant. Furthermore, Silwet L-7230 has an HLB of 6.3, while ROKAnol NL5 has an HLB of 11.6. This means that Silwet L-7230 had a higher hydrophobic proportion and ROKAnol NL5 had a higher hydrophilic proportion of the entire molecule. Hence, the cores of the Silwet L-7230 micelles were more hydrophobic and thus could solubilize more cinnamic acid.

When comparing both new systems with the well-established Triton X-114 mixture (average $10logP_{CA} = 1.2 \pm 0.2$), the new surfactants had similar capacity to accumulate the tracer as the standard amphiphile. Therefore, the application of the food-grade surfactant Silwet L-7230 and the cosmetic-grade surfactant ROKAnol NL5 for the cloud point extraction of cinnamic acid was promising and thus both systems were studied further.

6.2.4 PHYSICAL PROPERTIES OF THE COEXISTING PHASES

The density difference between the solvent and feed, as well as the viscosity of the phases, are essential parameters for the design of an efficient liquid-liquid extraction. The higher the density difference, the faster is the phase separation (see chapter 2.3). Additionally, if the viscosity of the disperse phase is too high, mass transfer limitation could occur [14]. Therefore, it was of importance to determine those properties for the new studied aqueous two-phase systems.

The measurement described in chapter 5.11.6 was applied for the determination of the density difference in the new surfactant-based biphasic systems. The density of the coexisting phases in the cloud point system of Silwet L-7230 and ROKAnol NL5 are presented in Figure 6.10.

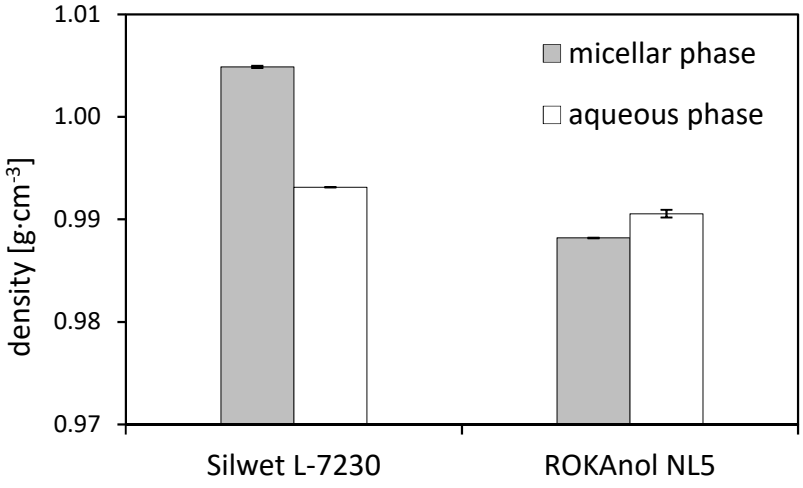

Figure 6.10: Density of the corresponding micellar and aqueous phases of the Silwet L-7230/water system (T=39 °C) and for the ROKAnol NL5/water system (T=45 °C). Error bars indicate the standard deviation, N = 3.

When comparing the densities of the coexisting phases, the surfactant-rich phase in the system Silwet L-7230/water was the denser one (see **Figure 6.10**). Hence, the extract was the dense phase and was collected at the bottom. The phase separation at 45 °C of the ROKAnol NL5/water system led to the formation of a lighter micellar phase. These results were in agreement with the pure substance densities of both surfactants. However, the density difference between the coexisting phases in the ROKAnol NL5 system (density difference = 0.002 g·cm^{-3}) was much lower in comparison to the Silwet L-7230 system (density difference = 0.011 g·cm^{-3}). The values were also lower than the general minimum density difference of 0.05 g·cm^{-3}, which was acceptable for a continuous extraction in a stirred column (see chapter 2.3). Nevertheless, Ritter et al. reported, that phase separation took place even at extremely low density differences, (e.g., density difference equal 0.002 g·cm^{-3} in the ternary two-phase system Triton X-114/glucose/water) [146]. Therefore, the Silwet L-7230/water and the ROKAnol NL5/water system was considered to be applicable for the cloud point extraction.

The viscosity is a further influencing parameter in the design of the extraction process. For instance, a disperse phase with high viscosity leads to broader droplet distribution in a stirred extraction column and thus to a lower interfacial surface area. In the best case, the viscosity of the disperse phase must be similar to the one of water (see chapter 2.3). Hence, the viscosity of the coexisting phases was measured as described in chapter 5.11.7. The shear rate within the column at an

agitation speed of 25 rpm was calculated according to **Equation 5-7** and found to be 5.0 s^{-1}. Therefore, results are shown for this shear rate in **Figure 6.11**.

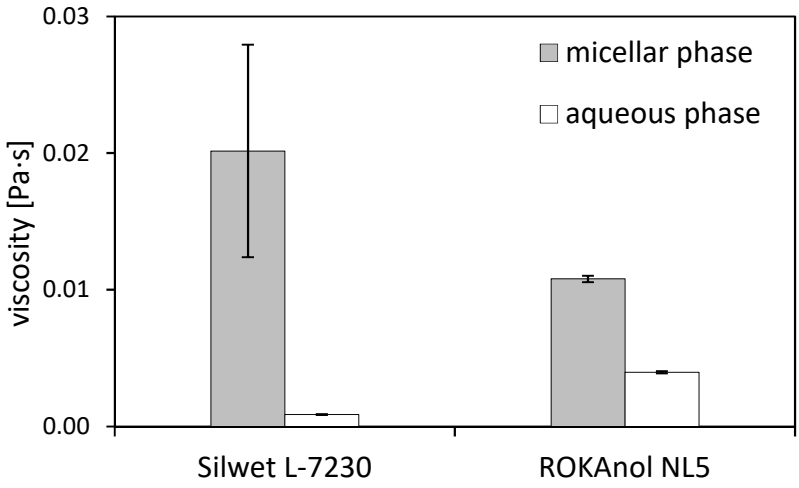

Figure 6.11: Viscosity of the corresponding micellar and aqueous phases of the Silwet L-7230/water system (T=39 °C) and for the ROKAnol NL5/water system (T=45 °C) at a shear rate of 5.0 s^{-1}. Error bars indicate the standard deviation, N=3.

The results of the corresponding viscosity measurements are presented in **Figure 6.11**. As expected, the viscosities of the surfactant-lean aqueous phases were similar to the values for water at the tested temperatures. The micellar phase of ROKAnol NL5 had a viscosity comparable to the surfactant-rich phase in the previously studied Trion X-114 system [43]. Therefore, ROKAnol NL5 was suitable for the extraction concerning its viscosity.

Further, the Silwet L-7230 – rich phase had a higher viscosity. Moreover, the measured values were strongly fluctuating. Samples from the extract phase showed a gel-like appearance at room temperature – although being of a lower Silwet L-7230 concentration than the solvent feed stream, which was a homogeneous liquid solution.

Due to this phenomenon, two different samples were investigated for their viscosity as a function of temperature: (1) an aqueous sample without previous clouding, with a surfactant concentration of 20 wt% Silwet L-7230; (2) an extract (20 wt% Silwet L-7230) obtained from the cinnamic acid extraction at 39°C. The results are presented in **Figure 6.12**.

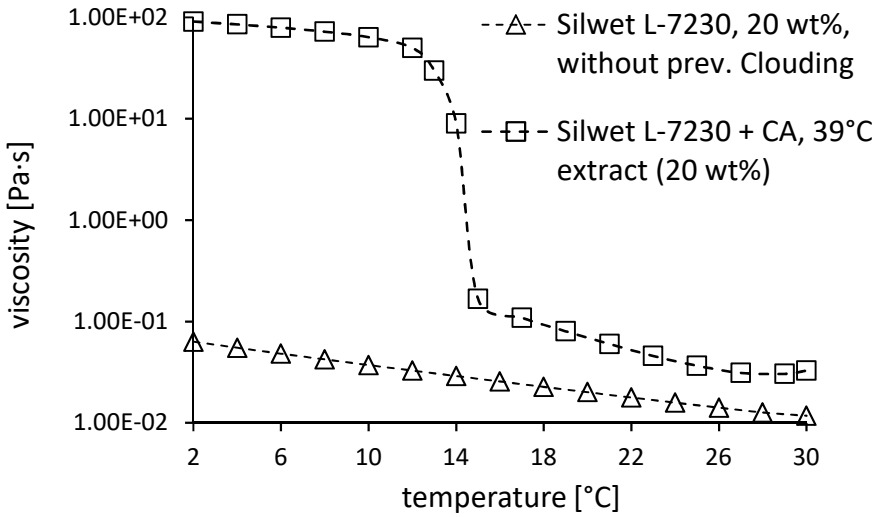

Figure 6.12: Viscosity of extract samples (retrieved at 39°C) and untreated aqueous Silwet L-7230 samples (20 wt%) without previous clouding as a function of temperatures between 2°C and 30°C at a shear rate of 5.0 s^{-1}.

Overall, the viscosity increased with decreasing temperatures, as presented in **Figure 6.12**. However, the extract samples' viscosity increased by up to three orders of magnitude if cooled below 15 °C. In comparison, the non-clouded aqueous Silwet L-7230 samples of equal concentrations showed no such behavior. That difference between the behavior of a micellar extract and an untreated surfactant solution has not been described yet. He et al. found trimethylsilane surfactants to be able to form crystalline structures at deficient concentrations [87]. Furthermore, Lavergne et al. stated that liquid crystalline phases in nonionic surfactant solutions can exhibit very high viscosities [34]. Hence, it can be considered that the sudden change in viscosity and rheological behavior denoted the formation of a liquid crystalline phase within the extract samples at the observed transition temperatures. Besides, it was further reported that micelles form entangled networks, whereby the extent of cross-linking increased above the cloud point [175]. Therefore, it is reasonable to assume that such entanglement could be responsible for the increased tendency of pre-clouded micellar phase to form liquid crystalline structures, compared to untreated surfactant solutions of equal concentration.

It is important to note that the micellar phase contained cinnamic acid. It was important to clarify the influence of cinnamic acid on the formation of a liquid crystalline structure. Surfactant-rich phases from clouding experiments without CA were compared to aqueous Silwet L-7230 solutions to and found to exhibit the

same behavior. Thus, the presence of cinnamic acid as a cause of the observed phenomenon was excluded.

Ultimately, the appearance of liquid crystalline structures of high viscosity further emphasizes that the phase behavior of Silwet L-7230/water was challenging for process control and a further processing of the extract. However, the sufficient density difference and high surfactant concentration in the extract made the system attractive for the design of a cloud point extraction.

The phase behavior, physical properties and extracting ability of the studied food- and cosmetic-grade surfactant systems indicated their applicability as solvents in the extraction of biological substances. Therefore, the CPE of cinnamic acid with Silwet L-7230 and ROKAnol NL5 was conducted in both batch and continuous mode. The performance of the single-stage process is discussed in the next chapter.

6.2.5 BATCH CLOUD POINT EXTRACTION OF CINNAMIC ACID

Trans-cinnamic acid was successfully accumulated in the surfactant-rich phase of both studied systems (see chapter 6.2.3). To compare them with regard to the process efficiency, the yield of the single-stage batch extraction at different initial surfactant concentrations was calculated according to **Equation 5-3**. The results obtained for both biphasic systems are presented in **Figure 6.13**.

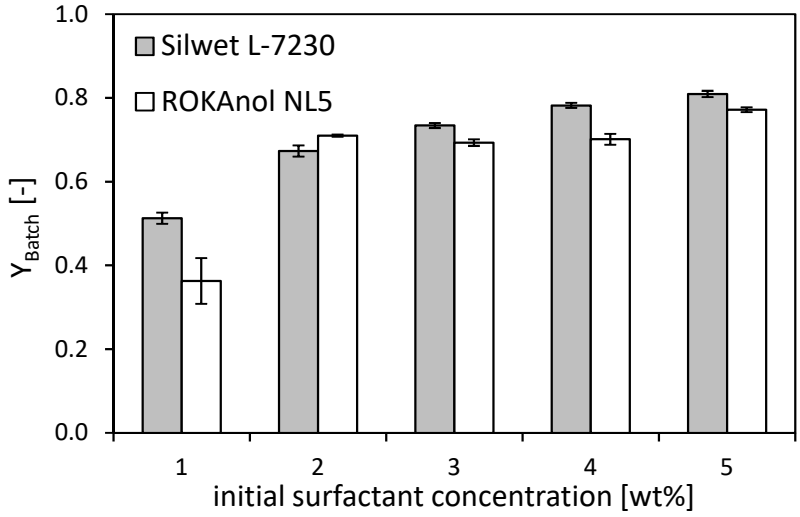

Figure 6.13: Cinnamic acid yield (Y_{Batch}) as a function of the initial surfactant concentration. Error bars indicate the standard deviation; N = 3.

According to Figure 6.13, the cinnamic acid yield of ROKAnol NL5 ranged between 36 ± 1 % for an initial surfactant concentration of 1 wt% and 69.3 ± 0.2% for 3 wt%. Further, the cinnamic acid yield was higher for Silwet L-7230 at 1 wt% initial surfactant concentrations. However, the yield as a function of the initial surfactant concentration exhibited the same trend for both surfactants and was comparable at initial surfactant concentrations > 1 wt%. Although an equal yield for different corresponding logP values might seem counterintuitive at first, one should consider the following: the micellar phase of Silwet L-7230 contained a higher surfactant amount than the micellar phase of ROKAnol NL5. However, the phase ratio in the ROKAnol NL5 system was higher. Consequently, an equal quantity of cinnamic acid in the micellar phase had to result in a higher cinnamic acid concentration in the micellar phase for Silwet L-7230. Hence, the corresponding logarithmic partition coefficient had to be higher as well.

The yield obtained within the food-grade and the cosmetic-grade system were in good accordance with the values for the Triton X-114 system (see Figure 6.1). A maximum yield of 80% was observed in case of all three surfactants. That observation proved the concept for applying a Silwet L-7230 and ROKAno NL5 for the cloud point extraction of cinnamic acid.

6.2.6 CONTINUOUS COUNTERCURRENT CLOUD POINT EXTRACTION OF CINNAMIC ACID

The transfer from batch to continuous mode enhances the productivity, as well as the extract purity in the liquid-liquid extraction process. For instance, a higher efficiency is obtainable in a countercurrent stirred column due to the higher number of theoretical stages (see chapter 2.3). Continuous countercurrent extraction of cinnamic acid was conducted as described in chapter 5.3 to demonstrate the potential of the food-grade and cosmetic-grade surfactant systems.

The parameters were set as summarized in Table 5.1. The choice of the process parameters was based on the LLE data and the batch experiments. Hence, the surfactant-rich phase (solvent) during the Silwet L-7230 experiments was pumped in at the top of the column as it was the heavy phase. During the ROKAnol NL5 experiments, the direction of the solvent was the opposite. The temperature was fixed at 39°C for Silwet L-7230 and 45°C for ROKAnol NL5. The ratio of the feed

(cinnamic acid solution) to the solvent (surfactant solution) was set in such a way, that a nominal surfactant concentration of approx. 3 wt% was ensured in the mixing zone. A lower stirring speed (15 rpm) was applied with the ROKAnol NL5 system due to the lower density difference.

The stability of the continuous extraction with both surfactants was compared based on the relative CA concentration (**Equation 5-5**) over the time. Hence, it was possible to observe normalized values, which were not influenced by the absolute concentration in the feed and raffinate. The corresponding plots are presented in **Figure 6.14**.

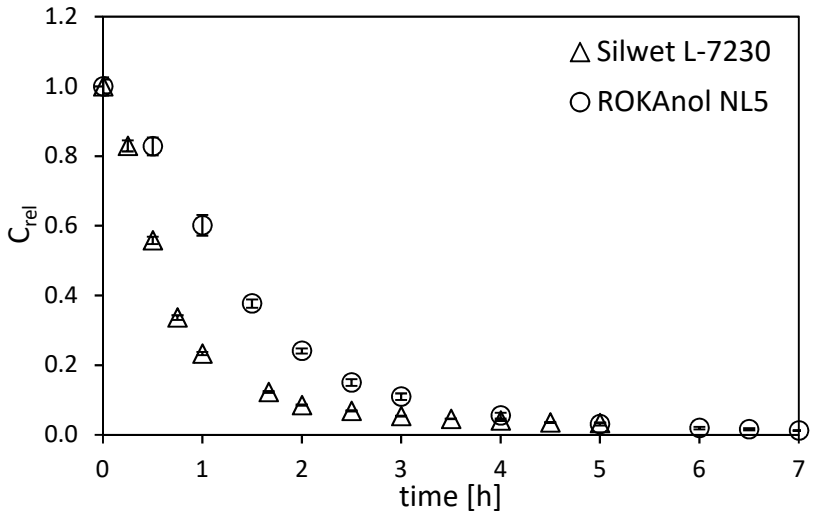

Figure 6.14: Time profiles of the relative cinnamic acid concentration ($c_{rel.}$) in the raffinate during the continuous extraction with Silwet L-7230 (39 °C) and ROKAnol NL5 (45 °C). Error bars indicate the standard deviation within each experiment. N=2.

As shown in **Figure 6.14**, the tracer's relative concentration in the raffinate initially decreased over time. That was due to the fact that the column was filled with feed at the beginning of all experiments. Subsequently, the tracer's relative raffinate concentration tended against a constant value (reaching the steady state). The steady state was reached after three hours at the experiments with Silwet L-7230. On the other hand, it took six hours to reach the steady state when performing the cloud point extraction with ROKAnol NL5. In comparison, the stationary state with the Triton X-114 system was reached after four hours at the operating temperature of 40 °C [43]. However, the lower density difference, as well as the opposite flow direction in case of ROKAnol NL5 could have resulted in the slower process stabilization. Fellechner et al. confirmed that observation, while observing a stationary state after 8 hours in the ROKAnol NL5 system [176]

Furthermore, the tracer's relative raffinate concentration in steady state was higher in the Silwet L-7230 raffinate than in the one of ROKAnol NL5. This was contrary to the expectation since the food-grade surfactant was denoted with a higher accumulation capacity for cinnamic acid. The yield, enrichment factor, and the number of theoretical stages were calculated as described in chapter 2.3 to evaluate the performace of the CPE. The corresponding results of the continuous cloud point extraction with Silwet L-7230 and ROKAnol NL5 is shown in **Table 6.2**.

Table 6.2: Performance of the cloud point extraction of cinnamic acid with food-grade and cosmetic-grade surfactant systems ($Y_{cont.}$): extraction efficiency, T_{CA}: enrichment factor, N_{theo}: number of theoretical stages)

surfactant	$Y_{cont.}$ [%]	$10logT_{CA}$	N_{theo}
Silwet L-7230	96.6 ± 0.1	2.35 ± 0.01	1.51 ± 0.01
ROKAnol NL5	103 ± 7	2.75 ± 0.06	5.6 ± 0.4

As shown in **Table 6.2**, the extraction efficiency was high enough to reach a yield of approx. 100% with both surfactants. Hence, the yield could be improved in comparison to the batch experiments. The enrichment of cinnamic acid in the micellar extract also attested for a pronounced accumulation of the solute in the extract. However, the number of theoretical stages reached with Silwet L-7230 was much lower than the value for ROKAnol NL5. Almost identical values describing the extraction performance in the system containing ROKAnol NL5 at 45 °C were reported by Fellechner et al [176]. On the one hand, this result illustrated the mass transfer limitations in the Silwet L-7230 system due to the high viscosity of the micellar phase. On the other hand, one observed 5.6 theoretical stages during the extraction with ROKAnol NL5. That illustrates the improvement of the separation in the ROKAnol NL5 cloud point extraction by the continuous process.

These results are comparable to the efficiency of the Triton X-114 continuous cloud point extraction of salicylic acid reported by Ingram et al. [43]. Moreover, the reached yield was higher than the result, achieved with Triton X-114 (see chapter 6.1.3). That is related to the lower total capacity, maintained during the experiments with Silwet L-7230 and ROKAnol NL-5.

Overall, the applicability of Silwet L-7230 and ROKAnol NL5 for a continuous extraction of aromatic compounds was confirmed at temperatures suitable for an

extraction of sensitive substances from biological materials. Further, the potential of the food-grade and the cosmetic-grade system was demonstrated in a batch and continuous extraction.

Ultimately, the results in chapters 6.1 and 6.2 prove the concept for a stable cloud point extraction in continuous mode, which is operated at mild conditions. Hence, the systems based on Triton X-114, Silwet L-7230 and ROKAnol NL5 are suitable for the direct recovery of sensitive solutes. Moreover, in case of good biocompatibility, the cloud point systems can be attractive as two-phase media for the direct ISPR from cell cultures as well.

However, such processes are beneficial, when the subsequent treatment of the extract stream is also not damaging the biomaterials. Therefore, several approaches for extract processing are discussed in the next chapter.

6.3 STRATEGIES FOR THE PROCESSING OF THE MICELLAR PHASE

The first issue concerning the extract is that the micellar phase is predominantly aqueous. This reflects in low solute concentrations in comparison with traditional organic solvents. Hence, alternative operations are needed to increase the solute and surfactant concentration in the extract. At first glimpse, this is possible by further increasing the temperature and thus elevating the surfactant concentration in the micellar phase according to the LLE (see Figure 6.8). However, in case of a thermally sensitive solute (e.g., natural antioxidants or unsaturated fatty acids), this approach may lead to solute degradation. As an alternative, the strategy to reach a higher solute concentration in the extract by recirculation of the solvent during the continuous cloud point extraction was evaluated. Additionally, the filtration of the final extract through a membrane with suitable cut-off may allow the retention of the loaded micelles from the aqueous bulk. The evaluation of these approaches is presented further in this chapter.

6.3.1 RECIRCULATION OF THE MICELLAR PHASE*

** The results in this chapter were part of the Master thesis by Dennis Wenzel [173].*

The recirculation of gathered extract was investigated to increase the concentration of cinnamic acid in the extract and to save surfactant. The surfactants Triton X-114, Silwet L-7230 and ROKAnol NL5, were used for the experiments as described in chapter 5.3. The recirculation was switched on after 150 min, as marked by the dotted line. However, the chosen process conditions for the continuous extraction with Triton X-114 did not fully correspond to the parameter combination, which was obtained from the response surface methodology (see chapter 6.1.2 - 6.1.4). Namely, the feed-to-solvent ratio was decreased from 6 to 5, the capacity – from 1 to 0.8, and the agitation speed – from 43 to 25. Hence, no maximum of the productivity was expected. Nevertheless, the new parameters allowed a comparison to Silwet L-7230 as well. The conditions for the CPE with recirculation of the solvent using Silwet L-7230 and ROKAnol NL5 were analogous to the experiment without recycling of the micellar phase.

In **Figure 6.15**, the continuous extraction of cinnamic acid with extract recirculation using Triton X-114 at 40°C is compared to the corresponding Silwet L-7230 and ROKAnol NL-5 process.

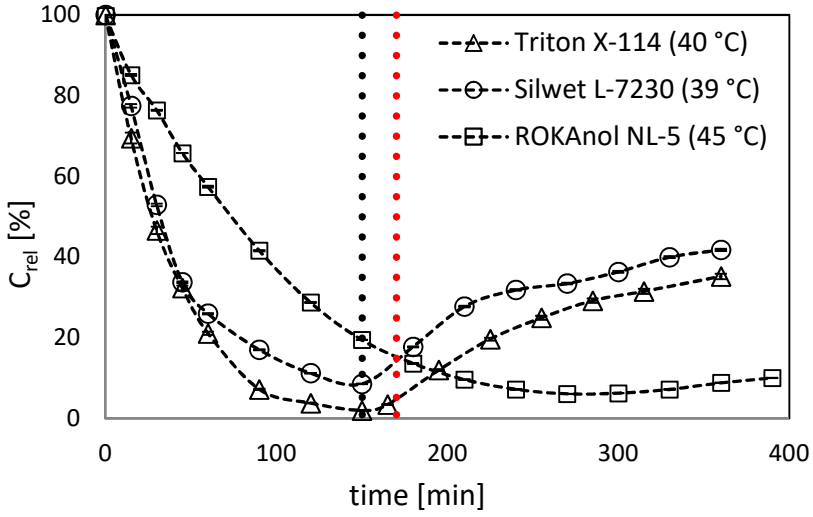

Figure 6.15: Time profiles of the relative raffinate concentration of cinnamic acid during the continuous extraction with Silwet L-7230 at 39 °C ROKAnol NL-5 at 45 °C and Triton X-114 at 40 °C, with recirculation of the extract. Error bars indicate the standard deviation within each experiment; N=2. The dotted line indicates the time of the recirculation start (in black for Silwet L-7230 and Trion X-114 and in red for ROKAnol NL-5). Dashed lines are added to guide the eyes.

As can be obtained from **Figure 6.15**, the tracer's relative raffinate concentration first decreased with time. The time profile of the cinnamic acid concentration in the raffinate was steeper for Triton X-114 and Silwet L-7230 than the one corresponding to ROKAnol NL-5. That was in accordance with the results shown in chapters 6.1.2 and 6.2.6 and could be explained with the lower density difference, the opposite flow direction, and the resulting slower separation in the settling zone in case of ROKAnol NL5. However, the cinnamic acid amount in the raffinate started increasing, as soon as the extract recirculation was initiated. Cause for that effect was the lower concentration gradient between feed and recirculated solvent than between feed and fresh solvent since the recirculated solvent was already loaded with cinnamic acid. Consequently, the time profile of the relative raffinate concentration showed an increasing trend, as the recirculated extract could take up less cinnamic acid with each recirculation run. That effect was more pronounced in case of Silwet L-7230 and Triton X-114. Again, due to the moderate reduction of the concentration gradient, the system based on ROKAnol NL-5 was reacting "slowly" to the loaded solvent. Therefore, only a slight increase of the relative

cinnamic concentration in the ROKAnol NL-5 micellar phase could be registered within that limited experiment duration.

Based on these results, it can be assumed that mass transfer of solute into the extract would get continously worse for longer process times. Therefore, the tracer's relative raffinate concentration would eventually increase up to the initial value of 100%, when no further cinnamic acid could be extracted. That observation is in good agreement with the theory concerning extraction processes in chapter 2.3.

Further, in Figure 6.15 can be observed, that the tracer's relative raffinate concentration decreased less pronounced for Silwet L-7230 than for Triton X-114 and ROKAnol NL-5, before extract recirculation was switched on. That was expected based on the better performance of the Triton X-114 and ROKAnol NL-5 in comparison with Silwet L-7230. However, the tracer's c profiles showed an equal incline after the beginning of extract recirculation for both Silwet L-7230 and Triton X-114. That may be due to the higher affinity of the Silwet L-7230 micellar phase to load cinnamic acid. Hence, when the mass-transfer is limited due to the lower concentration gradient, then the higher capacity of the Silwet L-7230 system is compensating for that limitation.

As shown in chapter 6.2.4, Silwet L-7230 extract turned to a liquid crystalline phase at room temperature. This phenomenon played a crucial role in the experiments with recirculation. Hence, after some time, recirculated extract was stuck in the solvent feed tube or re-entered the column in a liquid crystalline state. By this means, it was immiscible at the applied agitation speeds. Concerning that critical aspect, Silwet L-7230 was described as not suitable for the extraction with recirculation.

In addition, the constant change in the solute concentration in the extract led to elevated surfactant concentration as well. The plots in Figure 6.16. illustrate the concentration of the tracer and the surfactant over the time during the continuous extraction of cinnamic acid with Triton X-114.

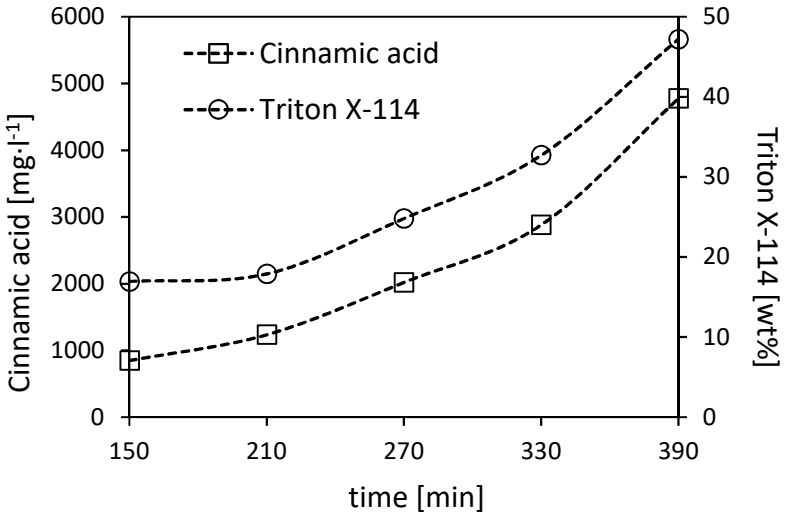

Figure 6.16: Cinnamic acid and surfactant concentration of recirculated extract phase as a function of time for the continuous extraction with Triton X-114 at 40 °C. Lines are added to guide the eyes.

As can be obtained from **Figure 6.16**, the concentration of cinnamic acid and Triton X-114 within the recirculated extract increased over time. That can be explained as follows:

Every run of recirculated extract phase was higher concentrated with cinnamic acid than the previous one. Therefore, also the extract surfactant concentration continuously increased due to the cloud point reduction caused by cinnamic acid at such high concentration levels. Consequently, the volume of extract phase at the bottom of the column, which could be recirculated, steadily decreased until the column bottom ran empty. For solving this problem in further experiments, it was necessary to either adjust the process temperature or to lower the recirculated extract's surfactant concentration by dilution. The dilution by mixing the extract with fresh solvent in order to minimize the latter effect was applied during the experiments with authentic feed solutions.

Overall, the recirculation of the extract phase until reaching its saturation with solute is beneficial due to the lower amount of surfactant for the extraction. Additionally, a higher loading with the target compound is also achievable. However, when further applying the approach, the operation of the process has to be adapted correspondingly.

6.3.2 NANOFILTRATION OF SURFACTANT SOLUTIONS

The filtration was tested in this work as a possible technique to further concentrate the micellar phase after the extraction. Filtration is a standard method to separate surfactants from wastewater [177]. Additionally, when there are solutes solubilized in micelles, the ultrafiltration can be applied for the enrichment of the micelles in the retentate [178]. In this work, the main idea was to implement a nanofiltration module and thus separate water mainly with the permeate. As a result, it was expected to keep the loaded micelles in the retentate and thus increase the surfactant and solute concentration in the extract.

The feasibility of the nanofiltration for surfactant accumulation was demonstrated through an experiment as described in chapter 5.6. The separation of Triton X-114 from water was subsequently evaluated by the permeate flux and the rejection of the amphiphile (**Equation 5-8**). The feed was set to 16.5 wt% surfactant concentration to "simulate" a micellar phase. The concentration of the surfactant in the permeate was 0.091 wt%, which resulted in a retention of 99.5 % for the Triton X-114. However, that value was reached at a low permeate flux of 0.860 L m^{-2} h^{-1}. In comparison, the permeate flux with pure water was 47.619 L m^{-2} h^{-1}. That result was expected, since the rejection was high. The sufficient retention of the nonionic surfactant was in good agreement with the data by Cornelis et al. [177]. Hence, the applied membrane Microdyn-Nadir NP 030 was suitable for the concentration of the micellar extract. The advantage of that approach is the operation at low temperatures, suitable for sensitive solutes. However, the fouling of the membrane in case of cells or other plant solids in the micellar phase must be accounted as well. Therefore, in case a filtration is chosen as an enrichment step for the extract, additional experiments with the extract from the original feed have to be conducted.

6.3.3 CLOUD POINT EXTRACTION WITH "LEAVE-IN" SURFACTANTS

Overall, the techniques described above, result in a higher solute accumulation and lower water content of the micellar phase. However, as described in the state of the art, the recovery of the target substance from the micellar extract is conducted by mass transfer to additional phase (vapor/gas or a second liquid phase) or by micelle breakage via cooling. The change of the emulsion type is another possibility to alternate the solute partitioning (see chapter 3.4). When designing a mild separation process using a surfactant with lesser environmental impact, the introduction of traditional organic solvent or heat for evaporation are not compatible with the process scheme. Additionally, the cooling of the system below the Kraft temperature of surfactants requires an extremely high energy input [151].

On the other hand, the CPE was utilized for isolation of phenolic compounds, antioxidants or pigments, which are mainly applied as ingredients in foods and cosmetics [72]. A standard technique for the even distribution of such substances in beverages or personal care products is the addition of commercial surfactants [91,92]. Therefore, it can be beneficial to design a cloud point extraction of the natural substance with a surfactant, which is applied in the final market formulation (leave-in surfactant). Hence, there will be no need for a cost-intensive separation (or just a rough separation) of the target molecule from the surfactant.

For instance, silicone polyether are applied as wetting or antifoaming agents, but also as additives in food. The studied Silwet L-7230 also represents a surfactant from this family. Additionally, various cosmetic products contain ethoxylated alcohols as secondary surfactants, from the family of ROKAnol NL5. Consequently, the studied Silwet L-7230 and ROKAnol NL5 are attractive as leave-in surfactants for the cloud point extraction of solutes for food or cosmetics.

Considering the remarks and observations in this chapter, an in situ continuous cloud point extraction with a leave-in surfactant can be beneficial in two ways. Firstly, the continuous application allows the recirculation of the solvent. Hence, a higher solute concertation is achievable. Additionally, the recycling of the micellar phase decreases the required amount of surfactant. Secondly, there is no need of a complete stripping of the amphiphile and the target compounds in the extract

due to the permission of the surfactant in the final formulation. Thus, the processing of the raw extract can be less laborious and complicated.

However, all the results presented so far corresponded to the model solute cinnamic acid. Biological feedstock, such as cell cultures, juices or other slurries possess a diverse composition. Hence, the multicomponent mixture can affect and destabilize the extraction system [148]. Therefore, the feasibility of the cloud point extraction with natural fruit juice and algae culture is discussed in the following chapter.

6.4 FEASIBILITY OF THE CLOUD POINT EXTRACTION FROM GENUINE FEEDSTOCK

Plant materials are rich in hydrophobic compounds, as described in chapter 2.8. Moreover, the valuable compounds in the natural sources can replace synthetic dyes and aromatic substances in foods and cosmetic formulations. The continuous cloud point extraction using nonionic surfactants at mild conditions is advantageous for the direct isolation of such hydrophobic compounds from plant suspensions. Hence, the feasibility of the micellar extraction was demonstrated through experiments with Triton X-114, Silwet L-7230, and ROKAnol NL5 with two authentic feed solutions.

Firstly, a fruit juice was utilized as a feed. It consisted of pressed and filtered pineapple juice, prepared as described in chapter 4.5. That feedstock was rich in phenolic compounds, pigments, and sugars (see 2.8). According to the state of the art, such fruit valuable compounds were separated successfully via cloud point extraction (see chapter 3.2.1). Therefore, the suitability of the new surfactant ROKAnol NL5 for the mild isolation of phenolic compounds from pineapple juice was investigated.

Secondly, cloud point systems were utilized as media for the in situ product removal from cell broths (see chapter 3.2.1). The most of the related contributions described an indirect isolation of target compounds. However, the studies of Glembin et al. reported a direct in situ removal of fatty acids from green microalgae cultures using nonionic surfactants [9,132]. That process was applicable, due to the good biocompatibility of Triton X-114 with the culture. Since green microalgae contain not only unsaturated fats but also pigments and antioxidants (see chapter 2.7), their cultures were utilized as feed in this work as well. To that purpose, the approach by Glembin et al. [9,132] was extended from batch to continuous mode. Additionally, the compatibility of the surfactant Silwet L-7230 and ROKAnol NL5 with the green microalgae *Acutodesmus obliquus* was studied.

Based on the results, the feasibility of the cloud point extraction from different genuine feedstocks could be evaluated. The results from the laboratory and technical scale studies are presented further in this chapter.

6.4.1 CLOUD POINT EXTRACTION FROM PINEAPPLE JUICE *

** The experimental work for this chapter was completed during the internship of Boryana Petrova.*

The cloud point system, based on ROKAnol NL5, was chosen for the batch extraction from natural fruit juice, due to its lighter micellar phase (see density difference in **Figure 6.10**). Consequently, less accumulation of solids in the extract was expected. The cloud point extraction with ROKAnol NL5 from pineapple juice was carried out according to the procedure in chapter 5.6., as an ISPR with the internal removal of the extract (see **Figure 2.10** a).The steps included defrosting of the feed, mixing of the samples with the surfactant and a final phase separation at 45 °C.

However, it is well known that processing influences the quality and composition of fruit juices [61,78]. Therefore, the influence of the three cloud point extraction steps on the phenolic content in the pineapple juice was preliminary determined. The evaluation was based on the gallic acid equivalents (GAE) method in chapter 5.11.3. The results for fresh and defrosted juice are presented in **Figure 6.17**.

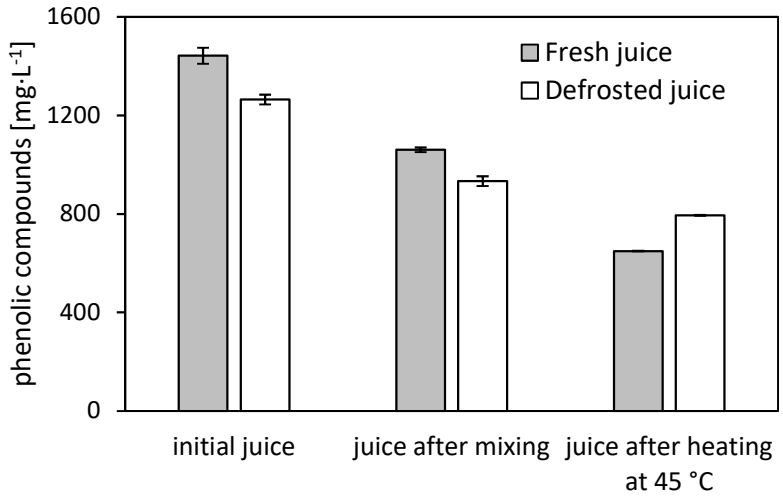

Figure 6.17: Phenolic content (GAE) in fresh and defrosted pineapple juice during the stages of the cloud point extraction in laboratory scale. Error bars indicate the standard deviation, N=3.

All process steps influenced the phenolic content of the juice. Initially, the amount of GAE in the fresh and the defrosted juice was above 1200 mg·L^{-1}. Those values were comparable to reported phenolic content in authentic fruit juice [77]. Freezing the juice to -20 °C led to an only slight reduction of the total phenolic content. That observation was in accordance with the rule, that frosting is the mildest approach for preserving the freshness of plants [61]. However, the

subsequent mixing and heating to 45 °C were characterized by a further reduction of the phenolic concentration in both juices. The observed trend was similar for the mixing step. The defrosted juice was stable during the exposure to 45 °C. Overall, during the processing, only 44 % and 61% of the GAE remained in the fresh and defrosted feedstock, respectively. As expected, the exposure to air induced the oxidation of the antioxidants and thus decreased the GAE value. Additionally, probably some of the thermal sensitive compounds were partially degraded at 45 °C [61].

Still, in comparison to processed pineapple drinks from the local market, the concentration of the phenolic compounds was 100-times higher. Hence, the cloud point extraction of the pineapple juice was beneficial at the proposed conditions. Whereby, the defrosted juice was more suitable as feedstock. Therefore, a cloud point extraction with ROKAnol NL5 was investigated.

The process performance was evaluated by their phenolic content. The GAE was determined in the feed after the mixing. Subsequently, the phenolic contents in the micellar and the aqueous phases were compared to the initial sample. Additionally, the antioxidant capacity was determined using the DPPH reduction according to the method in 5.11.4. The corresponding results are depicted in **Figure 6.18**.

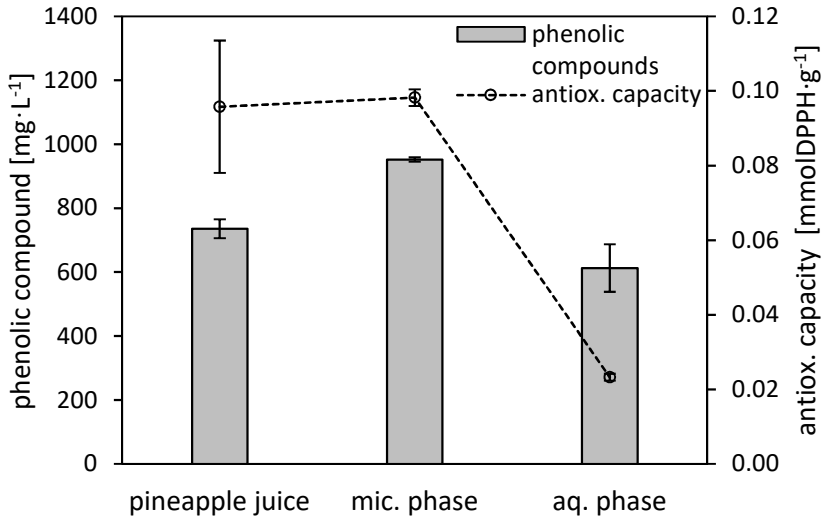

Figure 6.18: Phenolic content (GAE) and antioxidant capacity of the in the feed compared to the micellar and to aqueous phases after the cloud point extraction with ROKAnol NL5 at 45 °C. Error bars indicate the standard deviation, N=3.

The initial GAE concentration in the feed was lower than the phenolic content in the micellar phase. Additionally, as depicted in Figure 6.18, the GAE fraction in the aqueous phase was comparable to the initial value. Thus, an accumulation of phenolic compounds in the surfactant-rich phase was achieved during the CPE with ROKAnol NL5. Additionally, the reduction of the phenolic content in the aqueous phase was similar to the observations for defrosted juice (see figure Figure 6.17). That proved the concept that despite the reduction of the GAE value in the juice an accumulation of phenolic compounds using the cloud point extraction is possible. However, the yield of phenolic compounds in the extract was equal to 27 %. In comparison to the batch cloud point extraction of the model solute cinnamic acid (Y_{Batch}= 69 %), the observed yield from the authentic feedstock was lower. On the one hand, the degradation of the phenolic compounds may be responsible for the limited accumulation. On the other hand, the phenolic compounds in the pineapple juice might have lower affinity to solubilize in the micelles than the cinnamic acid. The incomplete recovery of phenolic compounds in a single-stage extraction was in the range of to the yields, observed by Gortzi et al. The authors reported yields of approx. 30 % for the model phenolic compounds gallic acid, rutin and epicatechin in the cloud point system of Genapol X-080 [111]. The recovery of phenolic compounds from 17 – 36 % was also reported for the extraction from fresh apple, sweet lemon and mango juices using different nonionic surfactants [115]. The limited yield of phenolic compounds could be enhanced by performing the cloud point extraction in continuous mode. However, the limited amount of feedstock was not sufficient to perform such experiments in technical scale.

Nevertheless, according to the mass balance, 90 % of the initial GAE were distributed between the coexisting phases. The value was higher than the results obtained for surfactant-free juice. The reason for that may be the preserving effect of ROKAnol NL5 micelles against interaction of the phenolic compounds with the environment.

Gallic acid and its equivalent molecules possess a high antioxidant activity. The reduction of the DPPH, presented in Figure 6.18, corresponded to the antioxidative capacity before and after the cloud point extraction. The amount reduced DPPH per gram sample was similar for the samples of the feed and the extract phase. Hence, the antioxidative effect was preserved in the micellar phase. However, a reduction of the DPPH-value was obtained for the aqueous phase. That was

contrary to the GAE-value in the surfactant-lean phase. It could be assumed, that the decrease in the antioxidant capacity was due to reduction reactions induced by air exposure and heating. Therefore, the UV-signal at 275 nm was unchanged since the aromatic group was still present in the solution. On the other hand, there were no available groups for the DPPH reduction. In can be concluded, that the observations regarding the antioxidant capacity were further evidence for the preserving effect of the surfactant in the micellar phase. The same tendency was reported for the antiradical activity of the micellar extract from the red-flesh orange juice. However, the authors did not present a more in-depth study on the influence of the micelles on the antioxidant activity [7].

Pineapple juice contains a significant amount of sugars. Solutes such as glucose and fructose can influence the phase separation in cloud point systems [90]. Therefore, the distribution of reducing sugars between the coexisting phases was analyzed according to the method in chapter 5.11.5. The comparison between the sugar content in the initial mixture to the micellar and the aqueous phase is presented in Figure 6.19.

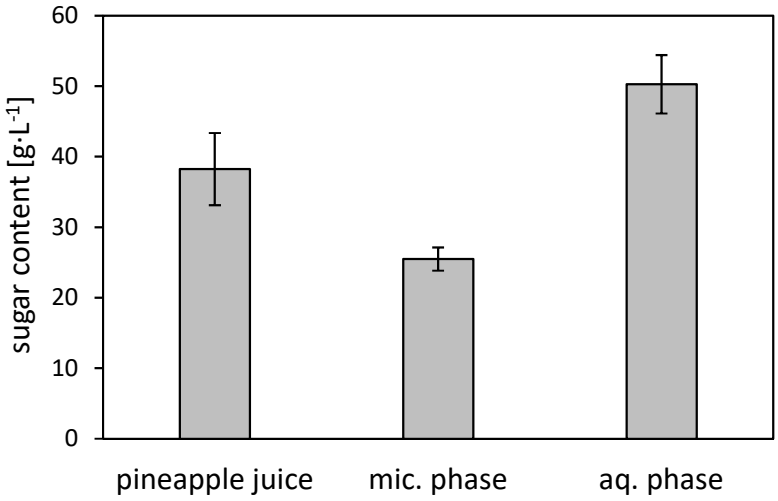

Figure 6.19: Sugar content in the feed compared to the micellar and to the aqueous phases after the cloud point extraction with ROKAnol NL5 at 45 °C. Error bars indicate the standard deviation, N=3.

The concentration of reducing sugars in the feed was 38 $g \cdot L^{-1}$. Subsequently, an uneven sugar distribution was observed. A two-times higher sugar concentration was constituted in the aqueous phase in comparison to the micellar phase. That result was in agreement with the observations by Ritter et al. In their contribution, the authors implemented sugars to elevate the density difference between the lighter micellar and the aqueous phase. Hence, it was possible to stabilize the cloud

point system for the continuous extraction in a stirred column. That was a result of the accumulation of the hydrophilic sugars in the surfactant-lean phase [90]. The same effect can be expected in case of the CPE from fruit juices. The influence of the fruit sugars can lead to more stable phase separation in a biphasic system with lighter micellar phase. Therefore, the sugar content must be considered when designing a direct product recovery from natural feedstock using a surfactant solution.

Lastly, a yellow coloring was observed in the micellar phase. The primary extract in depicted in the most left of **Figure 6.20**.

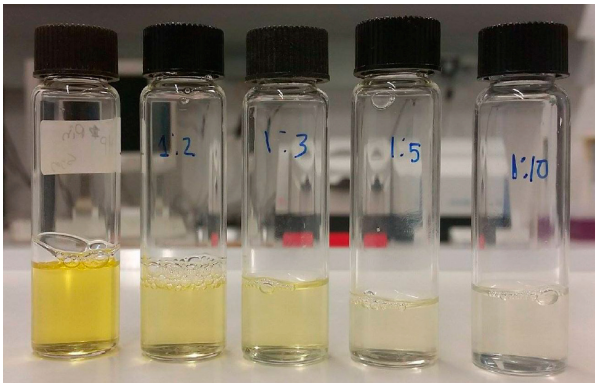

Figure 6.20: Pigment accumulation in the micellar phase. From left to right: no dilution, 1:2, 1:3, 1:5 and 1:10 dilutions.

The observed yellow color was evenly distributed and stable at further dilution, as illustrated in **Figure 6.20**. Additionally, the texture was homogeneous and free of visible solids. The coloring of the micellar phase was due to the accumulation of pigments. The exhibited affinity of the micellar phase to accumulate tocopherol, carotenoids or other yellow and red pigments was reported previously [6,7,122]. Such solubilized colorants can evenly distribute in beverages with high water content, without changing the texture [92]. Hence, the micellar phase could be applied as coloring agent with antioxidant activity in cosmetic formulations.

Overall, the cloud point extraction of phenolic compounds with the cosmetic-grade surfactant ROKAnol NL5 was feasible in batch mode. The conditions used for the separation of the model solute were applicable with the fruit juice as well. After maintaining stable phase separation, an accumulation of phenolic compounds and colorant was achieved. The target compounds maintained their antioxidant capacity into the micellar phase. Moreover, the sugars in the feed lead to further stabilization of the phase separation. Finally, a micellar phase with homogeneous

texture was produced. It can be concluded, the cloud point extraction with ROKAnol NL5 is suitable for the isolation of valuable compounds from fruit juices. In addition, the extract phase can be utilized as an ingredient for cosmetic formulations, due to the permission of the surfactant in such products. Ultimately, the concept for a cloud point extraction from a natural feedstock using leave-in surfactants was successfully implemented with the pineapple juice.

The results confirmed the suitability of the cloud point extraction for the recovery of valuable compounds from the sensitive fruit juice. In addition, the mild technique is also attractive for the product removal from living cell suspensions, such as green microalgae. The feasibility of the continuous cloud point extraction from microalgal cultures is thus presented in the next chapter.

6.4.2 CONTINUOUS IN SITU EXTRACTION FROM MICROALGAE CULTURES IN TECHNICAL SCALE*

** Some of the results in this chapter were published in the contribution: "In situ continuous countercurrent cloud point extraction of microalgae cultures"* [168]*. The biocompatibility experiments were conducted by Jens Johannsen and Marten Lange for their Bachelor theses* [179,180].

Glembin et al. demonstrated a direct in situ removal of fatty acids from the green microalgae *Acutodesmus obliquus* using the surfactant Triton X-114. The surfactant was chosen based on the good biocompatibility with the applied strain. Furthermore, the formation of the two phases was stable in the presence of algae cells. An accumulation of the product palmitic acid in the micellar phase was observed after performing a batch separation. Moreover, the feasibility of the cloud point extraction was confirmed in a pilot scale as well. However, the efficiency of the single-stage extraction was limited through the low solute concentration in the feed (approx. 0.20 $mg \cdot L^{-1}$) [9,132].

It was necessary to increase the ratio between the algae culture and the solvent to elevate the extraction efficiency. This is possible via a continuous countercurrent extraction with solvent recirculation. Therefore, the micellar in situ extraction from *A. obl.* with the surfactant Triton X-114 was developed in this work. The parameters for the countercurrent extraction from green microalgae are summarized in **Table 5.2**. The feed-to-solvent ratio and the column capacity were set in accordance to the extraction of cinnamic acid. However, the agitation speed was set to 40 rpm aiming to intensify the mass transfer.

As described in chapter 4.3, the green microalgae are cultivated in tap water. However, tap water contains impurities, which could influence the phase behavior of Triton X-114. Hence, an initial investigation on the effect of tap water on the continuous CPE with solvent recirculation was conducted using the technical scale equipment. The experiments were conducted analogically to subsequent continuous extraction from a microalgal culture with solvent recycling, whereby pure tap water was set as a feed (see chapter 5.8).

The influence of the feed was evaluated based on the surfactant distribution in the raffinate and extract over the time. The Triton X-114 concentration over the time in the corresponding stream is presented in Figure 6.21.

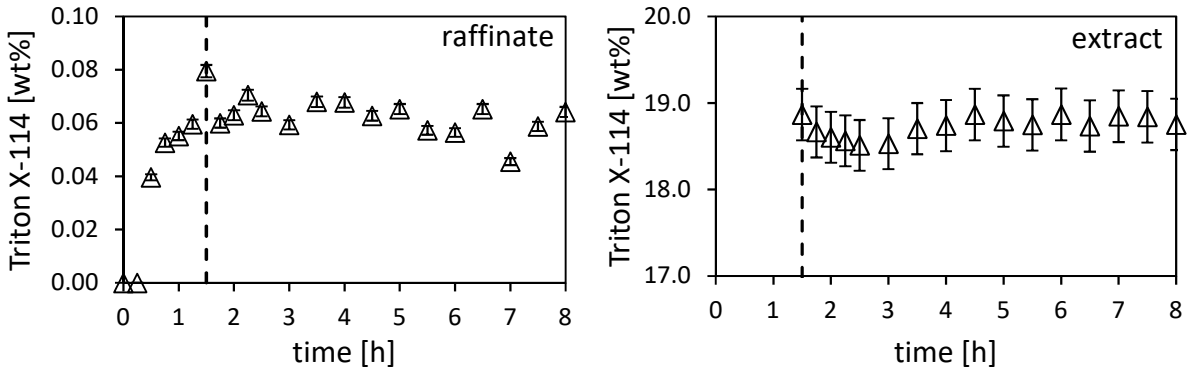

Figure 6.21: Triton X-114 concentration profiles in the raffinate and the extract during the experiment with tap water as feed. Error bars indicate the standard deviation within each experiment. N=2. The dashed line indicates the time of the recirculation start.

The duration of the validation experiments was 8 hours, whereby the extract recirculation was initiated after 1.5 hours. Die Triton X-114 amount in the raffinate was elevating until a stationary state was reached after 3.5 hours. The average surfactant concentration in the raffinate after the reaching of the stationary state was 0.061 ± 0.007 wt%. The corresponding fluctuation of 11% could be explained with the pulsation of the pumps and the sampling. It is important to note, that the Triton X-114 fraction in the raffinate was kept below the stress limit.

The micellar phase was let out of the column's bottom after 1.5 hours. The extract flow was directed to the solvent vessel, and thus the recycling of the solvent was initiated. There were no noticeable fluctuations of the surfactant concentration in the extract stream. The average Triton X-114 concentration was estimated to 18.8 ± 0.1 wt%. Since the initial solvent contained 20 wt% surfactant, the recirculation resulted in dilution of the micellar phase. As a result, a final concentration of 19.9

wt% was obtained in the solvent vessel. That result was contrary to the increase of the surfactant content in the micellar phase after the continuous extraction of the cinnamic acid (see Figure 6.16). That can be explained with the different composition of the tap water in comparison to the feed containing tracer molecules. It was possible that the species in the tap water had a slight effect on the equilibria, resulting in a lower Triton X-114 concentration in the micellar phase. Therefore, that effect had to be considered for the further experiments with feed containing tap water from the region of Hamburg.

The mass balance calculation according to Equation 5-11 resulted in a deviation of 2.12 %. Moreover, similar surfactant profiles in the extract and raffinate during the continuous cloud point extraction with Triton X-114 at 40 °C, without recirculation of the solvent were reported by Ingram et al. [43]. The authors observed a stationary state after 4 hour, which was in accordance with the observation in the present work. It can be concluded that the CPE was stable in the presence of tap water. However, the change in the solvent composition during the recirculation must be accounted to prevent insufficient Triton X-114 concentration in the mixing zone.

Further, a long-term continuous extraction of green microalgal culture was carried out as described in chapter 5.8. The process parameters were kept analogs to the tap water experiments. The feed consisted of *A. obl.* culture with CD=1.4±0.2 $g \cdot L^{-1}$. The microalgae cultivation was conducted as summarized in chapter 4.3. The feasibility of the technique was evaluated by comparing the Triton X-114 profiles in the extract and raffinate to the reference experiment with tap water.

The surfactant concentration profile in the raffinate over 24 hours is depicted in Figure 6.22.

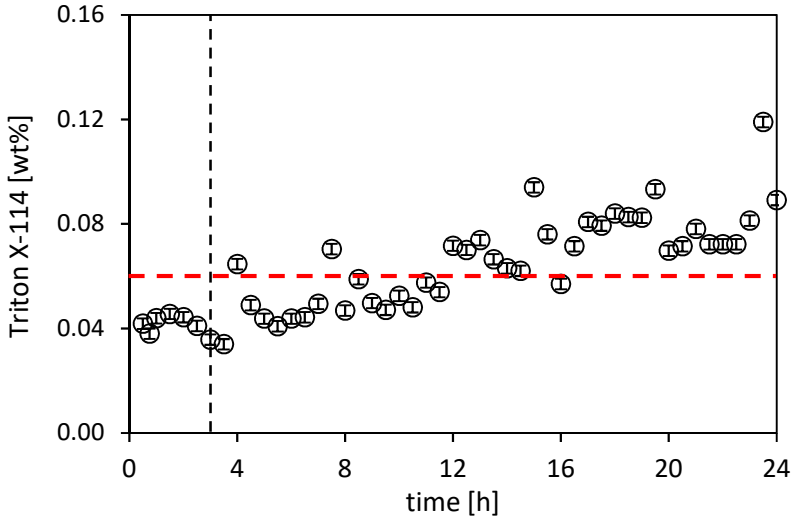

Figure 6.22: Triton X-114 concentration profile in the raffinate, during the experiment with microalgal culture as feed. Error bars indicate the standard deviation within each experiment. N=2. The black dashed line indicates the time of the recirculation start. The red dashed line corresponds to the average Triton X-114 concentration in the raffinate of the algae-free experiment.

The Triton X-114 concentration in the raffinate changed in the range from 0.03 to 0.12 during the 24 hours. Before the recirculation start (black dashed line in **Figure 6.22**) the values remained similar. However, after the initiation of the extract recirculation, an elevation of the Triton X-114 fraction was observed up to the end of the experiment. No apparent settling of a steady state value was observed. The accumulation of microalgae cells in the extraction column, which was observed during the complete experiment, might have been the reason for the unsettled surfactant profile in the raffinate

The average surfactant concentration in the algae culture leaving the extraction column was estimated to 0.06 ± 0.02. The results corresponded to the reference experiment (red dashed line in **Figure 6.22**). However, the high deviation and the constant elevation of the concentration only allowed a row comparison. Nevertheless, the stress limit of 0.2 wt% was not reached within 24 hours.

The surfactant concentration profile in the extract was evaluated as well. The plot in **Figure 6.23** illustrates the Triton X-114 fraction in the extract stream over the time.

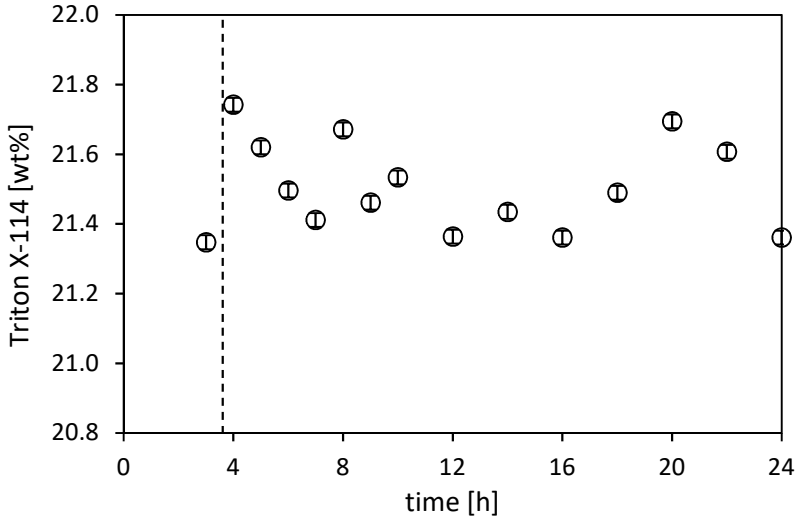

Figure 6.23: Triton X-114 concentration profile in the extract, during the experiment with microalgal culture as feed. Error bars indicate the standard deviation within each experiment. N=2. The black dashed line indicates the time of the recirculation start.

In contrast to the raffinate profile, the surfactant concentration in the extract remained at an average of 21.5± 0.1 during the entire experiment. The deviation of 0.6 % represented the stable micellar phase composition. The mean Triton X-114 fraction was higher than the corresponding value in the reference experiment with tap water. That could point out the influence of the algae culture on the phase behavior.

More precisely, the initial solvent composition was set to 20 wt% Triton X-114. At the end of the experiment, the fraction of surfactant in the solvent vessel was equal to 21.23±0.03, corresponding to an overall increase in the Triton X-114 concentration in the micellar phase. That observation was in accordance with the result of the cloud point extraction of the model solute cinnamic acid (see **Figure 6.16**). It could be assumed, that the accumulation of algae products in the extract induced an increase of the surfactant fraction.

Overall, the mass balance regarding the surfactant resulted in a deviation of 12.7 %, which was higher than the estimated value for the reference algae-free experiment. That could be explained with entrainment of micellar phase in the biomass, which was accumulated near the feed entrance at the bottom of the column. The intense algae flocculation in the column can be contributed to the cell reaction to the environmental stress. In such case, the cells built colonies, which eventually aggregate to more massive flocks [136].

The comparison between the continuous cloud point extraction in the presence and absence of algae cells illustrated the impact of the suspended cells on the process stability. Nevertheless, a stable extract composition and surfactant concentration below the stress limit were maintained during the long-term in situ extraction from *A. obl.* culture. The recirculation of the extract resulted in a reduction of the needed solvent and a culture-to-solvent ratio equal to 46.

Additionally, the total amount of extracted compounds from microalgae was calculated according to **Equation 5-9**. Overall, 0.4 ± 0.2 $g_{Algae\ product}/kg_{Culture}$ could be obtained. In comparison, the yield of 39.3 % of the tracer extraction led to 0.08 $g_{Cinnamic\ acid}/kg_{Feed}$ that were extracted at the optimal operating conditions according to the response surface method (see chapter 6.1.4). The reason for the difference may be lower partition coefficient of CA in comparison to other lipids and fatty acids in the algae culture [132].

A further important issue was the analysis of the solvent composition. An attempt to isolate the extracted compounds was made via analytical SEC (see chapter 5.11.2). A chromatogram of the analyzed extract is shown in **Figure 6.24**.

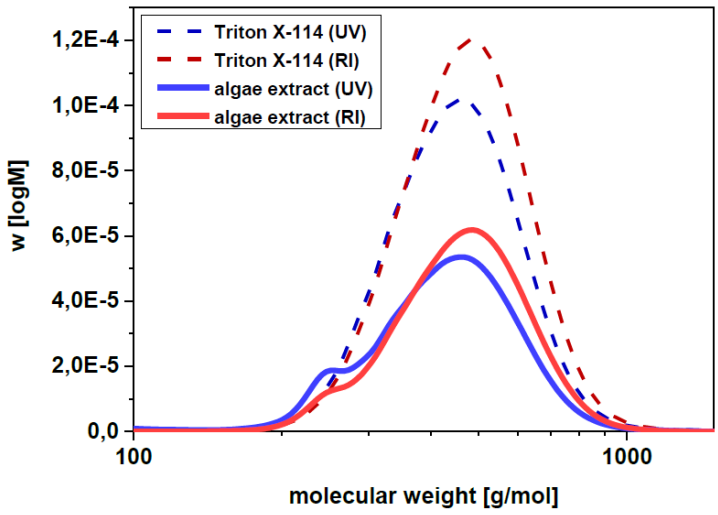

Figure 6.24: SEC chromatogram of the algae extract and aqueous Triton X-114 solution

The RI and UV signal of the sample separated using SEC were obtained as a function of the molecular weight of the fraction. The distribution in the extract was compared to a standard sample, which consisted only of Triton X-114 and water. Apparently, no compounds outside of the peak area of Triton X-114 were visible. Furthermore, the peak in the chromatogram of the microalgae products overlapped with the peak of the pure Triton X-114. Hence, no characterization of the extract

using SEC analysis was possible. Glembin et al. also reported an overlapping of the peaks corresponding to the surfactant and the microalgae products in the gas chromatography [9]. Overall, the analytical separation of the products from the surfactant Triton X-114 remained challenging, and thus no corresponding extract composition could be presented in this thesis. Nevertheless, a use of a surfactant, whose peak did not overlap with the products and a suitable analytical method, could allow a sufficient characterization.

Another aspect of the experiment with cell culture was to assess the biocompatibility of the continuous process. For this purpose, the photosynthetic activity of the algae in the raffinate was monitored during the continuous extraction with Triton X-114. The PA was normalized against a surfactant-free reference at room temperature. Hence, the relative photosynthetic activity of *A. obl.* cells in the raffinate over time could be calculated (see the method in 5.11.8). The corresponding results are presented in **Figure 6.25**.

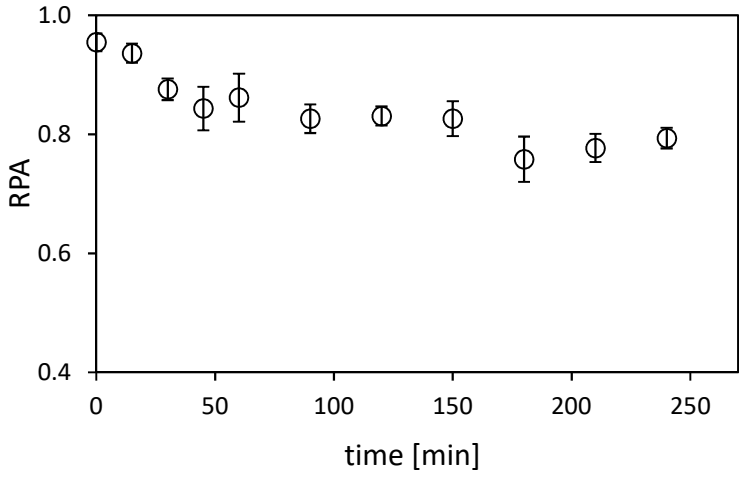

Figure 6.25: Relative photosynthetic activity of *Acutodesmus obliquus* cells in the raffinate over time. Error bars indicate the standard deviation, N=3.

The photosynthetic activity of the algae cells did not change significantly over the time. A slight decrease to approx. 80 % of the control was observed. However, the RPA values remained unchanged at 0.8. That referred to a good biocompatibility of the extraction set-up at residence time from 1 to 2 hours of the cells in the column. The RPA of the same microalgae strain during the batch cloud point extraction with Triton X-114 at 37 °C was investigated by Glembin et al. [9]. In contrast to the results in this thesis, the photosynthetic activity of *A. obl.* remained

at 98 % of the surfactant-free control. That can be explained by the higher operating temperature applied for the continuous extraction. However, the observed RPA reduction was still tolerable for the algae cells. This result proved the feasibility of the continuous cloud point extraction as a comparably mild technique for gaining valuable products from cell cultures.

In order to take a deeper look at the influence of the surfactant on the microalgae, scanning electron micrographs of untreated cells (**Figure 6.26**a) and cells from the surfactant-lean phase after a cloud point separation at 40 °C were taken (**Figure 6.26** b,c).

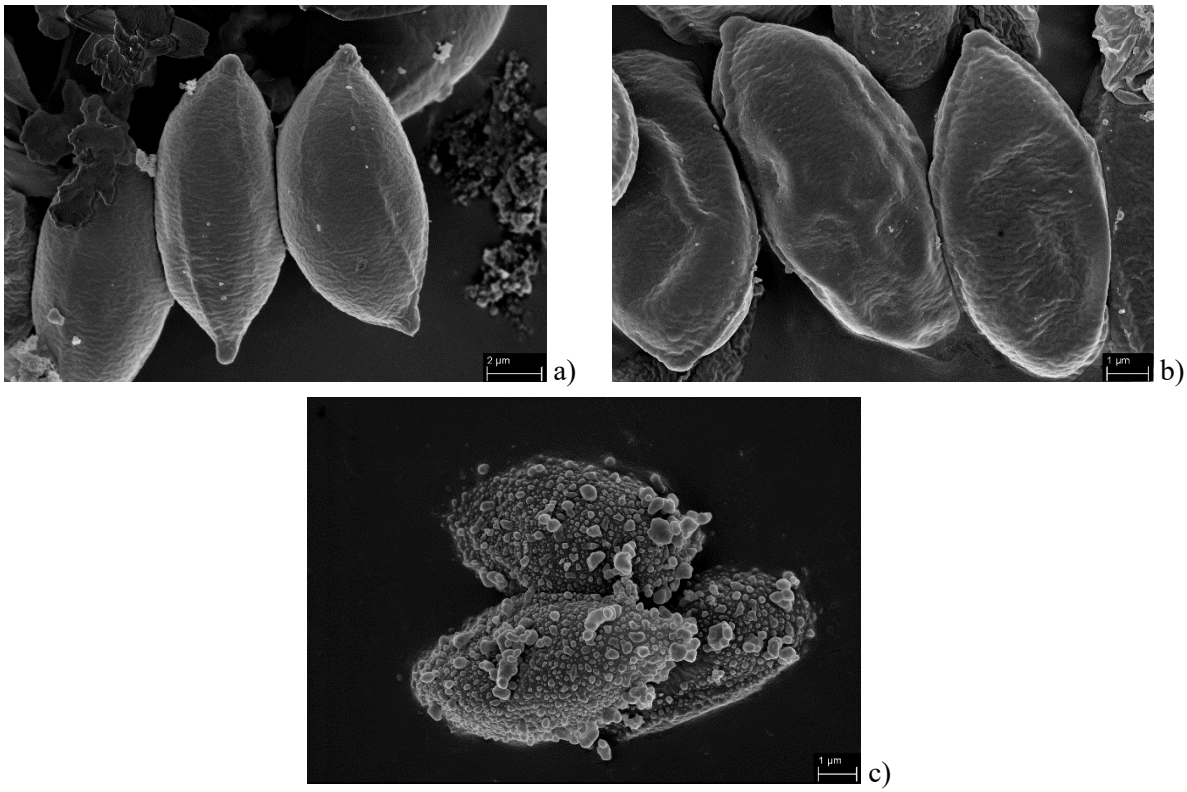

Figure 6.26: Scanning electron micrographs of *Acutodesmus obliquus* without surfactant (a), from the aqueous phase after the extraction (b, c).

The untreated cells (**Figure 6.26** a) did not show any abnormality in comparison to other micrographs of the same algae strain [66]. However, when observing the cells at Triton X-114 exposure at higher magnification (**Figure 6.26** b), some changes of the otherwise even surface were observed. Such effect was also observed Shafer and Bukovac and by Yuan et al. for different microorganisms in the presence of nonionic surfactants [139,140]. Dias et al. described changes of the membrane morphology of eukaryotic Protista, similar to the observations in this thesis as well [138].

In micrograph c, an even more pronounced change in the morphology of the microalgae was observed. Specific structures were arranged all over the cell surface. These could be explained with a possible adsorption of surfactant aggregates on the microalgae. However, the samples from the aqueous phase after the extraction were heterogeneous and thus no evident influence of the surfactant presence on the cells morphology could be derived.

Ultimately, the continuous extraction from the microalgae culture with the surfactant Triton X-114 was feasible and led to the accumulation of algae products in the extract phase. In the same time, the needed initial solvent volume was minimized. Moreover, the process was carried out without significantly decreasing the vitality of the cells.

On the other hand, two additional surfactants, viz. Silwet L-7230 and ROKAnol NL5 were identified as suitable for the continuous CPE in mild conditions. Therefore, it was of interest to examine their toxicity towards the green microalgae *A. obl*.

At first, the biocompatibility of the two surfactants was evaluated in mixtures with the algae culture at room temperature. The applied amphiphile concentration was set at 1 wt%. An incubation of the culture in the presence of Silwet L-7230 and ROKAnol NL5 was conducted over several days, and the RPA values were monitored. The corresponding results are presented in **Figure 6.27**.

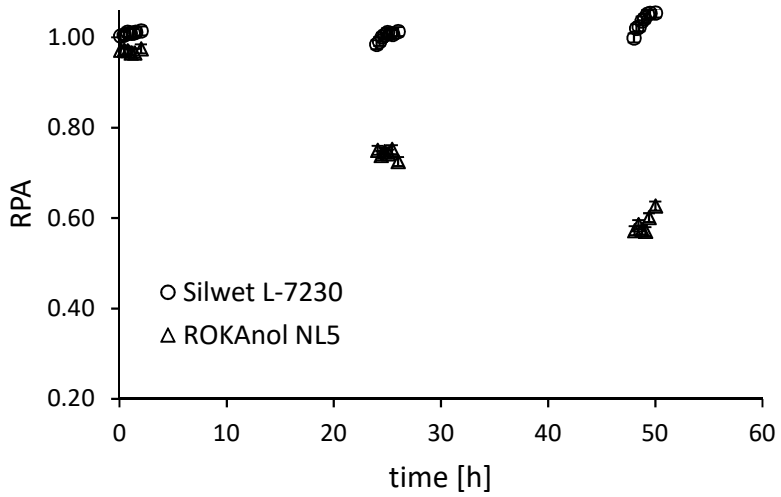

Figure 6.27: Relative photosynthetic activity of *Acutodesmus obliquus* in the presence of 1 wt% Silwet L-7230 and ROKAnol NL5, respectively. Error bars indicate the standard deviation, N=3.

The changes of the RPA over the time were obtained for both investigated surfactants. On the one hand, Silwet L-7230 did not induce the vitality of *A. obl.* over the duration of 50 hours. However, the samples containing ROKAnol NL5 were characterized by a reduction of the photosynthetic activity in comparison with the surfactant-free control. After one day of exposure, a decrease of less than 80 % of the corresponding control was observed. A slightly higher cell vitality of *A. obl.* (approx. 90% of the surfactant-free reference) was reported by Fellechner et al. However, the surfactant concentration during the incubation tests in their study never exceeded 1 wt% [176]. Both, the results in this work and in the contribution by Fellechner et al. prove the short-term compatibility of *A. obl.* with ROKAnol NL5. However, after 50 hours, the photosynthetic yield was equal to approx. 60 % of the reference sample. Hence, a long-term toxicity was observed for the surfactant ROKAnol NL5.

The difference in the toxicity of both surfactants could be explained by their hydrophilicity [134]. Since Silwet L-7230 was more hydrophobic than ROKAnol NL5, the amphiphile had a weaker affinity for the cells. On the other hand, ROKAnol NL5 was more hydrophilic and thus could interact better with the surface of the microalgae [137].

However, the retention time of the algae culture in the column during a continuous extraction process is not more than several hours. The algae cells maintained 97% of their photosynthetic activity during a short-term exposure to ROKAnol NL5 over 4 hours. That result was similar to the value obtained with Triton X-114 (99 % [132]) and with Silwet L-7230 (100%). It could be concluded, that the both tested surfactants were applicable for the extraction regarding the biocompatibility. However, the long-term exposure of *A. obl.* to ROKAnol NL5 had to be restricted.

Based on the good biocompatibility, the continuous countercurrent extraction with recirculation using Silwet L-7230 was conducted with a microalgae culture. The process parameters were set as described previously (see chapter 5.3).

However, the experiment with extract recirculation had to be aborted due to the formation of liquid crystalline extract. The highly viscous surfactant-rich phase plugged the upper part of the column. An illustration of the plugging is shown in Figure 6.28.

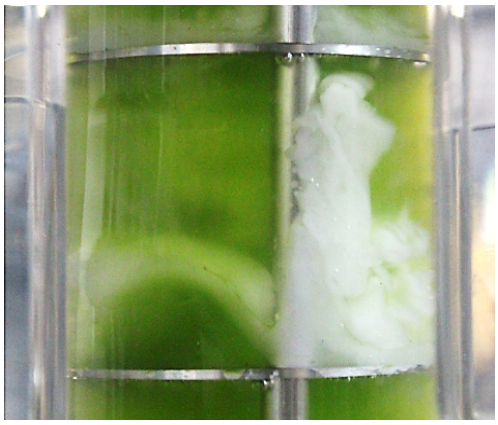

Figure 6.28: Illustration of the plugging caused by immiscible, liquid crystalline recirculated extract phase

Consequently, no further experiments were conducted with Silwet L-7230 and microalgae culture. However, ROKAnol NL5 was utilized as a solvent for the batch and continuous cloud point extraction from microalgal cultures in pilot scale. The corresponding results are described in chapter 6.5.5.

Overall, the successful implementation of the CPE from two different feedstocks, containing biomaterials, was presented in chapter 6.4. The choice of the extraction conditions, based on the observations of a model system, was transfer to the direct accumulation of phenolic compounds from pineapple juice and to the continuous in situ extraction from microalgae cultures. That after, a stable separation in the genuine bulks was observed in batch and in continuous mode, whereby an accumulation of products was stated in both processes. In addition, the feedstock characteristics (partially high phenolic content or high cell vitality) were influenced in a limited manner. On the one hand, the results proved the feasibility of the CPE as a mild technique for the direct ISPR from authentic feeds. On the other hand, different surfactant-based biphasic systems were compatible with two different natural suspensions. That emphasized the application potential of that diverse group of solvents for separations processes with biomaterials.

However, in order to make the cloud point systems attractive for large-scale operations, a proof for the applicability of the systems in pilot scale is demanded. Based on the continuous application with green microalgae in technical scale, a process for the in situ cloud point extraction from *A. obl.* cultures was designed and was implemented in pilot scale. The development and realization of the process are described in chapter 6.5.

6.5 CLOUD POINT EXTRACTION FROM MICROALGAE CULTURES IN PILOT SCALE*

** The realization of the surfactant-based in situ extraction from green microalgae in pilot scale was part of a project, financed by the German Federal Ministry of Economy and Energy. The experimental work was completed by Alexander Zilaev for his Master thesis* [160].

A plant for the continuous in situ CPE was realized in by-pass of the cultivation lines at the BIQ Algae House in Wilhelmsburg, Hamburg. The idea was to maintain a continuous extraction of algae products during the biomass recirculation in the flat-panel bioreactors. Therefore, as a final task in the current thesis, a plant with higher capacity than the technical scale equipment had to be realized. The objectives were: on the one hand to produce more significant amounts of microalgae extracts; on the other hand to study the continuous cloud point extraction in pilot scale.

Hence, it was required to design, construct and commission an extraction unit similar to the one used for the experiments in technical scale (see chapter 4.6). However, the technical column could process a feed stream up to 1 $L \cdot h^{-1}$ at a satisfactory steady condition. In contrast, the plant at the BIQ Algae House had to operate with a capacity of 25 $L \cdot h^{-1}$ (600 $L \cdot d^{-1}$) with an inlet temperature of 15 – 25 °C. Moreover, there was a maximal height limitation of 3 meters corresponding to the technical room at the BIQ Algae House. Additionally, the construction area was limited, and thus no column cascade or large tanks could be installed. Consequently, no substantial feed or solvent vessel were allowed. The process had to maintain lower energy and solvent costs. Hence, the recirculation of the extract phase was required. Moreover, the feed had to enter the column without additional pumping, only by using the hydrostatical pressure from the cultivation line.

In order to meet the mentioned requirements, the extraction unit at the BIQ Algae House was designed as described in chapter 6.5.1.

6.5.1 DESIGN OF A PLANT FOR CLOUD POINT EXTRACTION IN PILOT SCALE

According to those requirements, a borosilicate glass contactor from the type *Oldschue-Rushton* with an integrated heating jacket had to be constructed on site at the BIQ Algae House. Therefore, the diameter and the height had to be increased in order to operate at higher capacity according to chapter 2.4. At first, the inner diameter was scaled-up using the throughput calculation in **Equation 2-18**.

A throughput of 1.415 $m^3 \cdot (h \cdot m^2)^{-1}$ was calculated in accordance with the optimal column capacity for the continuous extraction of cinnamic acid without recirculation in technical scale (see chapter 6.1.4). That corresponded to an inner diameter of the pilot scale column of 0.15 m at a capacity of 25 $L \cdot h^{-1}$. Secondly, the theoretical height of the new column was estimated by **Equation 2-19** with α = 0.38. That resulted in a required active height of 3 meters. However, based on the height limitation in the technical room and the space needed for the stirrer motor, the height was set to 1.93 m. The limited height resulted in a lower number of stirring cells (20) and less settler volume (18 %) in the pilot scale contactor. All further geometry values were transferred in accordance with the proportion in the technical column. It is important to note, that the height limitation led to deviation from the geometrical similarity. Also, the proportion difference was expected to reflect on the transfer of the process parameters [18]. The characteristics of the pilot scale contactor are described in chapter 4.7 and are depicted in appendix A 5.

That after, a complete concept, including the periphery equipment and the indication and control units, was designed. The requirements concerning the solvent amount and the energy input for pumping were taken into account. **Figure 6.29** shows the P&I diagram of the pilot scale column and the associated extraction equipment.

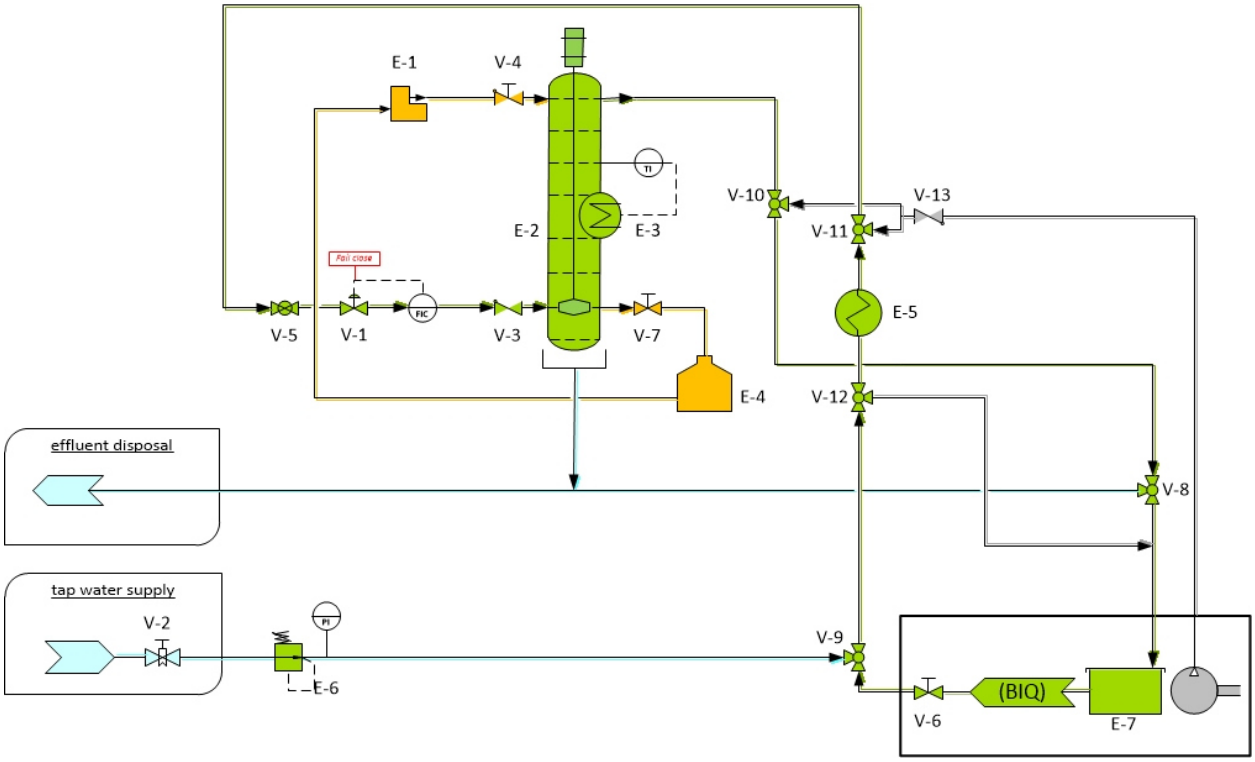

Figure 6.29: P&ID of the pilot plant at the BIQ Algae House (presented for a heavier solvent phase)

In light green, the microalgae circulation is shown, while orange symbolizes the solvent circulation. Furthermore, light blue denotes the fresh water supply and grey - the supply with pressurized air. Valves are denoted with V, while equipment parts are denoted with E. The microalgae cultivation tanks and the associated cultivation equipment are summarized as BIQ.

The plant operation was designed as described below.

Regular mode

For an extraction of microalgal products, the feed stream in form of microalgae culture left the cultivation tanks through an opened valve (V-6), was pre-heated in an heat exchanger (E-5) and entered the extraction column (E-2) at a rate determined by a flow control valve (V-1) or manually, using V-5. A pre-heating was necessary to reach the needed temperature of approx. 40 °C in the column. That after, the raffinate left the column through the top port. By changing the position of the valve V-8, the algae culture after the extraction could be disposed or further cultivated in the BIQ Algae House. Only the hydrostatic pressure from the cultivation lines was sufficient for the feed circulation.

The solvent, on the other hand, was pumped into the column by a gear pump (E-1). Subsequently, the surfactant-rich extract left the column as soon as the corresponding valve was opened (V-7) and was collected directly in the solvent tank (E-4). In this way, a recirculation of micellar phase was maintained.

Further, the column's ports were designed in such a manner, that described the orientation of the solvent and the feed could be arranged vice versa. Hence, a lighter extract phase could be collected via V-4 at the top of the column.

Rinsing mode

Tap water could also be used as a feed or for rinsing of the extraction column. The hydrostatic pressure in the water supply was kept constant by the pressure regulator E-6. The steady hydrostatic pressure of the aqueous stream was needed to maintain a constant level in the column. By changing the position of the valve V-9, the feed circulation from the "regular" mode could be performed with water.

Pressurized air circuit

To prevent the clogging with biomass, the respective valves (V-8, V-11, and V-10) were switched between a position for regular operation and a position for cleansing with pressurized air. Subsequently, the accumulated residual could either be lead into the cultivation tanks (E-5, BIQ) or discarded through the effluent disposal.

All valve positions for the different phases of operation are further summarized in appendix A 4.

Lastly, the extraction column was tempered through circulating hot water in its jacket (E-3). An additional temperating with a heating strap was introduced at the settler part, where the extract phase was collected. An insulation using glass-fiber isolation tape was installed on the settling volume in the top and bottom part of the contactor to minimize the heat loss.

The stable operation of the extraction column was relying on a constant feed rate. However, the flow had to be maintained without a pump. Moreover, a pulse-wise gas injection was carried out repetitively in each microalgae bioreactor, resulting in a continuous pulsation of the culture stream. Therefore, a precise control of the feed flow rate by V-1 was required. Aming to solve that issue, the feed flow had

to be measured on-line, and a control valve was used to automatically adapt the flow to the pulsations.

An adaptive control system for the feed flow was developed in collaboration with the "Electrical Engineering Research Workshop" at the Technical University of Hamburg (see chapter 4.7). The flow indication and control (FIC) was a combination of a magnetic-inductive flow meter, coupled with control valve with a pneumatic positioner. Additionally, the control system was designed to indicate the temperature in the column. The flow sensor, control valve, and temperature indicator were connected to PLC, which was further coupled to a LabVIEW software. Through the interface, it was possible to control the flow rate automatically. Also, a mode for calibration of the flow meter and the control valve was available. The process parameter could be logged in real time. A scheme of the control system is depicted in appendix A 3.

The installation of the column and the periphery, as well as the control system, were realized successfully at the site of the BIQ Algae House. That after, a final commissioning was conducted according to the steps in chapter 5.9.1.

6.5.2 PROCESS PARAMETERS OF THE CLOUD POINT EXTRACTION IN PILOT SCALE

The process parameters for the continuous liquid-liquid extraction in pilot scale were transferred based on the scheme in chapter 2.4. The technical scale process conditions for the continuous extraction with Triton X-114 were used as a base for the calculation (see chapters 6.1.3 and 6.1.4). At first, the stirring level was chosen based on the specific power input needed for the optimal extraction performance in technical scale.

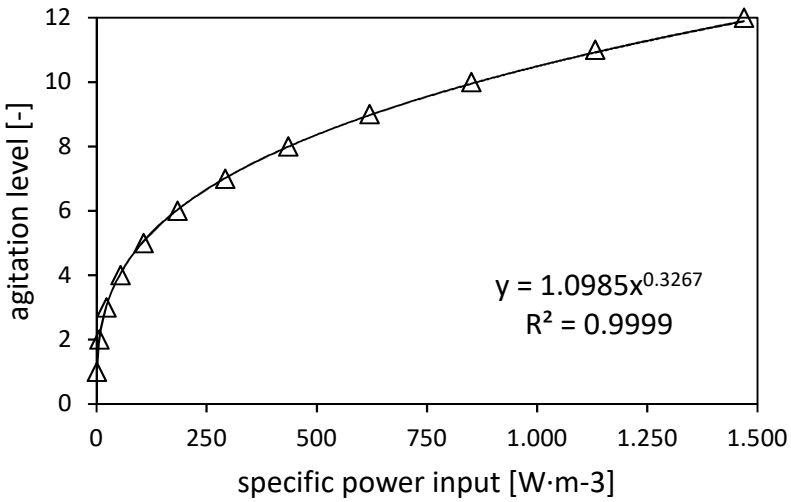

Figure 6.30: Correlation between the agitation level and the power input in the pilot scale column

According to the function in **Figure 6.30**, the agitation level of 0.5 was required to maintain the energy input with a deviation of 2.4 % in comparison with the technical scale. That agitation level referred to a stirring speed of 15 rpm (in comparison to 25 rpm in technical scale). A lower mixing speed was expected for the larger column according to the theoretical basics in chapter 2.4.

That after, a residence time of 2.29 h was calculated using the parameter for the technical contactor (**Equation 2-20**). Additionally, the velocity of the feed and the solvent streams were identical (2.76 $m \cdot h^{-1}$), based on the assumption, that the free cross-section was divided between the two currents according to the feed-to-solvent ratio (**Equation 5-10**). The residence time and the velocities were correlated through the free cross-section and the active volume of the column. In case of a maintained geometrical similarity, the parameters had to be identical to the pilot scale equipment. Since that was not the case in this thesis, an unchanged residence time could be implemented only together with a deviation in the velocity or vice versa. Therefore, two combinations of the parameters for the continuous extraction were studied, namely "constant residence time" and "constant velocities."

Ultimately, the process parameters for the continuous in situ extraction with Triton X-114 in pilot scale are presented in **Table 6.3**.

Table 6.3: Process parameter for the continuous cloud point extraction with Triton X-114 in pilot scale

parameter	combination	
	const. residence time	const. velocity
agitation level [-]	0.5	0.5
agitation speed [rpm]	14.58	14.58
residence time [h]	2.11	1.65
velocity [$m \cdot h^{-1}$]	2.16	2.76
column capacity [$L \cdot h^{-1}$]	15.4	19.7
feed-to-solvent ratio [-]	5	5
feed flow rate [$L \cdot h^{-1}$]	12.8	16.4
solvent flow rate [$L \cdot h^{-1}$]	2.57	3.28

All experiments in the pilot scale column utilizing Triton X-114 as feed were conducted based on the parameter combinations in **Table 6.3**.

6.5.3 VALIDATION OF THE PROCESS DESIGN USING THE BINARY SYSTEM TRITON X-114/WATER

The aim of the experiments with the binary mixture Triton X-114/water in the pilot plant was to evaluate the performance of the extraction column without additional influence from the microalgae. Hence, the distribution of the surfactant between the raffinate and the extract could be compared to the surfactant profiles from the corresponding experiment in technical scale (see chapter 6.4.2). Most importantly, the loss of Triton X-114 with the raffinate could be evaluated. Additionally, the stability of the feed and solvent flow rates could be monitored via the control systems. The results in this chapter represent the experiments utilizing the two parameter combinations in **Table 6.3**, namely "constant residence time" and "constant velocity".

The surfactant concertation profile in the raffinate, together with the raffinate flow rate, over the time at the parameter combination with constant residence time, are presented in **Figure 6.31**.

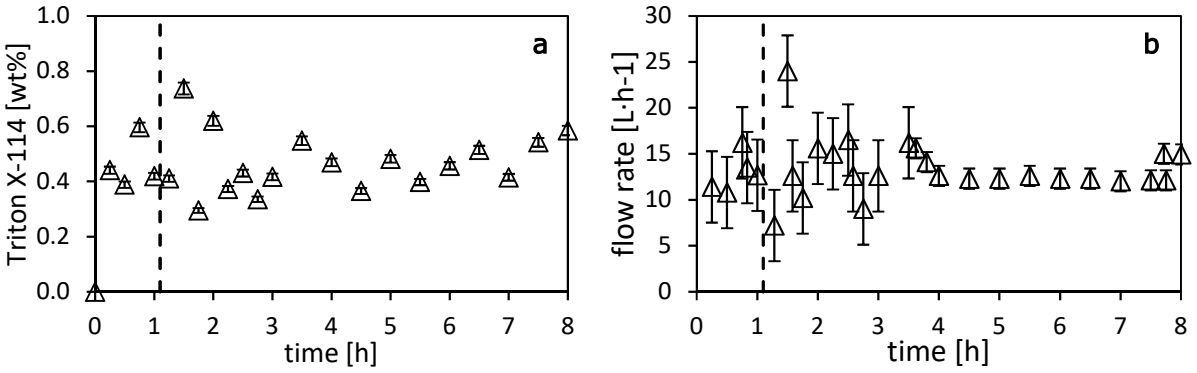

Figure 6.31: Profiles of the Triton X-114 concentration (a) and the flow rate (b) in the raffinate over the time during the experiments with "constant residence time" parameter setting. Error bars indicate the standard deviation within each experiment. The black dashed line indicates the time of the recirculation start.

The surfactant concentration in the raffinate (**Figure 6.31** a) was unstable in the first 3.5 hours of the experiment. Therefore, a stationary state was reached after approximately 4 hours. That after, the average Triton X-114 concentration in the raffinate was 0.47 ± 0.07 wt%. That fluctuation could be correlated to the changing raffinate flow rate (± 3.9 $L \cdot h^{-1}$) up to the 3.5 hours experiment duration (**Figure 6.31** b). Subsequently, a more stable flow rate of 12,8± 1,1 $L \cdot h^{-1}$ was observed. That corresponded to a deviation of 0.3% from the set feed flow rate.

A sufficient amount of micellar phase in the bottom of the column was observed after one hour. Thus, the recirculation was initiated after 1.1 hours (black dashed line in **Figure 6.31**). It is important to note, that the recirculation was started after 1.5 hours in the technical scale experiment. It can be concluded, that the hold-up in the mixing zone was similar. That was confirmed through the similar surfactant concentration in the pilot column (1.4± 0.6 wt%) as well.

The average Triton X-114 concentration in the raffinate was equal to 0.061 wt% during the corresponding experiment in technical scale. In comparison, the observed value in the pilot column was higher, even exceeding the stress limit. A possible explanation of the settling of the stationary state at a concentration above the stress limit is the difference in the geometry of both columns (**Table 4.3** and **Table 4.4.**). While the settler volume in the technical contactor was 50 % of the total one, the equivalent volume in the pilot column resulted in 19.5 %. Hence, the disperse phase, which was distributed with the equivalent energy input, had to separate for a shorter period. That resulted in a higher amount of the micellar

extract, which was "washed out" with the feed. Such deviations were expected due to the lack of geometrical similarity [14].

Further, the surfactant concentration and the corresponding flow rate profile of the extract are presented in **Figure 6.32**.

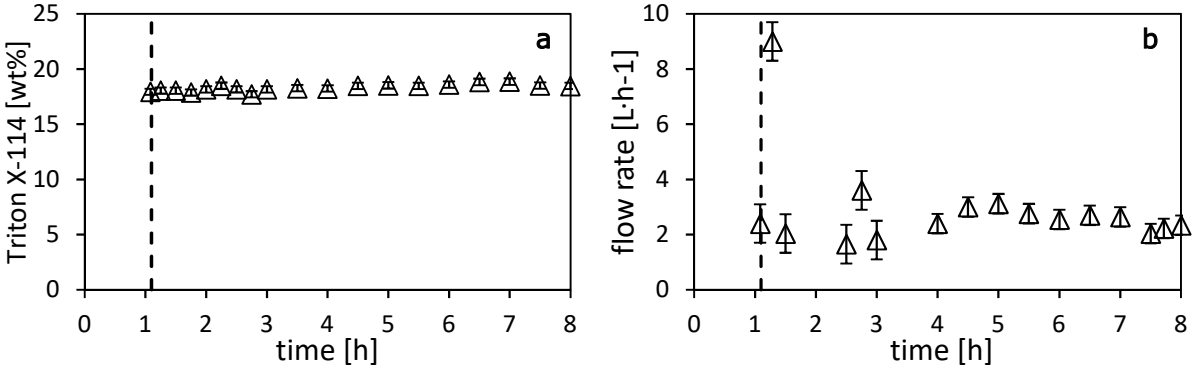

Figure 6.32: Profiles of the Triton X-114 concentration (a) and the flow rate (b) in the extract over the time during the experiments with "constant residence time" parameter setting. Error bars indicate the standard deviation within each experiment. The black dashed line indicates the time of the recirculation start.

The Triton X-114 fraction in the extract flow remained stable during the whole experiment (**Figure 6.32**. a). The fluctuation in the flow rate up to the 3rd hour did not destabilize the extract composition. The average surfactant concentration was 18.6 ± 0.2 wt%, which was deviating from the corresponding value in technical scale only with 0.2 wt%. Hence, the distribution of the surfactant between the two coexisting phases was not influenced by the different kinematic conditions.

Overall, a stable continuous process was maintained with regard to the fluctuations in the concentration and flow rates. Hence, the parameter combination at constant residence time was suitable for the direct extraction from microalgae.

However, the second parameter variation had to be tested as well. Directly after the experiment with constant velocity, the influence of the feed-to-solvent ratio was also examined.

The plots in **Figure 6.33** represent the surfactant concentration in the raffinate as well as the feed and raffinate flow rate over the time during the experiment with constant velocity.

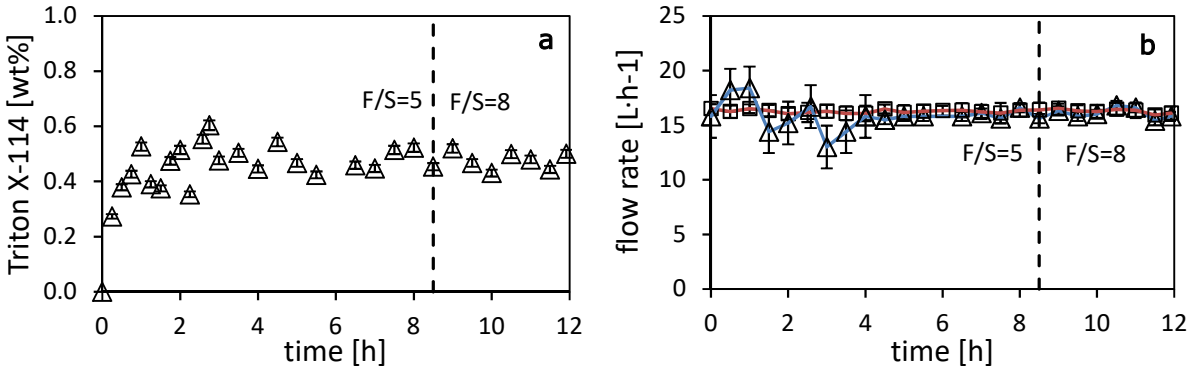

Figure 6.33: Profiles of the Triton X-114 concentration in the raffinate (a) and the flow rate of the raffinate (blue line) and the feed (red line) (b) over the time during the experiments with "constant velocity" parameter setting. Error bars indicate the standard deviation within each experiment. The black dashed line indicates the change of the F/S from 5 to 8. The recirculation was initiated after 1.3 hours.

The Triton X-114 fraction in the raffinate (**Figure 6.33** a, F/S = 5) was similar to the first experiment in pilot scale (**Figure 6.31** a). The stationary state was reached after 4 hours, whereby the recirculation of the extract was initiated after 1.3 hours (not denoted in the figure). The average Triton X-114 concentration in the raffinate amounted 0.47 ± 0.04 wt%. However, the deviation was lower as in the first test. That was due to the simultaneous observation of the raffinate flow (volumetric measurement) and the feed flow (control system). Hence, a faster adjustment of the streams was possible. As a result, the feed flow rate and the raffinate stream were equal to 16,2 ± 0,2 $L \cdot h^{-1}$ and 16,0 ± 0,4 $L \cdot h^{-1}$, respectively. That result confirmed the stability of the streams in the pilot scale column.

The influence of the feed-to-solvent ratio was investigated by increasing the ratio from 5 to 8 after an experiment duration of 8.5 hours. Hence, a higher surfactant loss was expected with the raffinate (see chapter 6.1.2). However, the Triton X-114 fraction did not exhibit any change.

Analogue observations concerning the surfactant concentration in the extract phase were made for the second experiment. The Triton X-114 fraction over the time is presented in appendix A 23. The average concentration of the surfactant in the micellar phase was 18,6 ± 0,5 wt%, which was equivalent to the first experiment and the extraction in technical scale.

The mass balance regarding the surfactant deviated with 3.4 %, which confirmed the reliability of the measured data.

Concluding, the different parameter combinations resulted in similar results. The expected change in the surfactant distribution between the two phases at higher feed-to-solvent ration was not detected. Hence, the effect of the limited settler volume was more pronounced than the parameter influence.

Ultimately, a stable continuous cloud point extraction with Triton X-114 was feasible in a pilot scale. The scale-up of the process parameters resulted in a stable surfactant distribution between the phases. No flooding was observed. Thus, a continuous stationary process was realized based on the parameter transfer. However, a higher surfactant loss was observed with the raffinate due to the deviation from the geometrical similarity. Therefore, an extra settling unit hat to be implemented to minimize the surfactant loss with the raffinate.

Based on the results in the biphasic system, the conditions under constant velocity were applied for the extraction from microalgal culture. The parameter combination was chosen since it allowed a higher column capacity. The results from the continuous in situ extraction from green microalgae using Triton X-114 in pilot scale are presented in the next chapter.

6.5.4 CONTINUOUS IN SITU EXTRACTION FROM MICROALGAL CULTURES USING TRITON X-114

The continuous surfactant-based in situ extraction from *A. obl.* using Triton X-114 was conducted over a period of 22 hours. Therefore, the results could be compared not only to the reference experiments in pilot scale with tap water but also with the long-term extraction from the same strain in technical scale (duration 24 hours, see chapter 6.4.2). The authentic microalgae culture, originating from the 4th-floor line of the BIQ, had a cell density of 1.6 ± 0.3 g·L^{-1}. Hence, the feed composition of both long-term experiments with *A. obl.* was similar.

The first step to evaluate the stability of the continuous extraction from green microalgae in pilot scale was the observation of the feed flow rate over the time. The corresponding values are presented in Figure 6.34.

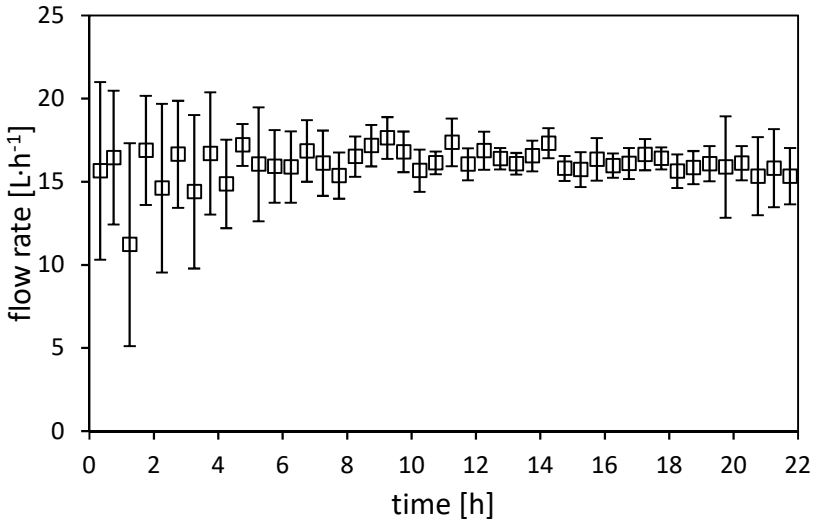

Figure 6.34: Feed (microalgae culture) flow rate during the long-term continuous cloud point extraction with Triton X-114 in pilot scale. Error bars indicate the standard deviation within each experiment.
The recirculation was initiated after 1.3 hours.

The feed flow rate was fluctuating pronouncedly in the beginning and at the end of the experiment. Deviations up to 6,11 $L \cdot h^{-1}$ were observed. In contrast, between the 8th and the 20th hour of the extraction duration, the flow rate was stable, with a lower fluctuation of 2.01 $L \cdot h^{-1}$. The reason for the unstable flow rate was the pulsation in the algae culture, originating from the periodical gas injections. As expected, the gas flow had a pronounced impact on the feed flow. However, an average flow rate of 16,1 ± 1,3 $L \cdot h^{-1}$ could be estimated. That value was in good agreement with the corresponding reference experiment with tap water in pilot scale.

The pulsation in the feed flow reflected on the surfactant concentration in the raffinate as well. The profile of the Triton X-114 fraction in the algae culture exiting the column is presented in **Figure 6.35**

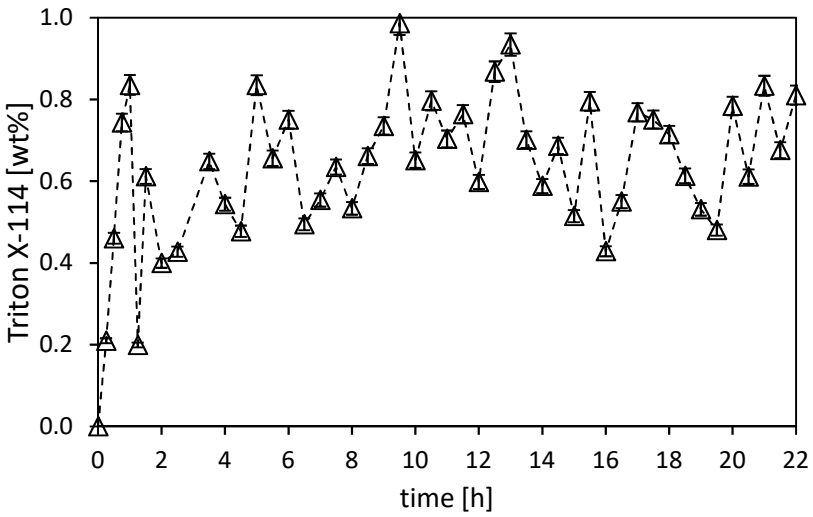

Figure 6.35: Surfactant concentration profile in the raffinate during the long-term continuous cloud point extraction with Triton X-114 in pilot scale. Error bars indicate the standard deviation within each experiment. N=2. The recirculation was initiated after 1.3 hours. A line was added to guide the eyes.

According to the changes in the feed flow, the surfactant concentration in the raffinate was fluctuating as well. Therefore, no stationary state could be registered. Further, an average of 0,6 ± 0,2 wt% for the Triton X-114 concentration in the raffinate was estimated. That value was only roughly comparable to corresponding tap water experiment in pilot scale (0.47 ± 0.04 wt%). However, the tendency of higher Triton X-114 fraction in the raffinate, during the continuous extraction from the microalgae, in comparison to the algae-free reference experiment was observed. That trend was valid for the technical and pilot scale experiments. Also, a formation of cell flocks around the feed entrance was observed during both extraction processes. Overall, a similar influence of the biomass on the process performance was stated in the corresponding experiments.

The Triton X-114 concentration profile was also applied for the evaluation of the surfactant-based in situ extraction. The corresponding time dependence is presented in Figure 6.36.

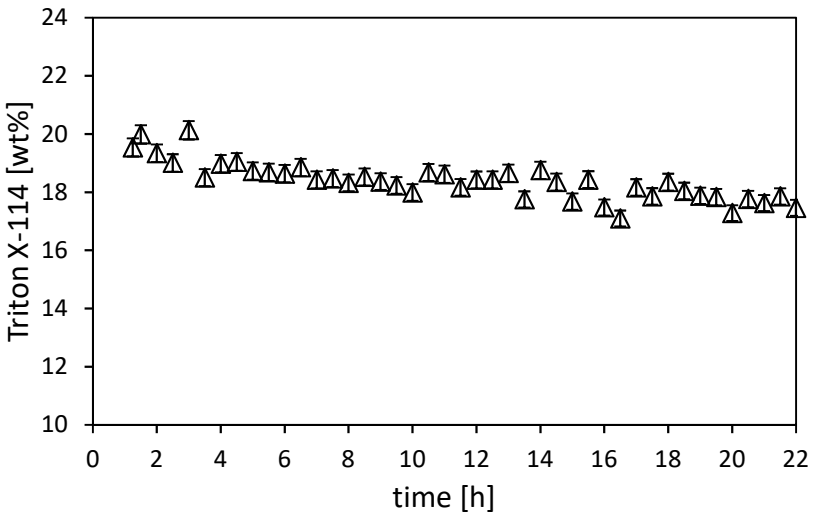

Figure 6.36: Surfactant concentration profile in the extract during the long-term continuous cloud point extraction with Triton X-114 in pilot scale. Error bars indicate the standard deviation within each experiment. N=2. The recirculation was initiated after 1.3 hours.

The Triton X-114 fraction in the extract stream remained stable during the complete experiment. Moreover, the composition of the surfactant-rich phase was in good agreement with the value from the algae-free experiment in pilot scale. However, an overall reduction of the surfactant concentration was observed. In contrast, no reduction of the surfactant concentration in the extract was observed during the continuous process with algae culture in the technical set-up. The reason for that difference may be the more noticeable surfactant loss with the raffinate combined with the entrainment of micellar phase in the biomass flocks.

In order to compensate the surfactant loss, a subsequent settling of the raffinate was conducted as described in chapter 5.10 (**Figure 5.2**). The additional phase separation took place at 33 °C, which was the room temperature. The surfactant concentration in the algae culture exiting the settler over the time is presented in **Figure 6.37**

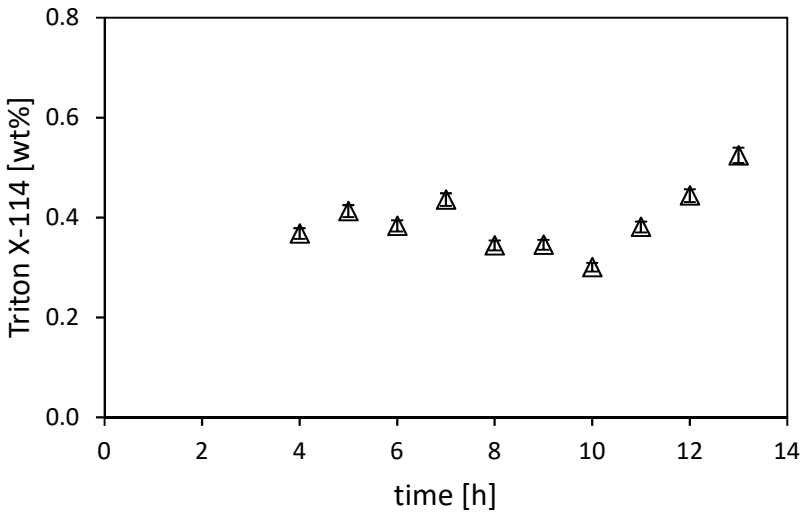

Figure 6.37: Surfactant concentration profile in the algae culture after the additional settling stage during the long-term continuous cloud point extraction with Triton X-114 in pilot scale. Error bars indicate the standard deviation within each experiment. N=2.

The average surfactant amount in the flow, leaving the settling vessel was equal to 0.37 ± 0.05 wt%. That mean value was lower than the one in the primary raffinate stream. Hence, a 20 % decrease in the Triton X-114 concentration was achieved through the introduction of additional settling volume. Moreover, the micellar phase, which was formed at the bottom of the vessel, amounted to 15.7 wt% Triton X-114. That value corresponded to the surfactant-rich phase composition at 33 °C (see appendix A 9). Thus, the "washed-out" disperse phase was collected in the settling vessel as well. Those observations proved the conclusion from the validation experiments with tap water that the settling volume in the column was not sufficient.

The total yield of algae products was determined according to **Equation 5-9**. Overall, 0.7±0.3 $g_{Algae\ product}/kg_{Culture}$ was obtained in the extract phase. The value was comparable to the technical-scale recovery. However, it was not possible to make a more precise comparison between the compositions of the algae extract based on Triton X-114 due to the described analytical limitations (see chapter 6.4.2). Therefore, no further interpretation concerning the influence of the process conditions on the extraction efficiency in technical and pilot scale was possible.

Nevertheless, a coloring of the extract was observed visually. The green-brownish color was accumulating over the time as depicted in **Figure 6.38**.

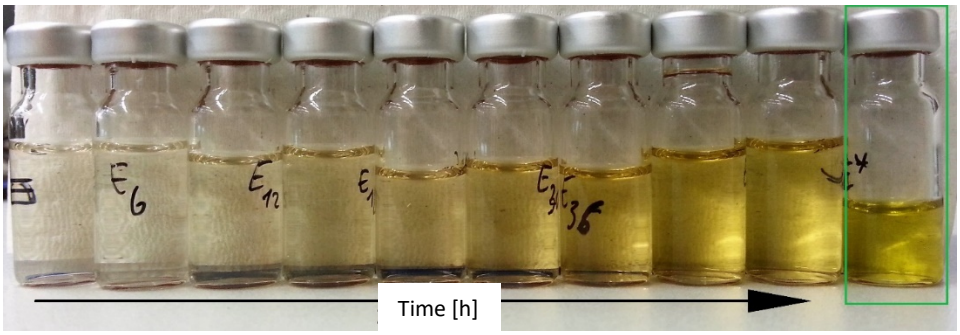

Figure 6.38: Illustration of the pigment accumulation in filtered extract samples collected during the long-term continuous cloud point extraction with Triton X-114 in pilot scale. The green box corresponds to the micellar phase in the additional settler.

The color of the samples persisted after the filtration through a syringe filter. Apparently, a pigment accumulation in the micellar phase was observed. The ability of Triton X-114 to recovery natural dyes from cell cultures was already reported by Hu et al. [44,129]. Moreover, Ulloa et al. described an efficient procedure to accumulate tocopherol from green microalgae cells using a cloud point system [122]. Thus, the accumulation of algae pigments in the micellar phase during the continuous extraction was also possible with the surfactant Triton X-114. However, the SEC analysis (see chapter 5.11.2 and 6.4.2) could not deliver further information concerning the pigment accumulation. In addition, no spectrophotometric measurement without sample fractionation was possible, due to the intense UV absorbance of Triton X-114. Therefore, no extract composition could be presented in this thesis.

Overall, a continuous in situ extraction from microalgae cultures using Triton X-114 was successfully implemented on pilot scale for the first time. The process was maintained over 22 hours, whereby the only fluctuation in the feed flow was observed due to the pulsation in the cultivation system. The concentration of the surfactant in the raffinate and extract was in good agreement with the algae-free experiments. Moreover, the surfactant loss in the raffinate could be minimized by introducing an additional settler unit. Finally, an advantageous accumulation of products was observed in the extract phase.

In addition, the surfactant ROKAnol NL5 was identified as suitable for the cloud point extraction from biomaterials. According to the results in **Figure 6.27**, the biocompatibility of ROKAnol NL5 allowed for a short-term exposition of *Acutodesmus obliquus* to the surfactant. Therefore, the feasibility of the in situ

extraction using ROKAnol NL5 was investigated in the pilot plant. The results from the experiments in batch and continuous mode are presented in 6.5.5.

6.5.5 IN SITU EXTRACTION FROM MICROALGAL CULTURES USING ROKANOL NL-5

At first, the cloud point extraction with ROKAnol NL-5 was performed in a batch mode. The aim was to examine the general applicability of the separation technique. Two different feedstocks from the BIQ Algae house were implemented: (1) an authentic culture with a CD equal to 1.0 ± 0.1 g L^{-1}; (2) a cell slurry from the flotation unit, regarded to as flotate (see chapter 4.4). That feedstock had a higher CD of 3.90 ± 0.01 g L^{-1}. The batch cloud point extraction was performed at 45 °C as described in chapter 5.10.

The following general observations were made. Firstly, a stable phase separation took place during the experiments with both feedstocks. As expected, the micellar extract was the upper phase.

Secondly, an intense pigment accumulation was observed in both extract phases. The color of the extract from the culture was green-brownish, while the coacervate of the flotate extraction was dark brownish. The coloring was more intense during the ROKAnol NL5 extraction than in the Triton X-114 experiments. A possible explanation for that can be the more pronounced toxicity of the surfactant in combination with the higher extraction temperature (45 > 40 °C). Therefore, a partial lysis of the cells could occur and thus release more intracellular pigments [44,122,129].

Lastly, biomass flocculation was exhibited in both experiments, whereby more massive flocks occurred during the flotate extraction. That was expected considering the extreme stress conditions for the cells (45 °C in combination with long-term surfactant toxicity) [136]. However, in case of ROKAnol NL5, the biomass sedimentation towards the bottom of the vessel, while the extract accumulated at the top. Hence, the solids could not penetrate the micellar phase.

Due to analytical limitations, no surfactant concentrations could be determined for the coexisting phases. However, a UV-Vis spectrophotometric measurement was performed for each phase and was compared to a ROKAnol NL-5 aqueous solution. The corresponding spectra are presented in Figure 6.39.

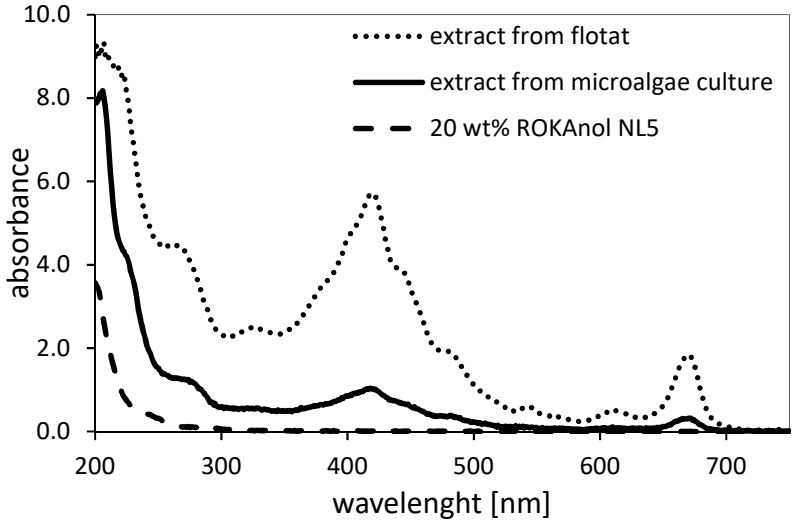

Figure 6.39: UV-Vis spectra of the micellar phase from the batch extraction of microalgae culture and flotate using ROKAnol NL5. The dashed line represents a mixture of ROKAnol NL5 and dist. water.

As depicted in **Figure 6.39**, UV-Vis spectra of the extracts could be obtained without being influenced by the surfactant. The absorbance of the 20 wt% Rokanol NL5 solution was neglectable. Overall, higher absorbance was observed for the extract from the flotate in comparison to the culture extract. That corresponded to the observed darker coloring of the micellar phase during the flotate extraction. Similar maxima in the spectra were obtained for both samples. The increase in the absorbance at 273 nm could be due to aromatic compounds. Also, the absorbance peaks at 337, 438, 614 and 664 were typical for plant pigments [75,111].

However, only a row estimation of the extracted compounds could be made based on the spectra. Nevertheless, the stable separation in the ROKAnol NL5/algae suspension was promising for a possible continuous extraction as well. Therefore, a first feasibility test of the continuous extraction from authentic *Acutodesmus obliquus* culture using ROKAnol NL5 was conducted in pilot scale. The process parameters were roughly chosen based on the observation in technical scale (see chapter 5.10).

Overall, a formation of a micellar phase was observed at the top of the column. In addition, after approx. 2 hours a recirculation of the extract was initiated as well. However, at the end of the experiment a weight loss of 58 % was stated for the solvent. Hence, a flooding could be assumed. Therefore, a more precise parameter transfer (as for Triton X-114) in combination with a reliable analytics for the

ROKAnol NL5 concentration were needed to maintain a steady state in the pilot scale equipment.

Nevertheless, a color accumulation in the extract phase was observed during the continuous extraction as well. The spectra of samples, obtained during the experiment are presented in **Figure 6.40**.

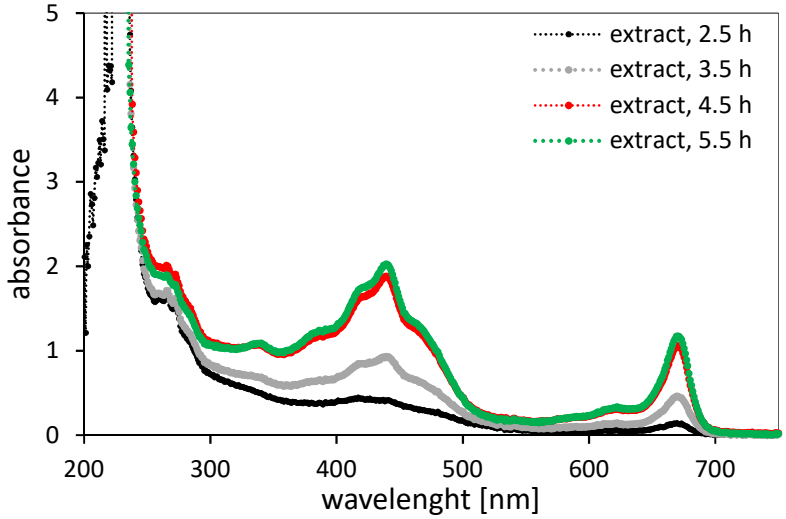

Figure 6.40: UV-Vis spectra of the extract stream from the continuous extraction of microalgae culture using ROKAnol NL5 after 2.5, 3.5, 4.5, and 5.5 hours after the beginning of the experiment.

The spectra obtained for the extract during the continuous experiment with ROKAnol NL5 possess an analogous pattern to the results from the batch extraction. In addition, at the areas of maximal absorbance, the intensity of the signal is increasing with the experiment duration. Hence, an accumulation of the algae products in the micellar phase could be concluded.

Overall, the experiments in pilot scale with the surfactant ROKAnol NL5 proved the applicability of the surfactant for the separation of algae products from the authentic algae culture. The spectrophotometric analysis indicated for an accumulation of pigments in the micellar phase. Therefore, an HPLC pigment analysis of the extracts was conducted in collaboration with the "Cell biology and phycology" department of the University of Hamburg. The corresponding pigment concentration in the different extracts is presented in **Table 6.4**.

Table 6.4: Pigment concentration [mg·L^{-1}] in micellar extracts obtained from the cloud point extraction with ROKAnol NL5 in pilot scale

extract from:	neoxanthin	violaxanthin	lutein
microalgae culture	-	-	0.092
flotate	0.088	0.089	0.493
continuous experiment	0.055	0.047	0.340

The pigment lutein was accumulated in all extracts. The highest accumulation of lutein was registered for the batch extraction from flotate, followed by the continuous experiment and the batch separation with algae culture. On the other hand, neoxanthin and violaxanthin were obtained only during the continuous experiment and from the flotate feedstock. The batch extraction from flotate led to higher concentration of neoxanthin and violaxanthin than the continuous approach. The more pronounced accumulation of lutein than of the other two pigments was in good agreement with the results by Wiltshire et al [65]. During their studies, the authors wholly permeabilized *Acutodesmus obliquus* dried biomass and thus achieved the highest recovery of lutein in the extract phase, composed of acetone and water. The corresponding violaxanthin and neoxanthin yield were lower. In this thesis, the highest pigment accumulation was achieved during the flotate extraction. That can be correlated to the higher cell density of the feedstock. However, a more systematic study was needed to characterize the influence of the process conditions and the feed composition on the extraction efficiency.

Overall, the results in chapter 6.5, presented the first known implementation of the surfactant-based in situ continuous extraction from green microalgae in pilot scale. By utilizing the technical scale study with a subsequent up-scale, the in situ product removal from *A. obl.* using the Triton X-114 cloud point system was realized in a stirred contactor with a higher capacity. Hence, the batch application, reported by Glembin et al. [9,132], was not only extended to a continuous application but was performed in a pilot plant. That process development was ultimately evident for the potential of the cloud point extraction for the large-scale product recovery from authentic biological feedstocks.

Based on the observations in this thesis, a general scheme for the design of an in situ cloud point extraction from a genuine feed solution is proposed in the next chapter.

6.6 IMPORTANT POINTS FOR THE DESIGN OF THE IN SITU CLOUD POINT EXTRACTION

This chapter provides an overview of the steps through the development of a surfactant-based in situ separation process of sensitive materials from an organic feed solution. The proposed scheme contains four stages, which aim to a final stable process with sufficient productivity.
The design scheme with the corresponding stages is presented below:

1. Feedstock characterization including:
    - general composition;
    - identification of target compounds based on their application;
    - suitable analytics for determination of the target compounds;
    - optimal temperature and pH range;
    - possible growth inhibition or product degradation;
    - availability and price of the feed solution.
2. Choice of a suitable surfactant based on:
    - cloud point temperature ≤ optimal temperature;
    - HLB ≥ 7;
    - availability on the market and price;
    - permission for the application of interest;
    - compatibility with the feedstock (viz. low toxicity, no side reactions, etc.);
    - influence of the feedstock on the phase behavior;
    - suitable analytics for the determination of the surfactants;
    - possible analytical procedure for the simultaneous determination of the surfactant and the products

A compatible surfactant-feedstock system can be identified based on the points 1 and 2. That after, a process concept maintaining the number of stages needed for the extraction as well as the required processing of the extract and raffinate can be designed according to point 3.

3. Development of a process concept considering:
    - accumulation of target compound in the extract;
    - physical properties of the extraction system (density, viscosity, surface tension)
    - feasibility tests in single-stage or multiple-stage units;
    - achievable yields and productivity;

- required extract processing (concentration, stripping, preservation, transformation);
- specific requirements concerning the raffinate after the extraction;
- economic assessment of different process alternatives.

When the concept for the cloud point extraction is designed, the plant's design can be developed based on the requirements in point 4.

4. Process design according to:
    - choice of an extractor type;
    - required units for the extract and raffinate processing;
    - needed additional instruments (stirrers, pumps, thermostats, etc.);
    - piping concept;
    - needed indication and control instruments;
    - specific requirements concerning the stream disposal.

According to the design, the needed apparatus and periphery can be selected and constructed by taking into account the following requirements:

5. Construction of the plant based on:
    - required throughput;
    - required energy input;
    - extractor(s) dimensions;
    - suitable material and diameter of the piping;
    - sufficient operating ranges of the additional instruments;
    - cost planning.

Based on the chosen units, the plant for the surfactant-based extraction can be taken into operation according to point 6.

6. Commissioning and operation:

- installation of the units and the instruments;
- installation of a control system;
- calibration of the instruments;
- scale-up of the process parameters;
- optimization of the process parameter;
- process stability tests;
- final long-term operation at the optimal operating conditions.

The points presented above give an overview of the main steps used for the process design in this thesis. It is important to note that due to the diversity of the surfactant-based systems, additional issues may occur in future process design. Neverthless, the steps can be useful as a compact base for the development of the ISPR utilizing a micellar two-phase system.

7 CONCLUSIONS

Nonionic surfactants are known to form ATPS at mild conditions. Biomolecules can accumulate in the micellar phase based on nonionic amphiphiles. These properties make the surfactants attractive for the in situ recovery of natural products. However, the application of surfarctant-based two-phase systems for the ISPR is mainly limited to laboratory or technical sclale processes in batch mode. The major goal of this work was to extend the direct ISPR from genuin feedstocks to the use of surfactant-based ATPS in a continous process at a technical and at a pilot scale.

At first, the usability of the nonionic surfactants for the ISPR was studied. Aiming to obtain a general impression on the suitability, tests were conducted with a model solute (cinnamic acid). In the first part of this work, the nonionic surfactant Triton X-114 was studied, due to its well-established use for the accumulation of organic molecules from aqueous solutions and its biocompatibility with microorganisms. A process in continuous mode was designed in a way that maintained mild conditions for a potential natural feedstock. The reached yield for the model solute was equal to 39.3 % and the productivity to 109.3 $g \cdot h^{-1}$. The successful product separation at process parameters, devoted to maintaining mild ISPR, illustrates the suitability of the well-known surfactant system for the continuous in situ extraction of dissolved biomaterials.

Based on the promising performance of Triton X-114, it was of interest to identify further amphiphiles, which can be used for the in situ extraction from authentic feedstocks. Among sixteen commercial surfactants applied in food or cosmetic, the aqueous surfactant systems containing Silwet L-7230 and ROKAnol NL5 separated rapidly into a surfactant-rich and an aqueous phase. Moreover, when using the same model system, a successful batch and a continuous cloud point extraction was realized with both Silwet L-7230 and ROKAnol NL5. These results represent the first known successful implementation of Silwet L-7230 and ROKAnol NL5 surfactant systems for the cloud point extraction in batch and continuous mode. The results also prove that the suitability of the nonionic surfactants for direct ISPR are not only limited to the well-established systems (e.g. Triton X-100, Tween 80), but can be realized also with commercial amphiphiles. Additionally, the efficiency of the continuous CPE was dependent on the used amphiphile. Thus, the influence

of the LLE and phase properties on the process performance using nonionic surfactants. Therefore, the development of separations in micellar systems should always be in alignment with the phase behavior of the amphiphile/water mixture. Overall, the results in this work could prove, based on the isolation of a model solute, that the conditions for a direct ISPR can be maintained using well-studied micellar ATPS as well as using commercial surfactants.

A common drawback of the product isolation in a micellar ATPS is the high water content in the extract (typical values such as 70 - 80% water at 40 °C), which results low solute concentration, especially in a single-stage process. Therefore, a strategy to elevate the target product concentration in the micellar phase was investigated in this work. At first, the feasible continuous process scheme with solvent recirculation in a micellar ATPS was demonstrated for the first time. The recirculation of the micellar phase is beneficial since it allows a higher ratio between feed and solvent because there is no limitation through the batch size. In addition, no further increase in the temperature is needed in order to elevate the micelle and solute concentration in the extract by the shift in the LLE. This setting can make the CPE more efficient and keep the conditions mild at the same time. This makes the recirculation of the micellar phase especially attractive for the product separation out of diluted cell cultures.

The complicated stripping of the surfactant from the solute in the micellar phase is highlighted as a main limitation for the CPE. In this work, the potential of the food-grade and cosmetic-grade surfactants for the extraction of solutes with a natural origin was discussed with regard to solute recovery from the micellar phase. Since surfactants, such as Silwet L-7230 or ROKAnol NL 5, are permitted for the final food or cosmetic formulation, no separation of surfactant and target product (or only rough separation is sufficient) was needed. In this case, the amphiphile was denoted as “leave-in surfactant.” The application of a leave-in surfactant for the cloud point extraction is an alternative approach, which was implemented in this work. The possibility to use nonionic surfactants with permission for consumer products as extraction agents makes the amphiphiles an alternative to traditional organic solvents.

According to the first three chapters of this thesis, the application of nonionic surfactants for the CPE in a continuous mode combined with a solvent recirculation is a beneficial technique for the ISPR, especially when the amphiphile is permitted for food or cosmetics and can be left in the product. However, the determination of the process parameters and operation mode was based on a model system. As a following milestone on the way to competitive ISPR using nonionic surfactants, it was essential to prove the concept using different authentic feedstocks.

The feasibility of the ISPR using "leave-in" amphiphiles was performed as a batch cloud point extraction from authentic pineapple juice. As a major result, 952 $mg \cdot L^{-1}$ phenolic compounds as well as yellow pigments accumulation were achieved. In addition, the micellar phase had a homogeneous structure. The antioxidant capacity was maintained unchanged in the micellar phase in contrast to the pure juice, where the antioxidant capacity was strongly minimized by the heat and air exposure. Lastly, the separation was stabilized by the sugars in the juice, which was a positive effect of the feedstock. These observations prove the suitability of the ISPR from fruit juices using "leave-in" surfactants. Therefore, the ISPR from the pineapple juice not only demonstrated a promising separation concept in batch mode but also presented a micellar phase that can be attractive as an ingredient for cosmetic formulations. Such kind of new applications for the surfactant-based extracts can compensate the need of surfactant stripping and thus make the CPE feasible for the production of ingredient systems. The successful CPE from pineapple juice was a first proof of the concept for direct ISPR using permitted surfactants.

On the other hand, the continuous CPE with recirculation of the micellar phase can be beneficial when the target products have to be isolated out of a diluted feedstock. By applying the strategy proposed in this work, the combination of laborious cell separation and subsequent extraction from the biomass can be replaced by an ISPR with a compatible nonionic surfactant. Additionally, by utilizing the recirculation of the solvent, a higher feed-to-solvent ratio is achievable. A successful implementation of this concept was presented in this work. Particularly, the continuous surfactant-based in situ extraction from the green microalgae *Acutodesmus obliquus* using Triton X-114 was realized over a period of 24 hours. Although the complete saturation of the micellar phase with algae products could

not be detected, culture-to-solvent ratio equal to 46 was reached in combination with a good biocompatibility of the surfactant with the microalgae cells. The surfactant-based cloud point extraction of microalgae in a continuous mode was demonstrated for the first time. The results corresponded to the already reported biocompatible cloud point extraction with Triton X-114 from *Acutodesmus obliquus* in batch mode, but also allowed an intensification of the CPE. In order to extend the field of the continuous ISPR using "leave-in" surfactants, the possibility to use Silwet L-7230 and ROKAnol NL-5 was also studied. The two amphiphiles were compatible with the studied microalgae. However, the attempt for the continuous extraction with solvent recirculation from the algal culture using Silwet L-7230 was aborted due to the complete clogging of the column with viscous liquid crystalline phase. This was an example, that the concept of a continuous CPE with solvent recirculation is not equally applicable using all surfactants that were selected using a model system. The process is highly dependent on the feedstock composition, which can affect the phase behavior of the surfactant and lead to unsatisfactory results. Nevertheless, the potential of the CPE as a separation technique that can be applied in a more intensive manner than a batch separation is promising in case the interactions of the surfactant and the feedstock are not negative. The continuous CPE from the algae culture was the second proof of the concept for a direct ISPR from an authentic culture.

Based on the findings in laboratory and technical scale, a surfactant-based in situ extraction from microalgae cultures in pilot scale was realized at the final stage of this work. A similar set-up to the technical extraction equipment, aiming to increase the capacity from 1 L h^{-1} to 25 L h^{-1}, was designed at BIQ Algae House in Hamburg. As a result, the first reported long-term continuous in situ extraction from authentic microalgae culture using nonionic surfactants was implemented in pilot scale. The constructed pilot set-up allowed an in situ extraction from algae suspension using the "leave-in surfactant" ROKAnol NL5. The new approach yielded valuable compounds such as lutein, neoxanthin, and violaxanthin, which are attractive for cosmetic and medical products. Hence, the production of a micellar extract, which can be potentially attractive for a cosmetic formulation, could be demonstrated not only in batch but also in a continuous mode.

Ultimately, this work contributed to the knowledge regarding the recovery of valuable compounds from natural feedstocks. The cloud point system was intensively studied as a tool for the mild recovery of organic solutes from authentic feed solutions. The successful in situ product removal from the plant suspensions using different nonionic surfactants confirmed that the CPE is an attractive technique for natural product separation. Moreover, nonionic amphiphiles, which are permitted in food and cosmetics, can be used as alternative to traditional organic solvents. However, there are aspects such as long-term effect of the cell culture, shelf-life of the micellar extract, achievable loading of the extract in comparison to organic solvents as well as the financial efficiency, which were not addressed in this work. Nevertheless, the presented applications in technical and pilot scale could convince that the cloud point extraction is suitable for not only operations in the laboratory practice, but also as a unit operation, that is relevant to an industrial process. Therefore, this thesis can be addressed as a contribution towards making CPE more attractive for the natural product separation in the large-scale production.

APPENDIX

A 1 MANNA LIN M: COMPOSITION

EG-Düngemittel

NPK-Dünger mit Magnesium 15 – 10 – 15 (2) und Spurennährstoffen

Für die Bodendüngung in Zierpflanzenbau, Obstbau und Baumschule

15	% N	Gesamtstickstoff 4,5% N Nitratstickstoff 10,5% N Ammoniumstickstoff
10	% P_2O_5	neutral-ammoncitratlöslich und wasserlösliches Phosphat 10 % wasserlösliches Phosphat
15	% K_2O	wasserlösliches Kaliumoxid
2	% MgO	wasserlösliches Magnesiumoxid
0,025	% B	wasserlösliches Bor
0,005	% Cu	wasserlösliches Kupfer als Chelat von EDTA
0,06	% Fe	wasserlösliches Eisen als Chelat von EDTA
0,025	% Mn	wasserlösliches Mangan als Chelat von EDTA
0,0025	% Mo	wasserlösliches Molybdän
0,02	% Zn	wasserlösliches Zink als Chelat von EDTA

A 2 LINES COUPLING AT THE BIQ ALGAE HOUSE

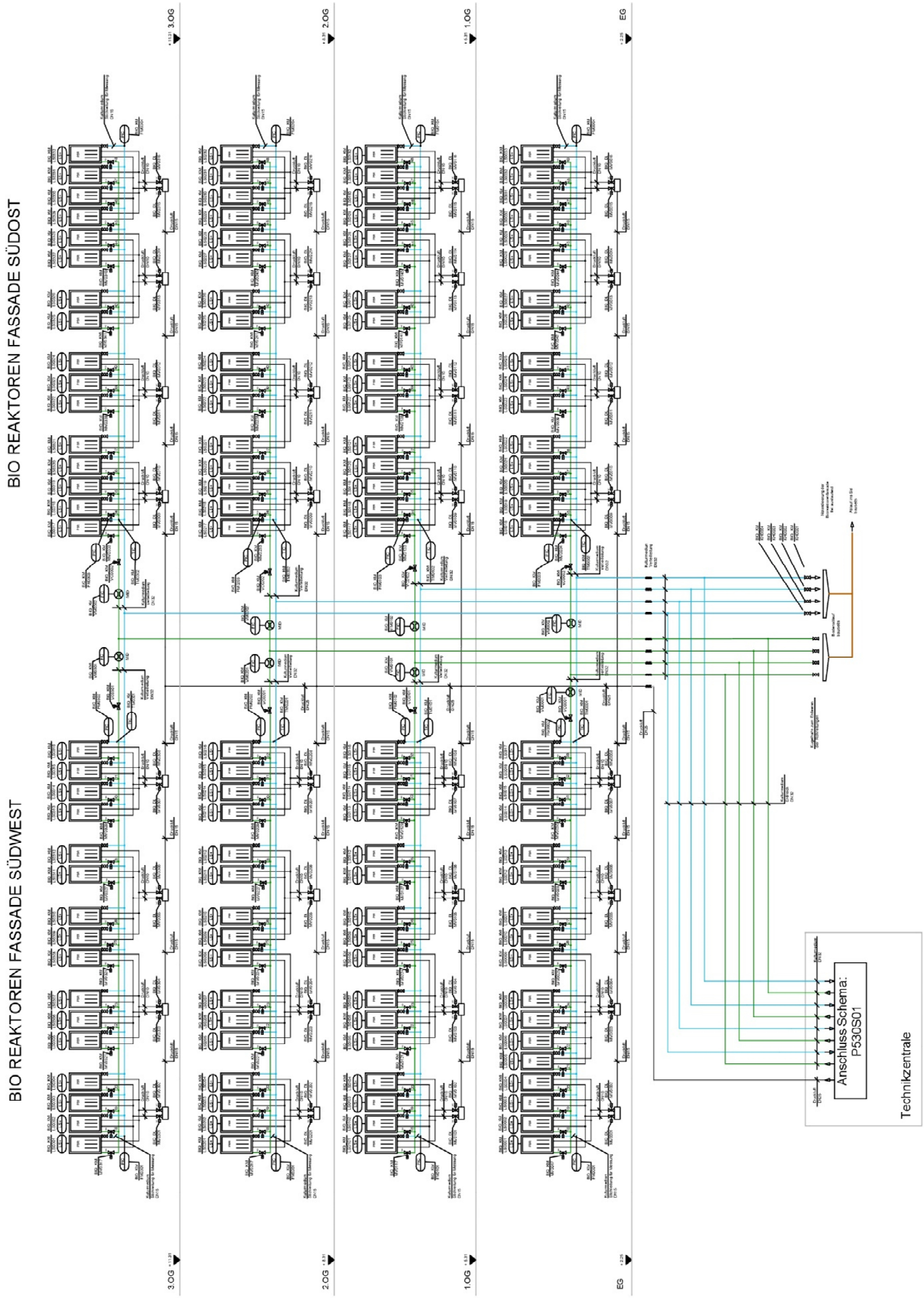

A 3 PILOT SCALE EXTRACTION COLUMN: CONTROL DIAGRAM

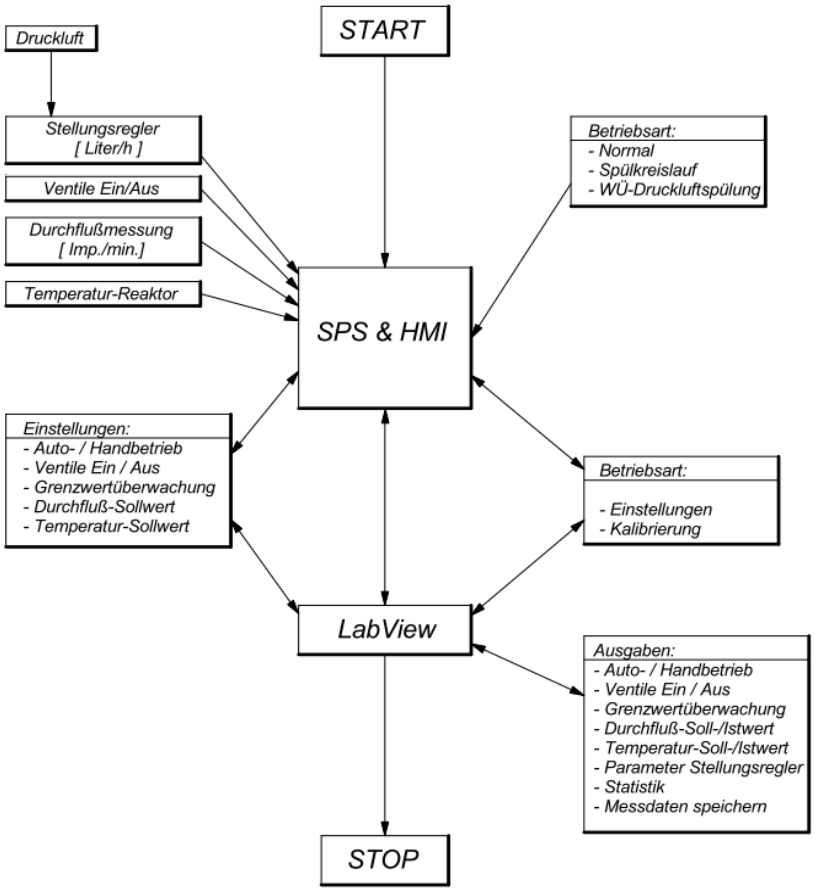

A 4 PILOT SCALE EXTRACTION COLUMN: VALVE POSITIONS

	Valve No.	Regular	Exception	Rinse circuit	Pressurized Air circuit
		Position	Position	Position	Position
Controlled Valves	V-1	open (FIC)	closed	open	open
3-Way (controlled)	V-11	open (AB)	open (AB)	open (AB)	closed (BC)
	V-12	open (AB)	open (AB)	open (AB)	closed (BC)
	V-13	open (AB)	open (AB)	open (AB)	closed (BC)
3-Way (manual)	V-9	open (AB)	open (AB)	closed (BC)	open (AB)
	V-10	open (AB)	open (AB)	closed (BC)	open (AB)
Manual Valves	V-2	closed	closed	open	closed
	V-4	open	open	closed	open
	V-6	open	open	closed	open
	V-7	open	open	closed	open
	V-8	open	open	open	open
Additional Valves	*V-3*	*Flap valve*			
	V-5	*Throttle valve*			
	V-14	*Flap valve*			

A 5 PILOT SCALE EXTRACTION COLUMN: SCHEMATIC DESIGN

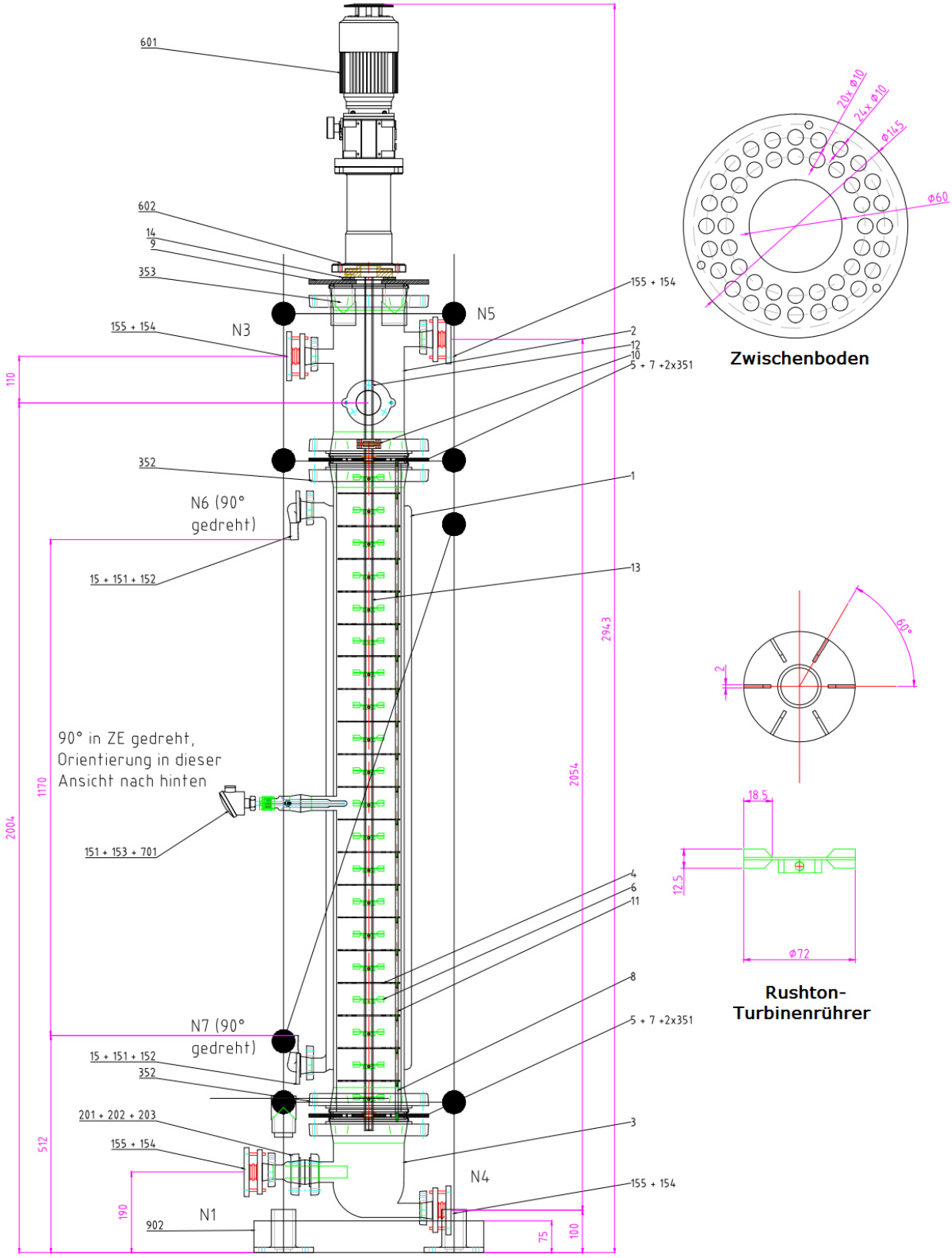

A 6 PROGRAMMABLE LOGIC CONTROLLER SIMATIC S7 (SIEMENS)

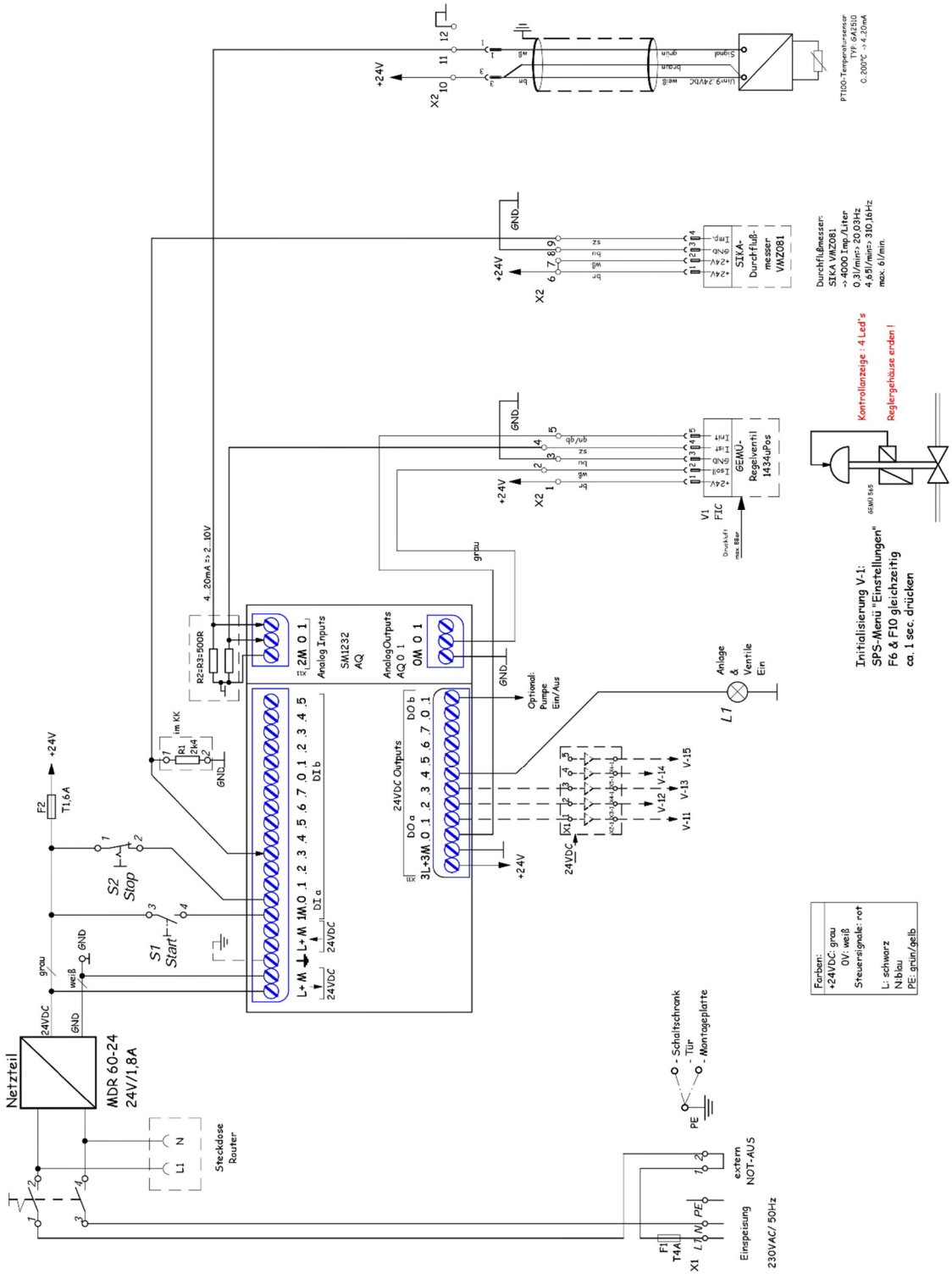

SPS: Simatic S7 CPU 1214C DC/DC/DC 6ES7214-1AG31-0XB0 24 V/DC
Software:

- TIA Portal Totally Integrated Automation System Portal, Version V13
- Simatik Step7 Basic, Version V13
- Simatik WINCC, Version V13

A 7 HMI-MODULE INTERFACE

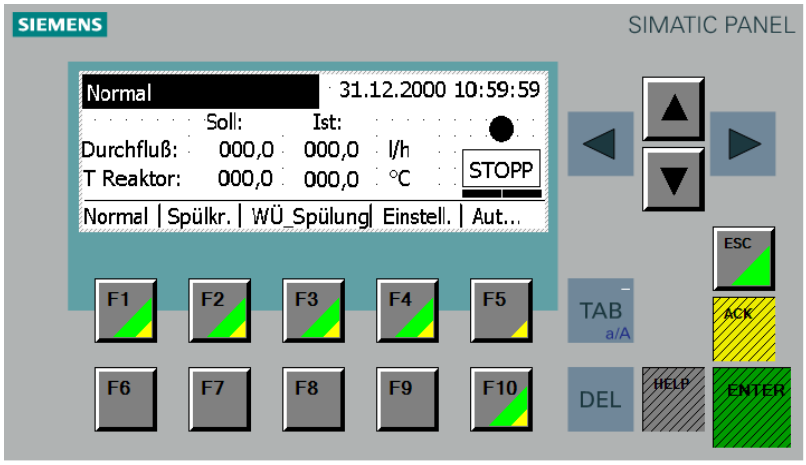

A 8 LABVIEW INTERFACE

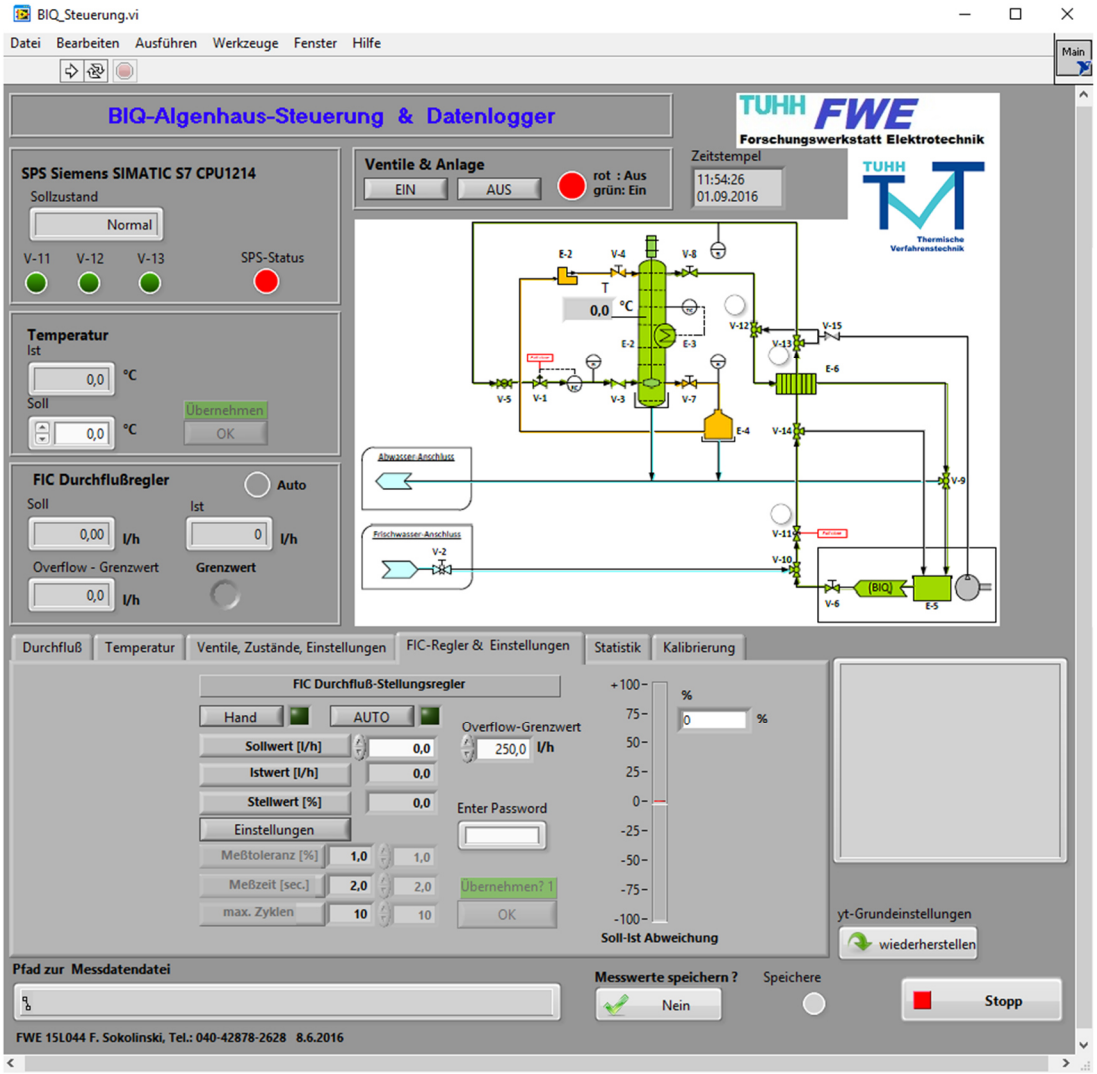

A 9 LIQUID-LIQUID EQUILIBRIUM TRITON X-114/WATER [43]

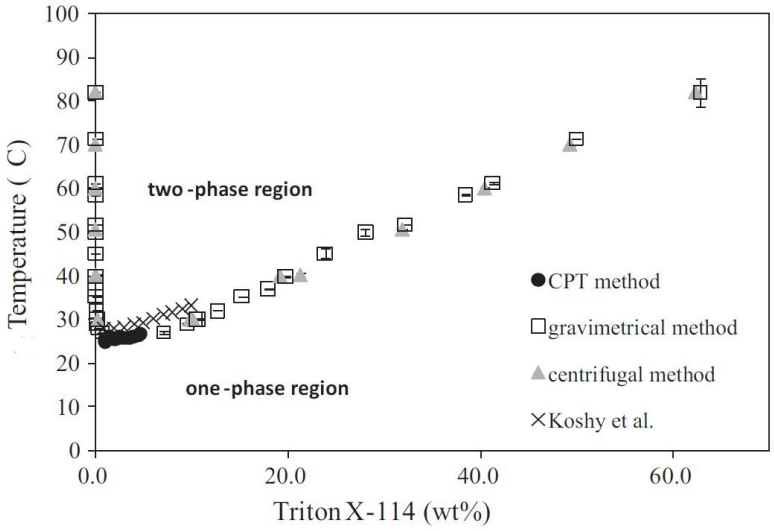

A 10 CALIBRATION CURVES OF THE PUMPS AT THE TECHNICAL PLANT

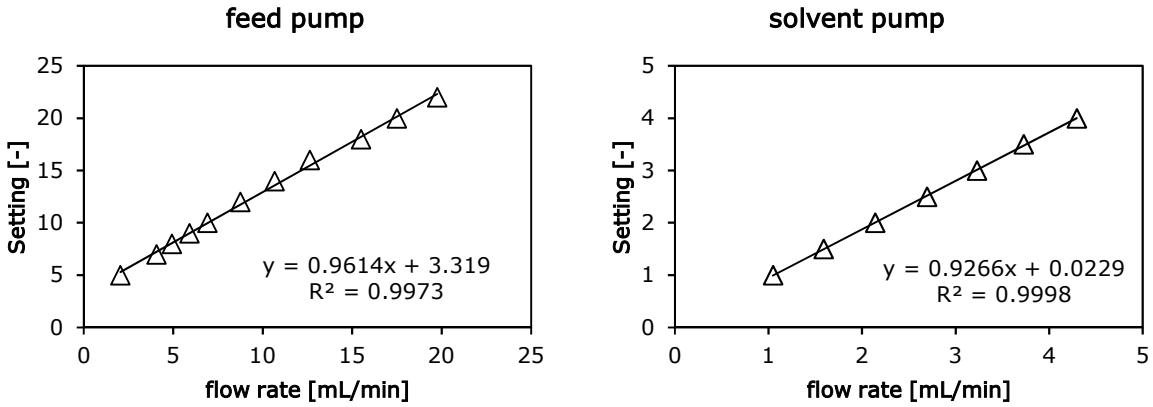

A 11 TRITON X-114 CALIBRATION CURVE (UV-VIS)

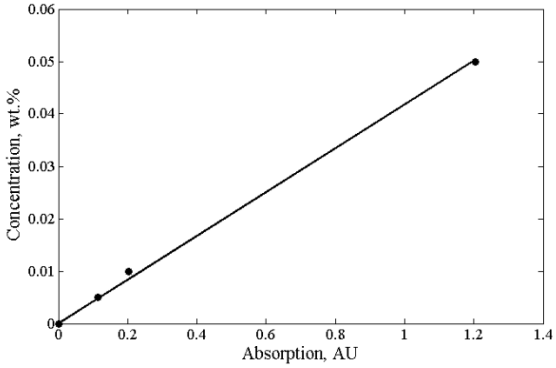

f(x) = a*x, a = 0.04176

Goodness of fit:
SSE: 2.454e-006;
R-square: 0.9984;
Adjusted R-square: 0.9984;
RMSE: 0.0009044

A 12 CALIBRATION CURVES OF THE PUMP AT THE PILOT PLANT

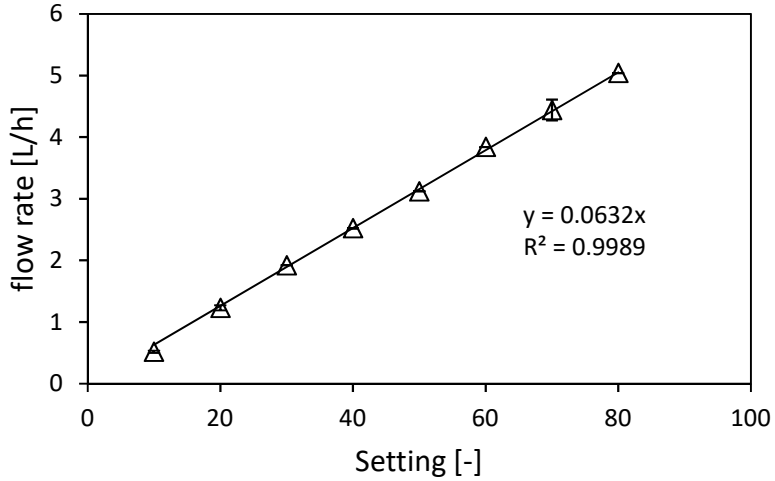

A 13 CALIBRATION OF POSITIONER AND CONTROL VALVE

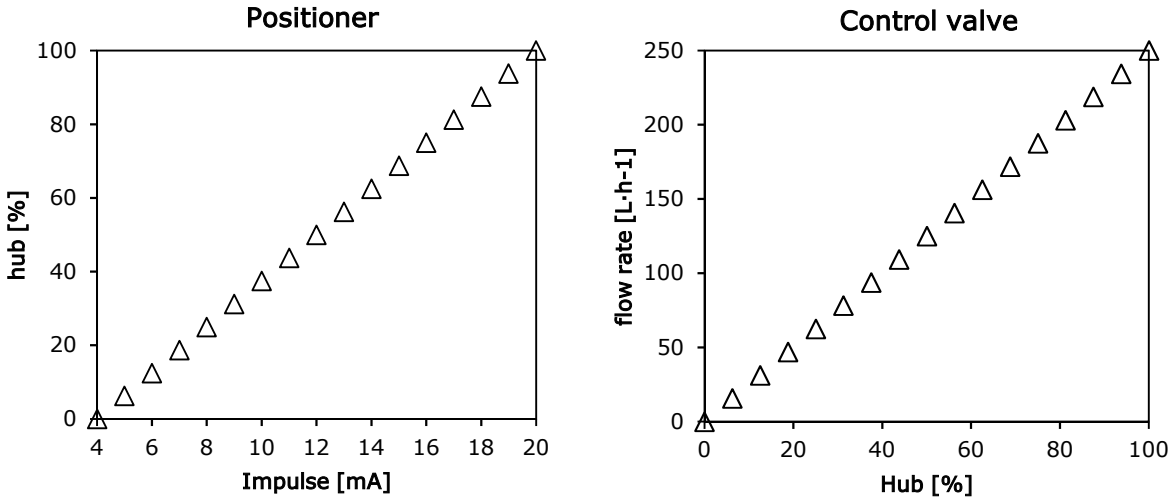

A 14 TRITON X-114 CALIBRATION CURVES (HPLC)

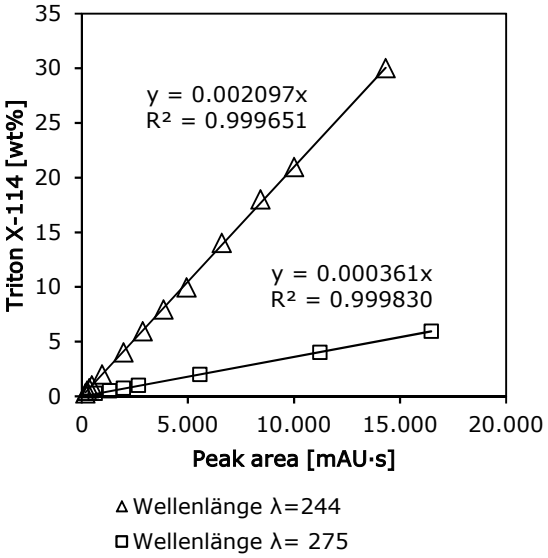

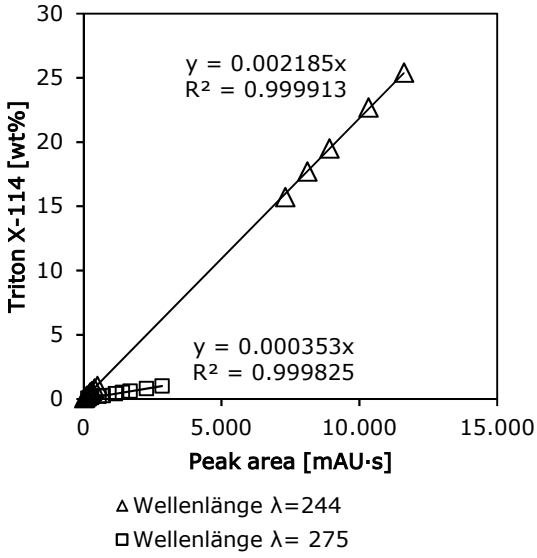

A 15 CINNAMIC ACID CALIBRATION CURVES (HPLC)

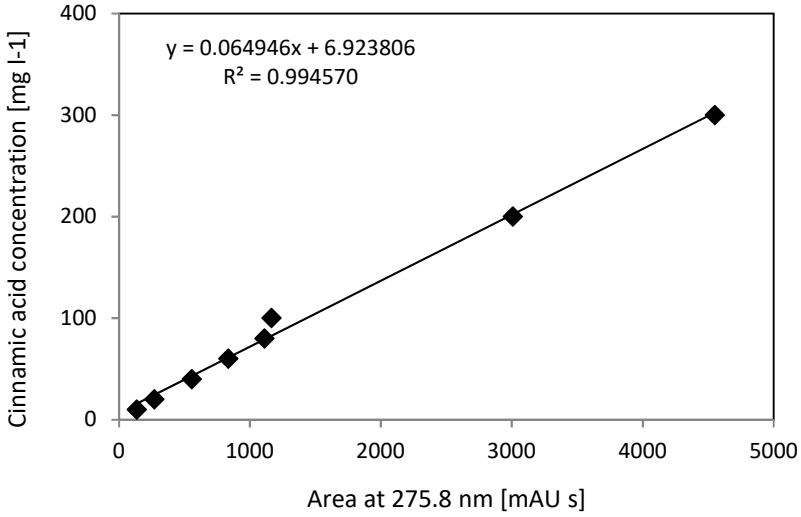

A 16 GALLIC ACID CALIBRATION CURVE (UV-VIS)

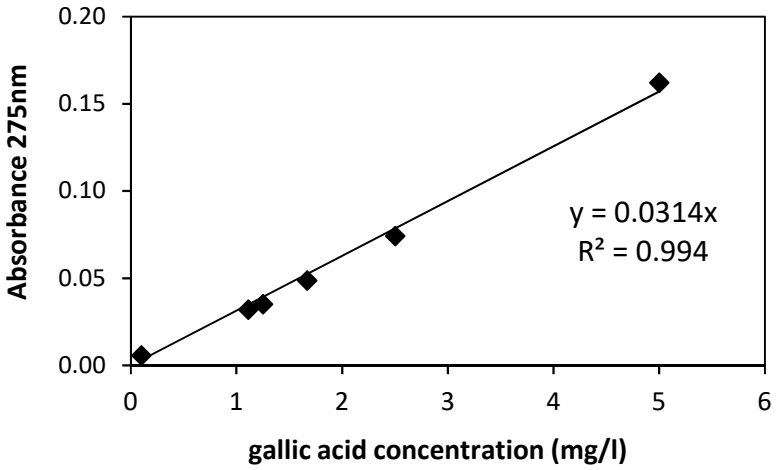

A 17 GLUCOSE CALIBRATION CURVE (UV-VIS)

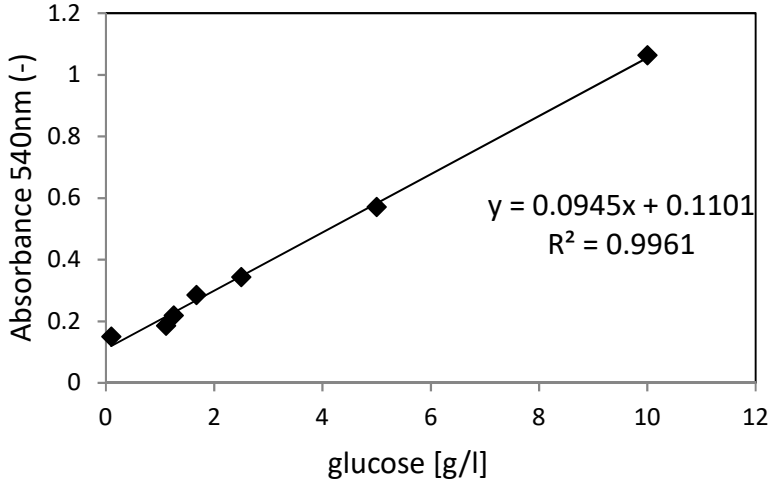

A 18 DESIGN OF EXPERIMENT: MEASURING POINTS AND RESPONSES

Parameter combinations (capacity b, agitation speed n and feed-to-solvent ratio v) and corresponding responses (cinnamic acid yield $Y_{cont.}$ and productivity F_{CA}) for the optimization of the continuous cloud point extraction of cinnamic acid with Triton X-114 at 40 °C

Run [-]	b [l·h^{-1}]	n [rpm]	v [-]	$Y_{cont.}$ [-]	F_{CA} [g.h^{-1}]	Run [-]	b [l·h^{-1}]	n [rpm]	v [-]	$Y_{cont.}$ [-]	F_{CA} [g.h^{-1}]
1	1.5	39.7	8.0	0.281	65.87	**11**	1.7	30.0	6.7	0.391	94.78
2	1.4	20.0	6.0	0.413	88.15	**12**	1.0	40.0	6.0	0.425	62.38
3	1.0	49.9	8.0	0.263	46.65	**13**	1.0	20.0	7.5	0.247	76.37
4	1.5	34.0	10.0	0.201	54.42	**14**	1.5	39.7	8.0	0.289	78.07
5	1.0	20.0	10.0	0.228	36.34	**15**	2.0	20.0	10.0	0.217	71.16
6	2.0	20.0	6.0	0.371	113.55	**16**	2.0	40.0	10.0	0.195	66.25
7	1.5	20.0	8.4	0.240	58.78	**17**	1.5	34.0	10.0	0.206	58.26
8	1.0	20.0	7.5	0.283	46.97	**18**	1.5	20.0	8.4	0.233	58.72
9	1.0	40.0	10.0	0.240	37.79	**19**	2.0	22.0	8.0	0.254	92.98
10	1.0	40.0	10.0	0.214	34.85	**20**	1.0	60.0	10.0	0.207	35.23

A 19 YIELD OPTIMIZATION

Model summary statistics of different data fits of the yield

Source	Std. Dev.	R-Squared	Adjusted R-Squared	Predicted R-Squared	PRESS
Linear	0.032	0.833	0.802	0.728	0.027
2-FI	0.035	0.843	0.771	0.549	0.045
Quadratic	**0.021**	**0.954**	**0.912**	**0.717**	**0.028**
Cubic*	0.014	0.990	0.960	-	-

Yield: Sequential Model Sum of Squares

Source	Sum of Squares	df	Mean Square	F Value	p-Value Prob > F
Mean vs Total	1.4569671	1	1.4569671		
Linear vs Mean	0.08322485	3	0.02774162	26.5904968	< 0.0001
2FI vs Linear	0.00102621	3	0.00034207	0.28384987	0.8362
Quadratic vs 2FI	0.01104797	3	0.00368266	7.97376135	0.0052
Cubic vs Quadratic	0.00357159	5	0.00071432	3.41167291	0.1021
Residual	0.00104687	5	0.00020937		
Total	1.55688461	20	0.07784423		

Yield: Lack of Fit test

Source	Squares	df	Square	Value	Prob > F
Linear	0.01564578	11	0.00142234	6.79328321	0.0233
2FI	0.01461956	8	0.00182745	8.72810063	0.0144
Quadratic	0.00357159	5	0.00071432	3.41167291	0.1021
Cubic	0	0			
Pure Error	0.00104687	5	0.00020937		

Yield: Normal probability plot of residues (a) and residuals vs. run (b)

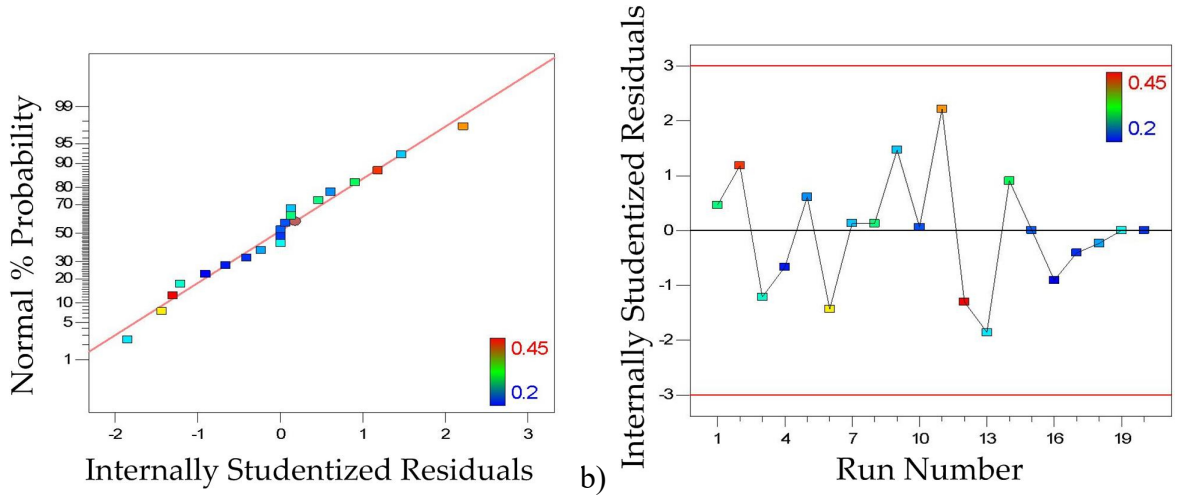

A 20 PRODUCTIVITY OPTIMIZATION

Model summary statistics of different data fits of the productivity

Source	Std. Dev.	R-Squared	Adjusted R-Squared	Predicted R-Squared	PRESS
Linear	**7.44**	**0.903**	**0.885**	**0.850**	**1373**
2-FI	7.59	0.918	0.880	0.814	1700
Quadratic	8.54	0.920	0.848	0.617	3505
Cubic*	10.18	0.943	0.785	-	-

**Cubic model is aliased*

Productivity: Sequential Model Sum of Squares

Source	Sum of Squares	df	Mean Square	F Value	p-Value Prob > F
Mean vs Total	81610.7179	1	81610.7179		
Linear vs Mean	8254.7955	3	2751.5985	49.7734704	< 0.0001
2FI vs Linear	136.190511	3	45.3968369	0.78863621	0.5215
Quadratic vs 2FI	18.8814302	3	6.29381008	0.08628194	0.9660
Cubic vs Quadratic	211.035377	5	42.2070754	0.40708074	0.8268
Residual	518.411597	5	103.682319		
Total	90750.0324	20	4537.50162		

Productivity: Lack of Fit test

Source	Squares	df	Square	Value	Prob > F
Linear	366.107318	11	33.2824834	0.32100443	0.9459
2FI	229.916807	8	28.7396009	0.27718902	0.9472
Quadratic	211.035377	5	42.2070754	0.40708074	0.8268
Cubic	0	0			
Pure Error	518.411597	5	103.682319		

Productivity: Normal probability plot of residues (a) and residuals vs. run (b)

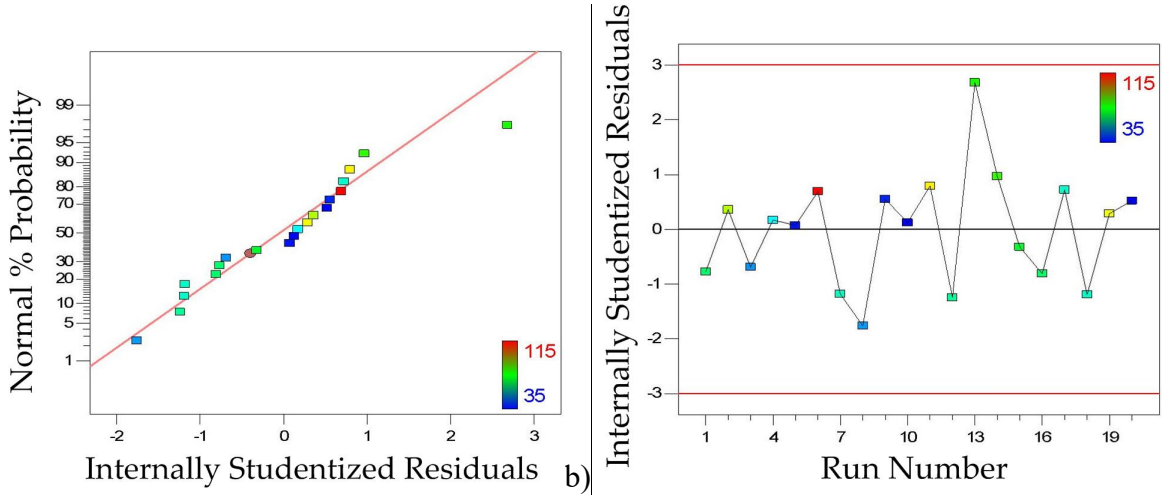

A 21 LIQUID-LIQUID EQUILIBRIUM SYNPERONIC 91/5 AND WATER

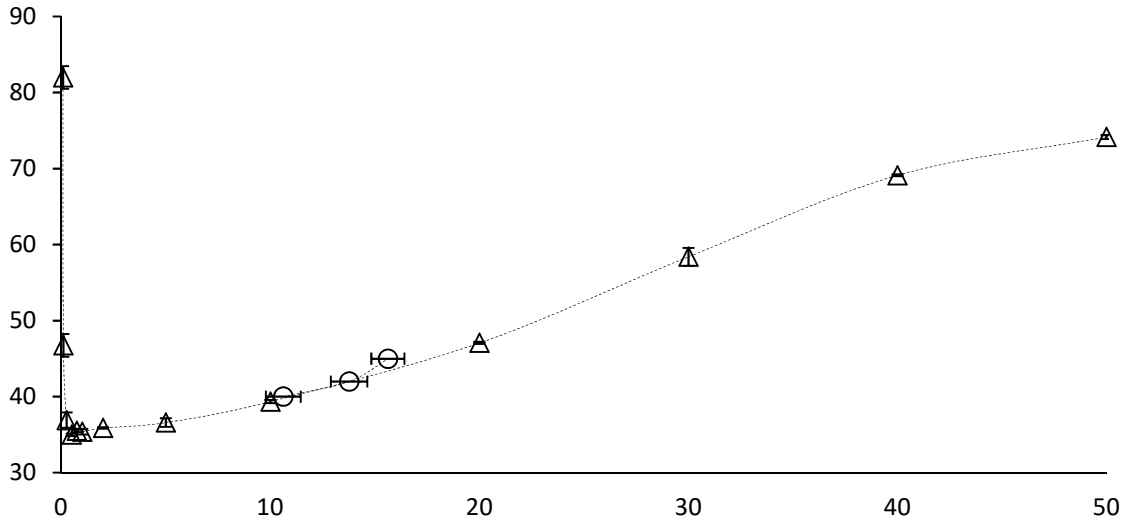

A 22 AGITATION LEVELS IN THE PILOT SCALE COLUMN

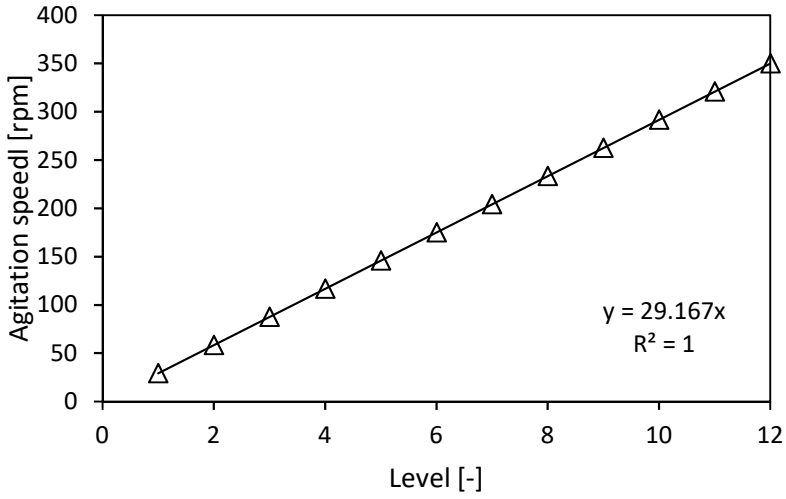

A 23 TRITON X-114 CONCENTRATION PROFILE IN PILOT SCALE

Profiles of the Triton X-114 concentration (a) in the extract over the time during the experiments with "constant velocity" parameter setting. Error bars indicate the standard deviation within each experiment.

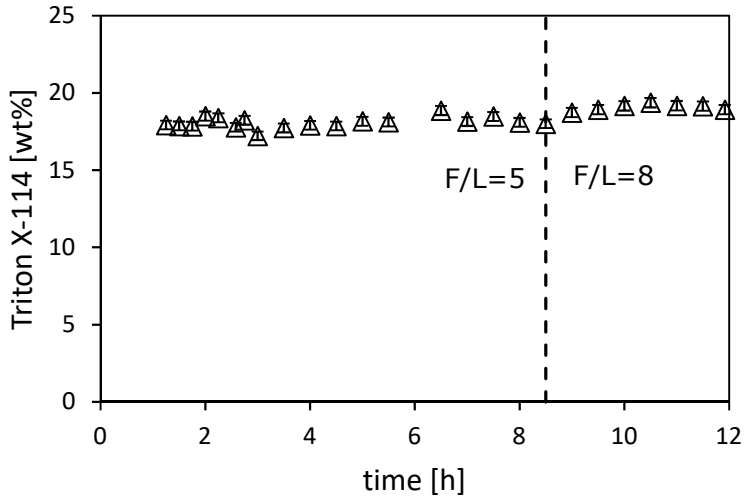

LIST OF FIGURES

LIST OF TABLES

LIST OF EQUATIONS

LIST OF ABBREVIATIONS AND SYMBOLS

Abbreviation	Meaning
A.obl.	Acutodesmus obliquus
ATPS	Aqueous Two-Phase Systems
CA	Cinnamic Acid
CD	Cell density
cmc	Critical Micelle Concentration
CPE	Cloud Point Extraction
CPT	Cloud Point Temperature
GAE	Gallic Acid Equivalents
HLB	Hydrophilic-Lipophilic Balance
HPLC	High Performance Liquid Chromatography
ISPR	In Situ Product Removal
LCST	Lower Critical Solution Temperature
LLE	Liquid-Liquid Equilibrium
OD	Optical Density
ORC	Oldshue-Rushton Column
PLC	Programmable Logic Controller
RDC	Rotating Disc Contactor
RPA	Relative Photosynthetic Activity
SEC	Size-Exclusion Chromatography

Symbol	Meaning
Greek symbols	
α	coexisting phase index [-]
β	coexisting phase index [-]
γ	activity coefficient [-]
$\dot{\gamma}$	shear rate [s^{-1}]
η	kinematic viscosity [Pa·s]
ε	extraction factor [-]
φ	coexisting phase index [-]
μ	chemical potential [$J \cdot mol^{-1}$]
ν	feed-to-solvent ratio [-]
π	Pi, = 3.14159 [-]
ρ	density [$g \cdot cm^{-3}$]
τ	residence time [s]
Latin symbols	
A	index for aqueous phase [-]
A_f	free cross-section [m^2]
b	column capacity [$L \cdot h^{-1}$]
$c_i^{\alpha}, c_i^{\beta}$	concentration of component i in phase α or β [$g \cdot L^{-3}$]
C	measured concentration [$g \cdot L^{-3}$]

d	diameter [m]
D_a	impeller diameter [m]
$\dot{E}$	extract stream [L·h^{-1}]
$\dot{F}$	feed stream [L·h^{-1}]
F_i	productivity [g·h^{-1}]
G	Gibbs free energy [J·mol^{-1}]
h	height [m]
i	component index [-]
$K_i^{\alpha\beta}$	partition coefficient [-]
m_i	mass of component I [g]
M	index for micellar phase [-]
N_{Re}	Reynolds Number [-]
N_P	Power Number [-]
$N_{theo.}$	number of theoretical stages [-]
n_i^{φ}	molar amount of component i of the phase φ [mol]
$P_i^{\alpha\beta}$	partition coefficient [-]
P^{φ}	pressure [Pa]
R	molar gas constant [J·mol^{-1}·K^{-1}]
$\dot{R}$	raffinate stream [L·h^{-1}]
S^{φ}	entropy [J·K^{-1}]
$\dot{S}$	solvent stream [L·h^{-1}]

s_x	standard deviation [-]
T	temperature [° C]
T_i	enrichment factor [-]
U^{φ}	internal energy [J]
v	velocity [$m \cdot s^{-1}$]
V^{φ}	volume [m^3]
w_i	weight fraction of component (i) [wt%]
x	molar fraction [-]
$\bar{x}$	mean value [-]
Y	yield [-]

BIBLIOGRAPHY

[1] Ceresana Research, Market Study on Surfactants, 2nd ed., Germany, 2015.

[2] DecisionDatabases.com, Global Surfactants Market Research Report - Industry Analysis, Size, Share, Growth, Trends and Forecast 2014 to 2021, 1st ed., India, 2015.

[3] K. Holmberg, Surfactants and polymers in aqueous solution, 2nd ed., Wiley, Chichester, 2007.

[4] W.L. Hinze, E. Pramauro, A Critical Review of Surfactant-Mediated Phase Separations (Cloud-Point Extractions): Theory and Applications, Critical Reviews in Analytical Chemistry 24 (2) (1993) 133–177.

[5] U.v. Stockar, L.A.M. van der Wielen, A. Bruggink (Eds.), Process Integration in Biochemical Engineering, 2003.

[6] L. Wang, Z. Wang, J.-H. Xu, D. Bao, H. Qi, An eco-friendly and sustainable process for enzymatic hydrolysis of penicillin G in cloud point system, Bioprocess Biosyst. Eng. 29 (3) (2006) 157–162.

[7] E. Katsoyannos, O. Gortzi, A. Chatzilazarou, V. Athanasiadis, J. Tsaknis, S. Lalas, Evaluation of the suitability of low hazard surfactants for the separation of phenols and carotenoids from red-flesh orange juice and olive mill wastewater using cloud point extraction, J. Sep. Sci. 35 (19) (2012) 2665–2670.

[8] T. Pan, S. Ren, M. Xu, G. Sun, J. Guo, Extractive biodecolorization of triphenylmethane dyes in cloud point system by Aeromonas hydrophila DN322p, Applied Microbiology and Biotechnology 97 (13) (2013) 6051–6055.

[9] P. Glembin, R. Racheva, M. Kerner, I. Smirnova, Micelle mediated extraction of fatty acids from microalgae cultures: Implementation for outdoor cultivation, Separation and Purification Technology 135 (2014) 127–134.

[10] K. Sattler, Thermische Trennverfahren, John Wiley & Sons, Hoboken, 2012.

[11] J. Gmehling, B. Kolbe, Thermodynamik, 2nd ed., VCH, Weinheim, 1992.

[12] J.M. Prausnitz, E.G.d. Azevedo, R.N. Lichtenthaler, Molecular thermodynamics of fluid-phase equilibria, 3rd ed., Prentice Hall PTR, Upper Saddle River, N.J, 1999.

[13] T. Ingram, I. Smirnova, F.J. Keil, Micellar systems for separation processes: Design of aqueous micellar two-phase systems based on thermodynamic models. Zugl.: Hamburg-Harburg, Techn. Univ., Institut für Thermische Verfahrenstechnik, Diss., 2012, VDI-Verl., Düsseldorf, 2013.

[14] R.H. Perry, D.W. Green (Eds.), Perry's chemical engineers' handbook, 7th ed., McGraw-Hill, New York, NY, 1999.

[15] A.B.d. Haan, H. Bosch, Industrial separation processes: Fundamentals, De Gruyter, Berlin, 2013.

[16] H. Walter, Partitioning In Aqueous Two - Phase System: Theory, Methods, Uses and Applications to Biotechnology, Elsevier Science, Oxford, 1985.

[17] R. Goedecke, Fluidverfahrenstechnik, Wiley-VCH, Hoboken, 2008.

[18] Peter Kolb, Hans-Jörg Bart, Hydrodynamics and mass transfer in an agitated miniplant extractor type Kühni. Dissertation, Technische Universität Kaiserslautern, 2004.

[19] C.A. Sleicher, Axial mixing and extraction efficiency, AIChE J. 5 (2) (1959) 145–149.

[20] V.N. Misra (Ed.), Proceedings of the International Symposium on Solvent Extraction (ISSE): September 26 - 27, 2002, Allied Publ, New Delhi, 2002.

[21] E. Bender, R. Berger, W. Leuckel, D. Wolf, Untersuchungen zur Betriebscharakteristik pulsierter Füllkörperkolonnen für die Flüssig/Flüssig-Extraktion, Chemie Ingenieur Technik 51 (3) (1979) 192–199.

[22] A.I. Johnson, E.A.L. Lavergne, Holdup in liquid-liquid extraction columns, Can. J. Chem. Eng. 39 (1) (1961) 37–41.

[23] R. Stockfleth, G. Brunner, J. Werther, Fluiddynamik in Hochdruckgegenstromkolonnen für Gasextraktion, VDI-Verl., Düsseldorf, 2002.

[24] J.S.R. Coimbra, F. Mojola, A.J.A. Meirelles, Dispersed Phase Hold-Up in a Perforated Rotating Disc Contactor (PRDC) Using Aqueous Two-Phase Systems, J. Chem. Eng. Japan / JCEJ 31 (2) (1998) 277–280.

[25] G.P. Towler, R.K. Sinnott, Chemical engineering design: Principles, practice, and economics of plant and process design, 2nd ed., Butterworth-Heinemann, Oxford, 2013.

[26] M.N. Jones, D. Chapman, Micelles, monolayers, and biomembranes, Wiley-Liss, New York, NY, 1995.

[27] M. Wolszczak, J. Miller, Characterization of non-ionic surfactant aggregates by fluorometric techniques, Journal of Photochemistry and Photobiology A: Chemistry 147 (1) (2002) 45–54.

[28] Németh, Rácz, Koczo, Foam Control by Silicone Polyethers-Mechanisms of "Cloud Point Antifoaming", J. Colloid Interface Sci. 207 (2) (1998) 386–394.

[29] W.C. Griffin, Classification of Surface-Active Agents by 'HLB', Journal of the Society of Cosmetic Chemists 5 (4) (1954) 249–256.

[30] T.E. Furia (Ed.), CRC handbook of food additives, 2nd ed., CRC Press, Boca Raton, Fla., 1990.

[31] D.F. Evans, H. Wennerström, The colloidal domain: Where physics, chemistry, biology, and technology meet, 2nd ed., Wiley-VCH, New York, NY, 1999.

[32] T.F. Tadros, Applied surfactants: Principles and applications, 2nd ed., Wiley-VCH, Weinheim, 2008.

[33] T.E. Sandoval, M.P. Gárate, Measurement of the phase behaviour of the binary systems {carbon dioxide (CO2)+non-ionic surfactants (CiEOj)}, The Journal of Chemical Thermodynamics 45 (1) (2012) 109–113.

[34] A. Lavergne, Y. Zhu, V. Molinier, J.-M. Aubry, Aqueous phase behavior of isosorbide-based non-ionic surfactants, Colloids and Surfaces A: Physicochemical and Engineering Aspects 404 (2012) 56–62.

[35] M. Kleman, The lamellar and sponge phases of dilute surfactant systems: Structures and defects at equilibrium and under shear, Pramana - J Phys 53 (1) (1999) 107–119.

[36] Kunieda, Umizu, Yamaguchi, Mixing Effect of Polyoxyethylene-Type Nonionic Surfactants on the Liquid Crystalline Structures, J. Colloid Interface Sci. 218 (1) (1999) 88–96.

[37] T. Gu, P.A. Galera-Gómez, Clouding of Triton X-114: The effect of added electrolytes on the cloud point of Triton X-114 in the presence of ionic surfactants, Colloids and Surfaces A: Physicochemical and Engineering Aspects 104 (2-3) (1995) 307–312.

[38] L. Koshy, A.H. Saiyad, A.K. Rakshit, The effects of various foreign substances on the cloud point of Triton X 100 and Triton X 114, Colloid Polym Sci 274 (6) (1996) 582–587.

[39] P. Trakultamupatam, J.F. Scamehorn, S. Osuwan, Removal of volatile aromatic contaminants from wastewater by cloud point extraction, Separation Science and Technology 37 (6) (2002) 1291–1305.

[40] P. Ball, Water as an active constituent in cell biology, Chem. Rev. 108 (1) (2008) 74–108.

[41] I. Fischer, M. Franzreb, Direct determination of the composition of aqueous micellar two-phase systems (AMTPS) using potentiometric titration—A rapid tool for detergent-based bioseparation, Colloids and Surfaces A: Physicochemical and Engineering Aspects 377 (1-3) (2011) 97–102.

[42] W. Kimchuwanit, S. Osuwan, J.F. Scamehorn, J.H. HARWELL, K.J. HALLER, Use of a Micellar-Rich Coacervate Phase to Extract Trichloroethylene from Water, Separation Science and Technology 35 (13) (2000) 1991–2002.

[43] T. Ingram, S. Storm, P. Glembin, S. Bendt, D. Huber, T. Mehling, I. Smirnova, Aqueous Surfactant Two-Phase Systems for the Continuous Countercurrent Cloud Point Extraction, Chemie Ingenieur Technik 274 (6) (2012)

[44] Z. Hu, X. Zhang, Z. Wu, H. Qi, Z. Wang, Export of intracellular Monascus pigments by two-stage microbial fermentation in nonionic surfactant micelle aqueous solution, Journal of Biotechnology 162 (2-3) (2012) 202–209.

[45] A. Freeman, J.M. Woodley, M.D. Lilly, In Situ Product Removal as a Tool for Bioprocessing, Nat Biotechnol 11 (9) (1993) 1007–1012.

[46] W. van Hecke, G. Kaur, H. de Wever, Advances in in-situ product recovery (ISPR) in whole cell biotechnology during the last decade, Biotechnology Advances 32 (7) (2014) 1245–1255.

[47] A. Bednarz, A. Jupke, A.C. Spieß, A. Pfennig, Aerated extraction columns for in situ separation of bio-based diamines from cell suspensions, J. Chem. Technol. Biotechnol. 94 (2) (2019) 426–434.

[48] K. Schügerl, Integrated processing of biotechnology products, Biotechnology Advances 18 (7) (2000) 581–599.

[49] A. Eggert, T. Maßmann, D. Kreyenschulte, M. Becker, B. Heyman, J. Büchs, A. Jupke, Integrated in-situ product removal process concept for itaconic acid by reactive extraction, pH-shift back extraction and purification by pH-shift crystallization, Separation and Purification Technology 215 (2019) 463–472.

[50] R. Pörtner, H. Märkl, Dialysis cultures, Applied Microbiology and Biotechnology 50 (4) (1998) 403–414.

[51] H. Mollet, A. Grubenmann, Formulierungstechnik, WILEY-VCH Verlag GmbH & Co. KGaA, Weinheim, Germany, 1999.

[52] J.J. Malinowski, Two-phase partitioning bioreactors in fermentation technology, Biotechnology Advances 19 (7) (2001) 525–538.

[53] D.M.M. Kleinegris, M. Janssen, W.A. Brandenburg, R.H. Wijffels, Two-phase systems: Potential for in situ extraction of microalgal products, Biotechnology Advances 29 (5) (2011) 502–507.

[54] P.M. Foley, E.S. Beach, J.B. Zimmerman, Algae as a source of renewable chemicals: Opportunities and challenges, Green Chem. 13 (6) (2011) 1399.

[55] R. Harun, M. Singh, G.M. Forde, M.K. Danquah, Bioprocess engineering of microalgae to produce a variety of consumer products, Renewable and Sustainable Energy Reviews 14 (3) (2010) 1037–1047.

[56] E.W. Becker, Micro-algae as a source of protein, Biotechnology Advances 25 (2) (2007) 207–210.

[57] C.D. Kang, S.J. Sim, Selective extraction of free astaxanthin from Haematococcus culture using a tandem organic solvent system, Biotechnol. Prog. 23 (4) (2007) 866–871.

[58] C. Posten, S. Feng Chen, Microalgae Biotechnology, 1st ed., 2016.

[59] B. Klejdus, J. Kopecký, L. Benesová, J. Vacek, Solid-phase/supercritical-fluid extraction for liquid chromatography of phenolic compounds in freshwater microalgae and selected cyanobacterial species, J. Chromatogr. A 1216 (5) (2009) 763–771.

[60] L. Onofrejová, J. Vasícková, B. Klejdus, P. Stratil, L. Misurcová, S. Krácmar, J. Kopecký, J. Vacek, Bioactive phenols in algae: The application of pressurized-liquid and solid-phase extraction techniques, J. Pharm. Biomed. Anal. 51 (2) (2010) 464–470.

[61] E. Charter, J. Smith (Eds.), Functional food product development, Blackwell, Chichester, West Sussex, Ames, IA, 2010.

[62] M.A. Borowitzka, Commercial production of microalgae: Ponds, tanks, tubes and fermenters, Journal of Biotechnology 70 (1-3) (1999) 313–321.

[63] S. Hindersin, M. Leupold, M. Kerner, D. Hanelt, Irradiance optimization of outdoor microalgal cultures using solar tracked photobioreactors, Bioprocess Biosyst. Eng. 36 (3) (2013) 345–355.

[64] M. Piorreck, K.-H. Baasch, P. Pohl, Biomass production, total protein, chlorophylls, lipids and fatty acids of freshwater green and blue-green algae under different nitrogen regimes, Phytochemistry 23 (2) (1984) 207–216.

[65] K.H. Wiltshire, M. Boersma, A. Möller, H. Buhtz, Extraction of pigments and fatty acids from the green alga Scenedesmus obliquus (Chlorophyceae), Aquatic Ecology 34 (2) (2000) 119–126.

[66] D.J. Patzelt, S. Hindersin, S. Elsayed, N. Boukis, M. Kerner, D. Hanelt, Hydrothermal gasification of Acutodesmus obliquus for renewable energy production and nutrient recycling of microalgal mass cultures, J Appl Phycol 27 (6) (2015) 2239–2250.

[67] M. Leupold, S. Hindersin, G. Gust, M. Kerner, D. Hanelt, Influence of mixing and shear stress on Chlorella vulgaris, Scenedesmus obliquus, and Chlamydomonas reinhardtii, J Appl Phycol 25 (2) (2013) 485–495.

[68] J. Burczyk, H. Szkawran, I. Zontek, F.C. Czygan, Carotenoids in the outer cell-wall layer of Scenedesmus (Chlorophyceae), Planta 151 (3) (1981) 247–250.

[69] J. Burczyk, J. Dworzanski, Comparison of sporopollenin-like algal resistant polymer from cell wall of Botryococcus, scenedesmus and lycopodium clavatum by GC-pyrolysis, Phytochemistry 27 (7) (1988) 2151–2153.

[70] N. Hanagata, T. Takeuchi, Y. Fukuju, D.J. Barnes, I. Karube, Tolerance of microalgae to high CO2 and high temperature, Phytochemistry 31 (10) (1992) 3345–3348.

[71] A. Makulla, Fatty acid composition of Scenedesmus obliquus: Correlation to dilution rates, Limnologica - Ecology and Management of Inland Waters 30 (2) (2000) 162–168.

[72] M. Attokaran, Natural food flavors and colorants, Wiley Blackwell; IFT Press, Chichester, West Sussex, Chicago, IL, 2017.

[73] S. Taylor, Advances in Food and Nutrition Research: Volume 58, 1st ed., Elsevier textbooks, s.l., 2009.

[74] A.M.F. Fileti, G.A. Fischer, J.C.C. Santana, E.B. Tambourgi, Batch and continuous extraction of bromelain enzyme by reversed micelles, Braz. arch. biol. technol. 52 (5) (2009) 1225–1234.

[75] H.-E. Khoo, K.N. Prasad, K.-W. Kong, Y. Jiang, A. Ismail, Carotenoids and their isomers: Color pigments in fruits and vegetables, Molecules 16 (2) (2011) 1710–1738.

[76] B. Fernandez de Simon, J. Perez-Ilzarbe, T. Hernandez, C. Gomez-Cordoves, I. Estrella, Importance of phenolic compounds for the characterization of fruit juices, J. Agric. Food Chem. 40 (9) (1992) 1531–1535.

[77] L. Wen, R.E. Wrolstad, Phenolic Composition of Authentic Pineapple Juice, J Food Science 67 (1) (2002) 155–161. https://doi.org/10.1111/j.1365-2621.2002.tb11376.x.

[78] X. Sui, Impact of Food Processing on Anthocyanins, Springer Singapore, Singapore, s.l., 2017.

[79] S. Ketnawa, P. Chaiwut, S. Rawdkuen, Aqueous two-phase extraction of bromelain from pineapple peels ('Phu Lae' cultv.) and its biochemical properties, Food Sci Biotechnol 20 (5) (2011) 1219–1226.

[80] F.A. Vicente, L.D. Lario, A. Pessoa, S.P.M. Ventura, Recovery of bromelain from pineapple stem residues using aqueous micellar two-phase systems with ionic liquids as co-surfactants, Process Biochemistry 51 (4) (2016) 528–534.

[81] E.G. Schwarz, W.G. Reid, SURFACE-ACTIVE AGENTS—THEIR BEHAVIOR AND INDUSTRIAL USE, Ind. Eng. Chem. 56 (9) (1964) 26–31.

[82] J.T. Davies (Ed.), A quantitative kinetic theory of emulsion type, I. Physical chemistry of the emulsifying agent, Butterworths Scientific Publications, 1957.

[83] H. Schott, Hydrophilic-Lipophilic Balance, Solubility Parameter, and Oil-Water Partition Coefficient as Universal Parameters of Nonionic Surfactants, Journal of Pharmaceutical Sciences 84 (10) (1995) 1215–1222.

[84] S.K. Hait, S.P. Moulik, Determination of critical micelle concentration (CMC) of nonionic surfactants by donor-acceptor interaction with Iodine and correlation of CMC with hydrophile-lipophile balance and other parameters of the surfactants, J Surfact Deterg 4 (3) (2001) 303–309.

[85] D. Nandni, K.K. Vohra, R.K. Mahajan, Study of micellar and phase separation behavior of mixed systems of triblock polymers, J. Colloid Interface Sci. 338 (2) (2009) 420–427.

[86] J.C. Lang, R.D. Morgan, Nonionic surfactant mixtures. I. Phase equilibria in C 10 E 4 –H 2 O and closed-loop coexistence, The Journal of Chemical Physics 73 (11) (1980) 5849–5861.

[87] M. He, R.M. Hill, Z. Lin, L.E. Scriven, H.T. Davis, Phase behavior and microstructure of polyoxyethylene trisiloxane surfactants in aqueous solution, J. Phys. Chem. 97 (34) (1993) 8820–8834.

[88] S.S. Soni, S.H. Panjabi, N.V. Sastry, Effect of non-electrolyte additives on micellization and clouding behavior of silicone surfactant in aqueous solutions, Colloids and Surfaces A: Physicochemical and Engineering Aspects 377 (1-3) (2011) 205–211.

[89] Iwanaga, Kunieda, Effect of Added Salts or Polyols on the Cloud Point and the Liquid-Crystalline Structures of Polyoxyethylene-Modified Silicone, J. Colloid Interface Sci. 227 (2) (2000) 349–355.

[90] E. Ritter, R. Racheva, S. Storm, S. Müller, T. Ingram, I. Smirnova, Influence of Inorganic Salts on the Phase Equilibrium of Triton X-114 Aqueous Two-Phase Systems, J. Chem. Eng. Data 61 (4) (2016) 1496–1501.

[91] L. Rhein, M. Schlossman, A. O'Lenick, P. Somasundaran (Eds.), Surfactants in Personal Care Products and Decorative Cosmetics, Third Edition, CRC Press, 2006.

[92] I. Kralova, J. Sjöblom, Surfactants Used in Food Industry: A Review, Journal of Dispersion Science and Technology 30 (9) (2009) 1363–1383.

[93] C.N. Mulligan, R.N. Yong, B.F. Gibbs, Surfactant-enhanced remediation of contaminated soil: A review, Engineering Geology 60 (1-4) (2001) 371–380.

[94] J.-W. Han, H.-S. Park, B.-H. Kim, P.-G. Shin, S.-K. Park, J.-C. Lim, Potential Use of Nonionic Surfactants in the Biodesulfurization of Bunker-C Oil, Energy Fuels 15 (1) (2001) 189–196.

[95] Z. Wang, Bioavailability of organic compounds solubilized in nonionic surfactant micelles, Applied Microbiology and Biotechnology 89 (3) (2011) 523–534.

[96] F.H. Quina, W.L. Hinze, Surfactant-Mediated Cloud Point Extractions: An Environmentally Benign Alternative Separation Approach, Ind. Eng. Chem. Res. 38 (11) (1999) 4150–4168.

[97] R.P. Frankewich, W.L. Hinze, Evaluation and Optimization of the Factors Affecting Nonionic Surfactant-Mediated Phase Separations, Anal. Chem. 66 (7) (2002) 944–954.

[98] R.B. Haga, V.C. Santos-Ebinuma, M. de Siqueira Cardoso Silva, A. Pessoa, C.O. Rangel-Yagui, Clavulanic acid partitioning in charged aqueous two-phase micellar systems, Separation and Purification Technology 103 (2013) 273–278.

[99] W.P.N. Silva, A.E.G.d. Nascimento, M.C.P.d.A. Moura, H.N.M.d. Oliveira, E.L.d. Barros Neto, Study of phenol removal by cloud point extraction: A process optimization using experimental design, Separation and Purification Technology 152 (2015) 133–139.

[100] M.d.A. Bezerra, M.A.Z. Arruda, S.L.C. Ferreira, Cloud Point Extraction as a Procedure of Separation and Pre-Concentration for Metal Determination Using Spectroanalytical Techniques: A Review, Applied Spectroscopy Reviews 40 (4) (2005) 269–299.

[101] R. Carabias-Martínez, E. Rodríguez-Gonzalo, B. Moreno-Cordero, J.L. Pérez-Pavón, C. García-Pinto, E. Fernández Laespada, Surfactant cloud point extraction and preconcentration of organic compounds prior to chromatography and capillary electrophoresis, J. Chromatogr. A 902 (1) (2000) 251–265.

[102] A. Ballesteros-Gómez, M.D. Sicilia, S. Rubio, Supramolecular solvents in the extraction of organic compounds. A review, Anal. Chim. Acta 677 (2) (2010) 108–130.

[103] J.H. Tan, S.F. Jin, H. Yang, A Cloud Point Extraction Approach Developed for Analyzing Pesticides Prometryne and Isoproturon from Multi-media, Clean Soil Air Water 41 (5) (2013) 510–516.

[104] S. Ameur, B. Haddou, Z. Derriche, J.P. Canselier, C. Gourdon, Cloud point extraction of Δ9-tetrahydrocannabinol from cannabis resin, Anal. Bioanal. Chem. 405 (10) (2013) 3117–3123.

[105] C. Bordier, Phase separation of integral membrane proteins in Triton X-114 solution, J. Biol. Chem. 256 (4) (1981) 1604–1607.

[106] S.S. Arya, A.M. Kaimal, M. Chib, S.K. Sonawane, P.L. Show, Novel, energy efficient and green cloud point extraction: Technology and applications in food processing, J. Food Sci. Technol. 56 (2) (2019) 524–534.

[107] B. Fricke, Phase separation of nonionic detergents by salt addition and its application to membrane proteins, Anal. Biochem. 212 (1) (1993) 154–159.

[108] T. Arnold, D. Linke, Phase separation in the isolation and purification of membrane proteins, Biotech. 43 (4) (2007) 427–440.

[109] P. Schneider, F. Bischoff, U. Müller, H.-J. Bart, K. Schlitter, V. Jordan, Plant Extraction with Aqueous Two-Phase Systems, Chem. Eng. Technol. 34 (3) (2011) 452–458.

[110] L. Chen, R. Li, X. Ren, T. Liu, Improved aqueous extraction of microalgal lipid by combined enzymatic and thermal lysis from wet biomass of Nannochloropsis oceanica, Bioresour. Technol. 214 (2016) 138–143.

[111] O. Gortzi, S. Lalas, A. Chatzilazarou, E. Katsoyannos, S. Papaconstandinou, E. Dourtoglou, Recovery of Natural Antioxidants from Olive Mill Wastewater Using Genapol-X080, J Am Oil Chem Soc 85 (2) (2008) 133–140.

[112] A.C. Leite, A.M. Ferreira, E.S. Morais, I. Khan, M.G. Freire, J.A.P. Coutinho, Cloud point extraction of chlorophylls from spinach leaves using aqueous solutions of non-ionic surfactants, ACS Sustainable Chem. Eng. 6 (1) (2018) 590–599.

[113] A. Chatzilazarou, E. Katsoyannos, O. Gortzi, S. Lalas, Y. Paraskevopoulos, E. Dourtoglou, J. Tsaknis, Removal of Polyphenols from Wine Sludge Using Cloud Point Extraction, Journal of the Air & Waste Management Association 60 (4) (2010) 454–459.

[114] A. El-Abbassi, H. Kiai, J. Raiti, A. Hafidi, Cloud point extraction of phenolic compounds from pretreated olive mill wastewater, Journal of Environmental Chemical Engineering 2 (3) (2014) 1480–1486.

[115] S. Sharma, S. Kori, A. Parmar, Surfactant mediated extraction of total phenolic contents (TPC) and antioxidants from fruits juices, Food Chem. 185 (2015) 284–288.

[116] K. Kiathevest, M. Goto, M. Sasaki, P. Pavasant, A. Shotipruk, Extraction and concentration of anthraquinones from roots of Morinda citrifolia by non-ionic surfactant solution, Separation and Purification Technology 66 (1) (2009) 111–117.

[117] E. Cordisco, C.N. Haidar, E.R. Coscueta, B.B. Nerli, L.P. Malpiedi, Integrated extraction and purification of soy isoflavones by using aqueous micellar systems, Food Chem. 213 (2016) 514–520.

[118] G.Y.T. Tan, W. Zimmermann, K.-H. Lee, J.C.-W. Lan, H.S. Yim, H.S. Ng, Recovery of mangostins from Garcinia mangostana peels with an aqueous micellar biphasic system, Food and Bioproducts Processing 102 (2017) 233–240.

[119] X. Tang, D. Zhu, W. Huai, W. Zhang, C. Fu, X. Xie, S. Quan, H. Fan, Simultaneous extraction and separation of flavonoids and alkaloids from Crotalaria sessiliflora L. by microwave-assisted cloud-point extraction, Separation and Purification Technology 175 (2017) 266–273.

[120] N. Phasukarratchai, S. Damrongsiri, C. Tongcumpou, Recovery of phorbol esters from pressed jatropha seeds by surfactant extraction and cloud-point separation, Industrial Crops and Products 95 (2017) 549–557.

[121] A. Singh, J.D. van Hamme, O.P. Ward, Surfactants in microbiology and biotechnology: Part 2. Application aspects, Biotechnology Advances 25 (1) (2007) 99–121.

[122] G. Ulloa, C. Coutens, M. Sánchez, J. Sineiro, J. Fábregas, F.J. Deive, A. Rodríguez, M.J. Núñez, On the double role of surfactants as microalga cell lysis agents and antioxidants extractants, Green Chem. 14 (4) (2012) 1044.

[123] Z. Wang, F. Zhao, X. Hao, D. Chen, D. Li, Microbial transformation of hydrophobic compound in cloud point system, Journal of Molecular Catalysis B: Enzymatic 27 (4-6) (2004) 147–153.

[124] Z. Wang, F. Zhao, D. Chen, D. Li, Biotransformation of phytosterol to produce androsta-diene-dione by resting cells of Mycobacterium in cloud point system, Process Biochemistry 41 (3) (2006) 557–561.

[125] Z. Wang, J.-H. Xu, W. Zhang, B. Zhuang, H. Qi, In situ extraction of polar product of whole cell microbial transformation with polyethylene glycol-induced cloud point system, Biotechnol. Prog. 24 (5) (2008) 1090–1095.

[126] C.-K. Lee, W.-D. Su, Separation of Phenylacetic Acid from 6-Aminopenicillanic Acid via Cloud-Point Extraction with N-Decyltetra(ethylene Oxide) Nonionic Surfactant, Separation Science and Technology 33 (7) (1998) 1003–1012.

[127] Z. Wang, Y. Guo, D. Bao, H. Qi, Direct extraction of phenylacetic acid from immobilised enzymatic hydrolysis of penicillin G with cloud point extraction, J. Chem. Technol. Biotechnol. 81 (4) (2006) 560–565.

[128] Z. Wang, L. Wang, J.-H. Xu, D. Bao, H. Qi, Enzymatic hydrolysis of penicillin G to 6-aminopenicillanic acid in cloud point system with discrete countercurrent experiment, Enzyme and Microbial Technology 41 (1-2) (2007) 121–126.

[129] Z. Hu, X. Zhang, Z. Wu, H. Qi, Z. Wang, Perstraction of intracellular pigments by submerged cultivation of Monascus in nonionic surfactant micelle aqueous solution, Applied Microbiology and Biotechnology 94 (1) (2012) 81–89.

[130] B. Kang, X. Zhang, Z. Wu, H. Qi, Z. Wang, Solubilization capacity of nonionic surfactant micelles exhibiting strong influence on export of intracellular pigments in Monascus fermentation, Microb. Biotechnol. 6 (5) (2013) 540–550.

[131] A.M. Lopes, P.O. Magalhães, P.G. Mazzola, C.O. Rangel-Yagui, J.C.M. de Carvalho, T.C.V. Penna, A. Pessoa, Green fluorescent protein extraction and LPS removal from Escherichia coli fermentation medium using aqueous two-phase micellar system, Separation and Purification Technology 81 (3) (2011) 339–346.

[132] P. Glembin, M. Kerner, I. Smirnova, Cloud point extraction of microalgae cultures, Separation and Purification Technology 103 (2013) 21–27.

[133] L.R. Chávez-Castilla, O. Aguilar, An integrated process for the in situ recovery of prodigiosin using micellar ATPS from a culture of Serratia marcescens, J. Chem. Technol. Biotechnol. 91 (11) (2016) 2896–2903.

[134] R. Ernst, C.J. Gonzales, J. Arditti, Biological effects of surfactants: Part 6—effects of anionic, non-ionic and amphoteric surfactants on a green alga (Chlamydomonas), Environmental Pollution Series A, Ecological and Biological 31 (3) (1983) 159–175.

[135] M.A. Lewis, Chronic toxicities of surfactants and detergent builders to algae: A review and risk assessment, Ecotoxicol. Environ. Saf. 20 (2) (1990) 123–140.

[136] M. Lürling, Effects of a surfactant (FFD-6) on Scenedesmus morphology and growth under different nutrient conditions, Chemosphere 62 (8) (2006) 1351–1358.

[137] K. Masakorala, A. Turner, M.T. Brown, Toxicity of Synthetic Surfactants to the Marine Macroalga, Ulva lactuca, Water Air Soil Pollut 218 (1-4) (2011) 283–291.

[138] N. Dias, R.A. Mortara, N. Lima, Morphological and physiological changes in Tetrahymena pyriformis for the in vitro cytotoxicity assessment of Triton X-100, Toxicology in Vitro 17 (3) (2003) 357–366.

[139] W.E. Shafer, Bukovac Martin, Studies on Octylphenoxy Surfactants: III. Sorption of Triton X-100 by Isolated Tomato Fruit Cuticles, J. Plant Physiology 85 (4) (1987) 965–970.

[140] X. Yuan, F. Ren, G. Zeng, H. Zhong, H. Fu, J. Liu, X. Xu, Adsorption of surfactants on a Pseudomonas aeruginosa strain and the effect on cell surface lypohydrophilic property, Applied Microbiology and Biotechnology 76 (5) (2007) 1189–1198.

[141] B. Yao, L. Yang, Pilot-scale Ultrasonic Assisted Cloud Point Extraction of Polycyclic Aromatic Hydrocarbons from Polluted Water, Separation Science and Technology 43 (6) (2008) 1564–1580.

[142] H. Benkhedja, J.P. Canselier, C. Gourdon, B. Haddou, Phenol and benzenoid alcohols separation from aqueous stream using cloud point extraction: Scaling-up of the process in a mixer-settler, Journal of Water Process Engineering 18 (2017) 202–212..

[143] P. Trakultamupatam, J.F. Scamehorn, S. Osuwan, Scaling Up Cloud Point Extraction of Aromatic Contaminants from Wastewater in a Continuous Rotating Disk Contactor. I. Effect of Disk Rotation Speed and Wastewater to Surfactant Ratio, Separation Science and Technology 39 (3) (2005) 479–499.

[144] P. Trakultamupatam, J.F. Scamehorn, S. Osuwan, Scaling Up Cloud Point Extraction of Aromatic Contaminants from Wastewater in a Continuous Rotating Disk Contactor. II. Effect of Operating Temperature and Added Electrolyte, Separation Science and Technology 39 (3) (2005) 501–516.

[145] E.A. Safonova, T. Mehling, S. Storm, E. Ritter, I.V. Smirnova, Partitioning equilibria in multicomponent surfactant systems for design of surfactant-based extraction processes, Chemical Engineering Research and Design 92 (12) (2014) 2840–2850.

[146] E. Ritter, R. Racheva, S. Jakobtorweihen, I. Smirnova, Influence of d -glucose as additive on thermodynamics and physical properties of aqueous surfactant two-phase systems for the continuous micellar extraction, Chemical Engineering Research and Design 121 (2017) 149–162.

[147] I. Fischer, C.-C. Hsu, M. Gärtner, C. Müller, T.W. Overton, O.R.T. Thomas, M. Franzreb, Continuous protein purification using functionalized magnetic nanoparticles in aqueous micellar two-phase systems, J. Chromatogr. A 1305 (2013) 7–16.

[148] T. Minuth, H. Gieren, U. Pape, H.C. Raths, J. Thömmes, M.R. Kula, Pilot scale processing of detergent-based aqueous two-phase systems, Biotechnol. Bioeng. 55 (2) (1997) 339–347.

[149] C. Kepka, E. Collet, J. Persson, Å. Ståhl, T. Lagerstedt, F. Tjerneld, A. Veide, Pilot-scale extraction of an intracellular recombinant cutinase from E. coli cell homogenate using a thermoseparating aqueous two-phase system, Journal of Biotechnology 103 (2) (2003) 165–181.

[150] K. Selber, F. Tjerneld, A. Collén, T. Hyytiä, T. Nakari-Setälä, M. Bailey, R. Fagerström, J. Kan, J. van der Laan, M. Penttilä, M.-R. KULA, Large-scale separation and production of engineered proteins, designed for facilitated recovery in detergent-based aqueous two-phase extraction systems, Process Biochemistry 39 (7) (2004) 889–896.

[151] H. Cheng, D.A. Sabatini, Separation of Organic Compounds from Surfactant Solutions: A Review, Separation Science and Technology 42 (3) (2007) 453–475.

[152] P.B. Dhamole, Z. Wang, Y. Liu, B. Wang, H. Feng, Extractive fermentation with non-ionic surfactants to enhance butanol production, Biomass and Bioenergy 40 (2012) 112–119.

[153] R. Lebeuf, E. Illous, C. Dussenne, V. Molinier, E.D. Silva, M. Lemaire, J.-M. Aubry, Solvo-Surfactant Properties of Dialkyl Glycerol Ethers: Application as Eco-Friendly Extractants of Plant Material through a Novel Hydrotropic Cloud Point Extraction (HCPE) Process, ACS Sustainable Chem. Eng. 4 (9) (2016) 4815–4823.

[154] M. Topf, T. Ingram, T. Mehling, T. Brinkmann, I. Smirnova, Product recovery in surfactant-based separation processes: Pervaporation of toluene from concentrated surfactant solutions, Journal of Membrane Science 444 (2013) 32–40.

[155] B.D. Ribeiro, D.W. Barreto, M.A.Z. Coelho, Use of micellar extraction and cloud point preconcentration for valorization of saponins from sisal (Agave sisalana) waste, Food and Bioproducts Processing 94 (2015) 601–609.

[156] R. Liang, Z. Wang, J.-H. Xu, W. Li, H. Qi, Novel polyethylene glycol induced cloud point system for extraction and back-extraction of organic compounds, Separation and Purification Technology 66 (2) (2009) 248–256.

[157] H. Ghouas, B. Haddou, M. Kameche, J.P. Canselier, C. Gourdon, Removal of Tannic Acid From Aqueous Solution by Cloud Point Extraction and Investigation of Surfactant Regeneration by Microemulsion Extraction, J Surfact Deterg 19 (1) (2016) 57–66.

[158] V. Patel, D. Ray, V.K. Aswal, P. Bahadur, Triton X-100 micelles modulated by solubilized cinnamic acid analogues: The pH dependant micellar growth, Colloids and Surfaces A: Physicochemical and Engineering Aspects 450 (2014) 106–114.

[159] N. Tietgens, Experimental determination of the optimal operating conditions for the continuous micellar in situ extraction from microalgae cultures. Master Thesis, Hamburg, 2015.

[160] A. Zilaev, Kontinuierliche mizellare in situ Extraktion wertvoller Verbindungen aus Mikroalgenkulturen im Pilotmaßstab: Scale-Up und Optimierung. Master Thesis, Hamburg, 2016.

[161] D. Yordanova, I. Smirnova, S. Jakobtorweihen, Molecular Modeling of Triton X Micelles: Force Field Parameters, Self-Assembly, and Partition Equilibria, J. Chem. Theory Comput. 11 (5) (2015) 2329–2340.

[162] A. Chaudhuri, S. Haldar, A. Chattopadhyay, Organization and dynamics in micellar structural transition monitored by pyrene fluorescence, Biochem. Biophys. Res. Commun. 390 (3) (2009) 728–732.

[163] D.C. Montgomery, Design and analysis of experiments, 8th ed., Wiley, Hoboken, NJ, 2013.

[164] E.L. Paul, V.A. Atiemo-Obeng, S.M. Kresta (Eds.), Handbook of industrial mixing: Science and practice, Wiley-Interscience, Hoboken, NJ, 2004.

[165] D. Peshev, L.G. Peeva, G. Peev, I.I.R. Baptista, A.T. Boam, Application of organic solvent nanofiltration for concentration of antioxidant extracts of rosemary (Rosmarinus officiallis L.), Chemical Engineering Research and Design 89 (3) (2011) 318–327.

[166] J.-P. Salminen, M. Karonen, Chemical ecology of tannins and other phenolics: We need a change in approach, Functional Ecology 25 (2) (2011) 325–338.

[167] G.L. Miller, Use of Dinitrosalicylic Acid Reagent for Determination of Reducing Sugar, Anal. Chem. 31 (3) (1959) 426–428.

[168] R. Racheva, N. Tietgens, M. Kerner, I. Smirnova, In situ continuous countercurrent cloud point extraction of microalgae cultures, Separation and Purification Technology 190 (2018) 268–277.

[169] V.I. Kirou, L.L. Tavlarides, J.C. Bonnet, C. Tsouris, Flooding, holdup, and drop size measurements in a multistage column extractor, AIChE J. 34 (2) (1988) 283–292.

[170] A. Forret, J.-M. Schweitzer, T. Gauthier, R. Krishna, D. Schweich, Liquid Dispersion in Large Diameter Bubble Columns, with and without Internals, Can. J. Chem. Eng. 81 (3-4) (2003) 360–366.

[171] P.D. Haaland, Experimental design in biotechnology, Dekker, New York, 1989.

[172] R. Racheva, A.F. Rahlf, D. Wenzel, C. Müller, M. Kerner, G.A. Luinstra, I. Smirnova, Aqueous food-grade and cosmetic-grade surfactant systems for the continuous countercurrent cloud point extraction, Separation and Purification Technology 202 (2018) 76–85.

[173] D.A. Wenzel, Development and scale-up of a continuous micellar in situ extraction process for valuable compounds from microalgae cultures. Master Thesis, Hamburg, 2015.

[174] C. Müller, Eignung von ROKAnol NL5 für die Cloud Point Extraktion von pflanzlichen Wertstoffen. Project Work, Hamburg, 2017.

[175] T. Kato, T. Terao, M. Tsukada, T. Seimiya, Self-diffusion processes in semidilute solutions of nonionic surfactant (C16E7) studied by light scattering and pulsed-gradient spin echo methods, J. Phys. Chem. 97 (15) (1993) 3910–3917.

[176] O. Fellechner, S. Rotzolk, I. Smirnova, Long-Chain Alcohol-Modified Micellar Systems and Their Application in a Continuous Extraction Process, Ind. Eng. Chem. Res. 58 (7) (2018) 2575–2582.

[177] G. Cornelis, K. Boussu, B. van der Bruggen, I. Devreese, C. Vandecasteele, Nanofiltration of Nonionic Surfactants: Effect of the Molecular Weight Cutoff and Contact Angle on Flux Behavior, Ind. Eng. Chem. Res. 44 (20) (2005) 7652–7658.

[178] T. Mehling, A. Zewuhn, T. Ingram, I. Smirnova, Recovery of sugars from aqueous solution by micellar enhanced ultrafiltration, Separation and Purification Technology 96 (2012) 132–138.

[179] J. Johannsen, Mizellare Gegenstromextraktion aus Mikroalgenkulturen mittels Triton X-114. Bachelorarbeit, Hamburg, 2014.

[180] M. Lange, Eignung nichtionischer Tenside für die in situ Extraktion aus Mikroalgenkulturen. Bachelorarbeit, Hamburg, 2016.

LIST OF PUBLICATIONS

List of the scientific publications as first author:

- R. Racheva, N. Tietgens, M. Kerner, I. Smirnova,
  Extension of the continuous countercurrent cloud point extraction for the in situ application with aqueous microalgae cultures,
  Separation and Purification Technol., 2017

- R. Racheva, A. F. Rahlf, D. Wenzel, C. Müller, M. Kerner, G. A. Luinstra, I. Smirnova,
  Aqueous food-grade and cosmetic-grade surfactant systems for the continuous countercurrent cloud point extraction,
  Separation and Purification Technol., 2018

LEBENSLAUF

Name Racheva

Vorname Ralena

Staatsangehörigkeit bulgarisch

Geburtsdatum 02.04.1988

Geburtsort, -land Sofia, Bulgarien

09.1995 - 08.2002 Grundschule in Sofia, Bulgarien

09.2002 - 08.2007 Staatliches Gymnasium für Mathematik und Naturwissenschaften, Sofia, Bulgarien

09.2007 - 10.2011 Studium der Verfahrenstechnik an der Universität für Chemische Technologie und Metallurgie Sofia und der Technischen Universität Hamburg-Harburg
Abschluss: Bachelor

11.2011 - 11.2012 Studium der Verfahrenstechnik an der Universität für Chemische Technologie und Metallurgie Sofia und der Technischen Universität Hamburg-Harburg
Abschluss: Master

11.2012 - 03.2013 Weiterbildung am Lehrstuhl für Analytische Chemie an der Universität für Chemische Technologie und Metallurgie Sofia

04.2013 - 03.2017 Wissenschaftliche Mitarbeiterin an der Technischen Universität Hamburg-Harburg

04.2017 - 10.2017 Anfertigung der wissenschaftlichen Publikationen und der Promotionsschrift

11.2017 - heute Technology Engineer bei Döhler GmbH, Darmstadt